A synthetic system to study the establishment of meiotic interhomolog-specific DNA repair by the Red1-Hop1-Mek1 complex

Inaugural-Dissertation

zur

Erlangung des Doktorgrades

Dr. rer. nat.

der Fakultät für Biologie

an der

Universität Duisburg-Essen

vorgelegt von

Vaishnavi Niraj Nivsarkar

aus Pune, India

durchgeführt am

Max Planck Institut für molekulare Physiologie

Abteilung für mechanistische Zellbiologie

April 2022

In the context of this doctoral work, the following articles were published:

- Dorota Rousová, **Vaishnavi Nivsarkar**, Veronika Altmannova, Vivek B Raina, Saskia K Funk1, David Liedtke1, Petra Janning, Franziska Müller, Heidi Reichle, Gerben Vader, John R Weir. (2021). 'Novel mechanistic insights into the role of Mer2 as the keystone of meiotic DNA break formation.' *Elife* DOI: 10.7554/eLife.72330

- **Vaishnavi N. Nivsarkar**, Linda Chen, Saskia K. Funk, John R. Weir and Gerben Vader. (2022). 'Studying meiosis in mitosis: Activating the meiosis-specific Red1-Hop1-Mek1 complex in mitotic budding yeast cells.' *BioRxiv* DOI: https://doi.org/10.1101/2022.04.06.487319

The experiments on which this work is based were carried out at the Max Planck Institute for Molecular Physiology in the Department of Mechanistic Cell Biology.

The thesis defense occurred on Tuesday, 23rd August, 2022 as an online disputation.

The examination committee was chaired by Prof. Dr. Dominic Boos and the examiners were Prof. Dr. Andrea Musacchio, Prof. Dr. Stefan Westermann and Prof. Dr. Gerben Vader.

INDEX

List of figures

List of Tables

List of Abbreviations

CDKs	cyclin-dependent kinases
ChIP	chromatin immunoprecipitation
CO	crossover
Co-IP	Co-immunoprecipitation
DDK	Dbf4-dependent kinase
DMSO	Dimethyl sulfoxide
DSB	double-strand break
G1	phase gap1 phase
G2	phase gap2 phase
GFP	green fluorescent protein
M	phase mitosis phase
NCO	non-crossover
BSCR	barrier to sister chromatid repair
IH	interhomolog
IS	intersister
NHEJ	non-homologous end joining
HR	homologous recombination
SSA	single strand annealing
SDSA	synthesis dependent strand annealing
BIR	break induced repair
MMS	Methyl methanesulphonate
dNTP	Deoxynucleotides
DNA	Deoxyribonucleic acid
DTT	Dithiothreitol
DSB	Double strand break
DAPI	4′,6-diamidino-2-phenylindole
dHJ	Double Holliday junctions
LB	Luria-Bertani
LiAc	Lithium acetate
PBS	Phosphate-buffered saline
PCR	Polymerase chain reaction
PEG	Polyethlene glycol
SC	Synaptonemal complex
SUMO	Small Uniquitin-like Modifier

Chapter 1

Introduction

A defining feature of eukaryotic organisms is sexual reproduction. To enable sexual reproduction, specialized reproductive cells, called gametes, are produced by sexually reproducing organisms. The process of gamete formation termed gametogenesis is a cellular differentiation program that dictates the formation of haploid gametes with half the chromosome number of the parental diploid progenitor cell (Gerton & Hawley, 2005; Kleckner, 1996). The fusion of two gametes from opposite mating types gives rise to a diploid progeny and thus maintains the ploidy (Hochwagen, 2008; Marston & Amon, 2004). Gametogenesis, or the budding yeast (*S. cerevisiae*) sporulation, occurs by a specialized type of cell division called meiosis that gives rise to spores in yeast or sperms and eggs in mammals. As a result of meiosis, genetic variation is introduced in the haploid gametes. Therefore meiosis needs to occur in a proper mechanism. Errors in meiosis are a leading cause of the missegregation of chromosomes into the daughter cells. This is commonly referred to as developmental aneuploidy. Examples of aneuploidy are trisomy (Cells carry three chromosomes of the same number) or monosomy (Cells have a single copy of a chromosome number). In humans, it is a hallmark of many diseases, such as infertility, birth defects, pregnancy miscarriage and growth defects (e.g. Down's syndrome; (Hassold & Hunt, 2001)). Several meiotic mechanisms manifest the occurrence of genetic diversity while avoiding aneuploidy-related defects. Further studies of these complex meiotic networks are required to understand how genetic diversity is introduced while maintaining genetic integrity.

1.1 The tell-tale signs of meiosis and mitosis

Mitosis and meiosis are two cell division programs that lead to the multiplication of cells. Both the cell division programs are well conserved in eukaryotes. Studies from organisms like yeast, plants and mammals (Clift & Schuh, 2013; Gray & Cohen, 2016; Handel & Schimenti, 2010; Hartwell, 1974; Mercier *et al*, 2015; Ohkura, 2015) have helped us gain a deeper understanding of these processes. During this Ph.D. study, I have performed experiments on *Saccharomyces cerevisiae* (*S. cerevisiae*; Budding yeast) as a model organism. Hence, the introduction from here on is focused on mechanistic insights of cell division in *S. cerevisiae*.

Mitosis, is an equational cell division. The mitotic division program is a part of vegetatively dividing cells. It prompts equal segregation of genetic material in the two daughter cells. Mitosis maintains chromosome content, with the resulting daughter cells carrying the same number of chromosomes as the parental cell. Prior to the mitotic division, DNA is replicated, leading to the duplication of chromosomes. The two identical sister chromatids are connected at the centromere and held together by multi-protein rings, called cohesin, along the entire chromosomal arms (Michaelis *et al*, 1997; Peters & Nishiyama, 2012; Watanabe, 2004). During mitotic division, the cohesin rings allow the sister chromatids to resist the mechanical forces generated by the microtubules that are attached to kinetochores (at centromere) and mediate pulling of chromatids to the opposite poles. This results in the alignment of chromosomes on the cell division plane. Microtubule-mediated pulling forces in the opposite direction leads to the segregation of sister chromatids in two daughter cells. As such, equal segregation of chromatids occur in mitosis.

In addition to sister chromatid segregation, the segregation of homologous chromosomes is an essential feature of the meiotic division (Kerr *et al*, 2012; Lee & Amon, 2001; Petronczki *et al*, 2003). Homologs are two identical chromosomes that are of maternal origin and paternal origin. Both the homologs as well as the sister chromatids are segregated in a two-step division during meiosis. The two divisions occurring in the meiotic program are - meiosis I (MI) and meiosis II (MII). The reduction in ploidy during meiosis is achieved due to two rounds of division without an intervening replication step. MI is a reductional division that ends in the segregation of homologous chromosomes, thus reducing the chromosome number half. MII is similar to mitosis; it is an equational division that results in the segregation of so-called sister chromatids. The meiotic cell division program is initiated with the replication of chromosomes, similar to the vegetative cell cycle. Sister chromatids are held together by cohesin rings. However, additional mechanisms are necessary to link the homologous chromosomes (homologs) that allow proper homolog segregation. Such homolog linkages are initiated by the introduction of DNA _d_ouble-_s_tranded _b_reaks (DSBs) in the genome during early MI (Keeney, 2008). Repair of the DSBs is attempted primarily by homologous recombination DNA repair mechanism, by preferentially using the homologous chromosome as a repair template (explained in detail in later sections). This results in linking the homologs together. The defining features of the meiotic program that deviate from mitosis are encoded in MI. These key meiosis-specific modifications are- i) Physical linkage of the homologs ii) Monopolar attachment of sister kinetochores during MI. iii) Protection of centromeric cohesin in MI and

iv) A second division step (MII) immediately followed by MI without an intervening replication step. Together, these events aid in mediating the meiosis-specific change in ploidy by half. Description of these modifications according to the cell cycle stages in which they occur, is followed in the subsequent sections.

1.2 Cell cycle phases

In general, eukaryotic cell cycles can be subdivided into several distinct phases. These phases are classically assigned based on cytological or metabolic events. Specifically, in mitosis, a growth phase 1 (G1), a synthesis phase (S), and a second growth phase 2 (G2) are recognized. The growth phases are thought of as metabolical preparation and control phases, preceding either DNA replication (occurring in the S-phase) (in the case of G1), or chromosome segregation phases (occurring during mitosis or meiosis) (in the case of G2). The main difference between mitotic and meiotic cell division programs can be recognized in the chromosome segregation phases. Whereas during mitosis a single chromosome segregation event involving sister chromatids takes places, the meiotic program contains two subsequent rounds of chromosomal segregation (Meiosis I (MI) and Meiosis II (MII)), effectively leading to a reduction in ploidy by half (Figure 1-1) (Marston & Amon, 2004). In vegetatively growing budding yeast cells, G2 and the following division (M) phase are metabolically and cytologically indistinguishable. Consequently, S-phase is directly followed by what can be considered a 'merged' G2/M phase. The final outcome of the mitotic cell cycle is the generation of two daughter cells that are genetically identical to their progenitor cell (*i.e.* in many eukaryotic organisms, including humans and budding yeasts, diploids cells are formed from diploid progenitors). In contrast, the outcome of the meiotic cell division program is the production of four specialized cells (*i.e.* reproductive cells or gametes) that contain a genome content that is half of that of their progenitor cells (*e.g.* haploid gametes are formed from a diploid progenitor cell) (Figure 1-1).

Cell cycle progression is driven by the controlled activity of cyclin-dependent kinases (CDKs). CDKs act in association with cognate regulatory subunits, called cyclins (or Cln/Clb in budding yeast) (Malumbres & Barbacid, 2005; Mendenhall & Hodge, 1998). Unlike in mammals, budding yeast cells express a single CDK, namely Cdc28. Cdc28, along with cell cycle phase-specific expression and activation of defined cyclins, is a major regulatory system that establishes order in cell cycle progression (Alberts, 2008; Marston & Amon, 2004). Errors in chromosome metabolism or genomic defects that occur during cell cycle progression, such

as stalled replication forks, DNA double-strand breaks, or incorrect microtubule-kinetochore interactions, can lead to cell arrest through the action of several dedicated cell cycle checkpoint mechanisms. Cell cycle checkpoints can halt cell cycle in the face of specific defects, and as such ensure cell cycle order and the propagation of a stable genome from one cell generation to the next. In the subsequent sections, I provide a brief overview of different stages of meiotic cell division program.
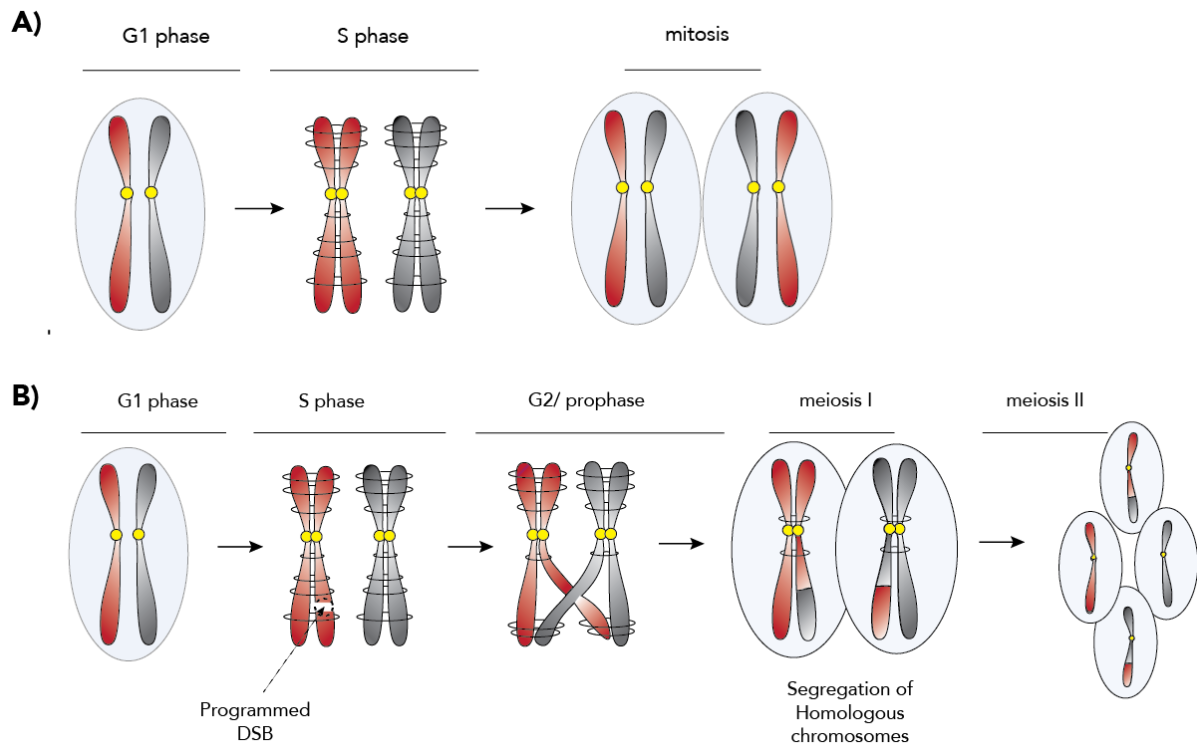
Figure 1-1: An overview of mitotic and meiotic cell division

Schematic of cells committed to mitotic and meiotic cell division. A) and B) A diploid cell consists of two sets of chromosomes originating from the two parental origins (depicted in Red and Grey). The decision to commit to mitotic/ meiotic cell division is made in G1 phase (growth phase). A single round of DNA replication is followed in the S-phase that leads to formation of sister chromatids held together at centromeres (yellow) and ring like protein complexes termed cohesin (black rings).

A) Following pre-mitotic S-phase, cells undergo equal segregation of chromosomes in the subsequent G2/M phase. There is no distinct G2 phase in budding yeast. The resulting daughter cells have the same number of chromosome as the parental cells.

B) Following pre-meiotic S-phase, a controlled introduction of DNA double stranded breaks takes place. The breaks are repaired by using the homologous chromosomes as

repair template in a homologous recombination DNA repair mechanism. This results in formation of interhomolog crossovers that links the two homologs together during early G2/prophase. A subsequent division step results in segregation of homologous chromosomes in MI. The sister chromatids are further segregated in MII resulting in four haploid gametes.

1.2.1 G1 phase

The decision to enter the mitotic or the meiotic cell division program is initiated in the G1 phase. Key changes in the signalling pathways during G1 culminate into entry into meiosis. Conditions promoting meiotic entry are - heterozygosity at the *mating type* locus (*MATa/ MATα*) (predominantly a diploid cell condition), nutrient deficiency (glucose and nitrogen starvation) and competence for respiration by presence of functional mitochondria in the cells (Colomina *et al*, 1999; Freese *et al*, 1982; Neiman, 2011; Smith & Mitchell, 1989; van Werven & Amon, 2011). Growth in a nitrogen-depleted environment and in the presence of a non-fermentable carbon source such as acetate (Freese et al., 1982; Mitchell, 1988, Neiman 2011), activates a meiosis-specific transcription factor Ime1 (*I*nitiator or *I*nducer of <u>*me*</u>iosis) (Colomina *et al.*, 1999; Smith & Mitchell, 1989; Smith *et al*, 1990) Ime1 is a master regulator that dictates entry into the meiotic cell cycle. In fact ectopic expression of Ime1 is sufficient to induce sporulation in mitotically dividing cells (Neiman, 2011; Smith *et al.*, 1990). Early meiotic genes are repressed in vegetatively dividing cells by Ume6, that is bound to regulatory elements in the promoter region of the meiotic genes. Ime1 regulates the transcription of the early meiotic genes by recruiting to their promoters and binding to Ume6, that allows the transcriptional activation of the early meiotic genes (Colomina *et al.*, 1999; Goldmark *et al*, 2000; Strich *et al*, 1994; van Werven & Amon, 2011).

To ensure unanticipated entry into meiosis during vegetative growth, mitotic G1-CDKs inhibit Ime1 expression. As a result, meiosis-specific genes are transcriptionally repressed in mitosis (Colomina *et al.*, 1999; Goldmark *et al.*, 2000; Kassir *et al*, 1988). It is therefore essential to substitute for the G1 CDK-Cln activity in the meiotic cell division program. This is carried out by Ime2. Among several targets of Ime1 are the two important players: Ime2 and Ndt80 (A detailed description of Ndt80 and its function is in the later sections)(Marston & Amon, 2004). Ime1 and Ime2 are inducers of meiosis and promote pre-meiotic S-phase entry (Marston & Amon, 2004; Smith *et al.*, 1990). Ime2 is a meiosis-specific CDK-like kinase. It mediates the degradation of pre-meiotic S-phase CDK inhibitors (such as Sic1) and carries out

inhibition of APC/C proteolytic activity (Bolte *et al*, 2002; Dirick *et al*, 1998; Marston & Amon, 2004), thus promoting the activation of Cdc28-Clb5/6 (S-phase CDKs). Accumulation of S-phase CDKs initiates DNA replication.

1.2.2 S-phase

During S-phase, DNA is replicated to generate identical copies of chromatids called "sister chromatids" that are engaged together via centromeres and ring-like protein complexes termed cohesin (Figure 1-1). The basis of replication is well conserved in pre-mitotic and pre-meiotic S-phase, with subtle differences that define the respective cell cycle progression (Collins & Newlon, 1994; Newlon, 1988). Entry into the mitotic S-phase is dictated by the activity of CDK (Cdc28) and G1-phase cyclins (Colomina *et al.*, 1999; Marston & Amon, 2004). Downregulation of G1-phase cyclins is essential for the decision of meiotic S-phase entry (Colomina *et al.*, 1999; MacKenzie & Lacefield, 2020). The role of G1 phase cyclins is taken over in meiosis the expression of Ime1 and Ime2, which take over the Cln-CDK activity and commit cells to the pre-meiotic S-phase as described in the above section (Dirick *et al.*, 1998; Marston & Amon, 2004). Later on in the S-phase, DNA replication is triggered by the CDK activity of Cdc28-Clb5/6 (Benjamin *et al*, 2003; Dirick *et al.*, 1998; Stuart & Wittenberg, 1998). After commitment to the S-phase, the basic mechanism of DNA replication is similar in mitosis and meiosis, with several shared proteins that drive DNA synthesis during both the cell cycles (Marston & Amon, 2004).

Despite the similarities, the meiotic S-phase is extensively prolonged compared to the mitotic S-phase (with the pre-meiotic S-phase nearly 1.5-3 times longer than the pre-mitotic) (Padmore *et al*, 1991; Williamson *et al*, 1983; Zickler & Kleckner, 1999). Several hypothesized theories attempt to understand the delayed meiotic S-phase (Blitzblau *et al*, 2012; Cha *et al*, 2000; Murakami & Keeney, 2014). In recent studies, the phenomenon is proposed to be due to delayed initiation of replication on several replication origin sites (Blitzblau *et al.*, 2012). The inefficiency in replication origin firing during meiosis could be a result of nutrient starvation conditions used for induction of meiosis. Alternatively, the extended pre-meiotic S-phase is thought to be by virtue of either reduced dNTP levels or decreased level of CDK activity (Blitzblau *et al.*, 2012; Sando & Miyake, 1971). Although attempts have been made to hypothesize the cause of delayed meiotic replication, the ultimate reason behind it is not fully understood.

In budding yeast meiosis, the 'post-S phase' is marked by DNA double-stranded breaks (DSBs) that are introduced in a programmed manner by the endonucleolytic activity of Spo11 (The mechanism of DSB introduction is discussed in detail in the later sections). The DSBs are repaired by homologous recombination mechanism leading to physical linkage between the two homologs. Under normal circumstances, meiotic DSBs are introduced on replicated chromosomes (Blitzblau *et al.*, 2012). This is because the replication forks are hindered by the DSB sites and introduction of DSBs in a succeeding step after replication avoids any deleterious chromosomal structures and cell viability defects. Nonetheless, earlier experiments have marked that DNA synthesis is not per se a requirement for programmed DSB formation during meiosis (Blitzblau *et al.*, 2012; Hochwagen *et al*, 2005; Murakami & Nurse, 2001), as mutants impeding S-phase replication initiation were observed to introduce normal levels of DSBs even on unreplicated chromosomes (Blitzblau *et al.*, 2012). To avoid deleterious effects of DSB introduction preceding the replication step, surveillance mechanisms, such as replication checkpoint, ensures that cells progress into the meiotic program only after proper replication occurs. Consequently, DSBs are prevented on unreplicated chromosomes (Blitzblau & Hochwagen, 2013; Ogino & Masai, 2006; Subramanian & Hochwagen, 2014; Tonami *et al*, 2005). These mechanisms are known to act on a local chromosomal level *i.e* delayed replication on one chromosomal arm prolongs DSB formation on that arm itself, without hindering the DSB activity on other chromosomes (Borde *et al*, 2000; Hochwagen & Amon, 2006). Cells progress into the G2/ prophase after bulk DNA replication is completed.

During S-phase, replication initiates at sites of replication origin, with replication forks emanating out of the origin sites. Throughout S-phase, DNA is replicated in a continuum with the initial firing of the early origin sites followed by late origin firing. Unfavourable conditions during DNA replication (such as stalled replication forks triggered by difficult to repair DNA structures, clashes of ongoing replication with the transcriptional machinery or diminished dNTP levels) can lead to replication stress (Finn *et al*, 2012; Hustedt *et al*, 2013; Zeman & Cimprich, 2014).A particular perilous consequence of such problems can be the collapse of a replication fork that culminates into DNA breaks (Cimprich & Cortez, 2008). Stalled replication forks initiate a replication checkpoint response in cells that slows down the replication process (Hustedt *et al.*, 2013; Putnam *et al*, 2009). As a result of replication checkpoint activation, late replication origins are inhibited from firing, consequently allowing the ordered progression of the stalled replication forks originating from the early origin sites (Finn *et al.*, 2012). Replication checkpoint also leads to cell cycle arrest to ensure chromosomal integrity during S-phase before proceeding to the cell division phase.

A yet another checkpoint termed the intra-S phase checkpoint is activated in response to DNA damage in S-phase (Finn *et al.*, 2012; Grenon *et al*, 2006; Hustedt *et al.*, 2013; Putnam *et al.*, 2009). DNA damage in the form of lesions or DSBs may occur due to replication fork collapse or exposure to DNA damaging agents. This leads to activation of intra-S phase checkpoint (DNA damage checkpoint specific to the S-phase). Although separable, both, the intra-S phase and the replication checkpoints partially overlap and activate similar downstream genes and are activated in response to similar DNA structures. Intra-S phase checkpoint activation results in the activity of phosphoinositide 3-kinase related proteins Mec1 and Tel1 (similar to mammalian ATR and ATM kinases, respectively) and their effector kinase namely - Rad53. Out of the two, activity of Tel1 is functionally redundant to Mec1 kinase (Mantiero *et al*, 2007; Morrow *et al*, 1995) (A detailed explanation of the role of Mec1 and Tel1 is followed in the later section). Mec1 is a sensory kinase that is activated in response to replication stress by two independent pathways. A 9-1-1 complex dependent pathway is proposed to specifically signal replication stress on the lagging strand whereas pol ε, along with replication factors Dpb11 and Sld2 operate on the leading strand (Puddu *et al*, 2011). Mec1, via downstream signalling mediates activation of Rad53, by phosphorylation of Rad53 adaptor proteins Mrc1 (in response to replication stress) or Rad9 (in response to DNA damage) (Finn *et al.*, 2012; Hustedt *et al.*, 2013; Tannous & Burgers, 2021). Rad53 and Mec1 play a critical role in promoting cell viability during the S-phase by stabilizing replication forks, preventing late origin firing and preventing meiotic/ mitotic entry in case of erroneous DNA replication/ damage (Tannous & Burgers, 2021). Furthermore, Mec1 activity is required in order to increase the dNTP levels that are needed for efficient DNA synthesis. This is an activity that is inherent to S-phase, explaining why *MEC1* is an essential gene (Forey *et al*, 2020) and constitutively expressed, even in the absence of DSBs.

1.2.3 G2/ Prophase of meiotic cell division program

In budding yeast, the G2/ prophase is dedicated to identifying homologous chromosomes and establishing interhomolog (IH) physical linkage. Such linkages are necessary for proper alignment of homologs on the metaphase plate and their subsequent error-free segregation. As cells progress after the replication of DNA, there is no clear distinction between S-phase and the initiation of the meiotic program in budding yeast. Concomitant to DNA replication, DSBs are introduced and repaired in an extended gap phase known as meiotic prophase (or G2/ prophase). Based on cytological observations, the early meiotic prophase is

further divided into distinct stages, *i.e.* leptonema, zygonema, pachynema, diplonema/ diakinesis (Figure 1-2) (Subramanian & Hochwagen, 2014).

Replication of chromosomes in S-phase is followed by the condensation of genetic material into chromosomal structures. During early meiotic prophase, telomeres get tethered to the nuclear membrane. Rapid telomere led chromosomal movements facilitate initial nonhomologous chromosomal coupling (Tsubouchi & Roeder, 2005; Xu & Kleckner, 1995). The pairing of nonhomologous chromosomes is thought to drive the search for homology, culminating in stable homolog association during late prophase (Marston, 2014; Tsubouchi & Roeder, 2005; Xu & Kleckner, 1995). The initiation of the meiotic prophase *i.e* the leptonema stage, is marked by chromosomal structural and organisational reformations. Amidst leptonema, DNA becomes organised into 'loop-axis' like structures (with DNA loops emanating out of chromosomal axis) by virtue of aberrant changes in the chromosomal axis (Blat *et al*, 2002; Panizza *et al*, 2011). The chromosomal axis is predominantly defined by assembly of meiosis-specific proteins - Red1, Hop1, cohesion complex and condensin (Bailis & Roeder, 1998; Blat *et al.*, 2002; Kim *et al*, 2010; Klein *et al*, 1999; Smith & Roeder, 1997). Red1 (*RED*uctional division) and Hop1 (*HO*molog *P*airing) are recruited to chromosomes soon after DNA <u>is</u> replicated (Niu *et al*, 2007; Panizza *et al.*, 2011; Smith & Roeder, 1997) and prior to DSB formation that aid in the formation of the loop-axis chromosomal architecture (Blat *et al.*, 2002; Keeney *et al*, 2014; Lam & Keeney, 2014). The loop-axis configuration facilitates the introduction of programmed DSBs occurring during the late leptonema stage. The DSBs are repaired by homologous recombination mechanism in the late meiotic prophase I. The breaks repaired in meiotic G2/ prophase by homologous recombination, preferentially use the homologous chromosomes as a repair template (Carpenter, 1994; Schwacha & Kleckner, 1995; Szostak *et al*, 1983). The selective usage of the homolog template for repair is also known as interhomolog bias (Goldfarb & Lichten, 2010; Lao & Hunter, 2010; Schwacha & Kleckner, 1997). The DSB repair is initiated in the zygonema stage (Figure 1-2). Fragmented DNA ends search for homologous sequences in the genome. Only a fraction of these DSBs are repaired by interhomolog recombination (Goldfarb & Lichten, 2010; Humphryes & Hochwagen, 2014; Kim *et al.*, 2010). The final products of these recombination events are non-crossovers (NCOs) or crossovers (COs), the latter resulting in physically linking the two homologs together. Followed by crossover mediated homolog linkage, a proteinaceous structure starts to assemble at the interface of two homologs (presumably at sites of COs) referred to as synaptonemal complex (SC; (Page & Hawley, 2004)) (Figure 1-2). The SC acts as a zipper-like structure that closely pairs the two homologs together (Subramanian & Hochwagen, 2014; Zickler &

Kleckner, 1999). The SC formation is initiated at the sites of crossovers (Henderson & Keeney, 2004) and the complex continues to polymerize along the entire chromosomal length. The physiology and assembly of the SC is indicative of the progression from zygonema to pachynema stage, with the latter marked by fully assembled SC (Figure 1-2).
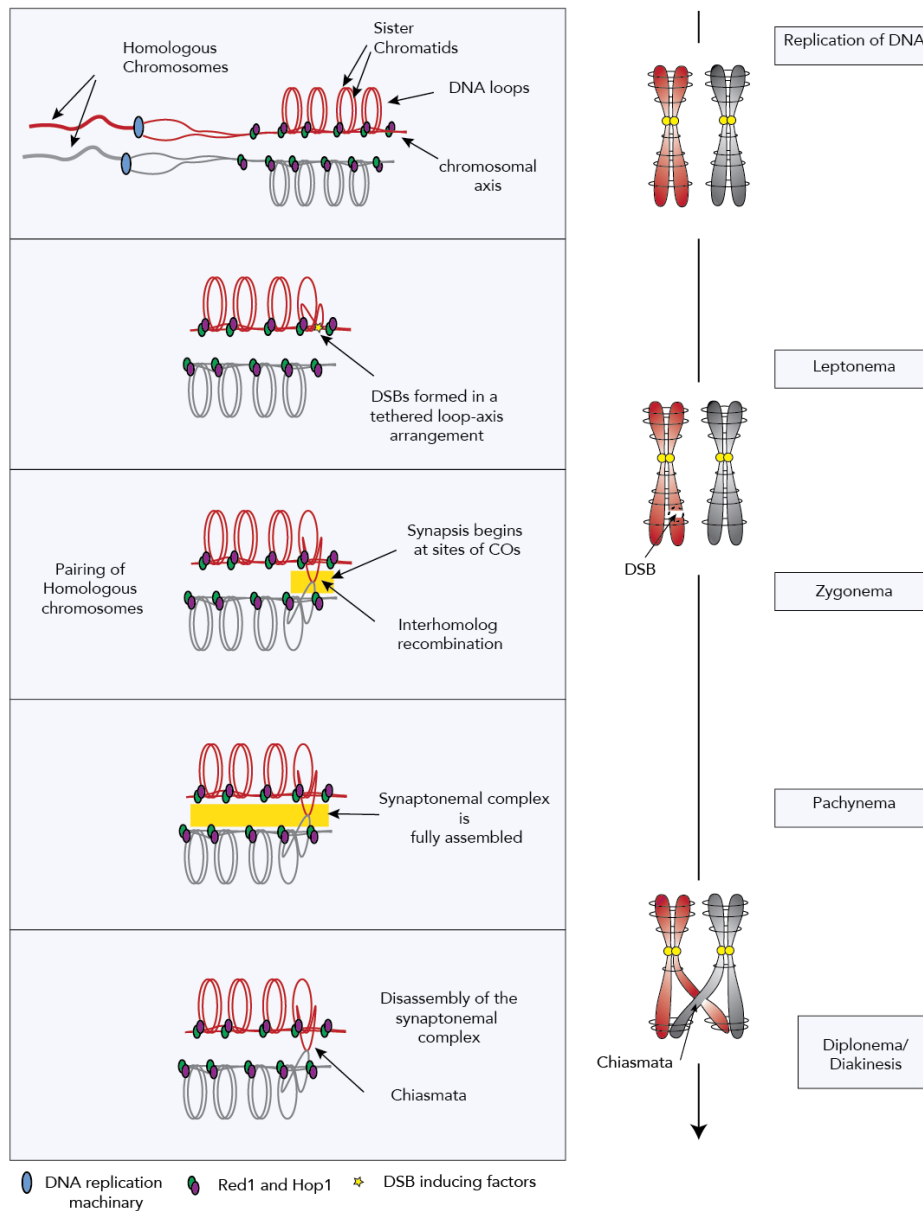
Figure 1-2: Meiotic cell division program. Meiotic DSB formation and repair events in G2/ prophase I

A prerequisite for faithful homolog segregation during MI is the establishment of interhomolog linkage via structures called chiasmata. These structures are developed during G2/ prophase I, following S-phase DNA replication events. The G2/ prophase I is further divided into following stages – leptonema, zygonema, pachynema, diplonema and diakinesis. Upon replication of

DNA, chromosomes are arranged in loop-axis like organisation. The axis comprises of meiosis specific proteins like Red1, Hop1 and cohesin complexes. The DNA loops emanate out of the chromosomal axis. Such a chromosomal organisation is crucial for programmed introduction of DSBs. In leptonema, programmed DSB introduction occurs in the DNA loops that are tethered to the axis where DSB machinery is recruited. In zygonema, DSB repair is initiated via homologous recombination by preferentially using the homologous chromosome. This leads to formation of interhomolog crossovers. The synaptonemal complex starts to assemble at sites of crossovers and is fully assembled between the homologs in pachynema. The synaptonemal complex is disassembled in diplonema/ diakineses and the exposed crossover sites are resolved to form chiasmata, thus physically linking the two homologs. (Figure adopted from (Subramanian & Hochwagen, 2014) and Kuhl, 2018)

The disassembly of the SC is lastly achieved in diplonema. At this stage, the DNA repair is complete, with exposed DNA crossovers. Lastly, in diakinesis, the homologs are physically linked by 'chiasmata' - the final outcome of crossover recombination (Carpenter, 1994; Kleckner, 1996) (Figure 1-2). Paired chromosomes in such a way are known as bivalents.

Introduction of programmed DNA breaks is a crucial guiding event that helps in physically linking the homologs together. As a consequence of this event, linked homologs, ensure proper segregation in MI. Another consequence of the interhomolog linkage is the exchange of genetic material during meiosis.

1.2.4 Meiosis I and Meiosis II

Following G2/ prophase, cells undergo two rounds of chromosomal segregation (MI and MII) without an intervening replication step. Segregation events occurring in meiosis II share similar features to mitotic segregation. At the onset of metaphase in mitosis and meiosis II, spindle microtubules attach to sister chromatids, via multi-protein complexes termed kinetochore (Musacchio & Desai, 2017). The kinetochore is assembled at centromeres of the monocentric budding yeast chromosomes (De Wulf *et al*, 2003; Earnshaw & Tomkiel, 1992; McAinsh *et al*, 2003; Westermann *et al*, 2003). The spindle microtubules originating from the two opposite spindle poles attach to the two sister kinetochores. This particular type of arrangement is called spindle bi-orientation (or amphitelic attachment) (Marston & Amon, 2004). Chromosomes are arranged on a metaphase plate (the future cell division plane) as a consequence of tension exerted via the 'pulling forces' generated from the microtubules

(emanating from opposite spindle poles) and the cohesin mediated cohesive forces counteracting and resisting the microtubule mediated pulling. Upon proper chromosomal orientation on the metaphase plate, cohesin is degraded to allow chromosomal segregation. Degradation of cohesin at the onset of anaphase is triggered by the action of a protease, termed Separase (budding yeast Esp1) (Ciosk *et al*, 1998). Separase mediates cohesin degradation by proteolytic cleavage of cohesive subunits Rec8 and Scc1. Separase activity is inhibited until the onset of anaphase due to the inhibitory effect by its binding partner securin (Ciosk *et al.*, 1998; Hornig *et al*, 2002; Luo & Tong, 2017). At the metaphase-to-anaphase transition, APC/C mediated ubiquitination of securin, induces proteosomal degradation of the inhibitor, thus advancing the activation of separase (Lee & Amon, 2001; Marston & Amon, 2004). Unlike in meiosis and in mammalian mitosis, where cohesin is lost in a stepwise manner (Brar *et al*, 2006), in budding yeast mitosis, simultaneous degradation of cohesin occurs along the entire chromosomal length (Uhlmann *et al*, 1999). In anaphase of mitosis (and anaphase II of meiosis), the forces generated by spindles lead to segregation of the sister chromatids.

In order to generate haploid gametes in meiosis, two rounds of error-free segregation of chromosomes occur, that require certain modifications to the mitotic chromosome segregation machinery – i) Homolog pairs linked by chiasmata (along with cohesin complex) ensure the proper alignment of homologs on metaphase-I plane. ii) Cohesin is maintained at centromeres until the onset of Anaphase II to prevent premature sister chromatid dissociation. iii) During Metaphase I, sister chromatids attach to microtubules originating from the same spindle pole leading to an arrangement defined as mono-orientation (or syntelic attachment) (Marston & Amon, 2004).

Following prophaseI, homologs are linked by chiasmata. The chiasma-mediated homolog interactions are stabilised by sister chromatid cohesin on chromosome arms that lie distal to the chiasma location. Cohesive linkages must be maintained for proper chromosomal orientation on the metaphase plate in MI. Release of cohesin on chromosome arms distal to the chiasma facilitates homolog segregation. Similar to mitosis, cleavage of cohesin is mediated by the activity of separase as mentioned above. However, centromeric and pericentromeric cohesin must be protected until the onset of anaphase II to avoid premature disjunction of sister chromatids. This is achieved by stepwise loss of sister cohesin (Marston, 2014; Marston & Amon, 2004; Watanabe, 2012). The ability of centromeric cohesin to resist separase mediated cleavage is achieved by Rec8-containing cohesin (Marston, 2014; Tóth *et al*, 2000). Rec8 is a meiosis-specific subunit of cohesin that replaces the mitotic cohesin subunit Scc1. Cohesin

cleavage is promoted by Rec8 phosphorylation, via the combined activity of casein kinase, Cdc5 and DDK. Phosphorylation of Rec8 in pericentromeric and centromeric cohesin (and thus cleavage of cohesin in this region) is protected by Shugosin (Sgo1) that localises to this region. Sgo1 recruits PP2A-Rts1 complex at centromeric region that prevents Rec8 phosphorylation. Another meiosis-specific protein Spo13, is also known to protect centromeric cohesin in MI.

As opposed to mitosis or MII, sister chromatids are co-segregated in MI. In particular, MI is marked by mono-oriented sister chromatids *i.e* both the sister chromatids are attached by spindle microtubules originating from the same spindle pole (syntelic attachment). Although sister chromatids are pulled towards the same pole, homologs are segregated to opposite poles due to their bi-orientation (attachment of homologs from spindles generated from opposite spindle poles). Studies have shown the importance of kinetochore geometry and spindle tension-dependent chromosomal reorientation machinery to play a role in this process (Marston, 2014; Marston & Amon, 2004; Watanabe, 2012). Mono-orientation of sister chromatids is achieved by fusing the two sister kinetochores together so that they are recognised as a single unit for spindle attachment. In particular, monopolin complex plays a vital role in this so-called "fusion" process (Marston, 2014; Marston & Amon, 2004; Petronczki *et al.*, 2003; Rabitsch *et al*, 2003; Tóth *et al.*, 2000). In the absence of monopolin, sister chromatids are attached in a bi-oriented manner. An error correcting mechanism is in place to avoid erroneous spindle attachments (monotelic, merotelic - single kinetochore attachment or unattached kinetochores). A checkpoint called spindle assembly checkpoint (SAC) is activated in response to erroneous spindle attachments and causes arrest (in metaphase I or metaphase of mitosis) until proper microtubule-kinetochore attachments are achieved (Gardner & Burke, 2000; Shonn *et al*, 2000).

As sister chromatids are fused, tension is generated when bivalents are captured by microtubules from opposite spindle poles. Chiasma and the sister chromatid cohesin generate the required opposing forces to the spindle mediated pulling forces to form tension that helps in orienting the chromosomes on the metaphase plate. The spindle assembly checkpoint is silenced in response to proper kinetochore-microtubule attachments, leading to anaphase onset and degradation of cohesin on the chromosomal arms. Homologs are pulled as a result of spindle forces in opposite direction and MI is completed with segregation of the homologous chromosomes.

In budding yeast, CDK activity is lowered at the MI to MII transition to prevent DNA replication (high CDK activity is essential for the formation of pre-replicative complex) and trigger spindle disassembly (low CDK activity) (Marston & Amon, 2004). The specialised chromosome segregation in MI is followed by a second round of segregation in MII that is similar to the mitotic segregation event in many ways. Sister chromatids are bi-oriented due to the lack of monopolin complex at kinetochores. The centromeric cohesin complex that is protected from degradation in MI, maintains the sister chromatid linkage and generates tension by resisting the spindle pulling forces. At the onset of anaphase II, separase is once again activated (Marston & Amon, 2004). As centromeric cohesin is no longer protected due to shugosin, cleavage of cohesin at this stage triggers segregation of sister chromatids (Marston and Amon 2004). In this way, reduction of ploidy is achieved with a final outcome of four haploid gametes at the end of meiosis II.

1.3 Programmed DSB induction in meiosis

Physically linking the homologs is a prerequisite for faithful homolog segregation during MI. The reciprocal recombination event that culminates in homolog linkage is initiated by the introduction of programmed DSBs during the early G2/ prophase of MI. DSBs are randomly and purposely introduced throughout the genome and later repaired by a homologous recombination mechanism to generate chromosomal structures (such as crossovers that are resolved to give chiasmata) that link the homologs together. The key endonuclease responsible for DSB formation is a meiosis-specific protein referred to as Spo11 (Bergerat *et al*, 1997; Cao *et al*, 1990; Keeney *et al*, 1997). Spo11 is evolutionary conserved across eukaryotes. The function of Spo11 orthologs is well demonstrated in yeast, fungi, Drosophila and mammals (Bowring *et al*, 2006; Steiner *et al*, 2002; Storlazzi *et al*, 2003). Spo11 has been identified as a homolog of archaeal Topo VI A subunit (a type II DNA topoisomerase) (Bergerat *et al.*, 1997; Keeney, 2001, 2008; Keeney *et al.*, 1997). Topoisomerases catalyse DNA topological changes to relax/ supercoil the DNA by covalently linking to DNA via transesterification reaction. Such linkages sever the DNA backbone generating DNA double-stranded breaks. Following the formation of breaks, Spo11 attached to DNA is removed by the action of Mre11 present in the MRX (Mre11, Rad50 and Xrs2) complex and Sae2 (de Massy *et al*, 1995; Garcia *et al*, 2011; Keeney & Kleckner, 1995; Lam & Keeney, 2014; Liu *et al*, 1995; Neale *et al*, 2005; Zakharyevich *et al*, 2010), thus releasing Spo11-attached short oligonucleotide fragments. Further, the blunt DNA ends are resected by the endonucleolytic action of Mre11 and Exo1 to generate 3' single-stranded DNA overhangs (Sun *et al*, 1991; Zakharyevich *et al.*, 2010). RecA

family proteins Rad51 and Dmc1 (in case of meiosis), bind the overhanging DNA tails and form nucleoprotein filaments that catalyse the recombination process (Chen *et al*, 2008; San Filippo *et al*, 2008). Details of the recombination events and involved proteins are described in further sections.

The formation of DSBs is tightly regulated in the context of higher-order chromosomal structures called 'loop-axis' organisation (Figure 1-3) (Kleckner, 1996, 2006; Zickler & Kleckner, 1999). After DNA replication, sister chromatids are paired and organised into a chromosomal axis with DNA loops (~10-20 kb in length; (Lam & Keeney, 2014) emanating out of it. The loop axis organisation is essential to maintain normal levels of DSBs, that are preferentially introduced in the DNA loop region than the chromosomal axes (Blat *et al.*, 2002; Glynn *et al*, 2004; Kleckner, 2006; Kugou *et al*, 2009; Lam & Keeney, 2014; Pan *et al*, 2011; Panizza *et al.*, 2011). Contrastingly, elements necessary for recombination are assembled on the axis. The paradoxical nature of DSB sites in the loops and the recombination events on the axis could be explained by the tethered loop-axis model (TLAC; (Blat *et al.*, 2002; Kleckner, 2006; Lam & Keeney, 2014; Panizza *et al.*, 2011). According to this model, the loops containing DSB sites get tethered to the recombination sites on the axis to promote DSB repair. The so-called tethering is presumably achieved by the interaction of DSB machinery proteins such as Mer2 with the axis proteins (Hop1) and by simultaneous interactions of Spp1 with histone modifications (H3K4me2/ me3) and with Mer2 (Acquaviva *et al*, 2013; Dehé *et al*, 2006; Lam & Keeney, 2014; Murton *et al*, 2010; Rousova *et al*, 2021; Shi *et al*, 2007; Sommermeyer *et al*, 2013). Similar Mer2-Hop1 interactions are also confirmed in *S. pombe* (Rec15-Hop1) (Kariyazono *et al*, 2019) and mammalian orthologs (IHO1-HORMAD1) (Stanzione *et al*, 2016). Thus the tethered loop-axis arrangement influences the location of introduced DSBs.

DNA sequences normally enriched with Spo11 induced breaks are the so-called 'hotspots' (Figure 1-3) (Gerton *et al*, 2000; Khil *et al*, 2012; Mieczkowski *et al*, 2007; Pan *et al.*, 2011). Such hotspots are also observed in other eukaryotes and are well-studied in humans and mice (Fowler *et al*, 2014; Pratto *et al*, 2014; Smagulova *et al*, 2011). They are mainly located outside the coding regions, presumably to preserve genetic integrity (Figure 1-3). Hotspots are often observed at promoter sequences (Cooper *et al*, 2016; Kaplan *et al*, 2009; Pan *et al.*, 2011). Conversely, certain sequences are primarily inhibited from the formation of DSBs. Examples of these so-called 'cold regions ' are repetitive DNA arrays (Petes, 2001; Sasaki *et al*, 2010; Vader *et al*, 2011), pericentromeres, centromeres and telomeres (Blitzblau *et al*, 2007;

Buhler *et al*, 2007; Pan *et al.*, 2011; Rockmill *et al*, 2006; Vincenten *et al*, 2015) where reduced DSB activity is observed. DSBs in these regions are likely to cause a significant threat to genomic stability; thus, to protect the genome, an active inhibition mechanism functions at the cold regions. Although Spo11 can potentially induce DSBs throughout the genome, its activity is specific and non-random, thus preferring certain DNA sequences over others (Figure 1-3) (Cooper *et al.*, 2016).

DSB induction is temporally controlled in a short interval window, ~1-1.5 hours after DNA replication. One way of temporal control is via the expression of genes necessary for DSB induction only during early meiotic prophase after completion of premeiotic DNA replication. Although DSBs are formed during the short early meiotic time window that follows the S-phase replication event, premeiotic replication is not a requirement per se for induction of DSBs (Blitzblau *et al.*, 2012; Hochwagen *et al.*, 2005).

Apart from temporal regulation, DSBs are also spatially regulated (Figure 1-3). The genomic DSB landscape is controlled by a DBS interference principle whereby sequences adjacent to DSBs are suppressed from any further break activity by the action of Mec1/ Tel1 kinases (Cooper *et al.*, 2016; Garcia *et al*, 2015; Zhang *et al*, 2011). This regulation has a cis/ trans element to it. This entails suppression of DSBs in a narrow 70-100 kb region near a DSB site on the same chromatid [Cis regulation, (Garcia *et al.*, 2015)] and suppression at the corresponding site on sister/ homologous chromosome [Trans regulation, (Cooper *et al.*, 2016; Zhang *et al.*, 2011)]. The trans interference, although not well studied, ensures the availability of an intact chromosomal template for homologous recombination repair.

Spo11 is part of a multi-protein DSB complex (termed DSB machinery). The DSB forming machinery consists of 10 accessory proteins. These accessory proteins can be further divided into three subgroups - the so-called 'core proteins' (Spo11, Rec102, Rec104 and Ski8), the MRX complex (Mre11, Rad50 and Xrs2) and the RMM proteins (Rec114, Mei4 and Mer2) (Claeys Bouuaert *et al*, 2021; Lam & Keeney, 2014; Yadav & Claeys Bouuaert, 2021). The association of these complexes and recruitment to DNA hotspots is primarily dictated by the chromosomal architecture as mentioned above. In the next section, RMM proteins and Mer2 in particular, are discussed in detail as they are of importance to the current doctoral work.
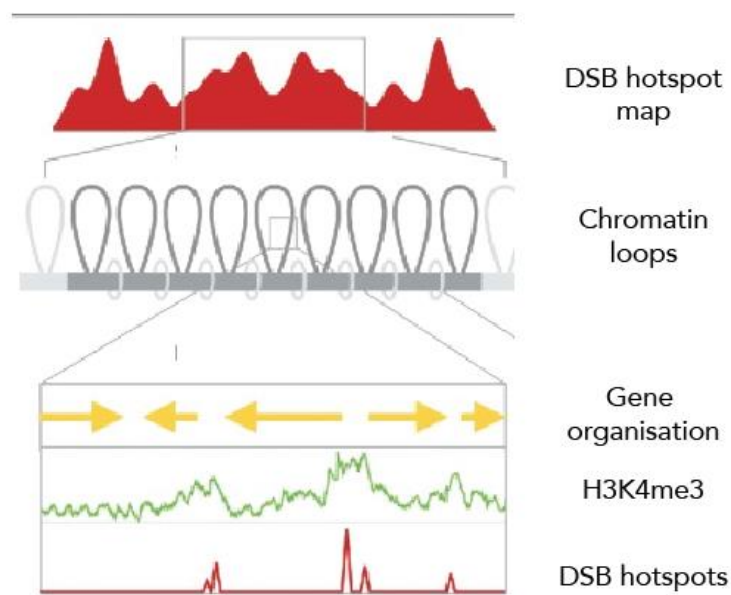
Figure 1-3: Schematic of meiotic DSB hotspot

Model representing DSB hotspot map in *S. cerevisiae*. Budding yeast chromosomes form loop-axis like organisation at the onset of meiosis. The loops (grey) are tethered to the axis where DSBs occur. Chromosome sites where DSBs occur frequently are termed hotspots (Red). The hotspots are mainly restricted to intergenic regions (such as gene promoters; Genes are shown in yellow). The DSB patterning is marked by histone modifications such as H3K4me3 (depicted in green). (Figure modified and adopted from (Cooper *et al.*, 2016))

1.3.1 Mer2: an important protein of the DSB machinery

In general, the introduction of DSBs is temporally regulated by the activity of cell cycle kinases, CDK-S (CDK with Clb5/6) and DDKs (Benjamin *et al.*, 2003; Murakami & Keeney, 2008; Smith *et al*, 2001; Stuart & Wittenberg, 1998). CDKs/ DDKs dictate DSB formation, particularly via phosphorylating their target - Mer2, an RMM complex protein (RMM complex is a part of the Spo11 DSB machinery) (Henderson *et al*, 2006; Sasanuma *et al*, 2008; Wan *et al*, 2008). Consequently, Mer2 plays a crucial role in Spo11-induced DSB formation. *merΔ* cells show significantly reduced spore viability (Rockmill *et al*, 1995; Rousova *et al.*, 2021), possibly via impaired DSB formation and lack of interhomolog crossovers (Rousova *et al.*, 2021). Mer2 orthologs in different species contain evolutionarily conserved protein sequences with functional implications in DSB formation (Kariyazono *et al.*, 2019; Rousova *et al.*, 2021; Stanzione *et al.*, 2016). A splice variant of Mer2 is also expressed

in vegetatively dividing cells and associates with chromatin in foci (Henderson *et al.*, 2006; Li *et al*, 2006); however the function of Mer2 outside the meiotic context is unknown.

During meiosis, Mer1 mediated splicing of Mer2 mRNA results in an increase in the concentration of functional Mer2 protein (Engebrecht *et al*, 1991; Nandabalan & Roeder, 1995; Spingola & Ares, 2000). Mer2 is phosphorylated in cells in an S-Cdk/Clb5/Clb6 dependent manner on residue S30 (Henderson *et al.*, 2006; Wan *et al.*, 2008). This particular post-translational modification is essential for DSB formation and spore viability (Henderson *et al.*, 2006; Panizza *et al.*, 2011; Wan *et al.*, 2008; Yadav & Claeys Bouuaert, 2021). *mer2-S30A* mutants are defective in DSB formation, possibly due to impaired recruitment of other DSB machinery factors to chromosomes (Henderson *et al.*, 2006). Even so, the mutant exhibits no difference in Mer2 chromosomal recruitment. The Mer2 S30 phosphorylation allows subsequent phosphorylation at S29 by DDK (Wan *et al.*, 2008; Yadav & Claeys Bouuaert, 2021). Phosphorylation of residues S30 and S29 in Mer2 assists in the binding of other Spo11 accessory factors such as Rec114, Mei4 and Xrs2 to Mer2 and aids in their recruitment to chromosomes (Henderson *et al.*, 2006; Wan *et al.*, 2008). Essentially, S-phase CDK initiates meiotic recombination by a predominant pathway that is dictated by phosphorylation of Mer2.
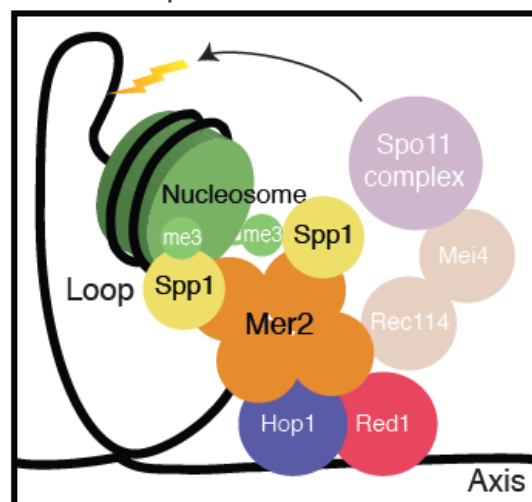
Figure 1-4: Hypothetical model of Spo11 DSB machinery with Mer2

Model representation of Mer2 and its interacting partners. The meiotic DNA loop-axis organisation provides the architecture necessary for introduction of DSBs. The axis consists of long filaments of axial elements Red1 (in red), Hop1 (in blue) and cohesin (not shown). Mer2 (tetramer shown in orange) interacts with Hop1. Furthermore, Mer2 also interacts with DNA loops (presumably containing the nucleosomes) via Spp1 (in yellow) that interacts with

modified nucleosomes. Recently Mer2 was also shown to form independent interaction with unmodified nucleosomes (Rousova *et al.*, 2021). Extruded loops are the sites of DSBs where the Spo11 complex (pink), tethered to the axis, forms DSBs. (Figure adopted from (Rousova *et al.*, 2021))

1.3.1.1 Mer2 and its role in the RMM complex

RMM proteins interact with chromatin during the early meiotic leptonema stage (Yadav & Claeys Bouuaert, 2021), even before the formation of DSBs. The RMM subcomplex consists of Rec114, Mei4 and Mer2. Even though Mer2 is seen to be expressed in mitotic and meiotic conditions, Rec114 and Mei4 are entirely meiosis-specific. Mer2 is a coiled-coil homotetramer that forms an independent subcomplex, while Rec114-Mei4 interacts as a 2:1 heterotrimer to form the other subcomplex of RMM (Claeys Bouuaert *et al.*, 2021). Independent Mer2 foci (without the need for other RMM subcomplex cofactors, or CDK/ DDK mediated phosphorylation) are observed on chromosomes; however, Rec114-Mei4 recruitment highly depends on Mer2 (Claeys Bouuaert *et al.*, 2021; Maleki *et al*, 2007; Panizza *et al.*, 2011). As mentioned above, the phosphorylation of Mer2 is thought to be essential for its interaction with other cofactors of the RMM complex (Yadav & Claeys Bouuaert, 2021). The interaction of the Mer2 proteins with the axial elements (via Mer2-Hop1 interaction; (Rousova *et al.*, 2021) and to the Spo11 core complex (Claeys Bouuaert *et al.*, 2021) could result in tethering the DNA loops to the meiotic axis (Figure 1-4) (The loop axis tethering in the context of Mer2 is explained in detail in the succeeding section) that subsequently helps in DSB formation. Upon achieving normal levels of DSBs, further DNA breaks are suppressed, presumably via a negative feedback loop mechanism, in which the RMM complex protein Rec114 is phosphorylated by Tel1, leading to its suppression and demoting the introduction of Spo11 DSBs (Carballo *et al*, 2008; Yadav & Claeys Bouuaert, 2021; Zhang *et al.*, 2011).

1.3.1.2 Mer2, Spp1 and nucleosome association presumably tethers the DSB machinery to the DNA loops.

In addition to interactions with the RMM complex proteins, Mer2 is also known to interact with Spp1, a PHD domain-containing protein (Acquaviva *et al.*, 2013; Sommermeyer *et al.*, 2013). Spp1 is a cofactor of the histone H3K4 methyltransferase - Set1 complex (or COMPASS). Spp1 is a canonical part of the COMASS but during meiosis, the interaction of Spp1 with Mer2 is important for meiotic recombination (Adam *et al*, 2018). Spp1 interacts with

the Mer2 complex and with Set1 (COMPASS complex) independently (Karanyi *et al*, 2018; Rousova *et al.*, 2021; Sommermeyer *et al.*, 2013). Set1 complex (COMASS) deposits the meiotic specific H3K4me3 mark on nucleosomes (Acquaviva *et al.*, 2013). The H3K4me3 posttranslational modification marks most recombination sites in yeast and mammals (Baudat *et al*, 2010; Myers *et al*, 2005; Smagulova *et al.*, 2011). Spp1 binds to nucleosomes marked by H3K4me3 modifications. Interaction of Spp1 with H3K4me3-nucleosomes and Mer2, is thought to promote the recruitment of nucleosome-containing DNA loops to the axis associated Spo11 DSB machinery (Acquaviva *et al.*, 2013; Rousova *et al.*, 2021; Sommermeyer *et al.*, 2013). Thus, linking the DSB machinery to the nucleosome containing DNA loops, tethers the loops to the chromosomal axis and aids in the formation of DNA breaks in the loop regions (Figure 1-4) (the so-called tethered loop-axis model) (Blat *et al.*, 2002; Kim *et al.*, 2010; Kleckner, 2006; Lam & Keeney, 2014; Panizza *et al.*, 2011). Interaction of Mer2 with DNA loops occurs via three well studied interactions – direct binding of Mer2 with DNA (Claeys Bouuaert *et al.*, 2021), independent interaction with nucleosomes (located in the loop region) (Rousova *et al.*, 2021) or interaction with nucleosomal modifications (H3K4me3) via Spp1 (Acquaviva *et al.*, 2013; Sommermeyer *et al.*, 2013). The Mer-Spp1 interaction is robust, with Mer2 having a high affinity for Spp1 (K_D of 25 nM) (Rousova *et al.*, 2021). It does not need any additional accessory factors for the interaction, as evidenced by *in vitro* and *in vivo* experiments (Acquaviva *et al.*, 2013; Rousova *et al.*, 2021; Sommermeyer *et al.*, 2013). The complex has a 2:4 (Mer2:Spp1) stoichiometry *in vitro* (Rousova *et al.*, 2021). Consequently, the binding of Spp1 to Mer2 triggers Spp1 dimerization (Rousova *et al.*, 2021)The central evolutionarily conserved Mer2 core (residues 140-256) interacts with the C-terminal of Spp1 (Adam *et al.*, 2018; Rousova *et al.*, 2021). A single amino acid substitution, Mer2 V195D disrupts its interaction with Spp1 (Adam *et al.*, 2018).

Recently it was also shown that Mer2 binds to unmodified mononucleosomes and the interaction is independent of the known Spp1-Mer2 complex interaction with H3K4me3 (Claeys Bouuaert *et al.*, 2021; Rousova *et al.*, 2021). This binding of Mer2 with nucleosomes was observed to generate a 4:1 Mer2-mononucleosome complex *in vitro* (Rousova *et al.*, 2021) Mer2 interaction with Spp1 and nucleosomes provides a speculative model of how Mer2 associates the axis tethered DSB machinery to nucleosome containing DNA loops (Rousova *et al.*, 2021) (Figure 1-4).

1.3.1.3 Mer2-Hop1 interaction is required for binding of Spo11 complex with the meiotic chromosomal axis

In addition to its interaction with Spp1 and nucleosomes, Mer2 also interacts with HORMA domain protein - Hop1 (Panizza *et al.*, 2011; Rousova *et al.*, 2021). Mer2-Hop1 interaction aids in recruiting Mer2 to chromosomal axis (Panizza *et al.*, 2011; Stanzione *et al.*, 2016). Mer2 chromosomal binding sites overlap with the Hop1 and Red1 chromosomal sites (Panizza *et al.*, 2011). Deletion of *RED1* or *HOP1* severely reduced Mer2 chromosomal binding as evidenced by ChIP experiments (Panizza *et al.*, 2011). Mer2 also regulates the recruitment of Spo11 machinery to chromosomes by associating with the meiotic axial element protein Hop1. The interaction of Mer2 orthologs with Hop1 orthologs is also studied in fission yeast and mammals (Kariyazono *et al.*, 2019; Stanzione *et al.*, 2016). Recently, the interaction of budding yeast Mer2 with Hop1 was also shown by *in vitro* protein purification and co-immunoprecipitation assays (Rousova *et al.*, 2021). Experiments suggest that Mer2-Hop1 binding is driven by Hop1 HORMA domain-mediated interaction (Rousova *et al.*, 2021). Deleting the Hop1 HORMA domain disrupts the Hop1-Mer2 interaction in vitro. Even though Mer2 chromosomal levels were seen to drop upon *red1Δ* severely, no Red1-Mer2 interaction was seen *in vitro*, suggesting that Red1 has an indirect influence on Mer2 recruitment (possibly via Hop1) (Panizza *et al.*, 2011; Rousova *et al.*, 2021). Mer2 presumably binds to the pool of Hop1 that is bound to Red1 as evidenced by *in vitro* biochemical studies (Rousova *et al.*, 2021). In this way, Mer2 plays a crucial role as a connecting element between the chromosomal axis, DSB machinery and the DNA loops (Figure 1-4).

1.3.2 Repair of DSBs and crossover formation in meiosis

Meiotic DSBs, produced by Spo11 are repaired in sequential steps. Understanding the meiotic DSB repair process helps us gain insights into how interhomolog crossovers are formed. After induction of breaks, Spo11 remains covalently attached to the 5' ends of the DNA strands (Bergerat *et al.*, 1997; Keeney *et al.*, 1997). Eventually, as a result of the endonucleolytic activity of Sae2 and MRX complex (de Massy *et al.*, 1995; Garcia *et al.*, 2011; Keeney & Kleckner, 1995; Liu *et al.*, 1995; Neale *et al.*, 2005; Zakharyevich *et al.*, 2010), Spo11-attached DNA oligos are released from the DNA ends. Further, Exo1 exonuclease activity leads to DNA end resection to generate 3' single-stranded DNA filaments (Figure 5) (de Massy *et al.*, 1995; Garcia *et al.*, 2011; Keeney & Kleckner, 1995; Liu *et al.*, 1995; Neale *et al.*, 2005; Zakharyevich *et al.*, 2010). The long DNA 3' tails coated with RPA proteins bind

ssDNA in a helical fashion (Chen *et al.*, 2008; Symington, 2016). RPA is later replaced by eukaryotic homologs of RecA-like recombinases and strand exchange proteins - Rad51 and Dmc1, that act in conjugation (Bishop *et al*, 1992; Cloud *et al*, 2012; Hong *et al*, 2001). Rad51 is constitutively expressed in eukaryotes while Dmc1 is meiosis-specific, with an essential role in interhomolog bias (Bishop *et al.*, 1992; Cloud *et al.*, 2012; Lao & Hunter, 2010; Oh *et al*, 2007). *dmc1Δ* cells accumulate extremely high levels of DSBs in meiosis and cause cell cycle arrest (Bishop *et al.*, 1992; Schwacha & Kleckner, 1995). The Rad51-Dmc1 bound nucleoprotein filament invades the homologous chromosome to form D-loop like structures (Figure 1-5) (Adzuma, 1992; Brown & Bishop, 2014; Hong *et al.*, 2001; Hunter & Kleckner, 2001; Lao & Hunter, 2010). The strand invasion step marks the designation of DSBs to the homologous recombination repair pathway. The D-loops captured by the template DNA and further DNA synthesis leads to a stable repair intermediate structure termed 'single end invasion' (SEI) with the 3' ss-DNA strand attached to the template DNA (Figure 1-5) (Hunter & Kleckner, 2001; Lao & Hunter, 2010). At this stage, if the invading 3' ss-DNA strand dissociates from the homolog and is captured by the 3' end of the DSB, then such a repair mechanism is termed synthesis-dependent strand annealing (SDSA) (Nassif *et al*, 1994; Pâques & Haber, 1999) (Figure 1-6). If the 3' ss-DNA of the SEI undergoes further DNA synthesis and capture by the second end of the DSB, a stable joint molecule forms called the double-Holliday junction (dHJ) repair intermediate (Bzymek *et al*, 2010; Holliday, 2007; Szostak *et al.*, 1983). dHJs can be repaired by two distinct pathways – resolution or dissolution. Resolution results in repair outcomes termed crossovers (COs; mainly favored) or non-crossovers (NCOs) (Allers & Lichten, 2001; Börner *et al*, 2004) (Figure 1-5). The outcome of the dHJ dissolution, SDSA mechanism and some fraction of dHJ resolution are the NCO products (Allers & Lichten, 2001; Cromie *et al*, 2007; Lam & Keeney, 2014; McMahill *et al*, 2007). The NCOs have a close to null (or minimal) DNA exchange between the donor template and the receiving DNA (containing the DSB site) (Figure 1-5). During meiosis, interhomolog COs occur with reciprocal exchange of chromosomal DNA between the homologs.

Two major pathways achieve crossover designation. The Class I crossovers obtained via the ZMM pathway (a primary pathway for majority of meiotic COs) or the Class II crossovers orchestrated by Mus81-Mms4 (accounts for 15-35% of COs) (de los Santos & Hollingsworth, 1999; de los Santos *et al*, 2003; Gray & Cohen, 2016). The ZMM family proteins are called the pro-crossover factors due to their active role in stabilizing and resolving the dHJs. The members of the ZMM family consist of proteins regulating DNA metabolism, Mer3 helicase, MutS homologs – Msh4/Msh5, Zip2, Zip3 family members, SC member Zip1 etc (Börner *et al.*, 2004;

de los Santos *et al.*, 2003; Hollingsworth *et al*, 1995; Jessop & Lichten, 2008; Oh *et al.*, 2007; Tang *et al*, 2015). The class I crossovers is characterized by the accumulation of MutSγ (the Msh4/Msh5 heterodimer) followed by MutLγ (Mlh1 and Mlh3) homolog accumulation (Gray & Cohen, 2016; Hollingsworth *et al.*, 1995; Li & Heyer, 2008). MutSγ plays an active role in stabilizing the DSB repair intermediates, particularly the dHJ structures, preventing their dissolution (Novak *et al*, 2001). MutLγ is a resolvase capable of cutting the dHJs that ultimately leads to crossover-like structures (Hunter & Borts, 1997; Wang *et al*, 1999). MutLγ, together with Exo1 and Sgs1, functions in resolving class I crossovers (Gray & Cohen, 2016; Zakharyevich *et al.*, 2010).
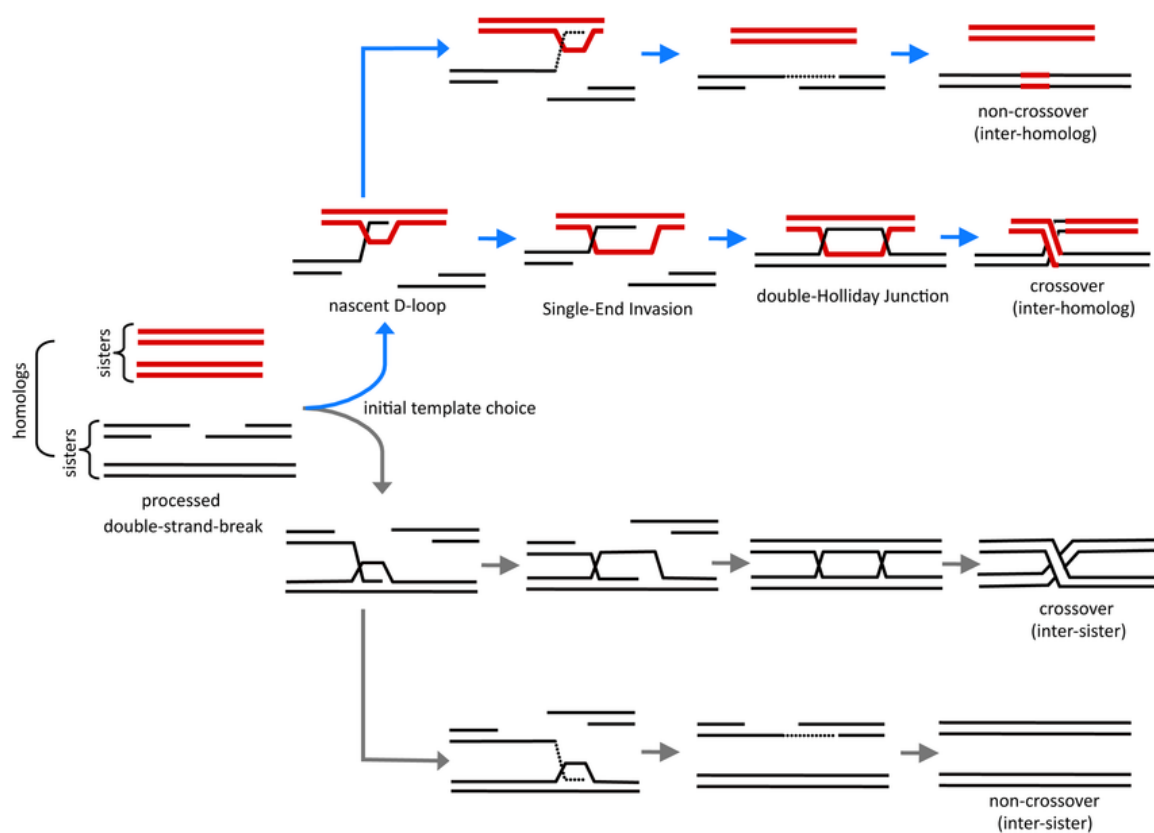
Figure 1-5: Outcomes of homologous recombination in meiosis and mitosis
DSBs occurring during mitosis due to exposure to harsh chemicals or replication fork collapse and those deliberately introduced during meiosis by the activity of Spo11 are repaired using homologous recombination mechanism. During meiosis the DSBs are resected by Sae2, MRX complex and Exo1. The resected 3' ssDNA filaments undergo a search for homologous sequences to be used as a repair template. During meiosis, DSBs are primarily repaired using the homologous chromosome (homologs shown in red and black). The resected strands invade the homolog to form D-loop structures. Following synthesis of DNA at the invading end, a repair intermediate termed single end invasion is formed. When the invading strand dissociates

and re-ligates to the opposite end of the DSB, the outcome of the repair is a non-crossover. In the case where the single end invasion intermediate further undergoes DNA synthesis and the invading strand is captured by the other end of the DSB, a structure called double Holliday junction is formed. The double Holliday junctions are primarily repaired as crossovers. When this occurs with the homologous chromosome as a repair template, it is called as interhomolog crossovers. During mitosis, the sister chromatid is the preferred choice of template due to its physical proximity to the DSB site. The outcome of homologous recombination in mitosis is intersister crossovers or non-crossovers. (Figure adopted from (Lao & Hunter, 2010)).

The class II crossovers are mediated by Mus81-Mms4, which function along with Sgs1 to resolve the repair intermediates or joint molecules (de los Santos *et al.*, 2003). Class I and Class II pathways have significant crosstalk to compensate for functional impairment in either of the two pathways, ultimately maintaining the overall crossover frequency (Gray & Cohen, 2016).

Crossover formation between the two homologs is essential for the proper segregation of homologous chromosomes. In order to ensure that at least one crossover/ chiasma is present per chromosome, more DSBs are introduced in the genome during meiosis than the total number of chromosomes present *i.e* ~160 DSBs per cell (Pan *et al.*, 2011). The crossover frequency, distribution and timing are regulated by two principles – i) Crossover interference: formation of a second crossover at sites nearby an already existing crossover is prevented to avoid deleterious chromosomal structural effects (Muller, 1916; Shinohara & Shinohara, 2004; Sturtevant, 1915). ii) Crossover homeostasis: crossover frequency maintenance even when DSB induction is altered (Martini *et al*, 2006). Although the later phenomenon aids in understanding how crossovers are maintained, further experiments are needed to provide clarification and evidence of this concept. In this way, crossover regulation, particularly between the homologs (interhomolog crossovers), ensures proper physical linkage between the homologous chromosomes in MI.

1.3.3 Cell cycle and ploidy dependence on the mechanism of DSB repair

DSB repair is possible via several different pathways in cells. The repair products vary depending on the mechanism of repair. The two primary mechanisms in yeast are – i) *Non-homologous end joining* (NHEJ), an error-prone repair mechanism and ii) *Homologous recombination* (HR) which is error-free (Aylon & Kupiec, 2005; Dudásová *et al*, 2004; Li &

Heyer, 2008) (Figure 1-6). Studies suggest that HR repair is prevalent in *S. cerevisiae* compared to the preferential utilization of the NHEJ repair mechanism in mammals, for example (Aylon & Kupiec, 2005; Dudásová *et al.*, 2004). DSB repair is regulated by several factors activated according to the cell cycle stage and ploidy.

DNA breaks can be formed in the genome due to several endogenous and exogenous factors (Friedberg *et al*, 2006). For example, during S-phase DSBs are formed as a result of stalled replication forks. The replication fork collapse leads to topological tension in DNA strands leading to DNA breaks (Li & Heyer, 2008; Schwartz & Heyer, 2011). In addition to these spontaneous S-phase induced DSBs, exposure of cells to radiomimetic chemicals (*e.g.* Bleomycin family drugs, γ-radiation) are deleterious to the DNA, causing genomic fragmentation. Therefore, various surveillance mechanisms are in order, to ensure that DSBs are repaired before cell division. These mechanisms function in two ways - i) *Cell cycle checkpoints* - activation of cell cycle checkpoints causes arrest in cell cycle progression giving time for DNA repair. More prominently, they prevent the propagation of damaged genomes by halting the cell cycle. ii) *DSB repair* - DNA repair mechanisms that enable DNA damage repair.

In haploid yeast, spontaneous DSB induction in G1 results in the repair of DSBs by Non-homologous end joining, NHEJ (Finn *et al.*, 2012; Li & Heyer, 2008; Schwartz & Heyer, 2011) (Figure 1-6). NHEJ is the default mechanism used in this cell cycle stage as there is no sister chromatid or a homologous chromosome template. During S-phase and G2/ mitotic phase, the availability of the sister chromatid after replication of the DNA leads to a preference for homologous recombination repair. HR is the error-free mechanism of repair and is thus favoured when homologous sequences (*i.e* sister chromatid or the homologous chromosome) are available.

The resection of the DSB ends is the most crucial step in designating the DSBs for HR (resected strands) or NHEJ repair pathway (minimal resection) (Figure 1-6) . Even though NHEJ and HR can be favoured at any given time, a cell cycle-dependent regulation of DSB end resection controls the choice of DSB repair pathway. A low resection rate is observed in G1, influenced by reduced CDK activity and binding of a particular Ku complex to DNA ends, (Aylon & Kupiec, 2005; Clerici *et al*, 2008; Ira *et al*, 2004) in turn leading to NHEJ mediated repair. NHEJ is based on the repair of broken DNA ends by extension and ligation (Schwartz & Heyer, 2011; Symington, 2016). As no search for homology is needed in this case, the repair

ends undergo little to no resection. NHEJ is initiated with blunt DNA ends, while HR occurs after processing DNA ends and DNA end resection. During S- and G2/ prophase, cell cycle-specific kinases (CDK) activity predominantly initiates DSB end resection and thus homologous recombination (HR) is favoured (Aylon & Kupiec, 2005; Finn *et al.*, 2012; Huertas *et al*, 2008; Ira *et al.*, 2004).

As explained earlier, the HR repair outcome is either non-crossover (NCO) or crossover (CO) products. The NCOs and COs are the final products of several repair pathways (Figure 1-5). They are formed depending on how the repair intermediates are processed. For example, in single strand annealing (SSA) repair pathway (Figure 1-6), the homologous sequences on the opposite resected strands anneal and extend to join the DNA gap resulting in non-crossovers (Bhargava *et al*, 2016; Schwartz & Heyer, 2011); Synthesis dependent strand annealing (SDSA) leads to displacement of the D-loop and reannealing to the opposite DSB end, again resulting in non-crossovers (Nassif *et al.*, 1994; Pâques & Haber, 1999) (Figure 1-6). Continuous extension of the D-loop by DNA synthesis till the end of the chromosome is called break-induced repair (BIR) (Figure 1-6). This forms single Holliday junctions (sHJ) that are resolved to give non-crossovers. (Schwartz & Heyer, 2011). A fraction of the DSBs undergoing HR lead to either dissolution of dHJs with non-crossover products or the resolution of dHJs via particular cell cycle-specific resolvases to form crossover products (Figure 1-5, 1-6). Depending on the template used, they are either IS (sister chromatid) crossovers or IH (homologous chromosome) crossovers.

Differences in DSB repair in haploid versus diploid cells are very well studied. However, certain speculations about the repair mechanisms, particularly in the G1 phase of haploids and diploids remain controversial. Despite the requirement for S-phase dependent CDK activity in HR repair, several evidences suggests that the presence of the homologous chromosome in the G1 phase of diploid cells leads to HR recombination (Lee & Petes, 2010; Smith *et al*, 2019). A recent study done in mammalian cells also confirmed the activation of HR in G1 phase ((Yilmaz *et al*, 2021). HR being error-free repair mechanism, it seems logical that the cells favour HR whenever a repair template is available. Experiments performed by Smith and colleagues (Smith *et al.*, 2019) pointed towards an increased genomic mobility of DNA sequences near DSBs in diploid G1 arrested cells. An increase in mobility is suggestive of a search for the homologous sequences by the resected strands. Rad51 foci were also observed in these experiments (performed in G1 arrested diploid cells) that are a hallmark of HR repair, along with the detection of mitotic reciprocal crossovers in G1 arrested diploid cells (Lee & Petes,

2010). These results indicate that ploidy, along with the cell cycle stage, may also play a role in deciding the fate of a DSB. Although the exact molecular mechanisms behind the differential repair of G1-phase haploids and diploids are unknown, it is speculated that it could be a result of heterozygosity of the mating-type locus or the mere presence of homologous sequences on the homologous chromosomes (Smith *et al.*, 2019).
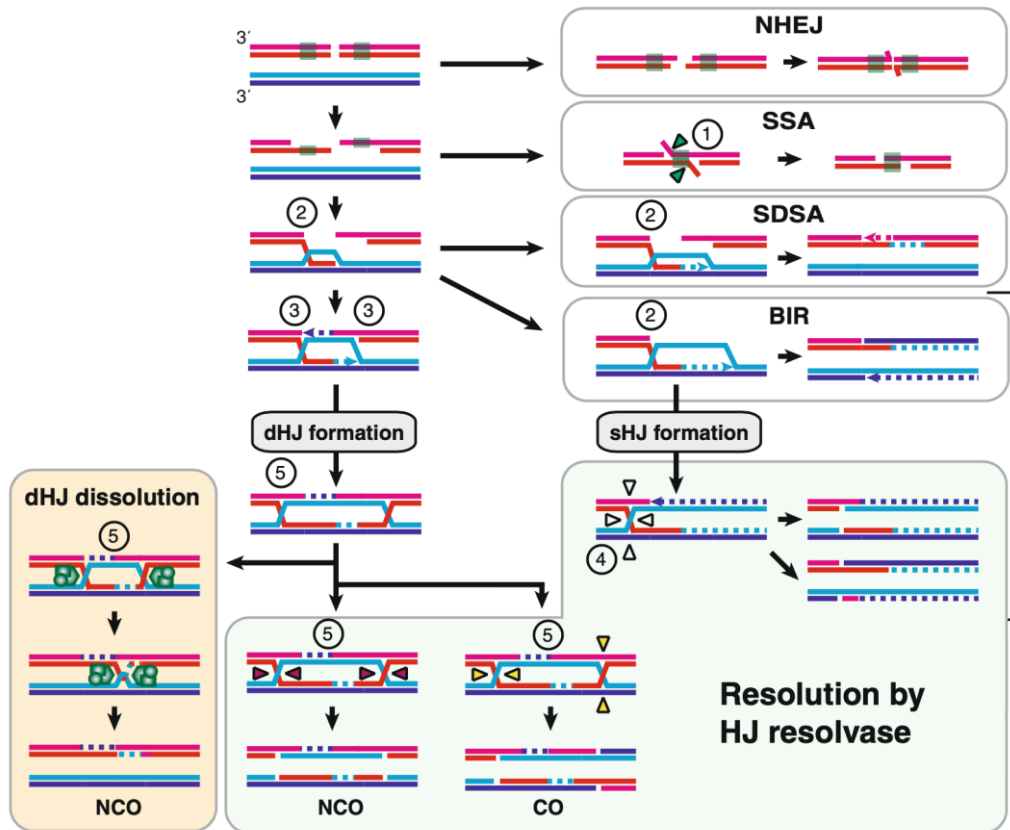
Figure 1-6: DSB repair pathways

Various DSB repair pathways operate to repair DSBs. The mechanism of DSB repair is primarily dictated by cell cycle stages and ploidy effects. One homolog is depicted with red and pink sister chromatids while the other homolog is with blue and dark blue sister chromatids. During G1 phase the NHEJ mechanism is prevalent. In NHEJ the broken ends are religated using minimal sequence homology. Alternatively, DSB ends are resected to generate ssDNA filaments that undergo different modes of repair. Presence of direct DNA sequence repeats (shown in green boxes) in the ssDNA filaments can lead to single strand annealing (SSA). Dissociation of the invading strand and relegation to the other end of the DSB causes repair by SDSA mechanism. Formation of an intact replication fork and continuous extension of the D-loop till the end of the chromosome is defined as the break-induced replication (BIR). When the invading strand undergoes synthesis and further capture by the opposite DSB end, it forms

double Holliday junctions (dHJs). The dHJs undergo dissolution by the action of certain complexes (green trimers) or resolution with the help of different resolvases (shown in white, yellow and red arrows). The dissolution of dHJs give rise to non-crossover products while depending on the action of resolvases the dHJ resolution leads to non-crossovers or crossover products. (Figure adopted from (Schwartz & Heyer, 2011).

1.4 Predictive models for interhomolog bias

Faithful homolog segregation during Meiosis I is ensured by physically linking the two homologs together. This process is achieved by repairing Spo11-induced DNA breaks by homologous recombination but via preferential usage of the homologous chromosome as a repair template, thus generating interhomolog crossovers that physically link the homologs. Studies monitoring the repair intermediates and the final crossover ratios between inter-sister (IS) and interhomolog (IH) repair suggest a change in IH:IS ratio from 1:4 in mitosis (Bzymek *et al.*, 2010; Humphryes & Hochwagen, 2014) to 5:1 in meiosis (Kim *et al.*, 2010). Possible explanations for the preference for the homologous chromosome during meiosis are included in several prevailing models in the field that attempt to capture the essence behind this process.

DNA breaks that occur in mitotically-dividing cells after replication of chromosomes are repaired by a homologous recombination mechanism but by mainly using the sister chromatid as a repair template (Bzymek *et al.*, 2010). The default use of the sister chromatid template could be explained due to its physically proximal and an attempt to ensure genetic integrity. During meiosis, several factors lead to the limited use of sister chromatids for DSB repair. This phenomenon is encoded in the activity of a meiosis-specific serine/ threonine kinase 'Mek1' (*ME*iotic *K*inase), that phosphorylates strand exchange proteins and promotes the inhibition of the sister chromatid mediated repair (Callender *et al*, 2016; Niu *et al*, 2009). This so-called barrier-to-sister chromatied recombination (BSCR) was discussed in a model by Goldfarb and Lichten in 2010 (Goldfarb & Lichten, 2010). Their model suggests that Mek1 kinase forms a "kinetic constraint" by "slowing down" the rates of DSB repair at the sister chromatid. This allows for the search of repair templates on homologous chromosomes. As searching for the homologous chromosome is time-consuming, slowing down the default sister repair mechanism would provide time and promote homolog-based HR repair. Unlike in *S. cerevisiae,* many other organisms have developed mechanisms to move homologous chromosomes in physical proximity to each other. For example, in fission yeast, microtubule or actin-dependent chromosomal movement help in the alignment of the homologs

(Hochwagen, 2008). Although such mechanisms are not entirely absent in *S. cerevisiae* (Marston, 2014; Tsubouchi & Roeder, 2005), the repair by homolog is spatially unfavourable compared to the intersister repair (as sister chromatids are held together by cohesion and spatially more proximal to sites of DSBs). This further emphasizes the need for the kinetic constraint model. The idea was based on several experimental observations that demonstrated similar rates of formation of intersister and interhomolog repair intermediates in meiosis (Goldfarb & Lichten, 2010), despite which sister-chromatid mediated repair is less favourable in meiosis. Mek1 activity plays a significant role in creating a barrier for inter-sister repair. To put a constraint only on the sister chromatid, Mek1 must be locally activated at sites of DSBs and avoid its 'inhibitory activity' on the homologous chromosomes.

Yet another model proposes that Mek1 does not indirectly cause the repair bias by sister chromatid inhibition but actively favours the homologous chromosome (Schwacha & Kleckner, 1997; Xu & Kleckner, 1995). Sister chromatids are tightly bound by Rec8 mediated cohesive forces, thus establishing sister chromatid repair as a default repair mechanism even in meiosis. To encounter these forces, an active preference for homolog is established by Mek1 and accessory meiosis-specific proteins. In principle, one can imagine that DSBs are likely to occur on any of the chromosomal templates and how Mek1 can distinguish homologous sequences from the sister chromatid or the homologous chromosome is not truly understood.

In line with the kinetic constraint model, Subramanian and colleagues put forth a spatial proximity model in 2016 (Subramanian *et al*, 2016). According to this model, Mek1 is locally recruited and activated at sites of DSBs and forms a localized zone of repair suppression (Figure 1-7). As the sister chromatid is physically proximal to the site of DSBs (along with activated Mek1), it lies in the zone of repair suppression. The zone entails a region of localized Mek1 activity where Mek1 mediates phosphorylation of its downstream targets in its vicinity. As homologous chromosomes are farther away, they escape the Mek1 mediated 'inhibitory' effect and are therefore favoured for repairing the breaks. In this Ph.D. work, I attempt to this physical proximity model and understand the mechanism behind the interhomolog preference in meiosis.
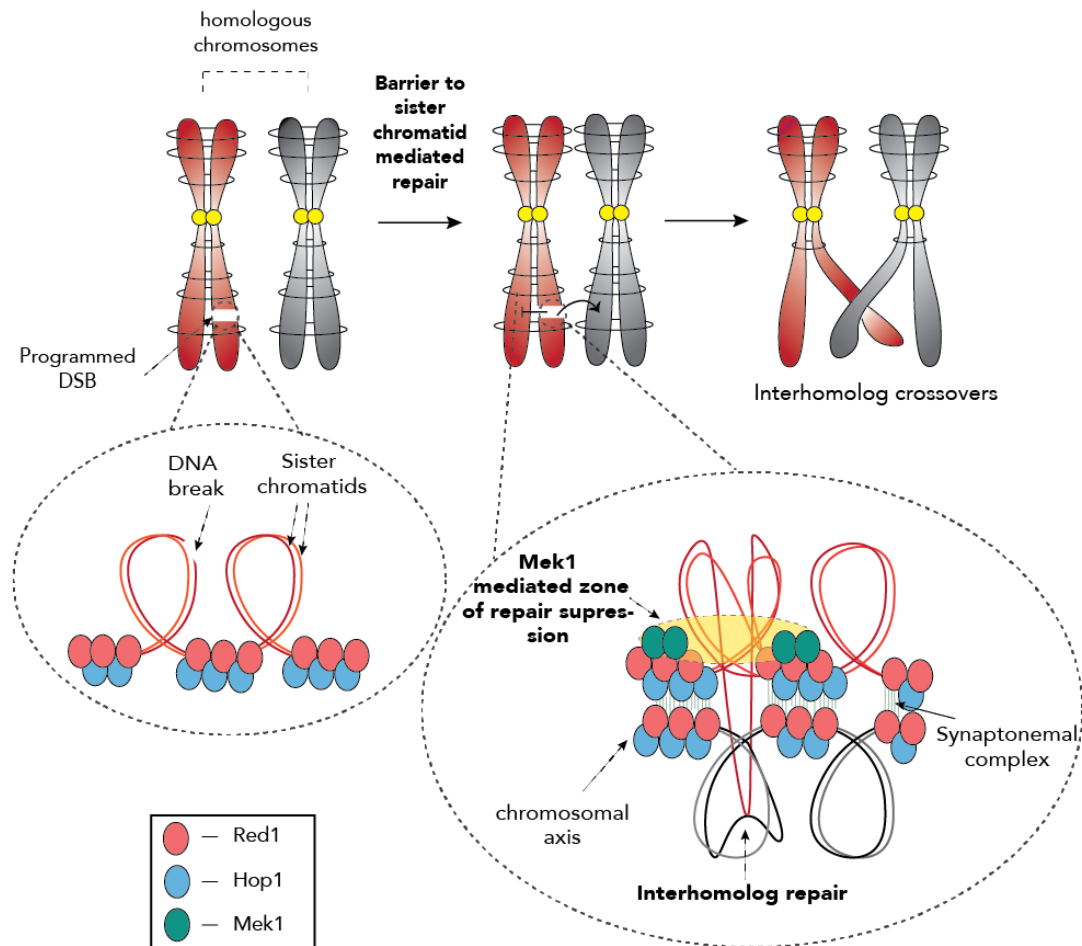
Figure 1-7: A hypothetical spatial proximity model explaining the interhomolog bias in meiosis

Schematic representation of the spatial proximity model proposed in *Subramanian et al. 2016*. Homologous chromosomes are depicted in red and grey. Programmed introduction of DSBs occurring by virtue of the DNA loop-axis architecture. The DSBs face a Mek1 kinase (green) mediated barrier to sister chromatid repair. Mek1 is recruited to chromosomal axis presumably near sites of DSBs. The recruitment and activation of Mek1 is dependent on its interaction with Hop1 (blue) and Red1-Hop1 complex (Red1 is in Red). Hop1 drives dimerization of Mek1 which then leads to its activation. Mek1 forms a so-called 'zone of repair suppression' (yellow bubble) in its vicinity. As the sister chromatids are physically proximal to the sites of DSBs, they lie in this zone and are inhibited from using as a template for repair. The distally located homologous chromosomes escape this Mek1 mediated repair suppression and are thus favoured as a repair template. (Concept adopted from (Subramanian *et al.*, 2016).

As mentioned above, the meiosis-specific Mek1 kinase plays a central role in IH recombination (Figure 1-7). However, not only Mek1 but three additional meiosis specific elements are essential for the formation of homolog bias-

1) *The upstream DNA break sensory kinases*: Mec1/ Tel1 are kinases that detect DNA breaks in meiosis and mitosis. The kinase regulation brings upon DNA damage checkpoint activation in mitosis (mainly via phosphorylation of Rad53 and other proteins) and recombination checkpoint activation in meiosis (via phosphorylation of Hop1).

2) *Axis elements*: The meiotic chromosomal axis consists of - a coiled-coil protein Red1, the HORMA domain-containing protein Hop1 and the meiosis-specific cohesion factor Rec8, plays an essential role in recruiting Mek1 to sites of DSBs. Further, The axis-loop structure is physically involved in meiotic DSB formation and DSB repair.

3) *The DNA strand exchange factors*: The interplay between the strand exchange proteins such as - Rad54, Rad51 and Dmc1 is crucial to understand the dynamics of interhomolog crossovers. Mek1 is involved in mediating IH bias by modulating these strand exchange factors.

Involvement of these elements is discussed in detail in the next sections.

1.5 Comparing DSB signalling by Mec1/ Tel1 kinases in mitosis and meiosis

DNA damage is deleterious to the cells. As a result, cells have developed active surveillance mechanisms to detect and promote the repair of the damage to their genome. Dedicated protein kinases can 'sense' DNA breaks and activate signaling cascades that lead to cell cycle arrest and promote the repair of detected lesions. PIKKs (Phosphatidylinositol 3-kinase-related protein kinases) are a family of such kinases that respond to DNA stress in eukaryotic cells (Lempiäinen & Halazonetis, 2009). Among the most recognized members of this family are the Mec1 and Tel1 kinases in budding yeast (Homologs of mammalian ATR and ATM, respectively). Both the kinases are active during mitotic as well as meiotic division programs and aid in checkpoint activation, DSB repair and replication defects.

Mec1 maintains a low basal activity throughout the cell cycle. As a result of DSBs, the kinase activity is amplified, consequently aiding in DSB signalling and DSB repair. Being an essential gene, deletion of *MEC1* is lethal to the cells. The lethality is rescued by deleting the ribonucleotide reductase inhibitor *sml1* (Chabes *et al*, 1999; Zhao *et al*, 1998). The *mec1Δ sml1Δ* condition in used in several experiments to monitor the effects of *mec1*. In terms of activation cues, Mec1 senses resected DNA ends and primarily gets recruited to RPA coated ssDNA filaments (Zou & Elledge, 2003). Such DNA structures occur during nucleotide excision repair, DSB repair, replication fork blocks and DNA replication, all of which promotes Mec1 activation (Tannous & Burgers, 2021). Mec1 is activated throughout the cell cycle in response to DNA stress. For example, Mec1 is constitutively expressed during S-phase at unperturbed DNA replication forks, maintaining the replication activity (Forey *et al.*, 2020; Tannous & Burgers, 2021). Replication fork blocks and the associated DSBs also mediate Mec1 activity that aids in intra-S phase checkpoint activation (Finn *et al.*, 2012; Paulovich & Hartwell, 1995). During G1, for example, RPA coated ss-DNA resulting from nucleotide excision repair of DSBs, initiates Mec1, while in G2, it is activated in response to DSBs and mediates the DNA damage checkpoint activation and DSB repair (Finn *et al.*, 2012; Paulovich & Hartwell, 1995). Depending on the cell cycle stage and the DNA stress, different activator proteins aid in invoking the function of Mec1 and similarly, the kinase activity is propagated by phosphorylation of several distinct downstream target proteins.

Tel1 is another PIKK family protein that gets activated in response to DNA double-stranded breaks and is involved in telomere length regulation (Greenwell *et al*, 1995). Tel1 detects blunt DNA ends (Fukunaga *et al*, 2011; Mantiero *et al.*, 2007) and its function is invoked in response to severe DSB stress. Furthermore, Tel1 promotes efficient DSB resection and aids in Mec1 mediated checkpoint activation (Mantiero *et al.*, 2007). It is also known to stabilize replication forks at DSB sites, regulate telomere length, and aid in DSB repair at telomeric sites (Baldo *et al*, 2008; Doksani *et al*, 2009). Tel1 is functionally redundant to Mec1 (Mantiero et al. 2007, (Mantiero *et al.*, 2007; Vialard *et al*, 1998)) and in most cases, *tel1Δ* does not lead to severe DSB repair defects. Tel1 is activated at sites of DSBs via MRX complex (Usui *et al*, 2001) and together, they mediate the Tel1-Mre11 checkpoint pathway that acts in parallel to the Mec1 mediated checkpoint pathway in mitosis.

Mec1/ Tel1 are serine/ threonine kinases that recognize the [S/T]Q motifs in their substrates and phosphorylate these sites (Traven & Heierhorst, 2005). Depending on the type of DNA aberration, the kinases phosphorylate a range of effector proteins such as Mrc1 and

Rad53 in response to stalled replication forks (Melo & Toczyski, 2002), Rad9-Rad53 upon DNA damage in S/G2/ mitotic cell cycle stages (Finn *et al.*, 2012) and Hop1 in response to Spo11-induced damage in meiosis (Carballo *et al.*, 2008). Independent of damage, Mec1 is constitutively active in S-phase (Forey *et al.*, 2020). Mec1 is also known to phosphorylate S129 residue on Histone H2A, a modification that is commonly seen as a marker for the presence of DSBs. From the point of activating the DNA damage response, the Mec1/ Tel1 signalling pathways diverge, leading to the activation of distinct DNA damage checkpoint proteins. In mitosis, this leads to activation of DNA damage checkpoint and in the case of meiosis, the recombination checkpoint is activated. These checkpoints are briefly described below.

1.5.1 DNA damage checkpoint:

DSBs must be repaired to maintain genetic integrity and surveillance mechanisms are activated in response to DNA damage that induces transient cell cycle arrest and allows time for repair of damage sites. In mitotically dividing cells, DSBs lead to the activation of DNA damage checkpoint that can be commonly represented as following steps (Putnam *et al.*, 2009)-

DSB => damage signal => sensor kinases => signal transduction => effector proteins => DSB repair

In *S. cerevisiae*, the DNA damage checkpoint can be activated in various cell cycle stages to ensure that the progression of the cell cycle is blocked while DSBs are repaired. It leads to G1/S transition arrest, blocking the G2/M transition and an intra-S checkpoint in response to DNA damage in S-phase. Principle sensory complexes detect DSBs and further mediate early steps in checkpoint activation via activation of Mec1/ Tel1 kinases. For example, Tel1 is activated by the action of DNA end binding complex - MRX and Mec1 is activated via Ddc2 – an ssDNA recognizing protein (Nakada *et al*, 2003; Usui *et al.*, 2001). Mec1/ Tel1 generates a checkpoint response by phosphorylating [SQ/TQ] sites of downstream effectors. One of the many target effector proteins of Mec1/ Tel1 is the kinase Rad53 which plays a crucial role in checkpoint arrest (Enserink *et al*, 2006; Grenon *et al.*, 2006; Sanchez *et al*, 1996; Sun *et al*, 1996). Mec1/ Tel1 mediates activation of Rad53 by phosphorylating Rad9, an activator of Rad53 (Grenon *et al.*, 2006; Sun *et al*, 1998; Vialard *et al.*, 1998). The phosphorylated Rad9 then interacts with the forkhead-associated domain (FHA) of Rad53 and brings upon its dimerization and activation (Finn *et al.*, 2012; Schwartz *et al*, 2002; Sun *et al.*, 1998). The dimerized Rad53 trans-autophosphorylates itself and brings upon cell cycle arrest by phosphorylating several downstream target proteins. One such example of Rad53 target protein

is Pds1, an anaphase suppressing protein, that is stabilized in a Rad53 dependent manner (Agarwal *et al*, 2003). Intriguingly the activity of Rad9-Rad53 is suppressed during prophase I of meiosis and its function is taken over by a similar adaptor-kinase complex Hop1-Mek1. The Mek1 kinase leads to activation of the recombination checkpoint in meiosis, as described below.

1.5.2 Recombination checkpoint:

DSBs introduced during early meiotic prophase due to Spo11 activity are just as deleterious as the spontaneously occurring DSBs. Even so, the introduction of DSBs is necessary for the formation of interhomolog crossovers. Therefore, surveillance mechanisms are in place that highly regulates the repair of DSBs before the progression of the cell cycle. The underlying meiosis-specific surveillance mechanism is the recombination checkpoint or pachytene checkpoint (Kar & Hochwagen, 2021; Subramanian & Hochwagen, 2014). Factors detecting DSBs during recombination (meiosis) and DNA damage checkpoints (mitosis/ vegetative growth) are similar – Mec1/ Tel1. The main downstream adaptor protein phosphorylated by Mec1 in meiosis is Hop1 and not Rad9, as in the case of mitosis. In fact, Rad9-Rad53 remain inactive during Meiosis I and their role is taken over by their meiotic analogs Hop1-Mek1. Similar to Rad53-Rad9 interaction, Mek1 contains FHA domain, via which it interacts with its adaptor Hop1 (Carballo *et al.*, 2008; Chuang *et al*, 2012; Wan *et al*, 2004). Hop1 then facilitates in dimerization of Mek1 and activation (Carballo *et al.*, 2008; Chuang *et al.*, 2012; Niu *et al.*, 2007; Niu *et al*, 2005; Wan *et al.*, 2004). The requirement for Hop1-mediated activation is made redundant by tagging Mek1 with a dimerizing tag, GST (Niu *et al.*, 2007; Wan *et al.*, 2004). The active Mek1 trans-autophosphorylates itself and furthermore phosphorylates its downstream effectors such as Ndt80, and Rad54 (Chen *et al*, 2018; Hollingsworth & Gaglione, 2019; Niu *et al.*, 2009) (the role of Rad54 is discussed in detail in the later section). Activation of the recombination checkpoint is primarily mediated via Ndt80 (Chen *et al.*, 2018; Hollingsworth & Gaglione, 2019). Ndt80 is an essential transcription factor for the completion of recombination and meiotic progression. It binds to sequences (called middle sporulation elements) in the promoters of > 300 genes and assists in their activation. One of the genes activated by Ndt80 is Cdc5 which triggers Holliday junction resolution and Red1 degradation, allowing SC disassembly (Argunhan *et al*, 2017; Okaz *et al*, 2012; Prugar *et al*, 2017; Sourirajan & Lichten, 2008). Another important Ndt80 target is *CLB1*, which along with Cdc28 (CDK), triggers meiotic progression after maximum completion of DSB repair (Benjamin *et al.*, 2003; Shuster & Byers, 1989). A 57 amino acid stretch in the middle region of Ndt80,

termed 'bypass checkpoint domain' (bc) is responsible for meiotic checkpoint recombination delay (Wang *et al*, 2011). Mek1 negatively regulates Ndt80 by binding to a consensus sequence within this region and phosphorylates Ndt80 at multiple sites (Chen *et al.*, 2018). Inhibition of Ndt80 by Mek1 (and other factors) leads to cell arrest until DSBs are repaired in meiosis. As a result of DSB repair during the late prophase, Mek1 is removed from the chromosomes resulting in activation of Ndt80 and progression through MI.

1.6 The meiotic chromosomal axis

The chromosomal axis plays a central role in assembling a structure that plays a dual function in meiosis, *i.e.* in DSB formation and DSB repair. From early meiotic prophase, the axial elements – Hop1, Red1 cohesin and condensins (proteinaceous complexes that help condense DNA loops and organize the structure of chromosomes) aid in the formation and stabilization of the meiotic chromosomal axis (Blat & Kleckner, 1999; Hollingsworth, 2010; Klein *et al.*, 1999; Lorenz *et al*, 2004; Smith & Roeder, 1997). The axis also allows the establishment of the chromosomal loop-axis structure, which is necessary for DSB formation. Later during meiotic progression, the axis elements form the lateral components of the synaptonemal complex. The synaptonemal complex assembles between the homologous chromosome and assists in homolog pairing and crossover resolution. The meiotic chromosomal axis structure and axial elements are well conserved in many eukaryotic species (van Heemst & Heyting, 2000; West *et al*, 2019; Zickler & Kleckner, 1999).

Red1 and Hop1 are central elements that form the core of the *S. cerevisiae* meiotic chromosomal axis. Together with meiotic cohesin (consisting of meiosis-specific Rec8 component), they form the chromosomal axis and later on form the lateral elements of the synaptonemal complex. Red1 and Hop1 are effective components for meiotic DSB forming pathways, maintenance of the recombination checkpoint, interhomolog bias and DSB repair. Red1 and Hop1 are recruited to the chromosomes even prior to DSB formation. Red1 and Hop1 remain on chromosomes until the pachytene stage and are removed from the axis via a meiosis-specific AAA+ ATPase Pch2, in late pachytene/ diplonema stage following majority repair of DSBs (Börner *et al*, 2008; Vader, 2015). The lateral elements are responsible for the assembly of the synaptonemal complex (which consists of meiotic cohesin kleisin subunit Rec8, the transverse element Zip1 and the axial lateral elements Red1/Hop1; (Klein *et al.*, 1999; Schalbetter *et al*, 2019; Smith & Roeder, 1997; Sym *et al*, 1993) and later for the assembly of the synaptonemal complex transverse elements (*i.e* Zip1). Recent studies have also shown that

they interact with cohesins, thus presumably supporting the sister chromatid compaction and overall chromosomal structure (Sun *et al*, 2015). As a result of DSB formation, Red1 and Hop1 are heavily phosphorylated (Carballo *et al.*, 2008; Cheng *et al*, 2013; Lai *et al*, 2011; Markowitz *et al*, 2017). In addition, Red1 is also SUMOylated in meiosis (Lin *et al*, 2010). These post-translational modifications aid in recombination and error-free segregation of chromosomes. A detailed description of the roles of Red1 and Hop1 in meiosis is provided in the following sections.

1.6.1 Meiotic chromosomal axial elements : Role of Red1 in meiosis

Red1 is a meiosis-specific protein that forms the chromosomal axis core. Red1 interacts with itself to form higher order homo-oligomeric filaments, it interacts with Hop1, a meiotic HORMA domain protein and with cohesin subunit Rec8 (Sun *et al.*, 2015; West *et al.*, 2019; West *et al*, 2018; Woltering *et al*, 2000). Together, these interactions presumably contributes to its role in axis assembly (West *et al.*, 2019). By interacting with the HORMA domain protein Hop1 (West *et al.*, 2018), it plays a central role in establishing the interhomolog bias. Consequently, *red1Δ* displays an increase in intersister crossovers changing the IH:IS (interhomolog : intersister) bias from 5:1 in wild type meiotic cells to 1:9 in *red1Δ* (Hong *et al*, 2013; Schwacha & Kleckner, 1997). Such a change in *red1Δ* is known to cause defects in chromosome segregation and significantly reduce spore viability (Wan *et al*., 2004). A meiotic prophase arrest is observed if proteins responsible for the processing of DSBs are deleted, such as dmc1Δ, (Bishop *et al.*, 1992). This is due to the accumulation of DSBs as interhomolog based repair is hindered. Deleting *RED1* in these strains suppresses the phenotype as it either causes repair of DSBs via using the sister chromatid or significantly reduces the introduction of DSBs (Niu *et al.*, 2005; Schwacha & Kleckner, 1997). Maintenance of appropriate Red1 stoichiometry is crucial for effective chromosome segregation. An overexpression assay confirmed Red1 related G2/ M arrest after overexpression of Red1 in vegetatively dividing cells (Sopko *et al*, 2006). This observation shows the importance of Red1 in establishing interhomolog recombination.

Red1 is a phospho-protein with multiple phosphorylation sites. It gets phosphorylated in the early meiotic prophase and remains phosphorylated until the completion of meiotic recombination (Lai *et al.*, 2011). Unlike earlier reports suggesting a role of Mec1/ Tel1 in Red1 phosphorylation, a much recent study pointed out that the phosphorylation of Red1 was instead dependent on Cdc28 (Lai *et al.*, 2011) and that the phosphorylation plays no significant role in

meiotic progression. Red1 is also modified by SUMO in meiosis. Interestingly, Red1 SUMOylation was dispensable for meiotic recombination initiation but plays a role in mediating Hop1 phosphorylation (Lin *et al.*, 2010).

Red1 is loaded along the chromosomes but exhibits increased localization in certain regions (Subramanian *et al*, 2019; Sun *et al.*, 2015). It is loaded to sites in a cohesion dependent and cohesion-independent manner (Sun *et al.*, 2015). Red1 was shown to interact with Rec8, a meiosis specific cohesion subunit (Sun *et al.*, 2015). The cohesion dependent loading of Red1 occurs via its interaction with Rec8. Unlike in *S. pombe* where the Red1 homolog (Rec10) interacts with Rec11 (*Sc*Scc3), a component of the cohesin complex (Sakuno & Watanabe, 2015), no interaction of Red1 was detected with other cohesion subunits (*e.g.* Scc1) (Sun *et al.*, 2015). Cohesin independent loading of Red1 to chromosomes occurs via Hop1 (Sun *et al.*, 2015). In summary, Red1 interacts with axial element Hop1 and cohesin, forms chromosomal axis via Red1-Red1 filaments (described in the later section), assists in interhomolog bias by aiding in Mek1 recruitment and activation and forms a crucial early meiotic component that facilitates chromosome segregation in MI.

1.6.2 Meiotic chromosomal axial elements : HORMA domain protein - Hop1

Hop1 belongs to the meiotic HORMA domain family of proteins. It is involved in meiotic DSB formation, interhomolog repair and meiotic chromosomal organisation (Carballo *et al.*, 2008; Hollingsworth *et al*, 1990; Panizza *et al.*, 2011; Prieler *et al*, 2005). It is loaded onto chromosomes in the early meiotic prophase to form the lateral element of the SC. It plays a crucial role in Spo11 induced DSB formation as deletion of *HOP1* decreases DSB formation by 10-folds (Blat *et al.*, 2002; Kugou *et al.*, 2009; Niu *et al.*, 2005; Prieler *et al.*, 2005; Woltering *et al.*, 2000). Later on, it is removed from the chromosomes by the activity of Pch2[TRIP13] (Börner *et al.*, 2008; San-Segundo & Roeder, 1999). *hop1Δ* displays reduced spore viability reflecting its role in meiotic chromosome segregation (Hollingsworth *et al.*, 1990). Hop1 is phosphorylated by Mec1/ Tel1 kinases in response to meiotic DSBs (Carballo *et al.*, 2008). Mec1/ Tel1 phosphorylate the [S/T]Q sites in Hop1. Three such residues together form a [S/T]Q cluster domain (SCD) in Hop1, which are important for its function (Carballo *et al.*, 2008). Particularly the phosphorylation at Hop1 threonine 318 is important and mutating the residue to alanine causes a reduced spore viability (Carballo *et al.*, 2008; Chuang *et al.*, 2012). This particular phosphorylation is thought to drive its interaction with Mek1.

 1.6.3 Structural properties of Red1-Hop1 interaction

Hop1 is a HORMA domain containing protein that interacts with the coiled-coil protein Red1 to form the chromosomal axis in meiosis (West *et al.*, 2018; Woltering *et al.*, 2000). Structurally, Hop1 contains an NH_2-terminally located HORMA domain ($Hop1^{1-255}$), a middle Zn finger motif ($Hop1^{320-380}$) and a C-terminal short peptide sequence called the closure motif (CM; $Hop1^{585-605}$) (West *et al.*, 2018). Hop1 is a member of the meiotic HORMA domain family proteins that share structural and functional characteristics. Three such proteins are well studied in budding yeast, Rev7, Mad2 and Hop1 (Rosenberg & Corbett, 2015). Structural similarities have been observed in Hop1 homologs in *S. pombe* Hop1, mammalian HORMAD1/HORMAD2, *C. elegans* HIM-3/HTP-1/HTP-2/HTP- 3 and plants ASY1/ASY2 (Caryl *et al*, 2000; Couteau & Zetka, 2005; Lorenz *et al.*, 2004; Wojtasz *et al*, 2009; Zetka *et al*, 1999) Proteins with HORMA domains can interact either with their binding partners or form intramolecular interactions via HORMA-CM interaction. Apart from the structural domains described above (HORMA domain and CM), these proteins contain two distinct structural regions, the NH_2-terminally located core and the C-terminal 'safety-belt' (De Antoni *et al*, 2005; Mapelli *et al*, 2007). Depending on the position of the safety belt, they can adopt two conformations - the 'closed' conformation in which the core interacts with the CM and the safety belt is wrapped around it and an 'open' conformation, the safety belt occupies the CM binding site of the core and prevents CM-HORMA interaction (Luo *et al*, 2000; Rosenberg & Corbett, 2015). Hop1 adopts a different conformation that is functionally similar to 'open' Mad2 called 'unbuckled' in which the safety belt is disengaged from the core to form a more extended molecule (West *et al.*, 2018). By interacting with its binding partner Red1, Hop1 adopts a closed conformation in which the CM of Red1 is bound to the core of Hop1 (West *et al.*, 2018). This in turn exposes the CM of Hop1. The current model of axis assembly proposes that another Hop1 molecule becomes recruited to chromosomes by binding to the exposed CM of the axis recruited Hop1 causing a chain of Hop1-Hop1 interactions and representing a "beads on a string" like architecture (West *et al.*, 2018) (Figure 1-8).

Red1 appears to contain three structurally conserved domains. An NH_2-terminal conserved region, followed by a short peptide sequence with limited sequence homology to the CM of Hop1 (West *et al.*, 2018; Woltering *et al.*, 2000). This is the Red1 closure motif ($Red1^{340-362}$) that binds to the HORMA domain of Hop1 (West *et al.*, 2018; Woltering *et al.*, 2000). The CM is linked to the C-terminally located coiled-coil region by an unstructured stretch of amino acids. The coiled-coil region of Red1 is responsible for its characteristic filament nature

(Red1$^{737-827}$) (West *et al.*, 2019). Red1 and its functional homologs in mammals (SYCP2/SYCP3) and in *Arabidopsis* (ASY3/ASY4) interact to form homo- or hetero-tetramers and arrange in higher-order structures to form filaments (West *et al.*, 2019). The filaments then associate to form bundles on the chromosome acting as large flexible scaffolds aiding in the loop-axis orientation (West *et al.*, 2019) (Figure 1-8). Mutations in the coiled-coil region such as deletion of the last 8 residues in *S. cerevisiae* - *Sc*Red1 or *Z. rouxii* - *Zr*Red1 leads to disruption of the filaments, while substituting the residues I743 and I758 with alanine in *Sc*Red1 presumably leads to disruption of higher-order structures in Red1, forming homo-tetramers and monomers respectively. The I743A and I758A mutants are responsible for poor SC assembly and spore viability defects (Eichinger & Jentsch, 2010; Lin *et al.*, 2010) confirming the importance of Red1 filament formation in meiosis.

Interaction of Hop1 and Red1 is essential for meiosis. Disrupting the interaction by making Red1-K348E mutation in the CM of Red1 leads to a reduced number of crossover and spore viability defects (Woltering *et al.*, 2000). Furthermore, disruption of the Red1-Hop1 complex also affects Mek1 activity (Hollingsworth & Gaglione, 2019; Niu *et al.*, 2007).
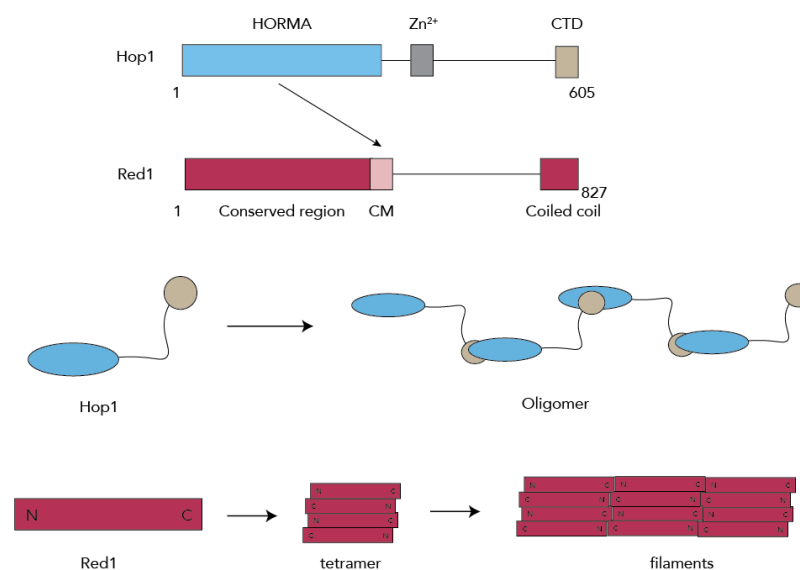
Figure 1-8: Structural properties of Red1 and Hop1

Hop1 (in blue) is a HORMA domain containing protein, with an NH$_2$-terminal HORMA domain, a zinc finger motif in the middle and a C-terminally located closure motif. Red1 (in red) is a coiled coil protein. It has an NH$_2$-terminal conserved region, followed by a closure motif (CM), the CM is followed by an unstructured region and at the very C-terminal is a coiled coil domain. Hop1 interacts via its HORMA domain with its own CM (intramolecular

interaction), CM of other Hop1 molecules to give Hop1-Hop1 oligomers or with other proteins containing a CM (such as Red1). Red1 is known to form higher order structures such as tetramers that come together to form large filamentous assemblies. Red1 filaments assist in axis formation during meiosis. (Figure modified and adopted from (Yadav & Claeys Bouuaert, 2021).

1.6.4 'Mek1' - A meiosis specific key kinase driving the interhomolog bias

One of the key regulators of interhomolog bias is the meiosis-specific kinase Mek1 that is recruited to chromosomes via its interaction with chromosomal axial elements. Mek1 performs dual functions in meiosis – i) It establishes interhomolog recombination by forming a barrier to intersister DSB repair; ii) It controls the rate of meiotic progression by mediating pachytene arrest and providing time for repair of DSBs. Mek1 kinase is activated in response to DSBs and remains active until the formation of synaptonemal complex. It is recruited to sites of DSBs via its interaction with axial element proteins Hop1 and Red1 and is activated upon Hop1 mediated dimerization (Niu *et al.*, 2007; Niu *et al.*, 2005). Mek1 is a meiotic paralog of Rad53 (Chuang *et al.*, 2012). Although Mek1 homologs are described in various fungal species (Cherry *et al*, 2012), no known homologs of Mek1 are confirmed in mammals or other higher-order species.

Mek1 protein consists of three functional domains: An NH_2-terminal FHA domain followed by a catalytic domain and a C-terminal domain. Mek1 binds to chromosomal axial element Hop1 via its FHA domain. Mec1 mediated Hop1 phosphorylation at T318 is required to recruit Mek1 to Hop1 and its activation (Carballo *et al.*, 2008). In addition, the C-terminal of Hop1 is required for Mek1 dimerization (Niu *et al.*, 2005). Hop1 function can be bypassed by ectopic Mek1 dimerization by GST; however, this does not bypass the requirement of Mek1 to bind to phosphorylated Hop1 prevailing its function (Niu *et al.*, 2005; Wu *et al*, 2010). Two conserved residues in the C-terminal domain of Mek1 (I459 and L460) are also shown to be essential for Mek1 dimerization (Niu *et al.*, 2007). The dimerized form of Mek1 activates itself by *trans* autophosphorylation of residues T327 and T331 in its activation loop (Niu *et al.*, 2007). These phosphorylation events are essential for the function of Mek1, and creating phospho-null mutants by mutating these residues results in reduced spore viability (Niu *et al.*, 2007). Moreover, the activity of Mek1 requires complex formation by Red1 and Hop1 (Hollingsworth & Gaglione, 2019; Niu *et al.*, 2007). A particular residue in the catalytic core site of Mek1 is seen to be necessary for its function and mutating it (Mek1-K199R) forms a

kinase-dead Mek1 allele (de los Santos & Hollingsworth, 1999; Wan *et al.*, 2004). Additionally, mutation of a conserved glutamine at position 247 in the ATP binding pocket of Mek1 creates an inhibitor-sensitive allele of Mek1 (*mek1-as1*) that induces kinase inhibition in the presence of small molecule inhibitors (Wan *et al.*, 2004).

Mek1 being a key component of meiotic recombination, deletion of this kinase or its accessory factors (*red1Δ* or *hop1Δ*) leads to repair of DSBs via intersister recombination (Callender & Hollingsworth, 2010; Hong *et al.*, 2013; Lao *et al*, 2013; Niu *et al.*, 2005; Terentyev *et al*, 2010). In *dmc1Δ* (meiotic recombinase that is crucial in interhomolog crossover formation) strains, DSBs are formed but remain unrepaired, leading to cell cycle arrest (Bishop *et al.*, 1992; Hunter & Kleckner, 2001; Niu *et al.*, 2005). This could be understood as most DSBs cannot be repaired by interhomolog recombination due to lack of Dmc1 and additionally, intersister recombination is also inhibited due to Mek1 activity. Mek1 kinase activity persists at high levels in the *dmc1Δ* strains to ensure DSBs are not repaired via the usage of sister chromatid. Deletion of *MEK1* in *dmc1Δ* leads to rapid repair of DSBs by IS recombination (Blat *et al.*, 2002; Lao *et al.*, 2013; Niu *et al.*, 2005).

One way that Mek1 promotes IH bias is by inhibition of a recombinase Rad51. Mek1 inhibits Rad51 by disrupting the Rad51-Rad54 interaction. The interaction of Rad51-Rad54 primarily mediates intersister recombination (Niu *et al.*, 2009) . Thus disrupting this interaction promotes interhomolog bias (Niu *et al.*, 2009). Mek1 mediates disruption of Rad51-Rad54 interaction by phosphorylating its downstream target proteins – Rad54 and Hed1 (Callender *et al.*, 2016; Niu *et al.*, 2009). A detailed description of Mek1 kinase, its downstream effectors, and the effect of the kinase on strand invasion proteins is provided in the following section.

Apart from its targets Rad54 and Hed1, two other targets of Mek1 are Histone 3 Threonine 11 and Ndt80 (Chen *et al.*, 2018; Hollingsworth & Gaglione, 2019; Kniewel *et al*, 2017). H3-T11 phosphorylation is a hallmark of Mek1 activity (Kniewel *et al.*, 2017). It gets transiently phosphorylated upon activation of Mek1 and remains phosphorylated only until Mek1 is active (*i.e* until synaptonemal complex formation). The H3-T11 phosphorylation is used as a marker for monitoring Mek1 activity. However, further studies are needed to identify the exact function of this modification. Mek1 negatively regulates Ndt80, a transcription factor that binds to promoters of >300 genes that are responsible for meiotic progression (Hollingsworth & Gaglione, 2019). Ndt80 affects several pathways that allow cells to proceed through the meiotic program. Mek1 inhibits Ndt80 by directly binding to the *bc* domain (bypass

checkpoint domain) of Ndt80, located in the middle region of Ndt80 (Chen *et al.*, 2018; Hollingsworth & Gaglione, 2019; Wang *et al.*, 2011). This leads to the arrest of cells in prophase and allows time for DSB repair. A description of Mek1-Ndt80 regulation was mentioned in the earlier section.

1.7 Effect of DNA damage signaling on strand invasion proteins

One way that Mek1 mediates interhomolog recombination is by inhibition of RecA like recombinase – Rad51. This is achieved by two distinct mechanisms i) Mek1 mediated phosphorylation of a meiosis-specific protein, Hed1, that binds to Rad51 and has an inhibitory effect on its activity (Callender *et al.*, 2016). ii) Mek1 phosphorylates Rad51's accessory protein Rad54, disrupting the Rad51-Rad54 complex which is known to be predominantly involved in intersister recombination (Niu *et al.*, 2009).

During meiosis, two RecA orthologs – 'Rad51' and 'Dmc1' are required for interhomolog recombination in many eukaryotic organisms. Rad51 is constitutively expressed in many eukaryotes, while Dmc1 is meiosis-specific. The activity of these recombinases is dictated by its interaction with two other proteins, Rad54 and Rdh54, that act as accessory factors. Rad54/ Rdh54 belong to Swi/Snf family of chromatin remodelling proteins (Humphryes & Hochwagen, 2014; Liu *et al*, 2014; Petukhova *et al*, 1998; Petukhova *et al*, 2000). The interaction of Rad54 to Rad51 is crucial in mediating the mitotic inter-sister recombination bias (Chen *et al.*, 2018; Crickard *et al*, 2018; Niu *et al.*, 2009). Rad54 has an essential role in recombination as it – i) Stabilizes Rad51 filaments, ii) Simulates Rad51 mediated strand invasion and iii) Removes Rad51 from DNA after joint molecules are formed (Heyer *et al*, 2006; Tan *et al*, 2003). Disrupting the Rad51-Rad54 interaction create hypersensitivity to DNA damaging conditions (Niu *et al.*, 2009). During meiosis, to form the barrier to sister chromatid repair (BSCR), the interaction of Rad54-Rad51, that favours intersister repair must be suppressed and instead the interhomolog strand invasion activity is taken over by Rad51 and Dmc1. Mek1 plays a role in biasing the recombination towards the homolog by phosphorylating Rad54 at T132 which disrupts its interaction with Rad51 (Niu *et al.*, 2009). The role of Mek1 in mediating the interhomolog bias is as such seen to be of importance, as both Rad51 and Rad54 are present during mitosis and meiosis, although a key Mek1 specific phosphorylation event on Rad54 changes the bias from the default 'intersister' to 'interhomolog' mediated repair.

In addition to phosphorylation of Rad54, an important target of Mek1 is Hed1 that aids in interhomolog bias (Busygina *et al*, 2008; Callender *et al.*, 2016; Tsubouchi & Roeder, 2005). Phosphorylation of Hed1 at T40 by Mek1, increases its stability. Hed1 binds to Rad51 and inhibits its activity by interfering with Rad54-Rad51 complex (Busygina et al., 2008; Tsubouchi and Roeder, 2006). Phosphorylation by Mek1 is not per se required for the function of Hed1 as ectopic expression of Hed1 in vegetatively dividing cells was shown to be sufficient for Hed1's inhibitory function (Busygina *et al.*, 2008; Tsubouchi & Roeder, 2005). Co-localization of Hed1 with Rad51 and reduction in interhomolog bias in *RAD54-T132A hed1Δ* has suggested both of these proteins being important targets of Mek1 kinase activity (Callender & Hollingsworth, 2010; Niu *et al.*, 2009).

The other important players of meiotic recombination are Rad51 and Dmc1 strand invasion proteins. Interhomolog recombination is driven by the Rad51-Dmc1 nucleoprotein filaments. Studies suggest that the activity of Rad51 is not needed in meiosis. Rad51 is solely required for loading of Dmc1 onto the ss-DNA filaments. In fact, Rad51 activity is downregulated in meiosis in order to prevent intersister DSB repair. Nonetheless, the presence of Rad51 is necessary for proper functioning of Dmc1, as interhomolog bias is affected in *rad51Δ* cells (Callender & Hollingsworth, 2010; Schwacha & Kleckner, 1997). Rad51 is stabilized after S-phase in vegetatively dividing cells as well as in meiotic cells by phosphorylation of its NH_2-terminal domain. During meiosis, as a result of Spo11 induced Mec1 activity, Rad51 gets hyperphosphorylated. This leads to further stabilization of the protein which is necessary for interhomolog recombination (Woo *et al*, 2020; Woo *et al*, 2021). Dmc1 is another crucial meiosis specific recombinase. In *dmc1Δ* mutants, DSBs remain unrepaired and become hyper-resected (Cartagena-Lirola *et al*, 2006; Reitz *et al*, 2019). This follows recombination checkpoint activation and cell cycle arrest. Persistent Rad51 foci are observed in this condition suggesting that Rad51 is bound to DSBs but unable to carryout repair (Bani Ismail *et al*, 2014). Rad51 is kept inactive by Mek1 activity in *dmc1Δ*. Inhibition of Mek1 activity in *dmc1Δ* strains allows Rad51 dependent intersister recombination (Niu *et al.*, 2007). Thus Mek1 mediated interhomolog bias is accomplished by its effect on Rad54 and Hed1 along with an important role of Rad51 and Dmc1 strand invasion proteins.

1.8 Objectives

Programmed induction of DSBs and subsequent repair of the breaks is crucial to establish the interhomolog linkage during meiosis I. DSBs occurring during mitosis, as a consequence of exposure to harsh chemicals, stalling of replication fork etc are predominantly repaired by homologous recombination mechanism using the sister chromatid as a repair template. The default use of the sister chromatid template can be justified due to its physical proximity to the sites of DSBs. Unlike in mitosis, the Spo11 induced programmed breaks occurring during meiosis are preferentially repaired by using the homolog as a repair template. The biased interhomolog repair, is mediated by a key meiosis-specific kinase Mek1. The activation of Mek1 is dependent on two other meiosis-specific proteins Red1 and Hop1. Therefore, in this Ph.D. thesis, I aim to study the biased interhomolog repair of DSBs that occurs in meiosis in the context of Red1-Hop1-Mek1 complex. Attempting to study the role of Red1/ Hop1 in mediating the DSB repair is complicated by the fact that both, Red1 and Hop1 are required in the upstream meiotic DSB induction process (Blat *et al.*, 2002; Kugou *et al.*, 2009; Niu *et al.*, 2005; Prieler *et al.*, 2005; Schwacha & Kleckner, 1995; Woltering *et al.*, 2000). Therefore, here I design a synthetic system whereby I conditionally express Red1-Hop1-Mek1 components in an ectopic environment *i.e* in mitotically dividing cells. Using this system and *in vitro* approaches, I investigate the following questions –

1. Understanding whether RHM complex can assemble and autonomously (without the need of other meiosis-specific components) perform the interhomolog bias in the ectopic environment.

2. Conditions necessary for activation of Mek1.

3. Studying the mechanism of interhomolog bias specifically in the context of the RHM complex.

4. Structural aspects of the RHM complex –

    i.   Designing a minimal Red1 construct by Red1 domain truncations, that is sufficient to activate the RHM complex.

    ii.   Understanding the Red1 associated growth defect.

    iii.   *In vitro* reconstitution of the RHM complex.

    iv.   Structural modelling of the RHM complex.

As a part of a second project, I investigate the programmed induction of DSBs in meiosis, specifically in the context of Mer2 (A Spo11 DSB machinery protein). For this project, the thesis aims to perform -

5. *In vivo* characterisation of the role of Mer2 in meiotic DSB induction.

Chapter 2

Materials

2.0 Materials

The following section contains a comprehensive list of all the materials, reagents, chemicals and other products used to perform this work.

2.1 Chemicals, enzymes, reagents and antibodies

All chemicals, reagents and enzymes used in this study are listed in the table 2-1 and antibodies in table 2-2

Table 2-1: Chemicals and reagents

Chemicals and Reagents	Supplier
Acetic acid	Sigma-Aldrich
Acrylamide	Carl Roth
Agar	Becton Dickinson
Agarose Standard	Carl Roth
Ammoniumperoxosulfate (APS)	Serva Electrophoresis
Ampicillin	Serva Electrophoresis
Bacto-Peptone	Becton Dickinson
Boric acid	Gerbu Biotechnik
Bromophenol blue	Sigma-Aldrich
Dextran sulfate sodium salt	Sigma-Aldrich
Difco yeast nitrogen base without AA	Becton Dickinson
Dimethylsulfoxide (DMSO)	Serva Electrophoresis
Dithiothreitol (DTT)	Serva Electrophoresis
DNA ladder GeneRuler™ 1kb	Fermentas
D-Sorbitol	Sigma-Aldrich
Dynabeads™ Protein G	Invitrogen
Ethanol (EtOH)	Carl Roth
Ethylenediaminetetraacetic acid (EDTA)	Gerbu Biotechnik
Formaldehyde, 10%, methanol free, Ultra Pure	Polysciences
Gibson Assembly® Master Mix	New England Biolabs

Glycerol	Gerbu Biotechnik
Glycine	Carl Roth
Green FastMix®	Takara Bio/ New England Biolabs/ VWR/ Quantabio
HindIII	New England Biolabs
Hydrochloric acid (HCl)	Fisher Scientific
Isopropanol	J.T.Baker Chemicals
Lithium acetate dihydrate (LiAc)	Sigma-Aldrich
LongAmp® Taq	Takara Bio/ New England Biolabs/ VWR/ Quantabio
L-Tryptophan	Sigma-Aldrich
Magnesium chloride (MgCl$_2$)	J.T.Baker Chemicals
Methanol (MeOH)	Sigma-Aldrich
Midori Green Advanced DNA stain	Nippon Genetics
Milk powder blocking grade	Carl Roth
Phenol/Chloroform/Isopropanol	Carl Roth
Phenylmethylsulfonyl fluoride (PMSF)	Serva Electrophoresis
Polyethylene glycol (PEG) 3350	Sigma-Aldrich
PonceauS solution	Sigma-Aldrich
Potassium acetate (KOAc)	Carl Roth
Potassium chloride (KCl)	J.T.Baker Chemicals
Potassium dihydrogen phosphate (KH$_2$PO$_4$)	Merck
Precision Plus Protein™ Dual Color Standards	Bio-Rad Laboratories
Proteinase K	Amresco
Proteinase K	Roche Diagnostics
Q5® High-Fidelity	Takara Bio/ New England Biolabs/ VWR/ Quantabio
Q5® High-Fidelity 2x Master Mix	Takara Bio/ New England Biolabs/ VWR/ Quantabio
RedSafe™ Nucleic acid staining solution	Intron Biotechnology
RNase A	Sigma-Aldrich
Salmon sperm DNA	Agilent Technologies
SeaKem® LE Agarose	Lonza
Sodium chloride (NaCl)	VWR chemicals

Sodium dodecryl sulfate (SDS)	Carl Roth
Sodium hydroxide (NaOH)	VWR chemicals
SYTOX® Green nucleic acid stain	Life Technologies
T4 DNA ligase	New England Biolabs
TaKaRa Ex Taq®	Takara Bio/ New England Biolabs/ VWR/ Quantabio
Tetramethylethylenediamine (TEMED)	Serva Electrophoresis
Tris-(hydroxymethyl)-aminomethane (Tris)	Carl Roth
Tween-20	AppliChem
VWR Taq	Takara Bio/ New England Biolabs/ VWR/ Quantabio
Yeast Extract	Becton Dickinson
Zymolyase ®T100	AMS Biotechnology
Methyl methanesufonate	Sigma aldrich
Nocodazole	Fisher Scientific
β-Mercaptoethanol	Serva Electrophoresis

Table 2-2: Primary and secondary antibodies

Primary and secondary (HRP conjugated) antibodies used in this study are listed here

Antigen	Origin	Dilution	Supplier
α-HA	Mouse Monoclonal	1:1000	Biolegend, USA
α-Pgk1	Mouse Monoclonal	1:1000	Thermo Fisher
α-Hop1	Rabbit	1:10000	Inhouse
α-GFP	Rabbit	1:5000	Inhouse
α-phospho H3 T11	Rabbit Monoclonal	1:1500	EMD Millipore 04-789
α-phospho H2A S129	Rabbit	1:500	Abcam Ab181447
Anti-mouse IgG	Sheep	1:5000	GE healthcare
Anti-rabbit IgG	Donkey	1:5000	GE healthcare

2.2 Commercially available kits

All commercial kits used in this study are listed in table 2-3

Table 2-3: Kits

Kit	Supplier
ECL™ Prime Western blotting Detection Reagent	GE Healthcare
Prime-It RmT Random Primer Labeling Kit	Agilent Technologies
QIAprep® Spin Miniprep Kit	
	Qiagen
QIAquick® Gel Extraction Kit	Qiagen
QIAquick® PCR Purification Kit	Qiagen
Wizard® SV Gel and PCR Clean-Up System	Promega Corporation

2.3 Instruments and Supplies

All instruments and their suppliers are listed in table 2-4

Table 2-4: Instruments and suppliers

Instruments and supplies	Supplier
7500 Fast Real-Time PCR system	Applied Biosystems
Agarose gel electrophoresis system	Carl Roth
Amersham Hybond™ – XL membrane	GE Healthcare Life Sciences
Axio Vert.A1	Zeiss
BD Accuri™ C6 Flow Cytometer	BD Biosciences
BioPhotometer®	Eppendorf AG
BioTrace™ NT nitrocellulose transfer membrane	Pall Corporation
Centrifuges 5424	Eppendorf AG
Centrifuges 5424R	Eppendorf AG
Centrifuges 5810R	Eppendorf AG
ChemiDoc™ MP Imaging System	Bio-Rad Laboratories
DeltaVision Elite Imaging system microscope	GE Healthcare

FastPrep®-24	MP Biomedicals
HB-1000 Hybridizer hybridization oven	Analytik Jena AG
Heraeus Instruments kelvitron®t B6030	Thermo Fisher Scientific/VWR International/ Memmert
HerathermT™ Microbiological Incubator	Thermo Fisher Scientific/VWR International/ Memmert
INCU-Line® IL23	Thermo Fisher Scientific/VWR International/ Memmert
Innova™ 2000 Platform Shaker	New Brunswick Scientific
LB 122 Contamination monitor equipment	Berthold Technologies
Mini PROTEAN® Tetra Cell	Bio-Rad Laboratories
Mini-PROTEAN® II Cell	Bio-Rad Laboratories
Minitron	INFORS AG
MP Imaging Plate Storage Phosphor Screen (20x 40 cm)	FujiFilm
NanoDrop 2000 Spectrophotometer	Thermo Fisher Scientific
Owl™ A2-BP large gel system	Thermo Fisher Scientific
pH-Meter 766 Calimatic	Knick
Power Source 300V	VWR International
See-saw rocker, SSL4	Bibby Scientific
Sonifier 450	Branson Ultrasonics Corporation
Stuart™ Scientific roller mixer SRT6	Bibby Scientific
TDM Tetrad Dissection Microscope Ci-L	Nikon
Test-tube rotator	Labinco
Thermocycler T3000	Biometra
Thermomixer comfort 5436	Eppendorf AG
Typhoon TRIO+ Variable mode imager	GE Healthcare Life Sciences
VXR basic Vibrax®	IKA® -Werke
Waterbath	Thermo Fisher Scientific/VWR International/ Memmert
X-Ray Cassette (35x43 cm)	Kisker Biotech

2.4 Buffers and Media

All buffers used in this study are listed in table 2-5 and all media in table 2-6 (both the tables adopted from Kuhl, 2018)

Table 2-5: Buffers

Method	Buffer/ Solution	Composition	Final concentration
Agarose gel electrophoresis	10x DNA Loading Buffer	EDTA Bromophenol blue Xylencyanoblue Glycerol	1 mM 0.25% (w/v) 0.25% (w/v) 50% (v/v)
	10x TAE Buffer	Tris-base Glacial acetic acid EDTA	400 mM 200 mM 10 mM
	5x TBE Buffer	Tris-base Boric acid EDTA	445 mM 445 mM 10 mM
Co-immunoprecipitation	1x Phosphate Buffered Saline (PBS)	NaCl KCl Na_2HPO_4 KH_2PO_4	137 mM 2.7 mM 8 mM 2 mM
	1xPBS-T	Tween-20 in 1xPBS	0.05% (v/v)
	IP buffer	Tris HCL, pH 7.5 Triton X 100 NaCl EDTA pH 8.0	50mM 1% (v/v) 150mM 1 mM
	Tris EDTA (TE) SDS Buffer	Tris (pH 8) EDTA (pH 8) SDS	10 mM 1 mM 1 % (w/v)
	TCA resuspension buffer	Tris-HCL 7.5 Urea	50 mM 6 M
Isolation of yeast genomic DNA	DNA Breakage Buffer	Triton X-100 SDS NaCl Tris (pH 8) EDTA	2% (v/v) 1% (w/v) 100 mM 10 mM 1 mM
	Spheroplasting Buffer	Sorbitol K_2HPO_4 KH_2PO_4 EDTA	1M 42 mM 8 mM 5 mM

	Spheroplasting Solution	β-Mercaptoethanol Zymolyase in Spheroplasting buffer	1% (v/v) 2.5% (v/v)
	Lysing Buffer	Tris (pH 8) EDTA	1M 500 mM
Southern blot hybridization and washing	20x SSC	NaCl Na-Citrate	3M 300 mM
	Hybridization Buffer	Sodium phosphate (pH7.2) NaCl EDTA SDS Dextran sulphate	250 mM 250 mM 1mM 7% (w/v) 5% (w/v)
	Low Stringency Wash Buffer	SDS in 2x SSC	0.1% (w/v)
	High Stringency Wash Buffer	SDS in 0.1x SSC	0.1% (w/v)
	Protein Breakage Buffer	Tris (pH 7.5) EDTA DTT	50 mM 1 mM 2.75 mM
SDS-PAGE	3x SDS Loading Buffer	Tris-acetate (pH6.8) β-Mercaptoethanol Glycerol SDS Bromophenol blue	190mM 6% (v/v) 30% (v/v) 9% (w/v) 0.05% (w/v)
	10 x SDS Running Buffer	Tris-base Glycine SDS	25mM 192mM 0.1% (w/v)
	Sodium Phosphate Buffer (pH 7.2)	Na_2HPO_4 NaH_2PO_4	1M 1M
Southern Blot	10x Western Transfer Buffer	TRIZMA base Glycine SDS	3% (w/v) 14.4% (w/v) 0.2 % (w/v)
Western Blot	Blocking Buffer	Milk powder in 1x PBS-T	4% (w/v)
	1x Phosphate Buffered Saline (PBS)	NaCl KCl Na_2HPO_4 KH_2PO_4	137 mM 2.7 mM 8 mM 2 mM

	1xPBS-T	Tween-20 in 1xPBS	0.05% (v/v)
	10x Western transfer buffer	Trizma base Glycine SDS	3% (w/v) 14.4% (w/v) 0.2% (w/v)

Table 2-6: Media

Liquid medium	Composition	Final concentration
Buffered YTA (BYTA)	Yeast extract Bactotryptone KAc Potassium phthalate	1 % (w/v) 2 % (w/v) 1 % (w/v) 50 mM
Luria-Bertani (LB)	Tryptone Yeast extract NaCl	0.5 % (w/v) 1 % (w/v) 0.5 % (w/v)
Minimal (MIN)	Difco yeast nitrogen without AA, AS Ammonium sulfate Inositol D-Glucose	0.15 % (w/v) 0.5 % (w/v) 2mM 2 % (w/v)
Sporulation (SPO)	KAc Acetic acid	0.3 % (w/v) 5 % (v/v)
Yeast extract peptone dextrose (YPD)	Bacto peptone Yeast extract L-Tryptophan D-Glucose	2 % (w/v) 1 % (w/v) 0.015 % (w/v) 2 % (w/v)/ 4 % (w/v)
Yeast peptone glycerol (YPG)	Bacto peptone Yeast extract L-Tryptophan Glycerol	2 % (w/v) 1 % (w/v) 0.015 % (w/v) 3 % (v/v)

2.5 Software and tools

All software used in this study are in table 2-7

Table 2-7: Software

Software and tools	Supplier
Illustrator CC	Adobe
ImageJ	NIH, USA
Photoshop	Adobe
FlowJo	FlowJo, USA
Word 16.16.27	Microsoft, USA
Excel 16.16.27	Microsoft, USA
Prism 8	GraphPad Software
Endnote 20.2	Clarivate Endnote
Reverse complement	https://www.bioinformatics.org/sms/rev_comp.html
Tm Calculator	https://tmcalculator.neb.com/#!/main
Saccharomyces GENOME DATABASE	http://www.yeastgenome.org

Chapter 3

Methods

3.1 Growth and maintenance of yeast strains

3.1.1 Growth conditions for *S. cerevisiae*

Depending on the experimental procedure, yeast strains were grown in liquid media or on solid media plates. The composition of liquid media are listed in (Table 2-6). 2% (w/v) agar was added to the YP-glucose (yeast extract, peptone, glucose) media to prepare solid media plates. To ensure the maintenance of mitochondria, strains were taken out of the -80°C stocks for each experiment and grown on YPG (yeast extract, peptone, glycerol) plates overnight in a Heratherm^{TM} incubator before transferring to YPD (yeast extract, peptone, glucose) plates. For the selection of prototrophic markers, strains were grown on YNB plates with mixtures of amino acids containing the particular amino acid deficiency. YPD plates containing antibiotics, geneticin (300mg/ml) or Nourseothricin (100mg/ml), were used to select strains with antibiotic resistance markers KAN and NAT, respectively. All liquid media cultures were grown at 30°C on shaking at 180 rpm in a Multitron incubator (Infors AG, Switzerland) unless specified otherwise. Without shaking, all solid media plates were grown at 30°C in a Heratherm^{TM} incubator (Thermo Fisher Scientific, USA).

3.1.2 Yeast stock maintenance

For long term storage, yeast strains were grown overnight at 30°C on a non-fermentable carbon source, YPG (yeast extract, peptone, glycerol) plates. 1ml of 15% glycerol was added to screw-cap microcentrifuge tubes. Strain patches were scrapped with autoclaved toothpicks and resuspended in the glycerol solution. The strains were thoroughly mixed by vortexing and immediately stored in a -80°C freezer.

3.1.3 Growth conditions and drug treatment for mitotic cultures

Strains were taken out of -80°C freezer and a small fraction of cells were patched on YPG plates using autoclaved toothpicks. Strains were grown at 30°C in Heratherm^{TM} incubators

overnight. Cells were transferred on a YPD plate (4% w/v glucose) and grown overnight at 30°C. 20 ml liquid YP-RG (2.4% Raffinose, 0.12% Glucose) primary cultures were grown overnight until saturation on shaking at 180 rpm. The next morning, cultures were diluted to a final OD_{600} of 0.48 and grown for further 3.5 hours after which galactose induction was done by adding 2% galactose. Samples were collected at indicated time points by harvesting 5 ml of cultures, with final 1.9 $O.D_{600}$. Procedures for time courses with different drug treatment regimens are mentioned in figure 3-1. For introducing DNA breaks, 0.01% (v/v) Methyl methanesulfonate (MMS, SIGMA-ALDRICH, Chemie) was added to the cultures 30 mins prior to galactose induction. For Phleomycin treatment, two doses of 50µg/ml Phleomycin (SIGMA-ALDRICH, Chemie) were added; first a 30 mins prior to galactose induction and a second 2 hours into galactose induction. Experiments involving Cell cycle arrest were performed by addition of α-factor (166 μg/ml, Inhouse synthesis) 1 hour before adding galactose and (50 μg/ml) 1hr after galactose induction (Method based on (Zhuk *et al*, 2016)). Cells were arrested in mitosis by Nocodazole treatment (15 μg/ml, Fisher Scientific) once, 3 hours after starting cultures and again (15 μg/ml) after 3 hours of galactose induction. Samples were collected for flow cytometry analysis to evaluate the cell cycle arrest.
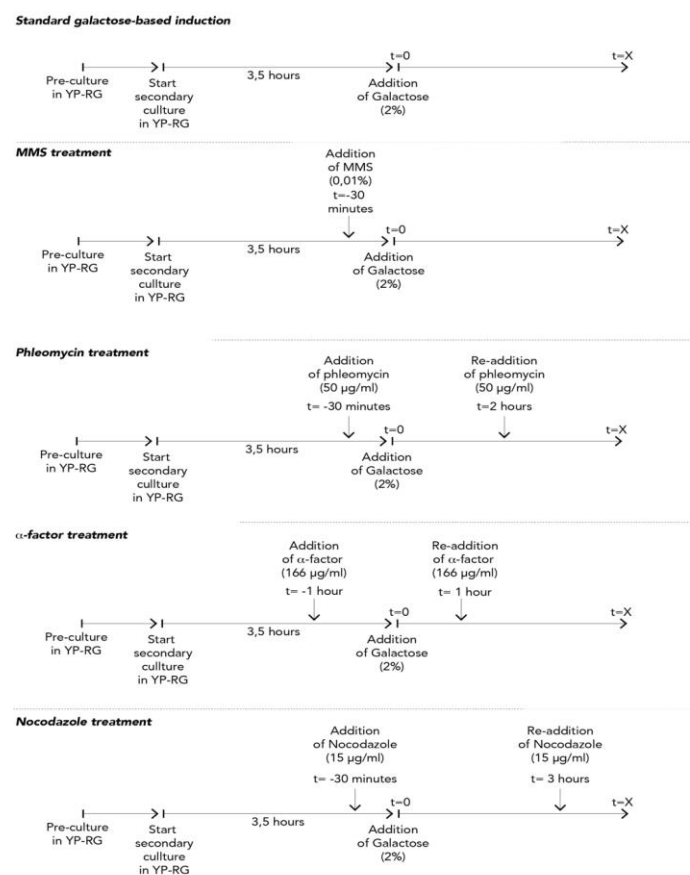
Figure 3-1: Time courses with various drug treatment regimens and cell cycle arrest protocols

3.1.4 Cell cycle synchronization in meiosis

For synchronous entry of cells into meiosis, cells were grown in nitrogen-deficient media containing acetate as a non-fermentable carbon source. For every experiment, strains were taken out of -80 ºC and thawed on YPG media overnight at 30 ºC. All yeast cultures were grown in 30 ºC Heratherm incubators unless mentioned otherwise. The next day strains were patched on 4% YPD plates and grown overnight. Cells were grown in liquid YPD media for 24 hours, 180rpm on a platform shaker (Innova) at room temperature before transferring to Buffered YTA (BYTA) media to a final OD_{600} of 0.3. BYTA cultures were grown overnight for 16 hours, 180 rpm in incubators (Multitron). The following morning cultures were centrifuged (Table top centrifuge 5810 R, Eppendorf, Germany) at 3000 rpm for 3 mins, washed twice with distilled water and resuspended in SPO media at a final OD_{600} of 1.9. The time of resuspension was considered as t = 0 hour in a time course and further time points were taken accordingly.

3.2 Yeast strain construction

3.2.1 Competent bacterial cell transformation for plasmid isolation

50µl of E. *coli* Omnimax cells were taken out of -80ºC storage and thawed on ice. 1µl of plasmid DNA was added to the competent cells, gently mixed by tapping and incubated on ice for 10 mins. Cells were given a heat shock at 42ºC for 45 seconds followed by immediate transfer to ice for 5 mins. 300µl of Luria Broth (LB) media was added to the transformation mix and incubated at 37ºC for 40mins on constant shaking. The transformation mix was then plated onto LB agar plates with appropriate antibiotic selection and grown overnight at 37ºC.

3.2.2 Plasmid isolation from bacterial cells

Colonies grown on LB plus antibiotic plates were picked and resuspended in a test tube with 5ml of LB media. Cultures were grown overnight at 37ºC , 180rpm in an incubator shaker (Infors HT). The culture was pelleted down and plasmid isolation was done following the protocol of QIAGEN miniprep kit according to the QIAGEN instruction manual.

3.2.3 Determination of DNA concentration

DNA concentration measurements were done by using NanoDrop Spectrophotometer (Thermo Scientific, USA). Concentration measurements were done by measuring absorbance at 260nm. Sample purity was monitored by measuring 260/ 280 nm absorbance ratio.

3.2.4 DNA sequencing

Samples for DNA sequencing were prepared following the protocols provided by the company GENEWIZ, UK. Samples were sequenced by Sanger sequencing method by GENEWIZ, UK.

3.2.5 Yeast transformation and Strain making

For transformation of yeast cells with the PCR product, yeast strains were grown overnight at 30ºC, 180 rpm in 25 ml YPD media in a Multitron incubator shakers (Infors). The next morning, cultures were diluted 1:25 in fresh YPD media. These secondary cultures were grown for ~4 hours till they reached OD_{600} 0.6-0.8. Cultures were harvested at 3500 rpm for 5 mins by centrifugation. Cells were then washed twice with 500µl LiAc-Sorbitol solution (1M LiAc, 1M Sorbitol freshly made and autoclaved). After the last wash, cells were resuspended again in 500µl of LiAc-Sorbitol solution. Yeast cells become competent for transformation by treatment with LiAc-Sorbitol solution.

For transformation purpose, PCR product was ethanol precipitated in 100% ethanol and resuspended in 50 µl of ddH$_2$O. A transformation mix was prepared in a microcentrifuge tube by adding 280 µl of 50% PEG4000 (polyethylene glycol, SIGMA-ALDRICH, Chemie), 20 µl of PCR DNA, 15 µl of salmon sperm DNA (Heated at 95ºC and pre-cooled in ice water for 5min. Invitrogen). The transformation mix was vigorously vortexed for ~ 1min. 100 µl of competent cells suspension were added to the mix and vortexed again. The transformation reaction was incubated at RT on a revolver tube rotator for 50 mins. Cells were then given a heat shock at 42 ºC for 15mins. In case the transformation PCR template consists of a drug resistance marker (*KANMX*, *NATMX*, *HPHMX*), 1 ml of YPD was added to the transformation reaction and the culture was allowed to grow at 30ºC on shaking for 2 hours. In case of marker genes (*TRP*, *URA*, *LEU* etc), the above step was skipped. The cultures were then pelleted by centrifugation at 3500 rpm for 5 mins and resuspended in fresh 300 µl of YPD media. The

transformation reaction was then plated onto desired selection plates and grown for 2-4 days at 30ºC. Colonies were picked and again streaked onto the appropriate selection plates. ~ 2 days later singlet colonies are picked and patched onto the appropriate selection plates. Colony PCR was done to test for positive clones.

3.2.6 Genomic DNA extraction and colony PCR

A small fraction of cells were scraped from a patch of strain grown on YPD agar plates using a toothpick. The cells were resuspended in 500 µl of TE buffer and pelleted by brief centrifugation (Table top centrifuge, Eppendorf, Germany). Supernatant was removed followed by the addition of 200 µl of DNA breakage buffer and 0.3 g of glass beads (Carl Roth, Karlsruhe, Germany) for mechanical cell lysis. 200 µl of phenol/chloroform/isopropanol (Carl Roth, Karlsruhe, Germany) was added for extraction of DNA and the cells were disrupted on a VXR basic Vibrax (IKA-Werke, Germany) for 6 mins. This was followed by centrifugation, carried out for 5mins at max speed on a table-top centrifuge for phase separation. The proteins and cell debris partition into the denser phenol layer while the upper aqueous layer consists of DNA. 100 µl of upper layer was carefully transferred into a microcentrifuge tube containing 1 ml of 100% ethanol. DNA was precipitated by centrifugation at max speed for 5mins. Ethanol was discarded followed by air drying of DNA pellet for 15 mins and resuspension of pellet in 50 µl of ddH$_2$O.

In order to perform colony PCR, colonies were picked and patched on YPD plates and grown at 30ºC overnight. Genomic DNA was extracted as described above and the extracted DNA was used as a template in PCR reactions. Primers flanking the region of interest were used to determine correct integration of the desired construct.

3.2.7 Mating type determination and creating diploids

To determine the mating type of a strain, the strain was patched on a YPD plate and grown overnight at 30ºC in Heratherm incubators. The next day a small amount of mating type tester strain was mixed with 300 µl of YPD and the mixture was spread on MIN plates. The mating type was determined by replica plating the desired strain onto the tester strain plates. Typically, a tester strain carries a unique auxotrophic marker that is not present in any of the other wt backgrounds. Since the strain of interest usually carries one or more auxotrophic

markers, only the strains that mate with the tester, form a prototrophic diploid and grow on the YPD containing MIN plates.

Diploid strains were created by mating the two haploid strains of opposite mating types (i.e. *MATa* and *MATα*). Using autoclaved toothpicks strains were scraped from a pre-grown strain patch and mixed on a YPD plate. More of *MATa* strain and less of *MATα* strain was used to prepare the mix. The mix was allowed to mate by overnight incubation at 30 ℃. Using a toothpick, a small amount of mix was streaked onto a YPD plate that was pre-spread with alpha-factor (10µg/ ml). Only diploids and *MATa* strains grow under these conditions. Shiny colonies were picked 2 days later, patched onto a YPD plate and grown overnight at 30 ℃. Diploids were replica plated onto MIN plates well spread with 300 µl of YPD with mating type tester strain resuspension.

3.2.8 Tetrad dissection, spore viability assay and sporulation efficiency

To obtain specific genotypic combination of strains, parental strains with desired genotypes and opposite mating types were mixed on YPD plate in a 1:1 ratio. The mix was allowed to grow for 2 days at 30℃ in Heratherm incubators. The mix was transferred into a 5ml SPO media and vortexed vigourously to obtain a homogenous solution. SPO cultures were grown overnight at RT on a rotator. 130 µl of the SPO culture was pipetted into a microcentrifuge tube and mixed with equal volumes of Zymolyase 100T (10mg/ml) followed by incubation at 42℃ for 8 -12 mins. Zymolyase is a yeast lytic enzyme that allows digesting of cell wall and formation of spheroplasts that can be dissected. Following enzymatic lysis, 500 µl of H_2O was added to the tubes to stop the reaction. ~60 µl of the cultures were added in a line on a plate and tetrad dissection was carried out using a dissection microscope (Nikon Eclipse Ci, Schuett-biotec).

For spore viability assay and sporulation efficiency, approximately 200 tetrads were dissected and the percentage of desired phenotypes were calculated. Sporulation efficiency was analysed by employing Axio Vert.A1 microscope observing 200 cells per condition and scoring the number of tetrads, monads, diads and no spores.

3.2.9 Epitope tagging and domain deletion mutants
For epitope tagging and creation of domain deletion mutants PCR products containing cassettes with desired tags were employed. Amplified PCR products were transformed into

competent yeast cells where they integrate at the desired sites based on homologous recombination mechanism to generate the desired genotype. For N-terminal epitope tagging, primers were designed covering 45 bps upstream and downstream of ATG start site and consisting of sequences corresponding to the plasmids with desired epitope tags. PCR amplification reactions using these plasmid templates and the primers was performed. These PCR products were concentrated by ethanol precipitation and transformed into competent yeast cells. The recombinant strains were then plated on appropriate selection plates to obtain transformant colonies. Positive colonies were confirmed by employing diagnostic colony PCR method.

pGAL1::(TAG) constructs were used for NH$_2$-terminal tagging and construction of overexpression strains. Red1 NH$_2$-terminal domain deletion mutants were designed by integrating *pGAL1::3HA* at desired sequence locations. For C-terminal deletion, *TRP1* cassettes were integrated at the desired sites in a *KANMX::pGAL1::3HA-RED1* containing strain. Gene deletion mutants were produced by using forward primer with 45 bp sequence upstream of the ATG start site of the desired gene and 45 bp downstream of the stop codon in the reverse prime. An insert marker cassette was used for gene deletion by integrating and replacing the desired gene (Longtine *et al*, 1998).

3.3 Molecular biology techniques

3.3.1 Polymerase Chain Reactions

PCR was used for amplification of desired cassettes and genes for genotypic modifications of yeast strains. PCRs were performed by following a standard PCR program on T3000 Thermocycler (Biometra) as mentioned below. An example of the PCR reaction mix is mentioned below. Modifications in the program and master mix reactions were done as per the requirements of the insert template that needs to be amplified.

Table 3-1: PCR mix reactions (50μL total volume)

Component	Volume (50 μl)
DNA template	1 μl
20 μM forward primer	2.5 μl
20 μM reverse primer	2.5 μl
dNTPs	4 μl

TaKaRa Ex Taq 10x buffer	5 µl
TaKaRa Ex Taq	0.4 µl
H$_2$O	34.6 µl

Table 3-2: Standard PCR thermo cycler program

Reaction step	Temperature (°C)	Time	No of Cycles
Initial denaturation	94	2 min	1
Denaturation	94	1 min	
Annealing	50	30 sec	2x30
Elongation	72	2 min 30 sec	
Final Elongation	72	10 min	1
Hold	4		

3.3.2 Agarose Gel electrophoresis

Agarose gel electrophoresis is used to separate DNA molecules based on their molecular weights. DNA being negatively charged, migrates in the gel exposed to electric field, in the direction of cathode (positive electrode). Higher molecular weight fragments migrate slower while the lower molecular weight fragments migrate faster, thus separating the DNA fragments based on size.

In this study 0.8%-1% (w/v) agarose gels were used. Required amount of agarose was added to 1xTAE buffer and warmed to mix evenly. Midori Green (Nippon genetics), a DNA binding stain is added to the agarose gel solution at a 1:25000 ratio and poured in a gel casting tray of the gel electrophoresis system (Carl Roth). Gels were run at 100V with a 1xTAE buffer.

3.4 Molecular genetics experimental procedures

3.4.1 Genomic DNA extraction and Southern blotting

Southern blotting is a DNA separation technique. This methods was employed to monitor DNA double stranded breaks. Samples were taken from synchronous meiotic cultures at desired timepoints and genomic DNA was extracted. Known DSB hotspots were further analyzed by restriction digesting of the hotspot region and separation by agarose gel. Parental

fragments of the hotspot region differ in size to the DSB induced fragments, the latter of which being of smaller sizes. Blotting followed by radioactive probe hybridization lead to signals that can be visualized on photographic screens. Southern blotting procedure was carried out following guidelines from (Vader *et al.*, 2011)

In order to isolate DNA fragments of the region of interest, cells were harvested at the desired time points by collecting 10 ml of meiotic cultures of OD_{600} 1.9. Cultures were killed by adding 0.1% sodium azide and pelleted by centrifugation at 3500 rpm for 3 mins on a table top centrifuge (5810 R, Eppendorf, Germany). Pellets can be stored at -20ºC. To proceed with genomic DNA isolation, pellets were transferred into microcentrifuge tubes by suspending in 1ml pre-cooled TE buffer. Spheroplasting was done by resuspending the pellets in freshly prepared spheroplasting solution (Add spheroplasting buffer supplemented with 1/100 ß-mercaptoethanol, 1/40 of the zymolyase stock.) and incubating at 37ºC on a rotating rack for 45 mins. Spheroplasts were lysed by incubating the samples with 100 µl of preheated lysing buffer and 15 µl of proteinase K (PCR grade, Roche diagnostic) at 65ºC for 2 hours. Further, precipitation was done by adding 150 µl of 5 M potassium acetate and incubating for ~ 1hr on ice until samples became semi-solid. Samples were centrifuged at 4ºC, 15 000 rpm on a table top centrifuge (5424 R, Eppendorf, Germany) for ~30 mins. Supernatants were precipitated by adding 600µl of lysates into 750 µl of ethanol in 2 ml microcentrifuge tubes. For DNA precipitation, lysates were thoroughly mixed in ethanol by inverting the tubes. DNA isolation was done by centrifugation at 4ºC for 10 mins at 14000 rpm on a table top centrifuge. Pellet was dissolved in 750 µl of TE buffer supplemented with RNase A (50 µg/ml; 1:600, SIGMA-ALDRICH) for 1 hr at 37 ºC. Samples were then stored at 4 ºC overnight.

The next day phenol-based DNA precipitation was carried out by adding 500 µl of phenol/chloroform/isopropanol to the samples and mixing by inverting tubes for 60 times. The samples were kept for 3 mins followed by repeating the mixing step. DNA was pelleted by centrifugation using a table top centrifuge (5424 R, Eppendorf, Germany) at 4 ºC for 10 mins and 600 µl of DNA containing upper layer was collected and added to 750 µl of isopropanol. The centrifugation step was repeated followed by washing with 70% ethanol. DNA was finally resuspended in 125 µl of TE and stored at 4 ºC.

To digest and acquire desired fragment of DNA, yeast genomic DNA was subjected to appropriate restriction enzymes. To analyse DSBs at the *YCR047C* hotspot, HindIII mediated digestion was carried out. For this purpose following digestion mix was made

30 µl of 10xNEB buffer (w/o BSA)

35 µl of genomic DNA samples

232.5 µl of H_2O

2.5 µl of HindIII

Digestion reaction was carried out at 37 ºC for 4 hours. Digested DNA was precipitated by adding 25 µl of 3M NaOAc, pH 5.5 and 650 µl of ethanol and incubating at -20 ºC for 30 mins. Precipitated DNA was pelleted by centrifugation at 4 ºC for 10 mins and the pellet was air dried. The pellet was then resuspended in 15 µl of TE and 5 µl of loading buffer (40% of 10xNEB buffer w/o BSA and 60% of 10x DNA loading buffer).

Separation of DNA fragments was done by agarose gel electrophoresis. 0.6% SeaKem Agarose (Lonza, USA) gel was prepared in 1xTBE buffer. The electrophoresis was performed at 70V for 16 hours in a gel separation system (Owl A2-BP large gel, Thermo Fisher Scientific). The gel was carefully removed and stained in an EtBr solution and DNA was visualised by UV light.

For blotting purpose, the gel was initially treated with 0.25M HCL for 40 mins on gentle shaking to depurinate the DNA followed by washing with H_2O and further denaturing the DNA by 0.4M NaOH treatment for 35 mins. This leads to formation of DNA single strands that can effectively bind to the membrane. Transfer apparatus was set by placing a wick (20 x 35 cm) of Whatman filter paper on an inverted gel tray of the Owl A2-BP large gel system (Thermo Fischer Scientific). 0.4M NaOH was poured in the apparatus to make sure that the two ends of the wick are evenly soaked in NaOH solution. Two gel-sized Whatman papers were placed on the wick and soaked with 0.4M NaOH. Gel was then carefully placed on the apparatus, upside down followed by carefully placing a Hybond-XL membrane (GE healthcare) soaked in water on top of it. Two Whatman papers were again soaked in 0.4M NaOH and placed on top ensuring no air bubbles are formed all the time. The edges of Whatman paper were protected by using parafilm. Finally a bunch of dry towels were covered on top evenly and a weight was placed. Transfer of DNA happens by gravity flow of the buffer.

The following day the membrane was removed and neutralised by incubating in 50mM sodium phosphate buffer, pH 7.2 for 30mins. Membranes were incubated in pre-warmed glass bottles containing 20 ml hybridization buffer and 300 µl of salmon sperm DNA (Invitrogen) at

65ºC in a HB-1000 hybridization oven (Analytik, Germany). Meanwhile, *YCR047C* probe was labelled with [α-^{32}P]dCTP (Perkin Elmer) using Prime-It RmT Random Primer Labeling Kit (Agilent Technologies) following the instructions mentioned in the kit protocol. Labeled probes were purified with 50 Micro column (GE Healthcare), illustra ProbeQuant G and denatured at 95ºC for 10 mins before added it to 5 ml, pre-warmed hybridization buffer and mixing it in the membrane containing bottles. Probes were allowed to hybridize with the membranes by overnight incubation.

The following day membranes were washed twice with pre-warmed low stringency SSC buffer (composition mentioned in materials) for 15 mins each followed by two high stringency SSC buffer washes for 30 mins. Membranes were finally covered with saran wraps, placed in an X-ray cassette and exposed to X-ray films for 7 days. Typhoon TRIO imager (GE healthcare) was used to image the films and quantification of DNA intensities was done using Adobe photoshop and ImageJ.

3.4.2 Trichloroacetic acid-based precipitation of yeast whole cell extracts

Samples were collected at desired timepoints by harvesting 5 ml of cultures of OD_{600} 1.9 and centrifuging on a table top centrifuge (5810R, Eppendorf) at 3000 rpm for 3 mins. Pellets were stored at -20 ºC. Pellets were subjected to TCA precipitation by resuspending in 5 ml of 5% pre-cooled TCA for 10 mins. Precipitates were collected by repeating the centrifugation step. Samples were then washed with pre-cooled acetone to remove the remaining TCA and allowed to dry overnight. Cell lysis and protein extraction was done by adding 200 µl of protein breakage buffer (4 ml of TE buffer, 11 µl of 1M DTT) and 0.3 g of glass beads. Mechanical cell lysis was done for 1 min by FastPrep 24 (MP biomedicals, USA). Yeast cell extracts were diluted by adding 100 µl of protein breakage buffer. 150 µl of 3xSDS loading buffer was added to samples and samples were boiled at 98ºC for 8 mins. SDS evenly imparts negative charge to the proteins.

3.4.3 Sodium dodecyl sulphate – polyacrylamide gel electrophoresis (SDS-PAGE)

SDS-PAGE is a technique that is used to separate proteins based on their molecular weights. SDS is a detergent that imparts negative charge evenly on denatured proteins. The negative charge is thus proportional to the molecular weight of the proteins. Separation is achieved based on the molecular weights. The lower molecular weight proteins tend to migrate

faster through the pores of the acrylamide gel matrix whereas the higher molecular weight proteins face a hindrance while migrating through the gel mesh and run at a slower rate. 15% SDS gels were used to separate histones and run at 70V for 100 mins. 12% SDS gels were used to resolve all other proteins. Gels were run at 70-100V until proper resolution was achieved. Gels were run in a Mini PROTEAN Tetra Cell (Bio-Rad, USA) with SDS running buffer.

3.4.4 Western Blotting for protein analysis

In order to analyse desired protein of interest from the whole cell yeast extract, western blotting was carried out on the SDS-PAGE separated proteins. The gels on which proteins reside was transferred on nitrocellulose membranes (Pall Corporation, USA) using a standard transfer apparatus (Mini PROTEAN 2-D Cell). Detection of lower molecular weight proteins such as histones and histone variants was facilitated by using methanol activated PVDF membrane. Completion of transfer was confirmed by staining the membrane with Ponceau S followed by washing with water. To avoid non-specific antibody binding, membranes were blocked with 5% milk, PBS-T buffer. To block PVDF membranes, 5% BSA TBST-T buffer was used. Blots were incubated in primary antibodies mixed in PBST-T/ TBS-T milk on a rotating rack (See-saw SSL4, Stuart See-saw rockers, Cole Parmer) at 4 °C overnight.

The next day blots were washed three times with 5% milk, PBS-T/ TBS-T buffers for 15 mins each followed by incubation in appropriate dilutions of (HRP)-conjugated secondary antibodies. Chemiluminescence was detected by using ECL prime/ ECL select western blotting detection reagents (Amersham) mixed in 1:1 ratio. Imaging was done by using ChemiDoc MP Imaging (BioRad).

3.4.5 Co-immunoprecipitation assay for detection of protein-protein interaction

In order to investigate protein-protein interactions occurring *in vivo* in yeast cells, 100 ml of cultures, final OD_{600} 1.9, were harvested at desired timepoints by centrifugation at 3000 rpm for 3 mins on a table top centrifuge. Pellets were transferred into clean microcentrifuge tubes, flash frozen in liquid nitrogen and stored at -20 °C.

Cells were mechanically lysed by adding 300 µl of IP buffer supplemented with protease inhibitors and 0.3 g glass beads. Cells were disrupted by bead beater (FastPrep24, MP biochemicals) twice for 60 seconds each on 6.0 setting while cooling in between the two cycles.

Lysates were further sonicated with a 30 sec on and 30 sec off cycle on a 25 cycles round. The sonicated lysates were transferred to clean pre-cooled microcentrifuge tubes and centrifuged at max speed for 20 mins. Cleared supernatant was transferred into a clean pre-cooled microcentrifuge tubes. Volumes were adjusted to 500 µl by adding pre-cooled IP buffer with protease inhibitor mix to each sample tube and then 50 µl was taken out in fresh tubes as input samples. ~1 µl of desired antibody was added to the remaining 450 µl of the sample and incubated on a rotating rack for 2 hours. Later, 30 µl of prewashed magnetic beads (Dynabeads Protein G coupled, Invitrogen, USA), resuspended in IP buffer, were added to the samples and the samples were further incubated at 4°C for 4 hours on rotation. Beads (containing bound samples) were then washed 3x10 mins, with IP buffer and finally transferred to fresh microcentrifuge tubes and resuspended in 40 µl of IP buffer. 20 µl of 3xSDS loading buffer was added to the samples and samples were heated at 98°C for 8-10 mins.

For input samples, proteins were precipitated with 10% of TCA. Excess TCA was washed out with 1 ml Acetone and the pellets were dried at RT. Further, pellets were resuspended in 40 µl of TCA resuspension buffer (2% SDS, 50 mM Tris, pH 7.5, 6 M Urea) and the pellets were manually broken down for better resuspension. After 30 mins of incubation, 20 µl of SDS loading buffer was added to it and samples were heated at 98°C for 8-10 mins.

3.4.6 Flow cytometry for cell cycle analysis

150 µl of cultures were collected in a pre-cooled microcentrifuge tube containing 350 µl of 100 % ethanol and stored at 4°C until all the time points were collected. Samples were spun at 7000 rpm for 3 mins in a table top centrifuge (5424, Eppendorf, Germany). Pellets were resuspended in sodium citrate solution [500 µl of 50 mM sodium citrate, 0.7 µl of RNase A (SIGMA-ALDRICH)]. Pellets were incubated overnight at 50°C in an incubator. The next day 10 µl of proteinase K (20mg/ml, VWR international) was added to the tubes and the samples were re-incubated at 50°C for 2 hours. 500 µl of 50 mM sodium citrate and 0.2 µl of SYTOX Green dye (Life technologies) was added to stain the DNA. Cells were briefly sonicated at the lowest power to avoid clumping and briefly vortexed just before analysis. Samples were analysed for DNA content using BD AccuriTM C6 (BD Biosciences, USA) flow cytometric data analysis was done by FlowJo Software (FlowJo LLC, Ashland, USA)

3.4.7 Live cell imaging and spindle staining

Live cell imaging and spindle staining was done to visualize metaphase/ anaphase arrest in Red1-expressing strains. Strains expressing GFP-Tub1 were cultured in YP-RG media following the standard mitotic growth culture protocol mentioned above and time points were collected at 0 hours and 4 hours. The imaging window of the MatTek dish (No. 1,5) was coated with concanavalin A (C2010-250MG). For this purpose, a fresh 1:10 dilution of the 1 mg/ml stock solution was prepared in PBS buffer. 60 μl of the diluted buffer was added to the glass window and spread equally using a pipette tip. The slide was incubated in the solution for 15 mins. Appropriate quantity of sample cells were collected in a microcentrifuge tube and sonicated for 1 min in a sonication bath. ConA solution was removed from the glass window using a pipette and the imaging surface was washed with 500 μl of PBS buffer. 60 μl of cells were added to the window and equally spread using a pipette tip. Cells were incubated in the window for 15 mins followed by 3x PBS washes. 500 μl of PBS was added to the slide window and immediately proceeded for imaging. Imaging was done by using Delta Vision microscope at 100X with appropriate software settings. Image analysis was done using ImageJ.

Chapter 4

Results

One of the defining features of meiosis is the formation of interhomolog crossovers during prophase I. The establishment of crossovers ensures proper homolog segregation during meiosis by enabling physical linkage between initially unpaired homologous chromosomes. In order to produce crossovers, DNA double-stranded breaks (DSBs) are introduced in a programmed manner during early meiosis by the action of meiosis-specific endonuclease Spo11 (Keeney *et al.*, 1997). Following this, the DSBs are predominantly repaired by employing an essentially error-free homologous recombination repair mechanism.

During meiosis in budding yeast, a preferential bias is observed for the usage of the homologous chromosome as a repair template instead of the default sister chromatid (predominantly observed in mitosis) for homologous recombination repair. The activity of such enforcement is encoded in a key meiosis-specific kinase - 'Mek1'. Mek1 is recruited and activated at sites of DSB via two other meiosis-specific accessory proteins - Hop1 and Red1, components of the meiotic chromosomal axis (Kniewel *et al.*, 2017; Niu *et al.*, 2007; Niu *et al.*, 2005; Wan *et al.*, 2004). Although studies have been done to understand downstream proteins, pathways and processes controlled by Mek1 activity, the exact mechanism behind homolog's biased use still remains to be studied and runs as a hypothetical model (Goldfarb & Lichten, 2010; Subramanian *et al.*, 2016). Moreover, understanding the mechanism of template bias is complicated by the fact that both Red1 and Hop1 positively regulate upstream DSB formation. Therefore deletion of *RED1* or *HOP1* influences the introduction of DSBs in meiosis and the subsequent repair process. Here I attempt a novel approach to study the meiotic interhomolog bias by expressing Red1, Hop1 and Mek1 in an ectopic environment *i.e*, in vegetatively dividing cells (where they usually are not expressed) by employing galactose-based inducible systems (Figure 4-1 A). In this Ph.D. work, I aim to use this synthetic system to - i) Devise a minimal meiosis-specific complex that is active outside its native environment (the meiotic prophase I) and which is involved in the template switch ii) Understand the conditions necessary for activation of Mek1 in the synthetic system iii) Study the mechanism for homolog template bias, specifically in the context of the spatial proximity model proposed by (Subramanian *et al.*, 2016).

4.1 Ectopically expressed dimerized Mek1 is active

To express meiosis-specific proteins in vegetatively dividing cells, I employed a galactose based inducible system. Using this system I initially attempted to express Mek1 kinase. As Mek1 activity is influenced by Hop1 mediated dimerisation during meiosis (Niu *et al.*, 2007; Niu *et al.*, 2005), I explored the expression of dimerised Mek1. Moreover, to propagate artificial dimerisation of Mek1, I used a GST tagging method. Artificial dimerisation can be induced by tagging proteins with GST (Tudyka & Skerra, 1997). GST-mediated artificial dimerisation of Mek1 is known to establish an active form of Mek1 (de los Santos & Hollingsworth, 1999; Niu *et al.*, 2007; Wan *et al.*, 2004; Wu *et al.*, 2010) during budding yeast meiosis. Therefore, I tested whether ectopic expression of GST-tagged Mek1 would be sufficient for activation of Mek1 in mitotically dividing cells. For this purpose, I created a galactose-inducible construction by integrating a *pGAL1::GST* fragment upstream of the Mek1 coding region, thereby replacing the endogenous Mek1 promoter. Cultures were grown in a carbon source medium (*i.e* raffinose), that keeps the *pGAL1* in an inactive state. Upon addition of galactose, the Gal4p transcription factor gets recruited to p*GAL1* driving the transcription of Mek1 (Johnston, 1987).

Primary cultures were grown overnight at standard conditions in YP-RG media followed by dilution to OD_{600} 0.48 the next day. The resulting secondary cultures were further grown for an additional 3.5 hours before the addition of galactose. The time of galactose induction was considered as 0 hours and the time course was carried out accordingly. Samples were collected at 0 hours and 4 hours by harvesting 5 ml cultures of OD_{600} 1.9.

Activation of Mek1 was monitored by observing a known Mek1 substrate, Threonine 11 of Histone H3, that is transiently phosphorylated by Mek1 kinase activity (H3-T11 phosphorylation) during meiosis (Kniewel *et al.*, 2017). Indeed, in my experiment, I observed H3-T11 phosphorylation, indicative of Mek1 activity at 4 hours by western blotting (Figure 4-1 C). A non-specific background signal was observed at the H3-T11 phosphorylation level in the culturing conditions, which could result from cross-reactivity of the specific antibody batch by non-specific epitope recognition. Alternatively, it could be due to the activation of certain kinase pathways in response to the used nutritional conditions (*i.e* growth in YP-Raffinose media) (Oh *et al*, 2020; Oh *et al*, 2018). As I observe a prominent H3-T11 phosphorylation signal in the GST-Mek1 expression condition, I conclude that artificial dimerization of Mek1 confers an active form in an ectopic system. Further, I explored Mek1 activity in a non-

dimerizing condition. In this case, Mek1 was tagged with GFP by integrating a *pGAL1::GPF* cassette upstream of the Mek1 coding region. As expected, no H3-T11 phosphorylation was detected for this strain at 4 hours after galactose induction.
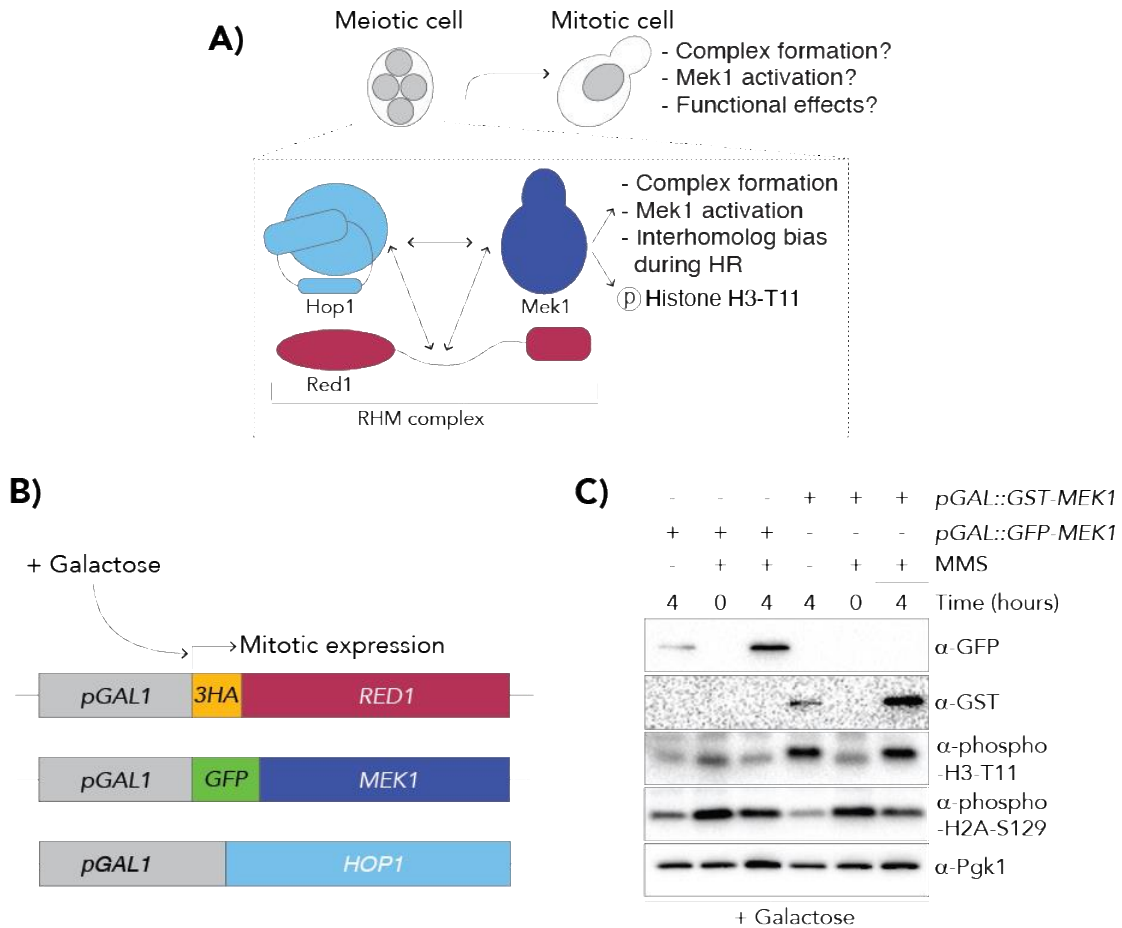
Figure 4-1: Ectopic expression system for Red1, Hop1 and Mek1 expression

A) Schematic overview addressing the aims of this work.

B) Schematic of alleles, genetically modified to introduce *pGAL1* upstream of the coding start sites of respective genes. Red1 is NH2-terminally epitope-tagged with 3xHA (strain yGV3726), Hop1 is untagged (yGV3243) and Mek1 is NH2-terminally GFP tagged (yGV2812). Expression of proteins is achieved by adding 2% galactose to the cultures.

C) Western blot analysis of Mek1 activation in mitotically dividing cells for *pGAL1::GST-MEK1* (yGV2774) and *pGAL1::GFP-MEK1* (yGV2812). Indicated timepoints are after addition of galactose. 0.05% (v/v) MMS was added, 0.5 hours before galactose induction. See the methods section for detailed time course protocol, growth conditions and drug treatment. α-H3 T11 phosphorylation antibody was used to detect Mek1

activation. α-H2A S129 ph was used to monitor Mec1/Tel1 activity. α-GST and α-GFP were used to detect Mek1 and Pgk1 was probed as a loading control.

During meiosis, Mek1 activation results from downstream signalling due to DNA double-stranded break formation. Therefore in order to mimic early meiotic conditions, DNA damage was introduced in cultures expressing GST-Mek1 and GFP-Mek1, by adding the DNA damaging drug, Methyl methanesulfonate (MMS; causes DNA methylation leading to damage) (0.01%), 0.5 hours before galactose induction. MMS is not per se a DSB inducing agent, although it is greatly used as a radiomimetic / DSB inducing agent in several studies (Mankouri & Hickson, 2006; Myung & Kolodner, 2003; Ui *et al*, 2005). HR is instead induced in this case, as a result of a replication block (Lundin *et al*, 2005). MMS is a methylating agent that methylates the oxygen or nitrogen residues on the DNA backbone. DNA backbone methylation usually triggers BER repair (Base Excision repair) leading to ssDNA formation. During S-phase, when replication forks encounter the ssDNA, they are stalled and collapse to induce DSBs. Thus, DSBs formed after treatment with MMS requires passage through S-phase (Lundin *et al.*, 2005). As a result of DSBs, Mec1/Tel1 are activated (Baldo *et al.*, 2008; Bandhu *et al*, 2014). DNA damage was monitored in this and all further experiments by observing the phosphorylation of Serine 129 at the histone H2A (H2A-S129 phosphorylation). This particular histone site is phosphorylated in response to Mec1 activity (Downs *et al*, 2000). Despite the rapid induction of DNA damage, GFP-Mek1 was inactive, while no change was observed in GST-Mek1 activity as monitored by H3-T11 phosphorylation levels. Together, this data suggests that GST-Mek1 is active in an ectopic environment without the need for any additional meiosis-specific components or the induction of DNA damage. However, DNA damage is not sufficient for activation of GFP-Mek1 under our growth conditions. This prompted us to test the requirement for other meiosis-specific components that might aid in Mek1 activation in the synthetic system.

4.2 Ectopic expression of Red1, Hop1 and Mek1

As no activation of Mek1 was observed for the GFP-Mek1 expressing condition even after DSB inducing, I investigated the requirement for other meiosis-specific factors that aid in this process. In meiosis, Red1 and Hop1 are accessory proteins to Mek1 that form the meiotic chromosomal axis during early G2/ Prophase even prior to DSB formation (Panizza *et al.*, 2011; Smith & Roeder, 1997; West *et al.*, 2019). Even though no direct interaction between Red1-Mek1 is observed to date, Red1 is known to influence Mek1 activation by interacting with Hop1

and forming chromosomal structures that aid in DSB repair. On the contrary, Hop1 is directly involved in the recruitment of Mek1 to chromosomes by binding to the Mek1 FHA domain and driving its dimerization (Carballo *et al.*, 2008; Chuang *et al.*, 2012; Niu *et al.*, 2007). As such, it is speculated that Hop1 may lead to a local increase in the concentration of Mek1, thereby facilitating its dimerization and activation (Carballo *et al.*, 2008; Niu *et al.*, 2007). Thus, after understanding the roles of Red1 and Hop1, I proceeded by co-expressing Red1 and Hop1 in my synthetic system. For this purpose, I again employed a galactose-based inducible system. *pGAL1* promoter was placed upstream of the coding regions of each of these genes with Red1 and Mek1 also carrying NH2- terminal tags - 3xHA and GFP, respectively, to aid in probing for their expression levels (Figure 4-1 B). An increase in expression of respective proteins was observed after galactose induction in a 2-4 hours time window by using western blotting (Figure 4-2 A). The earliest time point at which the proteins were detected is 2 hours after galactose induction.
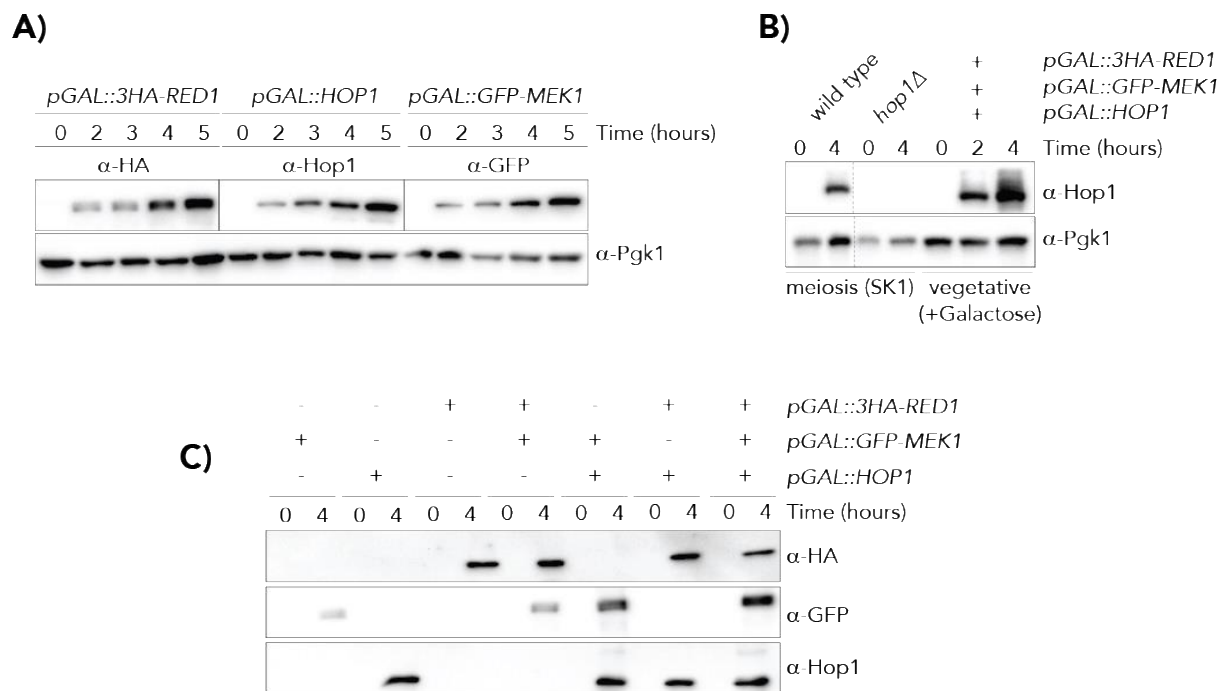
Figure 4-2: Ectopic expression of the components of the RHM complex

A) Expression levels of individual components of the RHM complex *viz* 3HA-Red1 (yGV3726), Hop1(yGV3243) and GFP-Mek1 (yGV2812). Indicated time points were after the addition of galactose. See methods for a detailed protocol of the time course. α-HA was used to detect Red1, α-Hop1 was used to detect Hop1 and α-GFP was used to detect Mek1.

B) Comparison of Hop1 expression in the ectopic mitotically dividing cultures relative to the expression of Hop1 in wild type meiotic expression condition. A Red1, Hop1 and Mek1 expressing strain (yGV4806) was used for the mitotic expression. A meiotic time course was done using SK1 strains [wild type condition (yGV49), *hop1Δ* (yGV4442)]. In case of mitotic cultures, indicated time points are after galactose induction. α-Hop1 was used to detect Hop1 by western blotting and α-Pgk1 was probed as a loading control.

C) Western blot detecting the expression of Red1, Hop1 and Mek1 in strains harbouring combinations of *pGAL1::3HA-RED1, pGAL1::HOP1* and *pGAL1::GFP-MEK1*. Indicated time points are after induction of galactose. α-Hop1, α-HA and α-GFP antibodies were used to detect Hop1, Red1 and Mek1, respectively. α-Pgk1 was probed as a loading control. Strains used are yGV3726, yGV3243, yGV2812, yGV3235, yGV3219, yGV3255 and yGV4806.

To further investigate the combined effect of Red1-Hop1-Mek1 in Mek1 activation, strains expressing 3xHA-Red1, Hop1 and GFP-Mek1 were crossed to generate all possible Red1-Hop1-Mek1 combinations. No expression of proteins was observed under conditions lacking galactose. However, an increase in expression of the respective proteins was observed in the combination strains using western blotting with antibodies α-HA, α-Hop1 and α-GFP that probed for Red1, Hop1 and Mek1, respectively (Figure 4-2 C). Increased levels of Mek1 protein were noted, for example, when Mek1 was present in combination with Red1 and/or Hop1. A further increase in stability of Mek1 was observed when it was co-expressed simultaneously with Hop1 and Red1, suggesting that co-expression of the three proteins may lead to the formation of a stable complex. As such, this hinted at a possible interaction between the three proteins.

To compare the protein levels observed in our synthetic system with those usually observed in physiological meiotic conditions, I compared expression levels of Hop1 in our system to the endogenous meiotic protein levels. Here, I have compared only Hop1 levels due to the lack of availability of α-Red1 or α-Mek1 antibodies. Nonetheless, this experiment provides an insight into how these components are expressed in our system compared to their physiological expression levels. I found that 2 hours after galactose induction yielded similar levels of Hop1 protein as endogenous in meiotically dividing cells, after 4 hours of meiotic induction (during meiotic prophase I) (Figure 4-2 B). Hop1 protein levels further increased at 4 hours in galactose. I conclude that, at least for Hop1, protein levels in the ectopic system are

comparable to endogenous meiotic conditions. Further experiments need to be done to investigate and compare expression levels for Red1 and Mek1 with physiological meiotic expression levels.
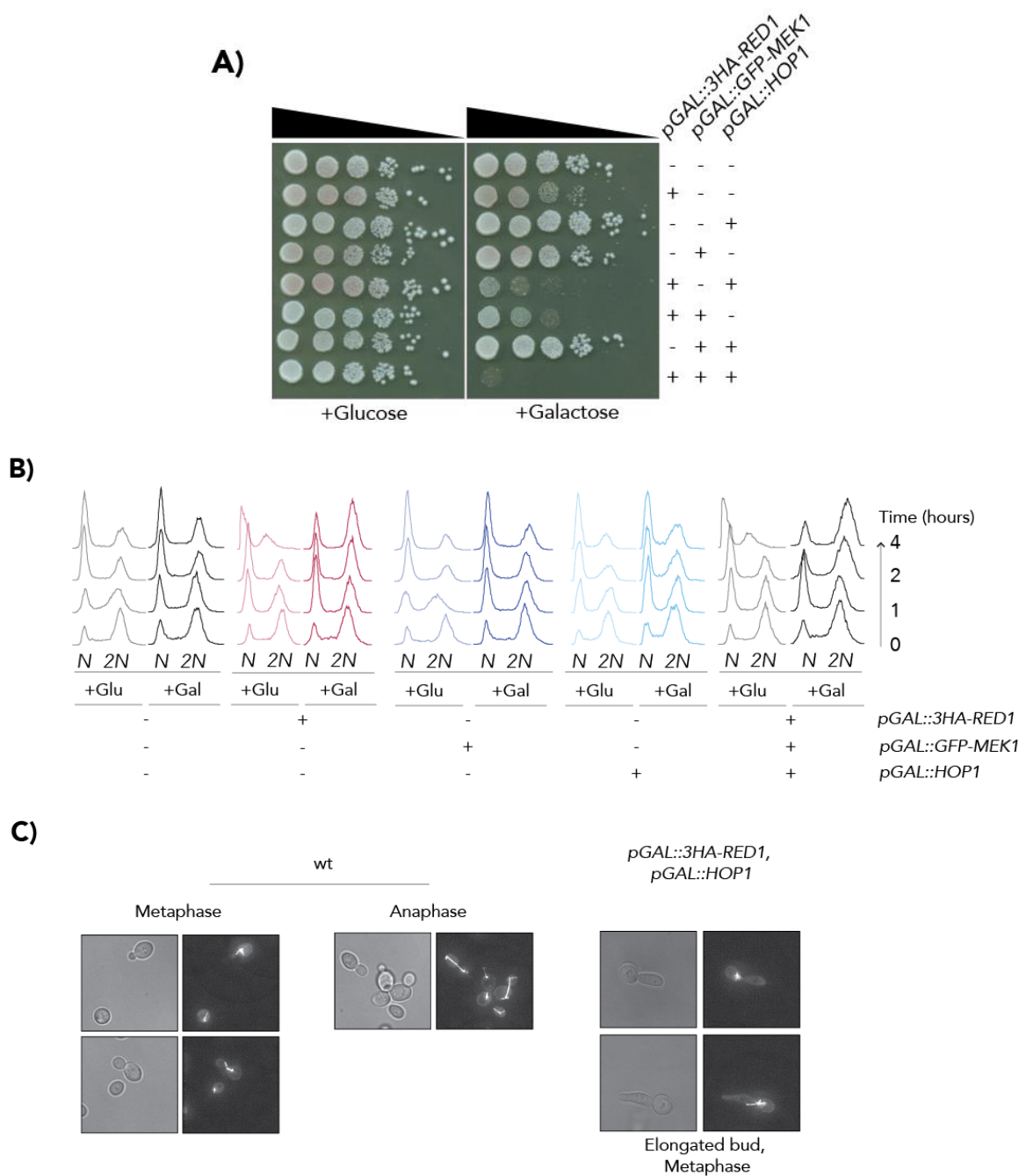
4.3 Ectopic expression of Red1 leads to a slow growth phenotype

Red1, Hop1 and Mek1 are meiosis-specific proteins. Therefore, I was curious to investigate the effect of their expression in the ectopic condition. To this end, I first aimed to observe potential cell growth phenotypes triggered by the expression of these factors (in isolation or combinations). I conducted a growth assay by spotting 10-fold serial dilutions of strains expressing Red1, Hop1 and Mek1 individually and in combinations, on YP-glucose (control; no expression) and YP-galactose plates (expression). I observed significant growth defects in the strain expressing Red1 on galactose plates (Figure 4-3 A). Hop1 and Mek1 expressing strains appeared to have no change in growth phenotype. The growth defect in Red1 was exacerbated when co-expressed with Hop1 or Mek1, and was aggravated further when all three of them were simultaneously expressed (Figure 4-3 A).

To investigate whether the growth defect corresponded to a possible cell cycle delay/ arrest, I performed flow cytometry analysis on cultures expressing RHM combinations and collected time points between 0-4 hours after galactose induction. I indeed observed an accumulation of Red1 expressing strains in 2N state (note these cells are haploid), indicative of a (post S-phase) arrest/delay possibly in G2/M (Figure 4-3 B). These findings are consistent with an earlier study (Sopko *et al.*, 2006) where a high throughput screening was performed to observe phenotypic effects of overexpression of 5280 genes in *S. cerevisiae*. Consistent with our data, the study also reports an accumulation of cells in 2N state after Red1 overexpression by flow cytometry profiles.

In order to further elucidate the nature of the cell cycle defect, I investigated the mitotic stage in which the arrest occurs. In addition, I monitored the morphology of the cells by confocal microscopy (DeltaVision Elite) by performing live-cell imaging experiments.

By observing the separation between spindle poles and spindle morphology, the cell cycle stage (*i.e* metaphase or anaphase) can be determined. In these strains, tubulin had a functional NH_2-terminal GFP tag (*GFP-TUB1*).

A)

+Glucose   +Galactose

pGAL::3HA-RED1	pGAL::GFP-MEK1	pGAL::HOP1
-	-	-
+	-	-
-	-	+
-	+	-
+	-	+
+	+	-
-	+	+
+	+	+

B)

Time (hours): 4, 2, 1, 0

N 2N	N 2N	N 2N	N 2N	N 2N	N 2N	N 2N	N 2N	N 2N	N 2N	
+Glu	+Gal	+Glu	+Gal	+Glu	+Gal	+Glu	+Gal	+Glu	+Gal	
-	+	-	-	-	-	-	-	-	+	*pGAL::3HA-RED1*
-	-	-	+	-	-	-	-	-	+	*pGAL::GFP-MEK1*
-	-	-	-	-	-	-	+	-	+	*pGAL::HOP1*

C)

wt   pGAL::3HA-RED1,
                                                       pGAL::HOP1

Metaphase   Anaphase

Elongated bud,
Metaphase

Figure 4-3: Effect of Red1-Hop1-Mek1 expression on cell cycle in mitotic dividing cells

A) Growth assay by spotting 10-fold serial dilutions of the indicated strains on glucose (control) and galactose plates. Strains used are the following, yGV104, yGV3726, yGV3243, yGV2812, yGV3235, yGV3219, yGV3255 and yGV4806. Images were obtained after 2-4 days of incubation.

B) Representative histograms of DNA content of cells in different cell cycle stages assessed by Flow Cytometry. Indicated time points are after galactose induction. 'N' and '2N' represent the G1 and G2/M phases, respectively. Cultures were grown in glucose containing media (+Glu) and induced with galactose (+Gal). DNA staining was

done with SYTOX Green. Strains used were yGV104, yGV3726, yGV3243, yGV2812, yGV4806.

C) Live cell microscopy and spindle staining of wild type and Red1-Hop1 (yGV3235) expressing strains. Both strains harbour a *GFP-TUB1* allele. Images are obtained via Delta Vision microscope in bright field and GFP settings. Fluorescent images depict spindles. Elongated buds are observed for Red1-Hop1 expressing condition.

As Mek1 is also tagged with GFP in our system, I decided to carry out morphology analysis on Red1-Hop1 strains to avoid background fluorescence from GFP-Mek1. For Red1-Hop1 expressing strains, bright field images alone indicated an increase in the population of cells with large elongated buds. This phenotype is typical of mitotic arrest in cases where cells are no longer able to undergo cytokinesis. Indeed, checkpoint mutants such as *rad53Δ,* under replication stress, were unable to orient the cytoskeleton resulting in elongated buds due to cytokinesis defects (Enserink *et al.*, 2006). Typically, cells arrest in metaphase due to errors in spindle attachment to kinetochores leading to spindle assembly checkpoint activation. Metaphase cells have spindles that are bright, and have a small dumbbell-like shape with small cytoplasmic microtubule protrusions (~1-2 mm in size) (Figure 4-3 C). Anaphase spindles, on the other hand, are large and can span the entire length of the cell, including the bud and are typically 7-8 mm in size (Figure 4-3 C). In the Red1-Hop1 expressing condition, all of the elongated-budded cells have short bright metaphase spindles with prominent cytoplasmic microtubules protruding out, thus indicating a possible metaphase arrest (Figure 4-3 C).

Currently, I do not understand the pathways involved in mediating the arrest. However, I was able to narrow down a small extreme C-terminally located fragment of Red1, known to form Red1 filaments, that causes the cell cycle arrest phenotype. These experiments are discussed in the later section.

4. 4 Red1, Hop1 and Mek1 interact and associate, forming a trimeric complex

Having established an ectopically controllable system to modulate the expression of meiotic proteins in cycling cells, I further aimed to examine a potential functional interaction between Red1, Hop1 and Mek1. For this purpose, I employed *in vivo* co-immunoprecipitation assays. α-HA IPs were performed in 3xHA-Red1 strains expressing different Red1-Hop1-Mek1 combinations. Through this approach, I could observe that Hop1 and Mek1 co-precipitated with Red1 in Red1-Hop1 and Red1-Mek1 expressing conditions (Figure 4-4 A). I

conclude that both of these proteins interact with Red1 individually, *i.e,* without the need for the third component of the complex. Under conditions where Red1, Hop1 and Mek1 are co-expressed, both Hop1 and Mek1 co-precipitated with Red1 upon Red1 pulldown, suggesting that <u>R</u>ed1-<u>H</u>op1-<u>M</u>ek1 interact to form a complex (RHM complex from here on) and are autonomously assembled in our ectopic system without the need for any other meiosis-specific proteins and/or modifications. I also performed a reverse Co-IP (*i.e.* α-GFP IP) on GFP-Mek1 and confirmed that Red1 and Hop1 co-precipitated with Mek1 in our expression condition (Figure 4-4 B). In addition to the known Red1-Hop1 interaction (West *et al.*, 2018), my data also indicates a novel interaction between Red1 and Mek1. This interaction is independent of the necessity for any other meiosis-specific proteins. This suggests a potential binding site in Red1 for Mek1.
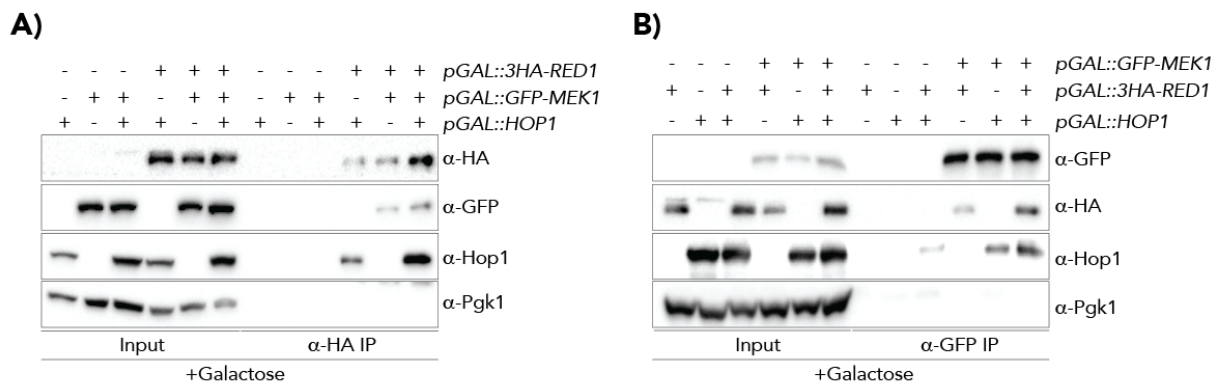
Figure 4-4: Co-immunoprecipitation experiments for assessing the association amongst Red1, Hop1 and Mek1

A) α-HA IP on 3xHA-Red1. Strains used are the following: yGV3243, yGV2812, yGV3235, yGV3219, yGV3255 and yGV4806. Samples were collected 4 hours after galactose induction. α-Hop1 was used to detect Hop1, α-HA was used to detect Red1, and α-GFP was used to detect Mek1. α-Pgk1 was probed as a loading control.

B) Red1, Hop1 and Mek1 interaction was confirmed by α-GFP IP on GFP-Mek1. The following strains were employed: yGV3243, yGV3726, yGV3235, yGV3219, yGV3255 and yGV4806. α-Hop1, α-GFP and α-HA antibodies were used to detect Hop1, Mek1 and Red,1 respectively.

4.5 Activity of Mek1 kinase in the ectopic RHM complex

The function of the RHM complex to form a template bias during DSB repair lies in the activity of the kinase Mek1. To determine whether Mek1 is active in our ectopic system, I again monitored H3-T11 phosphorylation levels when Mek1 was co-expressed with Red1 and Hop1. None of the binary combinations led to activation of Mek1, demonstrating that the expression and assembly of Mek1 in the RHM complex alone is not sufficient to trigger Mek1 activation. As mentioned earlier, in meiosis, Mek1 activity is associated with phosphorylation of Hop1 by Mec1/ Tel1 kinases in response to DSB formation by Spo11 (Carballo *et al.*, 2008). Therefore, to reproduce meiotic-like DNA damage conditions, I treated cultures co-expressing Red1-Hop1-Mek1 with MMS. Induction of DNA damage was monitored by observing H2A-S129 phosphorylation status. Interestingly, H3-T11 phosphorylation was observed when the RHM complex was expressed in the presence of MMS-induced DNA damage (Figure 4-5 A). As shown earlier, no activation of Mek1 was triggered when the RHM complex was expressed in the absence of MMS. Similarly, DSBs alone did not lead to an increase in H3-T11 phosphorylation.

MMS is a DNA alkylating agent that modifies purines in DNA to generate heat-labile DNA (Lundin *et al.*, 2005). Upon interaction with the replication fork, MMS-driven modified nucleotides can lead to fork collapse and the formation of DNA double-stranded breaks. As MMS-mediated DNA damage signalling is different from meiotic breaks formed by Spo11. Therefore, I confirmed my prior results of activation of GFP-Mek1 in the presence of RHM complex by employing other DSB inducing agents. Cultures were treated with Phleomycin (a bleomycin family drug) that triggers DNA double-stranded breaks (Moore, 1988). Similar to MMS-induced activation, Mek1 kinase activity was also observed after treatment with Phleomycin (Figure 4-5 B). Zeocin (A phleomycin D1 formulation) also led to similar results (data not shown).

To test the time window in which Mek1 gets activated in the ectopic system, I performed a time course by collecting samples at 0, 2, 3, 4 hours after galactose treatment. I observed an apparent increase of Red1/Hop1/Mek1 levels in cultures treated with galactose. At 4 hours the H3-T11 phosphorylation signal was comparable to the signal observed during meiotic conditions (Figure 4-5 C). Thus I conclude that a threshold level of Red1-Hop1-Mek1 is necessary to generate detectable levels of active Mek1. The rest of the experiments in this study

aimed to understand conditions for Mek1 activation were hence conducted at 4 hours after galactose treatment.
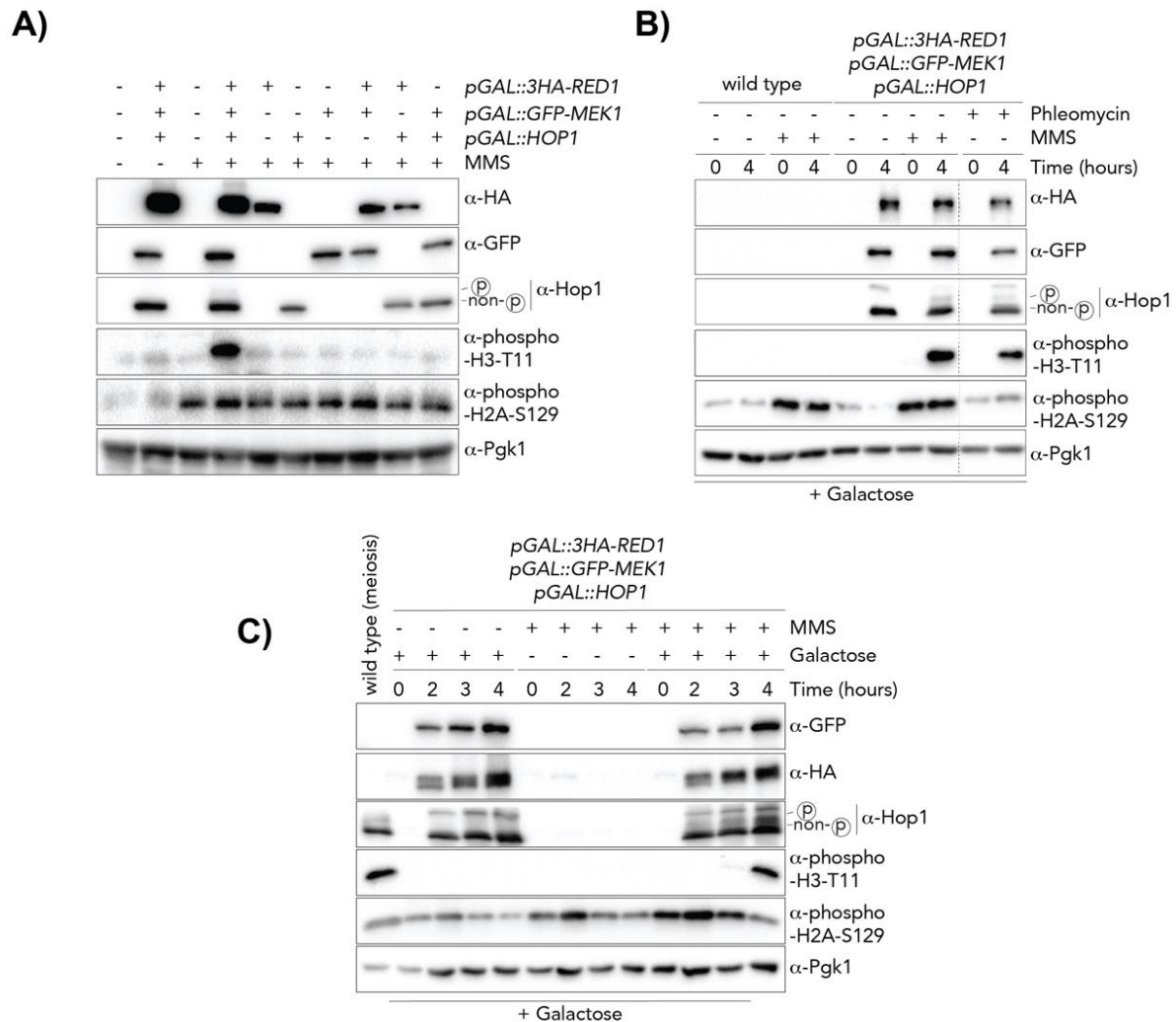
Figure 4-5: Conditions for activation of Mek1 in mitotically dividing cells

A) Activation of Mek1 monitored by western blot in strains harbouring combinations of *pGAL1::3HA-RED1, pGAL1::HOP1* and *pGAL1::GFP-MEK1*. Samples were taken 4 hours after galactose induction. 0.01% (v/v) MMS was added 0.5 hours prior to galactose induction. Activation of Mek1 was observed only for strains expressing Red1, Hop1 and Mek1 along with treatment with MMS. α-Hop1, α-HA and α-GFP antibodies were used for the detection of Hop1, Red1 and Mek1, respectively. A higher migrating Hop1 phosphorylated form is detected on the Hop1 blot, which likely represent a well-known phosphorylated version of Hop1 (Carballo *et al.*, 2008). α-H3 T11 phosphorylation antibody was used for visualizing activation of Mek1. α-H2A S129

phosphorylation was used to detect Mec1/ Tel1 activity. α-Pgk1 was probed as a loading control. Strains used are the following: yGV3243, yGV2812, yGV3235, yGV3219, yGV3255, yGV3726, yGV104 and yGV4806

B) Activation of Mek1 by using phleomycin as a DNA damaging drug. Strains used were wild type (yGV104) and Red1-Hop1-Mek1 expressing strain (yGV4806). Red1, Hop1 and Mek1 were detected using α-HA, α-Hop1 and α-GFP antibodies via western blotting. A higher migrating band is detected on a Hop1 blot representing the Hop1 phosphorylated form. α-H3 T11 phosphorylation represents Mek1 activity and α-H2A S129 phosphorylation detects Mec1/ Tel1 response to DSBs. Pgk1 is the loading control.

C) Mitotic time course to determine the time of activation of Mek1. Red1-Hop1-Mek1 expressing strains were grown overnight followed by dilution in the morning. 0.01% (v/v) MMS was added 3 hours later followed by (2%) galactose induction at 3.5 hours. Indicated time points are after galactose induction. Strain used was (yGV4806), that expressed Red1, Hop1 and Mek1. For the meiotic control, meiotic time course was done with an SK1 strain (yGV49). Red1, Hop1 and Mek1 were detected using α-HA, α-Hop1 and α-GFP antibodies. Activation of Mek1 was detected with α-H3 T11 ph and Mec1/ Tel1 activation was detected with α-H2A S129 phosphorylation. α-Pgk1 was probed as a loading control. Activation of Mek1 was first detected at 3 hours but represented a signal corresponding to meiotic levels at 4 hours.

4.6 Upstream DNA damage signalling and dependence of cell cycle on Mek1 activity

The Spo11 induced breaks in meiosis are repaired by mechanisms that initiate from detection of the breaks to activation of mediator kinases that phosphorylate strand invasion proteins. As mentioned earlier, Mec1/ Tel1 kinases are the primary sensory kinases that are activated in response to meiotic DSBs. Amongst many known targets of Mec1/ Tel1 are the meiotic axial element Hop1 (Carballo *et al.*, 2008; Cheng *et al.*, 2013). The phosphorylation of Hop1 is primarily driven by Mec1 (Carballo *et al.*, 2008; Penedos *et al*, 2015), and this event is essential for the RHM complex regulation. I decided to investigate the upstream signalling events responsible for the Mek1 activation in our ectopic system to determine whether a similar kinase pathway is also activated in the ectopic condition. I performed experiments by introducing *mec1*Δ (Figure 4-6 E) (with a *sml1*Δ background as only *mec1*Δ is

lethal, *i.e. mec1Δ smll1Δ*) into RHM expressing strain. Deletion of *MEC1* led to a marked reduction in H3-T11 phosphorylation signal, suggesting a role for Mec1 in Mek1 (Figure 4-6 E). Thus, similar to meiosis, Mec1 signalling appears to be crucial for DSB induced Mek1 activation in mitosis. *tel1Δ* , on the other hand, did not perturb Mek1 activation levels (Figure 4-6 E). Although in yet another *tel1Δ* strain condition, I observed a decrease in H3-T11 phosphorylation levels. I speculate this apparent discrepancy could be due to some unknown factors in both of these strains. For example, rad5 is a DSB repair pathway (Torres-Ramos *et al*, 2002) protein. Some of these strains carry a recessive *rad5* allele. It would be interesting to check whether RAD5/ *rad5* affects the *tel1Δ* pathway for Mek1 activation in our synthetic system.

The ectopic system herein developed allows us to investigate mechanisms of Mek1 activation that are usually difficult to address in meiotically dividing cells. One such example is investigating potential cell cycle-dependent effects on upstream DSB signalling that leads to Mek1 activation *i.e* It would be interesting to test if Mek1 can be activated outside the G2-like cell cycle stage. However, since Mek1 is a meiosis-specific protein, it is difficult to understand the effect of cell cycle regulatory proteins on Mek1 function in physiological meiotic conditions. As such, I expressed Red1-Hop1-Mek1 combined with the induction of DNA damage, in cells arrested in G1 (by addition of a-factor) or in G2/M (by treatment with Nocodazole). Synchronisation was confirmed by analysing samples via flow cytometry (Figure 4-6 B). Roughly 80% of cells were arrested in G1 at 4 hours, while ~ >90% of cells were in G2/M at this time (Figure 4-6 B). I initially looked at conditions where DNA damage was introduced by MMS (Figure 4-6 A). In accordance with the mode-of-action of MMS (described above), where MMS produces DSBs upon encounter of replication forks by methylated DNA; thus DSBs are produced in/ after S-phase with MMS treatment. Therefore, DSBs were not observed for α-factor arrested cultures treated with MMS by monitoring H2A-S129 phosphorylation levels. However, in G2/M arrested cells, DSBs were present as monitored by H2A-S129 phosphorylation, and a corresponding marked increase in H3-T11 phosphorylation signal was observed in response to DSBs (Figure 4-6 A). Thus activation of Mek1 was seen in G2/ M state.
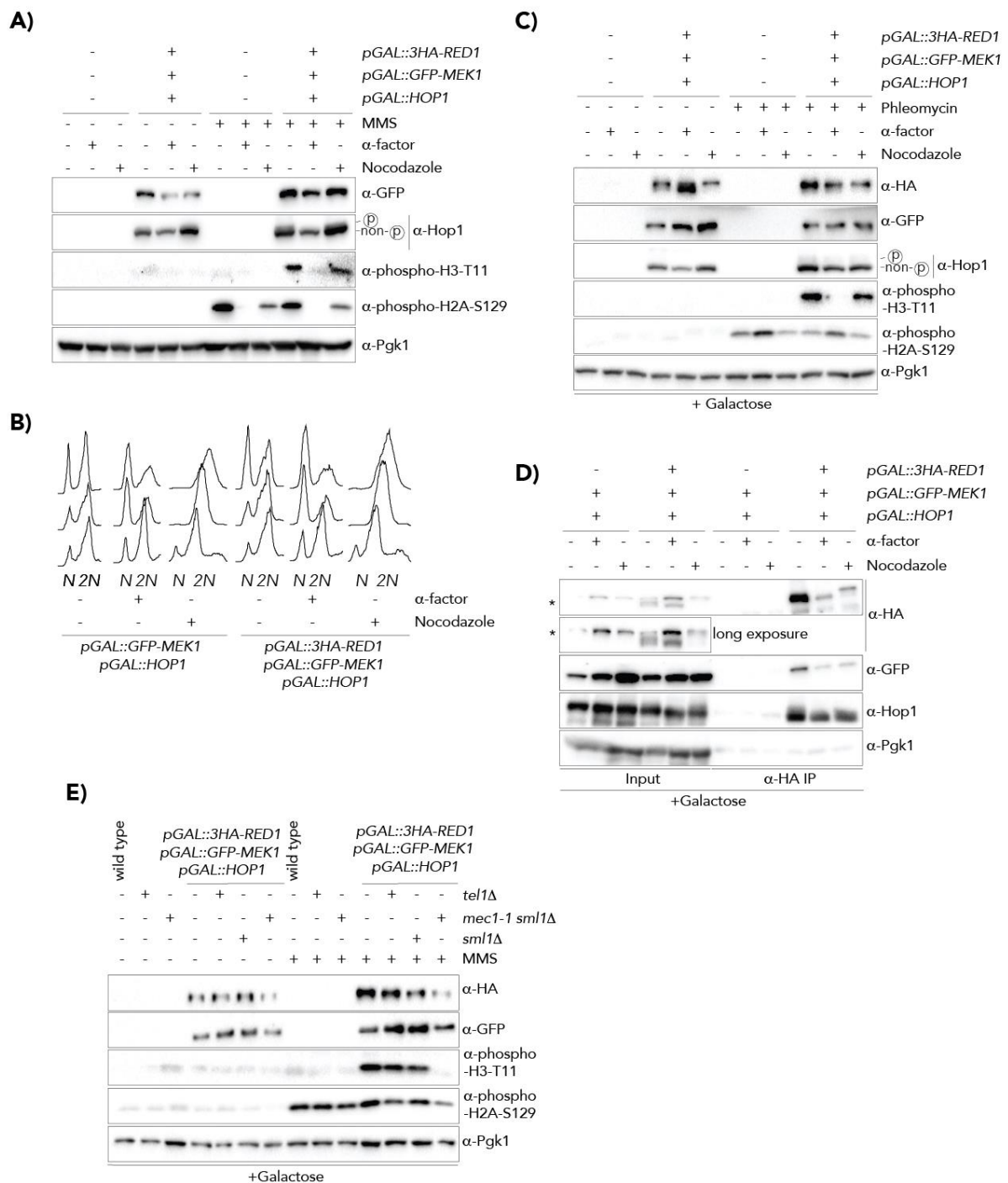
Figure 4-6 : Cell cycle dependence on activation of Mek1

A) Mek1 activation in different cell cycle phases. Cells were arrested in G1 by treatment with α-factor and in mitosis by treatment with nocodazole. Arrest was confirmed with flow cytometry analysis. Strain used was yGV4806. Samples were taken 4 hours after galactose induction. DSBs were induced by treatment with 0.01% (v/v) MMS. Expression of Mek1 and Hop1 was detected by probing with α-GFP and α-Hop1 antibodies respectively. α-H3 T11 phosphorylation was used to detect activation of

Mek1. α-H2A S129 phosphorylation was used to detect Mec1/Tel1 activity and thus monitor DNA damage. Slower migrating Hop1 band likely represents phosphorylated form of Hop1. Strains used were yGV104 and yGV4806.

B) Cell cycle profiles for G1 and G2/M arrested cells (from figure 4-6 A) by flow cytometry. 'N' and '2N' peaks represent cells in G1 and G2/M stage respectively. Samples were taken at 0, 2 and 4 hours after galactose induction (represented from bottom (0 hours) to up (4 hours). Strains used were yGV104 and yGV4806.

C) Same experiment as figure 4-5A but with phleomycin-induced DNA damage.

D) α-HA based co-immunoprecipitation assay. Co-IP was performed on Hop1-Mek1 (control) and Red1-Hop1-Mek1 expressing strains (yGV3219 and yGV4806). Cells were arrested in G1 by treatment with α-factor and in mitosis by treatment with nocodazole. * denotes background band was detected for α-HA probed blot. Increased interaction was noted for asynchronous cultures. Longer exposure image was taken for α-HA blot. Cell cycle progression was monitored by using flow cytometry analysis.

E) Analysis of Mek1 activation in cells expressing Red1, Hop1 and Mek1 in wild type, *sml1Δ, and mec1Δ sml1Δ*. MMS was used to induce DNA damage; cells were treated with MMS for 4.5 hours. Galactose-based induction was done for 4 hours. α- H2A S129 phosphorylation was used to detect Mec1/Tel1-dependent activation, α-H3 T11 phosphorylation was used to detect Mek1 activation. α-GFP was used to detect Mek1, α-HA was used to detect Red1. Pgk1 was probed as loading control. Yeast strains used yGV104, yGV3713, yGV3719, yGV4806, yGV5011, yGV5033, yGV5044.

To overcome the incompetence of MMS to induce breaks in G1, which precluded me from analysis of the RHM activation in different cell cycle phases, I explored phleomycin as a DSB inducing agent. Under these conditions, I observed H3-T11 phosphorylation signal for G2/ M arrested cells, confirming my previous result (Figure 4-6 C). Interestingly, G1 arrested cells were unable to trigger Mek1 activation (Figure 4-6 C). To investigate the lack of activation under these conditions, I monitored the H2A S129 phosphorylation signal. DNA Breaks were induced with phleomycin treatment in G1 arrested cells as Mec1 mediated H2A S129 phosphorylation was observed (Figure 4-6 C).

A possibility could be that the RHM complex cannot be formed in a G1 arrested state, which would lead to a lack of Mek1 activation. To test this, I performed α-HA IP by pulling down 3xHA-Red1 under different cell cycle synchronization conditions. I observed co-precipitation of Hop1 and Mek1 in G1 and G2/ M arrested cells suggesting that a complex can

be formed in these cell cycle stages. However, Mek1 remained inactive in the G1-phase despite the presence of all the conditions that I have investigated so far to enable Mek1 activation *i.e* formation of RHM complex, presence of DNA damage and Mec1 signalling. This suggests the role of other yet unknown proteins/ pathways activated in the S/ G2/ M phase that contribute to Mek1 activation. Further experiments need to be done to investigate these mechanisms. Speculations on why Mek1 is not active in G1 are mentioned in the discussion section.

4.7 Involvement of structural domains of Red1 in RHM complex activation

Many eukaryotic organisms form meiosis-specific chromosomal assemblies called the chromosomal axis. In most of the organisms, the chromosomal axis mainly consists of two proteins, a HORMA domain-containing protein (Hop1 in budding yeast) and a coiled-coil linker protein that forms filaments (Red1 in budding yeast) (Chambon *et al*, 2018; Ferdous *et al*, 2012; Osman *et al*, 2018; Vader & Musacchio, 2014; West *et al.*, 2019; Yuan *et al*, 2002; Yuan *et al*, 2000) and cohesin. The axis-like structure is not only necessary for DSB repair but is also involved in DSB formation (Hollingsworth, 2010; Humphryes & Hochwagen, 2014; Panizza *et al.*, 2011; Zickler & Kleckner, 1999). Therefore the axis elements are of primary importance in meiotic chromosomal segregation. From my previous results, I observe a crucial role of Red1 and Hop1 in Mek1 activation. Thus, in this part of the work, I decided to focus on the structural aspects of one of the axial elements - Red1. I investigate its role in the functionality of the RHM complex. In this study, I carried out experiments in collaboration with John Weir and colleagues (FML, Tübingen, Germany) to investigate - i) The involvement of Red1 domains in RHM complex formation, with an aim to generate a minimal truncated construct of Red1 that leads to an active complex, ii) Shedding light into the Red1 associated growth defect defined above (Figure 4-3 A-C) and iii) *in vitro* reconstitution and structural modelling of RHM complex.

Sequence alignment of Red1 across eukaryotic species, performed in a previous study, identified three distinct conserved regions in Red1 (West et al.2018). Red1 consists of an NH_2-terminal conserved domain ($Red1^{1-340}$) immediately followed by a short closure motif peptide ($Red1^{341-362}$) with limited sequence homology to the Hop1 closure motif (West *et al.*, 2018). This region is followed by a long unstructured sequence ($Red1^{363-737}$) and a conserved C-terminal coiled-coil domain ($Red1^{737-827}$).

Further investigations from the same group indicated that the Red1$^{735-827}$ region has a propensity to self-associate and form higher-order structures. Homologs of Red1 such as, SYCP2/SYCP3 in mammals form filamentous axis (Pelttari *et al*, 2001; West *et al.*, 2019) that lead to chromosome axis assembly and similar behaviour is also noted for Red1 homologs in *Arabidopsis thaliana - ASY3/ASY4* (Chambon *et al.*, 2018; West *et al.*, 2019). By expressing and purifying a homolog of *RED1* from *Zygosaccharomyces rouxii* (Zr), the filament-forming nature of Red1 was narrowed down to the most extreme C-terminally located 8 residues. Expression of a coiled-coil domain construct lacking these residues, *i.e Zr* Red1$^{705-791}$ led to complete disruption of filaments and instead formed homotetramers (West *et al.*, 2019). In support of this previous data of Red1 domains, I perform a detailed structure-function analysis to elucidate its domain-dependent role in the assembly and activation of the RHM complex.

To address our specific aims (mentioned above), I generated a truncated series of Red1 based on the established structural understanding (Figure 4-7 A) . The following constructs were designed: a deletion of the last C-terminal residues, based on sequence homology from the known *Zr* Red1$^{791-798}$ - construct (Red1$^{1-818}$), a deletion of the coiled-coil domain (Red1$^{1-730}$), a further truncation of the unstructured region (Red1$^{1-366}$), expression of the NH$_2$-terminal conserved domain (Red1$^{1-345}$), CM till the last residue (Red1$^{346-827}$) and expression of the C-terminal region without CM (Red1$^{367-827}$). All the constructs were galactose inducible and NH$_2$-terminally tagged with HA.

Next, I investigated the domains of Red1 responsible for RHM complex assembly in the synthetic system. For this purpose, I performed co-immunoprecipitation experiments with strains expressing different Red1^{truncation}-Hop1-Mek1 combinations. An α-HA IP was performed to pull down Red1. As expected, based on earlier studies, we observed an interaction between Red1 and Hop1 (Hollingsworth & Ponte, 1997; West *et al.*, 2018; Woltering *et al.*, 2000) in all truncation constructs except those lacking the CM in Red1 (*i.e* Red1$^{1-345}$ and Red1$^{367-827}$) (Figure 4-7 B,C). This confirmed that, similar to the behaviour in meiosis, the Red1-Hop1 association is dictated by a CM-HORMA domain interaction (West *et al.*, 2018; Woltering *et al.*, 2000). We note that Hop1 binds more efficiently to full-length Red1 as compared to a version that is NH$_2$-terminally truncated (Red1$^{346-827}$) (Figure 4-7 C), implying a possible involvement of the conserved domain adjacent to the CM in Hop1 binding.
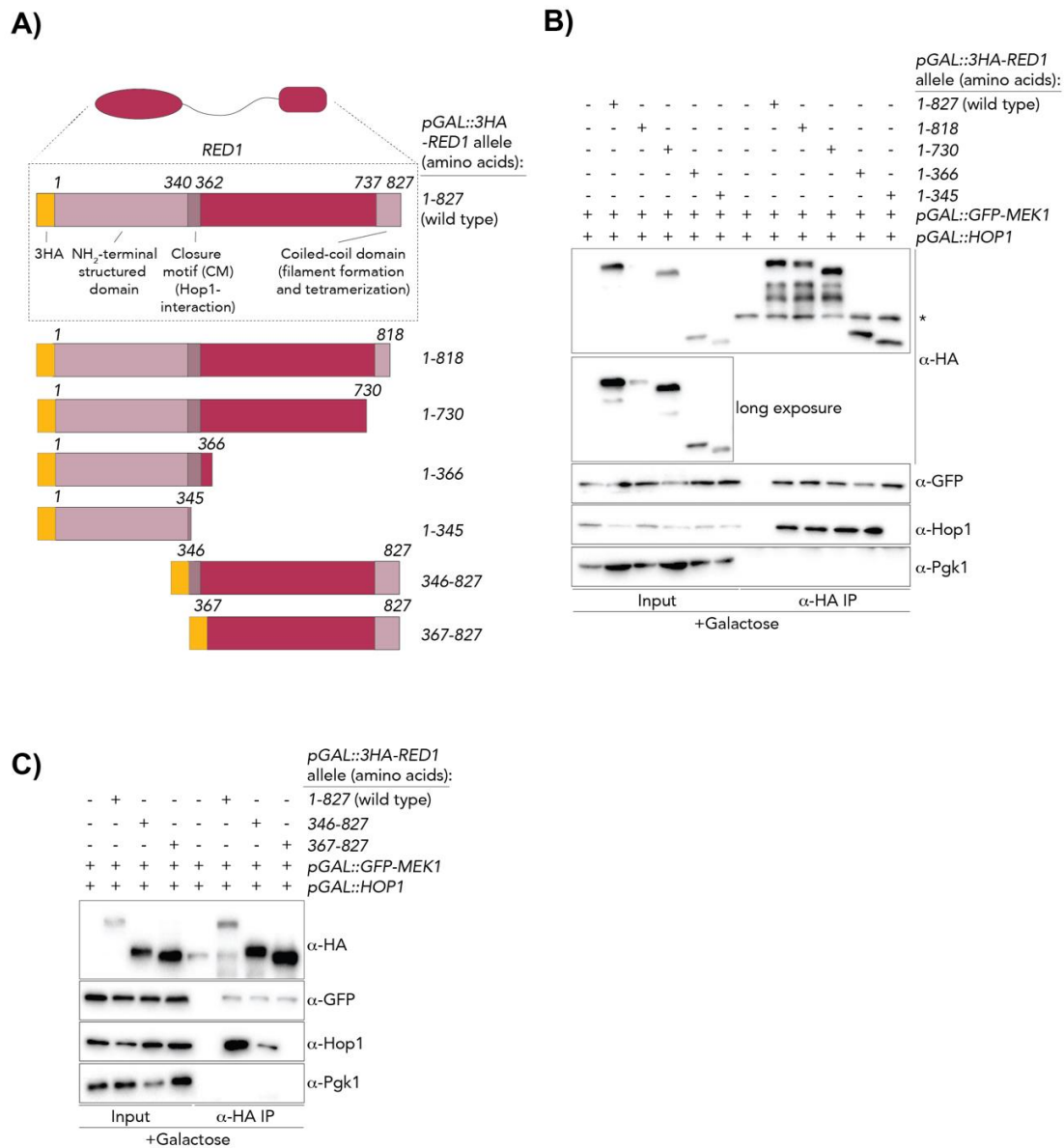
Figure 4-7: RHM complex assembly and activation of Mek1 in the context of Red1 domains

A) Schematic representation of domain deletion constructs of Red1, carrying integration of *pGAL1* promoter upstream of the start site of the Red1 coding region. All the constructs are NH₂-terminally tagged with 3xHA. The following constructs were designed: Red1[1-827], Red1[1-818], Red1[1-730], Red1[1-366], Red1[1-345], Red1[346-827] and Red1[367-827].

B and C) Co-immunoprecipitation assay with antibodies against HA (α-HA IP (Red1)). Cultures were harvested 4 hours after galactose induction. α-HA, α-Hop1 and α-GFP antibodies were used to detect Red1, Hop1 and Mek1 respectively. A consistent background band was observed for α-HA. Longer exposure was taken for α-HA blot. Strains used were: (yGV3219, yGV4806, yGV4393, yGV4395, yGV4397, yGV4400 for figure B and

yGV3219, yGV4806, yGV4207, yGV4402 for figure C). Pgk1 was used as a loading control.

I next focused on Mek1 and its association with Red1. A strain expressing Red1$^{1-345}$ showed Mek1 enrichment upon Red1 pulldown (Figure 4-7 B, C). However, the C-terminal region of Red1 (i.e Red1$^{346-827}$) also interacted with Mek1. Moreover, the interaction of Red1 with Mek1 was confirmed for Red1 constructs that did not interact with Hop1 (Red1$^{367-827}$ and Red1$^{1-345}$), thus confirming a direct Red1-Mek1 interaction and hinting at the presence of two distinct Mek1 binding sites in Red1.

Having implemented and demonstrated the expression and association of Red1, Hop1 and Mek1 in our truncated series of strains, I further decided to employ this set of tools to dissect the causality of our previous observations, precisely, the reason behind the Red1 associated growth defect. Therefore, I performed growth assays by spotting serial dilutions of the Red1^{truncation}-Hop1-Mek1 strains on glucose (control) and galactose containing plates (Figure 4-8 B). Our data indicates that the observed growth defects are suppressed upon deletion of the C-terminal residues in Red1 (Red1$^{1-818}$) (Figure 4-8 B). As this region is responsible for filament formation (West *et al.*, 2019), I speculate that the observed effect on cell cycle delay/ arrest is linked to Red1 filament formation (Figure 4-3 B and Figure 4-8 B).

As I planned to investigate a minimal RHM complex that renders active and functional Mek1 kinase in the ectopic system, I further employed the truncated Red1 series to investigate the minimal subunits of Red1 that allow Mek1 activation. To this end, I used MMS to introduce DSBs and analyzed H3-T11 phosphorylation signal in Red1^{truncation}-Hop1-Mek1 expressing strains. Under these conditions, I observed activation of Mek1 only when full-length Red1 was co-expressed (Figure 4-8 A), suggesting the integrity of the whole complex to be necessary for Mek1 activation. The results indicated that the NH$_2$-terminal domain of Red1 is important for the activation of Mek1. For example, in the Red1$^{1-366}$-Hop1-Mek1 strain, all three proteins interact, yet the condition does not satisfy Mek1 activation. Similarly, the coiled-coil domain deletion (Red1$^{1-737}$) also establishes a Red1$^{1-737}$-Hop1-Mek1 complex, yet no activation is observed. This could be due to structural changes occurring in the RHM complex, for which full-length Red1 is necessary. I noted that construct with mere deletion of the filament-forming region on the C-terminal of Red1 (Red1$^{1-818}$) was also insufficient in activating Mek1. Thus the higher-order Red1 assemblies are also involved in dictating the activation of Mek1. Previously, disruption of higher-order structures in Red1 was shown to produce defects in SC assembly and

low spore viability (Eichinger & Jentsch, 2010; Lin *et al.*, 2010). We speculate that the low spore viability in Red1 due to disruption of the higher-order structures could be due to the lack of Mek1 activation.
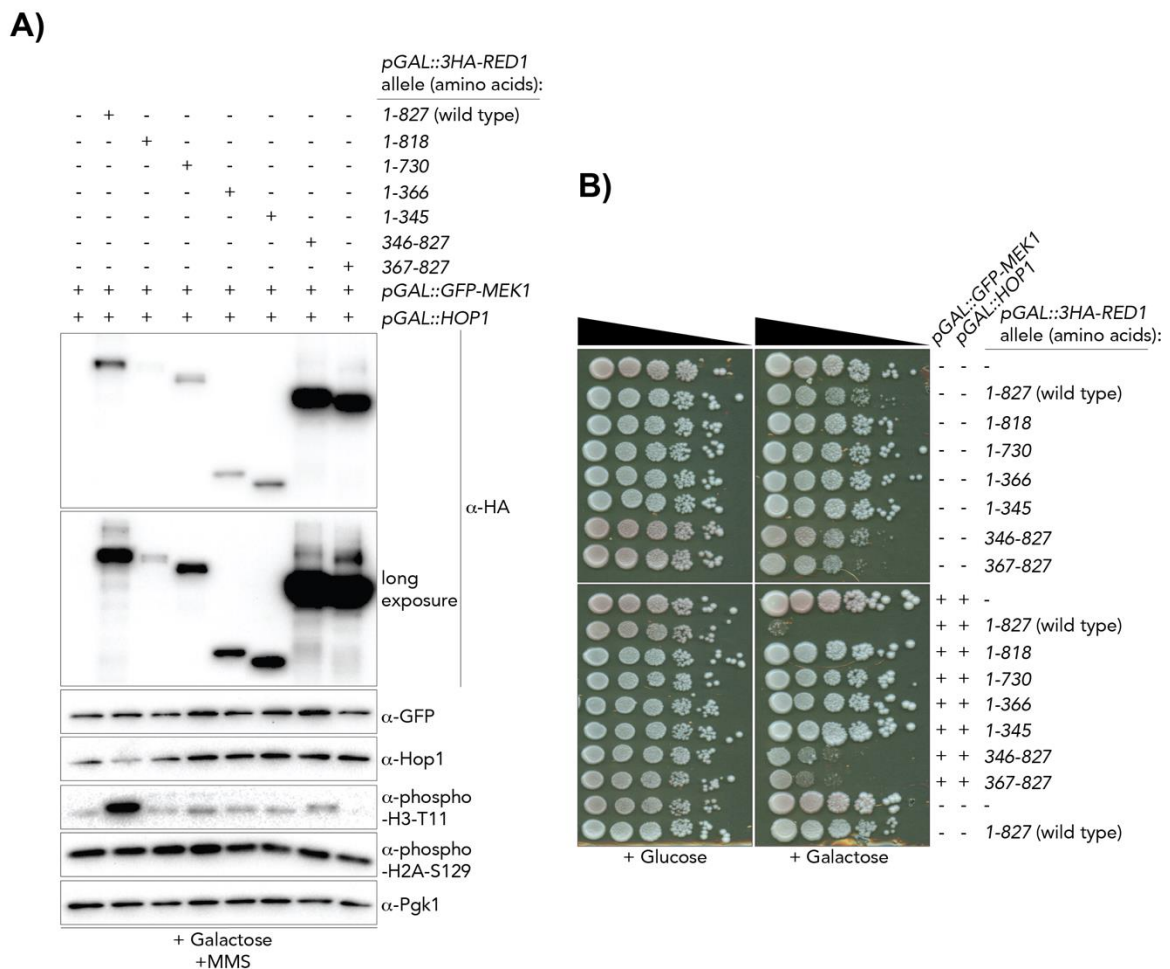
Figure 4-8: Involvement of Red1 domains in activation of Mek1.

A) Analysis of Mek1 activation in cells expressing Red1[trunctions] constructs and co-expressing Hop1 and Mek1. Samples were collected, 4 hours after galactose induction. 0.01% MMS was added for induction of DSBs. α-HA, α-Hop1 and α-GFP antibodies were used to probe for Red1, Hop1 and Mek1 respectively. A longer exposure was taken for the α-HA blot. α-H3 T11 phosphorylation was employed for monitoring Mek1 activity. A persistent background signal was observed for this blot. α-H2A S129 phosphorylation was used for detection of Mec1/ Tel1 activity (DNA damage signal). α-Pgk1 was probed as a loading control.

B) Growth assay by spotting 10-fold serial dilutions of the strains harboring Red1[trunctions] with and without co-expression of Hop1 and Mek1, on glucose (control) and galactose plates. The following strains were used: (yGV104, yGV4806, yGV3219, yGV3726,

yGV3798, yGV4402, yGV3799, yGV4190, yGV4191, yGV4194, yGV4207, yGV4193, yGV4393, yGV4395, yGV4397 and yGV4400).

## 4.8 *In vitro* biochemical reconstitution of the RHM complex- a structural study.

RHM complex is a master regulator of interhomolog bias in budding yeast meiosis. Understanding the structural aspects of the complex and biochemical characteristics that govern its association would help us gain insights into its function. With this aim, we collaborated with the group of John Weir (FML Tübingen, Germany) for *in vitro* reconstitution and structural analysis of the complex. All of the *in vitro* experiments described in this section were carried out by John R. Weir, Saskia Funk and Linda Chen (Weir Lab, FML Tübingen, Germany).

In the RHM complex, the two chromosomal axial proteins, Red1 and Hop1, form a structural scaffold that promotes the recruitment of Mek1 to chromosomes. Therefore we initiated our structural studies by observing Red1-Hop1 interaction. For this purpose, we successfully expressed and purified Red1-Hop1 complex with NH_2-terminally Strep-tagged Hop1 (2xStrepII-Hop1) and C-terminally MBP tagged Red1 (Red1-MBP) by streptavidin based affinity purification from insect cells (Figure 4-9 A). Red1 is known to form higher-order structures, such as tetramers that then associate to form filamentous assemblies (West *et al.*, 2019). For simplicity of purification, we employed a point mutant variant of Red1 (*i.e* Red1^{I743R}) that is known to disrupt the formation of higher-order structures (Eichinger & Jentsch, 2010; West *et al.*, 2019). With the purified Red1-Hop1 complex in the solution, we next investigated the mass of the complex. For this purpose, we performed mass analysis by employing mass photometry. Mass photometry is typically employed for samples at low concentrations. It can detect masses in the range 100 pM-100 nM. As low yields of proteins were obtained after purification, we employed this technique to calculate masses of the complex. The largest species observed had an experimental mass of ~209 kDa, suggesting the presence of a 1:1 Red1-Hop1 complex (the theoretically predicted mass is 212 kDa) (Figure 4-9 B). We also observed masses corresponding to free Red1^{I743R}-MBP (140 kDa) and Strep-Hop1 (81 kDa) [Actual theoretical masses are 138 kDa and 74 kDa respectively] (Figure 4-9 B). We conclude that a 1:1 stoichiometry for the Red1^{I743R}-Hop1 complex is present in our *in vitro* purified condition. Hop1 is a HORMA domain family protein that consists of two important functional regions, a HORMA domain and a closure motif (Aravind & Koonin, 1998; Rosenberg & Corbett, 2015; Vader & Musacchio, 2014). Typically, HORMA domain

containing proteins interact with their partners or with other Hop1 molecules (intra- or intermolecular interaction) by HORMA domain-CM interactions. Hop1 is also known to form higher order self-associated structures by binding of the HORMA domain with its own closure motif (or from another Hop1 molecule) to form a series of Hop1-Hop1 chain interactions (Also known as a beads-on-a-string model, (West *et al.*, 2018)). Even though we had an excess of Hop1 in the solution, we observed peaks corresponding to monomeric Hop1. This could be because the HORMA domain of Hop1 interacts with its own CM to form a compact 'closed' conformation. Indeed, from previous literature, it is predicted that Hop1 adopts such a 'closed' conformation in solution (West *et al.*, 2018).

In order to gain additional insights into the topological structure of the complex, we subjected our Red1^{I743R}-Hop1 samples to crosslinking mass spectrometry (XL-MS). To this end, crosslinking was performed by using DSBU crosslinker followed by proteolytic digestion and mass spectrometry as described in (Pan *et al*, 2018). Hop1 was seen to be extensively crosslinked compared to Red1, suggesting the presence of excess free Hop1 in the samples (Figure 4-9 C). Note that we use higher concentrations for mass spectrometry analysis thus, higher crosslinks could be due to excess free Hop1. Compared to Hop1, in case of Red1, a single long-distance crosslink was detected between the C-terminal end and the NH$_2$-terminal domain (Figure 4-9 C). This could be intra- or intermolecular interaction (or an artifact of the experiment). Intra- and intermolecular interactions cannot be distinguished using XL-MS. Also, due to the higher concentrations of Hop1 and Red1 used for this experiment, we might likely be observing higher order structures.

We detected several crosslinks between the region proximal to CM of Red1 and the HORMA domain of Hop1 (Figure 4-9 C). This observation goes along with the earlier studies where Red1 is shown to interact with Hop1 via CM-HORMA domain interaction (West *et al.*, 2018; Woltering *et al.*, 2000). In addition to this, extensive crosslinking was detected in the NH$_2$-terminal region of Red1 (that lies proximal to CM of Red1) and Hop1 HORMA domain (Figure 4-9 C). This indicates a possible involvement of NH$_2$-terminal domain of Red1 in interaction with Hop1. Our *in vitro* results are consistent with our *in vivo* observations, where deletion of the NH$_2$-terminal domain of Red1 leads to reduced Red1-Hop1 interaction as observed by Co-IP (Figure 4-7 C).
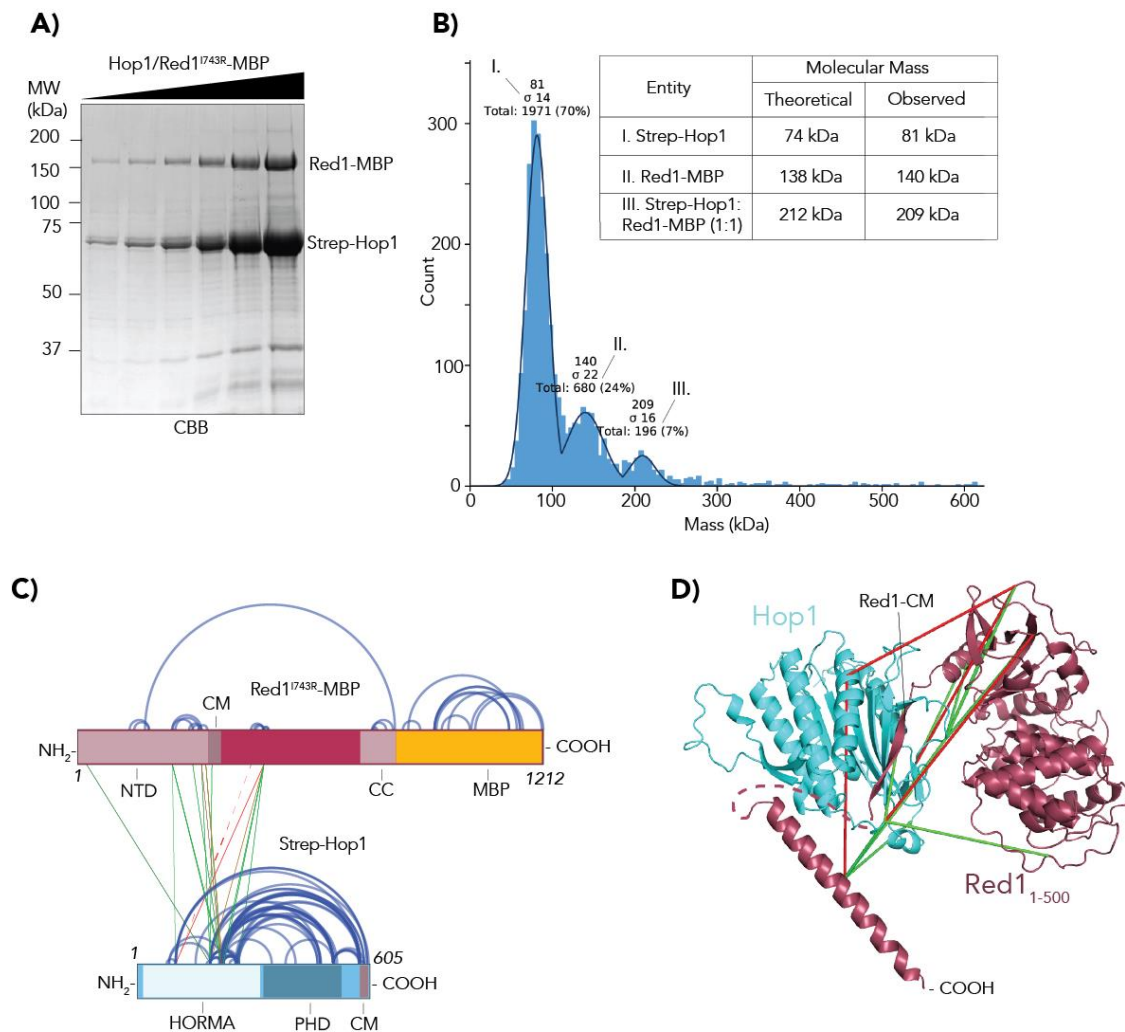
Figure 4-9: Purification and analysis of Red1-Hop1 complex

A) Purity of the Red1-Hop1 complex was tested by running an increasing concentration of Strep-Hop1 and Red1^{I743R}-MBP complex on 10% SDS-PAGE followed by Coomassie staining and imaging.

B) Mass photometry of the Red1-Hop1 complex. Purified Red1-Hop1 complex, diluted to ~30 nM concentration and subjected to mass photometric measurements (Refyen One mass photometer). Protocol and manufacturer's instructions were followed for the analysis.

C) Schematic representation of the crosslinks between Red1 and Hop1 obtained by XL-MS. A false discovery rate of <1% was set for analysis. Intramolecular crosslinks are depicted in blue. Intermolecular crosslinks are in Red or green according to whether they are consistent with the Alpha fold 2 model. In green are in the threshold distance of < 37 Å between Cα-Cα. Distances greater than the threshold are considered inconsistent and are represented in red.

D) An AlphaFold2 predicted model of Red1 $^{1-500}$-Hop1. Red1 is in maroon and Hop1$^{1-300}$ is in blue. The CM of Red1 inserted in the HORMA domain of Hop1 is highlighted. A loop in Red1$^{361-466}$ is replaced by a dotted line for clarity. Crosslinks obtained from XL-MS were superimposed onto the model by PyXlink Viewer (Schiffrin *et al*, 2020). Cα-Cα distances < 37 Å were taken to be potentially consistent and shown in green. Cα-Cα distances > 37 Å were likely to be inconsistent and shown in red. (This distance was chosen as a threshold as we are using a DSBU X-linker which has a distance of 12 Å. Depending on the distance between the Cα-Cα that are crosslinked one might observe a distance of 27 Å. In addition, we consider the approximate PAE for the model which is 10 Å. Thus we set a threshold of 37 Å)

Experiments in figure 4-9 A-D are performed by John Weir and Weir lab colleagues; XL-MS in (C) was performed by Franziska Müller and Petra Janning (MPI Dortmund, Germany) and analysed by John Weir.

To predict the interaction surface of Red1^{I743R}-Hop1, we employed the AlphaFold2 prediction algorithm (Figure 4-9 D, supplementary figure 2 A, B) (Jumper et al. 2021). Sequences corresponding to the first 500 residues of Red1 were used for Red1 structure prediction, whereas full-length Hop1 was used for Hop1 structure prediction. After processing 5 iterations of the AF2 algorithm, a highest ranking model was chosen based on pLDDT score, for further analysis (supplementary figure 2 A, B).

Based on our structural predictions, the NH$_2$-terminal domain of Red1 folds into two distinct structural domains. One, spanning the residues 1-230 and the other from 231-344. To compare the domain structures, the DALI server program was employed (Holm, 2020; Jumper *et al*, 2021). DALI search compares the 3D structure of the protein of interest to the known structures of proteins from the PDB database. By comparing the similarities between an unknown protein and a well characterized protein, it is possible to speculate the functions of the unknown protein. As a result, we revealed that Red1 NH$_2$-terminal domain is structurally similar to the NH$_2$-terminal domain of mammalian SYCP2 (crystal structure 5IWZ; Feng J et al. 2017). Next, we ran a DALI search on the individual domains of the Red1 conserved region. We identified the NH$_2$-terminal domain encodes Armadilo-like repeat domain (ARML) (residues 1-226) (Figure 4-10 A) and the domain adjacent to the CM to be Pleckstin Homology (PH) domain (residues 227-345) as previously described (Feng *et al*, 2017; Tromer *et al*, 2021; Ur & Corbett, 2021).

In order to understand Red1-Mek1 interaction, we made use of the Red1 predicted structures. The ARML domain of Red1 is highly structurally similar to an adaptor protein MO25β (PDB 3ZHP) that drives activation of several kinases (one example of MO25β binding kinase is STK24) (Figure 4-10 A-C). Based on this, the ARML region of Red1 might be involved in interaction with Mek1. Strikingly, in the predicted structure, the potential Mek1 binding site is occupied by the Red1 PH domain (Red1$^{227-345}$) (Figure 4-10 A-F). This suggests that the Red1-Mek1 interaction is hindered due to potential allosteric effects of the PH domain of Red1. Indeed this could be the reason why we did not observe Red1-Mek1 interaction in our *in vitro* experiments (data not shown). However, in the *in vivo* setting, we speculate that the Mek1 binding surface in Red1 is now available for binding due to possible Red1 binding to the chromosomes (possibly to cohesin). The speculated Red1-cohesin interactions might produce conformational changes that makes the Mek1 binding surface in Red1 available for binding to Mek1.

Additionally, to validate our AF2 predicted structure, we superimposed the Red1^{I743R}-Hop1 crosslinks obtained from the crosslinking mass spectrometry data onto the predicted structure. We retained a threshold distance of 37 Å between the Cα of the model, to be consistent crosslinks. Crosslinks with greater distances were considered to be inconsistent. 11 of the 16 crosslinks between Red1 and Hop1 were observed to be consistent. The model also shows a high degree of confidence in folding of the Red1 and Hop1 domains and the placement of the NH$_2$-terminal domain of Red1 relative to the Hop1 HORMA domain (Supplementary figure 2 A, B). The CM of Red1 was buried in the HORMA domain of Hop1, thus providing confidence in the model (Figure 4-9 D). We note that the algorithm placed the NH$_2$-terminal domain of Red1 in close proximity to the HORMA domain of Hop1 (Figure 4-9 D and Figure 4-10 E). Thus, from our *in vitro* and *in vivo* studies, we suggest that the NH$_2$-terminal of Red1 might play a significant role in interaction with Hop1 (Figure 4-7 C and Figure 4-9 C, D). Overall, the structural and *in vitro* analysis done by the Weir lab colleagues provided us with additional insights on the Red1-Hop1 complex.
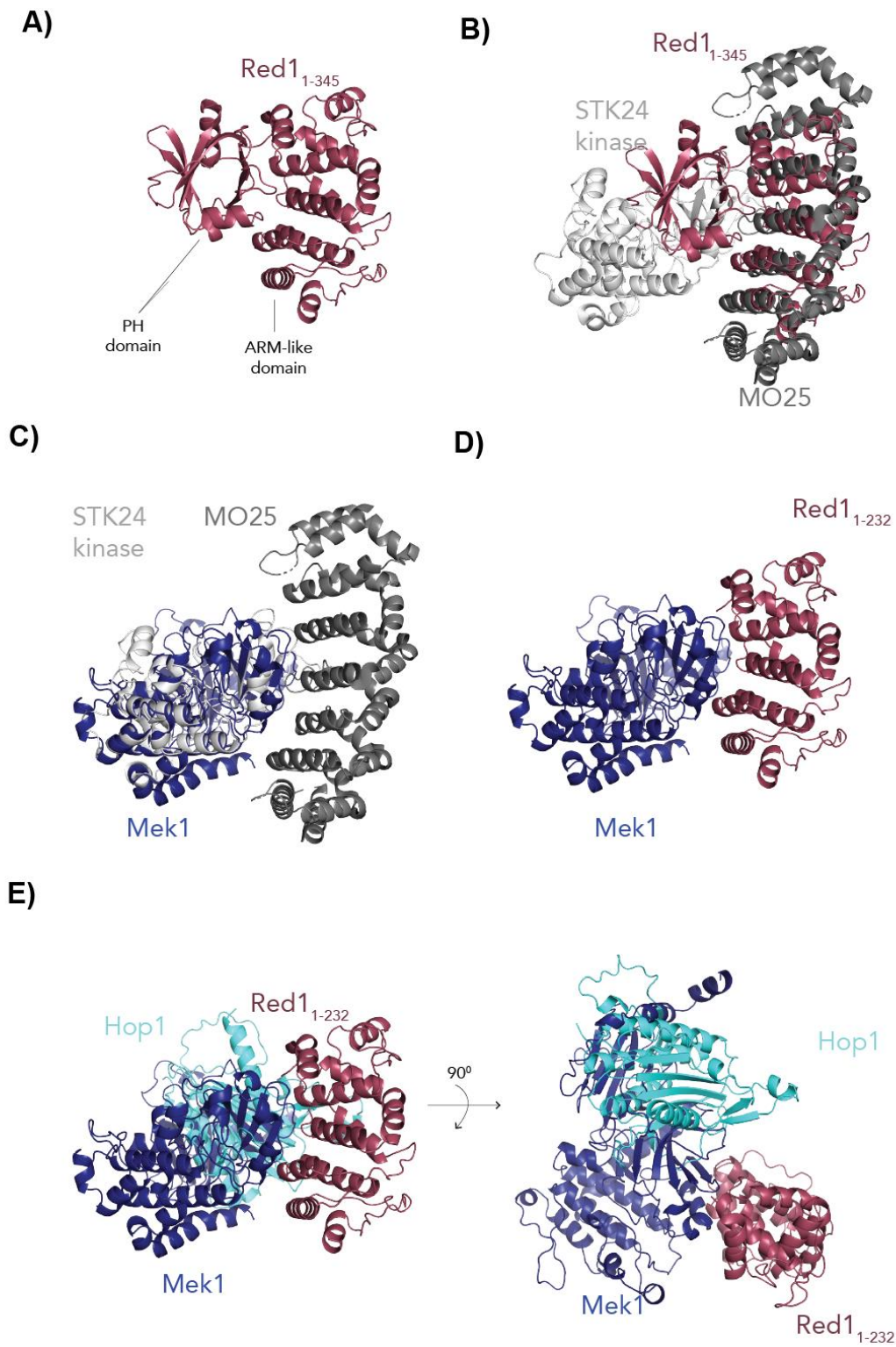
Figure 4-10: AF2 modelling and DALI search results for prediction of Red1-Hop1 interaction surface

A) Red1$^{1-345}$ structure predicted by AF2 modelling. Structure corresponding to the highest ranking pLDDT score (see supplementary figure 2 A, B).

B) Structural similarity in the ARML domain of Red1 (predicted by DALI search) and MO25β depicted by superimposing the structure of MO25β (crystal structure; PDB

3ZHP) with our predicted model of Red1. STK24 kinase (a known binding partner of MO25β) and MO25β interaction surface. MO25β is in dark grey, Red1 is in maroon and STK24 kinase is in light grey.

C) Mek1 superimposed on the STK24 occupy similar interaction surface on ARML domain. Mek1 is in blue, MO25β is in dark grey, and STK24 kinase is in light grey.

D) Prediction of Red1$^{1-232}$-Mek1 interaction via Red1 ARML domain. Red1 in red and Mek1 is in Blue.

E) Structural prediction of Red1$^{1-232}$, Hop1 and Mek1 interaction. Mek1 is in Blue, Red1 is in Red and Hop1 is in light blue.

Structural predictions in figure 4-10 A-F are done by John Weir, Linda Chen and Saskia Funk (Weir lab colleagues). Corresponding PAE plots are included in supplementary figure 2 A, B.

4.9 Functional assay to elucidate Mek1 function in an ectopic system

The activation of Mek1 alone (GST-Mek1) and in the presence of the RHM complex prompted us to revisit our hypothesis and test the functionality of Mek1 in our ectopic system. In meiosis, Mek1 plays a central role in mediating the interhomolog biased DSB repair. Using our synthetic system, I decided to investigate the function of Mek1 in forming the bias. Several models have been hypothesized earlier that attempt to understand the IH repair. I specifically focus on the 'spatial proximity model' described in (Subramanian *et al.*, 2016). According to this model, Mek1 forms a barrier-to-sister-chromatid-repair (BSCR) by presumably recruiting to sites of DSBs and actively suppressing the DSB repair in its vicinity. As the sister chromatid is physically proximal to the DSB sites, compared to the homologous chromosomes, they lie in this so-called 'zone of repair suppression' and are inhibited from being used as a repair template. This model is in accordance with several other hypothetical models proposed earlier in the literature.

A conceptually simple way to test the above-mentioned 'physical proximity' model of Mek1 activity is to observe the DSB repair in cells with only the 'sister chromatid' as an available choice for the repair template. This condition is present in haploid cells after genomic duplication in S-phase. In such a situation, a sister chromatid is available for repair and the only sequence homology comes from the sister chromatid (note that the homologous chromosome is absent). Therefore, expressing an active form of Mek1 (for example, GST-Mek1 that is shown to be active in previous experiments) would inhibit the repair of DSBs in its

vicinity *i.e* by using the sister chromatid. Due to no other template available for repair, the DSBs will persist under these conditions.

To test this hypothesis, I employed a growth assay whereby I spotted 10-fold serial dilutions of strains expressing GFP-Mek1 (control) and GST-Mek1, on glucose (control) and galactose plates supplemented with DSB inducing agents (0.005% MMS, 0.01%MMS and phleomycin) (Figure 4-11 A). To ensure the effectiveness of the drug, a *rad51Δ* strain, that displays growth defect upon DNA damage, was used as a control (Aouida *et al*, 2019; Woo *et al.*, 2020). Earlier observations show no activation of Mek1 in GFP-Mek1 expressing strains (Figure 4-1 A). Thus, no change in growth was observed for strains expressing GFP-Mek1 on drug-containing plates. On the contrary, a severe growth defect was seen on the DNA damaging plates (galactose with MMS and galactose with phleomycin) after GST-Mek1 expression. This suggested that the growth defect was not due to ectopic expression of Mek1 as GFP-Mek1 does not show any effect. Moreover, no effect was observed on galactose plates (without drugs) for GST-Mek1. Therefore, I speculate that the growth defect mainly observed on DNA damage-inducing plates, in the case of GST-Mek1, is a Mek1 functional effect and related to Mek1 induced inhibition of DSB repair.

Our results from haploid strains expressing GST-Mek1 suggested a growth defect which could presumably be a cell cycle arrest in response to unrepaired DSBs. As a next step, I looked at the effect of expressing Mek1 in a diploid condition. As Mek1-mediated repair inhibition is predicted to be local and near the sites of DSBs where Mek1 is rendered active, the presence of two extra homology sequences on the physically distal homologous chromosomes (in diploid condition) would provide a chance for DSB repair and bypass the arrest. In this experiment, I employed two strain variations, *i.e* a diploid with a single copy integration of *pGAL1::GFP-MEK1* or *pGAL1::GST-MEK1* (heterozygous condition) and a diploid with two copies of *pGAL1::GFP-MEK1* or *pGAL1::GST-MEK1* (homozygous condition). These conditions were used to interpret the dosage-dependent effect of Mek1. The strains were constructed by integrating *pGAL1-GFP/GST* upstream to the Mek1 coding region and crossed to get either a homozygous or heterozygous combination of alleles. Strains were spotted on YP-glucose (control) and YP-galactose plates supplemented with DNA damaging drugs (MMS and phleomycin). As expected, no growth defect was observed for haploid, homozygous and heterozygous GFP-Mek1 expressing strains in the DNA damaging condition. However, haploid strains expressing GST-Mek1, showed a growth defect on drug-containing plates. Interestingly, diploid strains heterozygous for *GST-MEK1* showed a marked return to normal growth on both

MMS and phleomycin-containing plates. This phenotype could be seen as DSBs are now able to get repaired due to the availability of a homologous chromosome. Thus, it is possible that in this particular condition, we observe the functional effect of Mek1 activity *i.e* inter-homolog homologous recombination.
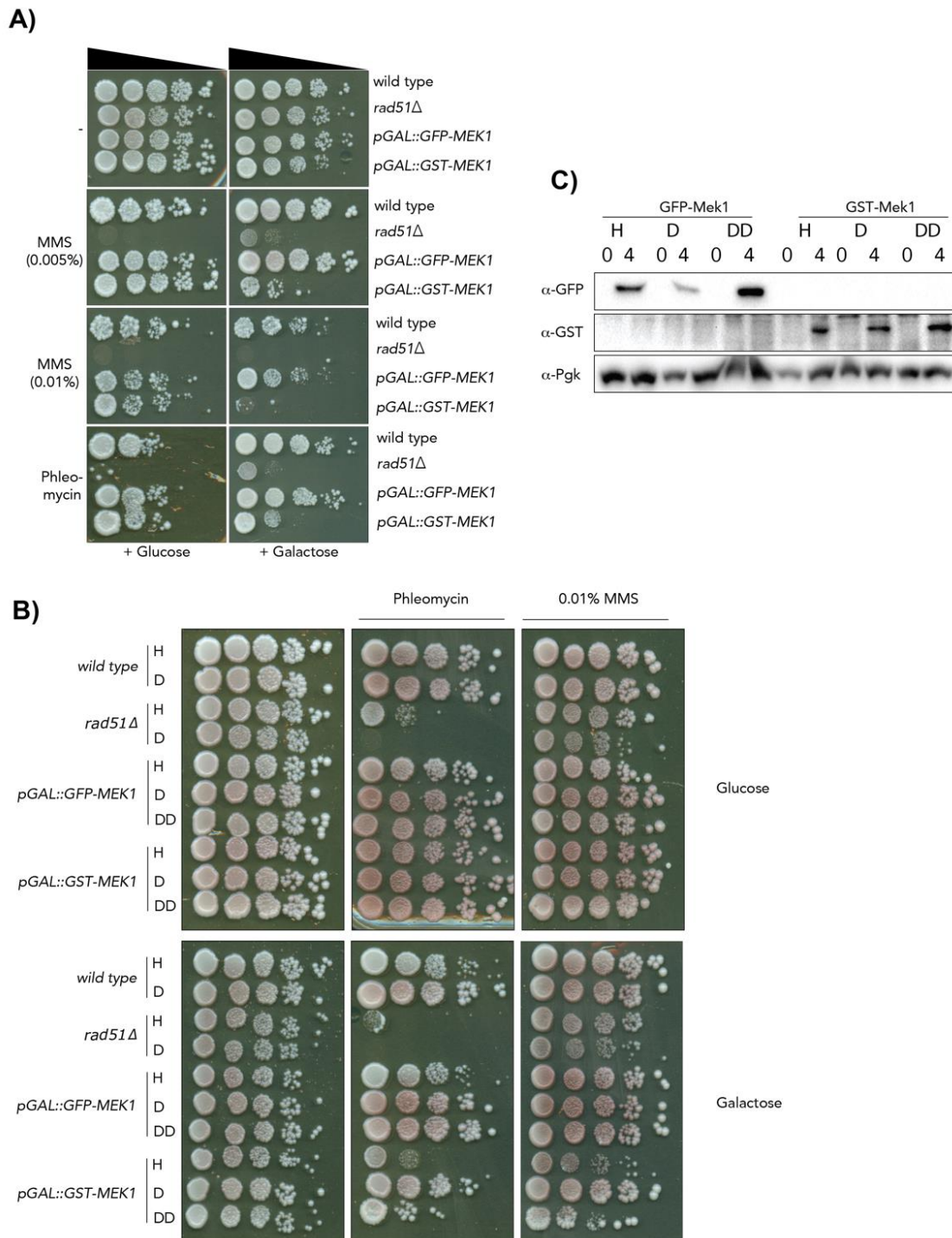

Figure 4-11: Spot assays depicting the functionality of GST-Mek1 in the ectopic system.

A) 10 fold serial dilutions of strains were spotted on glucose and galactose plates supplemented with DNA damaging drugs (0.005% MMS, 0.01% MMS and …phleomycin). Following strains were used: wild type (yGV104), *rad51Δ* (yGV3692), *pGAL1::GFP-MEK1* (yGV2812) and *pGAL1::GST-MEK1* (yGV2774). Plates were incubated for 2-4 days at 30°C before imaging.

B) Effect of ploidy and copy number variation on the activation of Mek1. Spot assay done as mentioned in A. Strains used were : yGV104, yGV2102, yGV3692, yGV5060, yGV2812, yGV5059, yGV3392, yGV2774, yGV5058, yGV5089.

C) Western blot for comparison of Mek1 expression levels in different strains with varying ploidy and copy number variation. Strains used were : yGV2812, yGV5059, yGV3392, yGV2774, yGV5058, yGV5089

I further investigated the result of expressing GST-Mek1 in a strain that is homozygous for *GST*-MEK1. As one can imagine, the expression levels of GST-Mek1 might vary for homozygous and heterozygous allelic conditions. Indeed, by western blot, I observed a slight increase in expression for the homozygous condition compared to the heterozygous condition. Results from the spot assay using the homozygous *pGAL1::GST-MEK1* strains revealed similar growth defects as observed for the haploid GST-Mek1 expressing strains. This result was consistently observed for DSBs induced with MMS as well as phleomycin. Increased expression of active Mek1 could somehow be causing a 'global inhibition' of DSB repair *i.e* the homolog is also inhibited from being used as a repair template. More validation experiments need to be done to confirm this speculation.

In this project, I studied meiotic recombination, specifically focusing on DSB repair occurring during meiotic prophase to gain additional insights into the role of Mek1 in mediating the interhomolog recombination bias. I confirm that Mek1 is active when expressed in a synthetic system that I designed. I found that the activation of Mek1 is dependent on utterly two other meiosis-specific proteins – Red1 and Hop1 and on the formation of DSBs. Red1, Hop1 and Mek1 interact together to form a complex. The other conditions necessary for Mek1 activity are the presence of a full length Red1 protein, G2/ M cell cycle phase -specific factors (not yet known) and activity of Mec1 kinase. Finally, using this synthetic system, I try and elucidate the function of Mek1 with experiments hinting towards an active and functional Mek1 that mediates inhibition of DSB repair using sister chromatid, leading to interhomolog recombination in mitotically dividing cells. Additional experiments are needed to elucidate the

nature of the observed functional phenotype. Possible implications of the functional experiment and future prospects are discussed in detail in the discussion section.

As a part of the second project carried out in collaboration with the group of John Weir (FML, Tübingen, Germany), we studied the early meiotic events, *i.e* programmed introduction of DSBs. DSB formation is catalyzed by Spo11 DSB machinery consisting of 3 sub-complexes and 10 different proteins. We focus on the role of one of the proteins - Mer2 that is known to play a significant role in DSB formation (Engebrecht *et al*, 1990; Murakami & Keeney, 2014; Rockmill *et al.*, 1995; Wan *et al.*, 2008).

4.10 Formation of DNA breaks and Spo11 DSB machinery in *S. cerevisiae* meiosis

4.10.1 An important role of Mer2 in the DSB machinery

During early meiotic G2/ prophase, DNA double-stranded breaks are introduced in a programmed manner by the endonuclease activity of Spo11. Numerous accessory proteins associate to form the Spo11 DSB machinery. In this study, we describe the role of one such Spo11 accessory factor, Mer2, known to be an important factor at various steps of DSB induction. Mer2 – a part of the RMM (Rec114-Mer2-Mei4) subcomplex, plays a crucial role in integrating the cell cycle signals in the initiation of DSB during early meiosis (Murakami & Keeney, 2014). It gets phosphorylated by cell cycle-specific kinases (CDKs/ DDKs) and this modification is essential for recruiting other Spo11 components to Mer2 and thus to chromosomes. Mer2 interacts with Spp1 and has recently been shown to interact with Hop1 and nucleosomes (Rousova *et al.*, 2021). These interactions (Mer2-Spp1, Mer2-nucleosomes and Mer2-Hop1) are speculated to aid in tethering the DNA loops to the chromosomal axis (Rousova *et al.*, 2021), forming the necessary chromosomal architecture for DSB induction. Thus Mer2 plays a central role in meiotic DSB formation and the deletion of *MER2* leads to spore viability defects (Rockmill *et al.*, 1995). In this part of the project, we try to address the role of Mer2 in DSB formation along with John Weir and Weir lab colleagues. All of the *in vitro* experiments mentioned in this section were carried out by colleagues from the group of John Weir, while I, and colleagues from the group of Gerben Vader lab have focused on the *in vivo* part.

To better understand the function of Mer2, we introduced separation of function alleles by mutating certain conserved residues as described below (Figure 4-12 A). Initially, we performed a sequence alignment on evolutionarily conserved Mer2 orthologs (Performed by Weir lab colleagues). Apart from the known central coiled-coil region, we also found a highly conserved sequence near the NH_2-terminal, spanning residues 52-71 (Figure 4-12 A). To gain insights into the function of Mer2, we designed two alleles by mutating conserved residues in the Mer2$^{52-71}$ region. The two alleles, namely *mer2-3a* and *mer2-4a* consists of the following mutations: W58A, K61A and L64A for *mer2-3a* and residues D52A, E68A, R70A and E71A for *mer2-4a* respectively (Figure 4-12 A). In a *mer2Δ* background, we integrated plasmids carrying the wild type and the mutant alleles, C-terminally tagged with HA. By employing western blot analysis we observed expression levels for strains expressing Mer2-3HA, Mer2^{3A}-3HA and Mer2^{4A}-3HA. We note differential migration patterns for Mer2 in wild type and mutant expression condition, that might indicate that the mutations affect the post-translational modifications of the protein. We next aimed to understand the functional implication of this conserved region. First, we analysed the spore viability (done by Gerben Vader, Vader lab). *mer2Δ* cells exhibited a high spore viability defect as observed earlier (Rockmill *et al.*, 1995) (Figure 4-12 C). Expression of protein from wild type *MER2* construct in the *mer2Δ* strains restores the spore viability defect implying the functionality of our *MER2* construct (Figure 4-12 C). Intriguingly, the spore viability defect did not improve upon Mer2$^{3A/4A}$ expression, suggesting a crucial role of the conserved residues in the function of Mer2. To further support our observations, we looked at the activation of Mek1, a key kinase that is regulated by DSB-dependent downstream signalling during meiotic prophase. We observed reduced activation of Mek1 in *mer2-3a* and *mer2-4a* strains (Figure 4-12 B) by probing for H3-T11 phosphorylation, a known Mek1 activation marker (Kniewel *et al.*, 2017). Our data also indicated a lack of Hop1 phosphorylation in Mer2$^{3A/4A}$ (Figure 4-12 B), suggesting that the DSB induction or the DSB-dependent downstream Mec1/ Tel1 signalling (as Mec1/Tel1 dependent Hop1 phosphorylation is affected) is disrupted in the mutant strains.

The function of Mer2 in meiotic DSB formation is central in enabling chromosome segregation and the formation of viable spores. As Mer2 is a key element of the Spo11 DSB machinery, it could be suggested that the *mer2* mutants fail to associate with some of its binding partners in the Spo11 complex, leading to the spore viability defects.

Experiments done by Weir lab and colleagues (data not shown here; (Rousova *et al.*, 2021)) indicate that the interaction of Mer2$^{3A/4A}$ with Hop1, Spp1 or nucleosomes is not affected
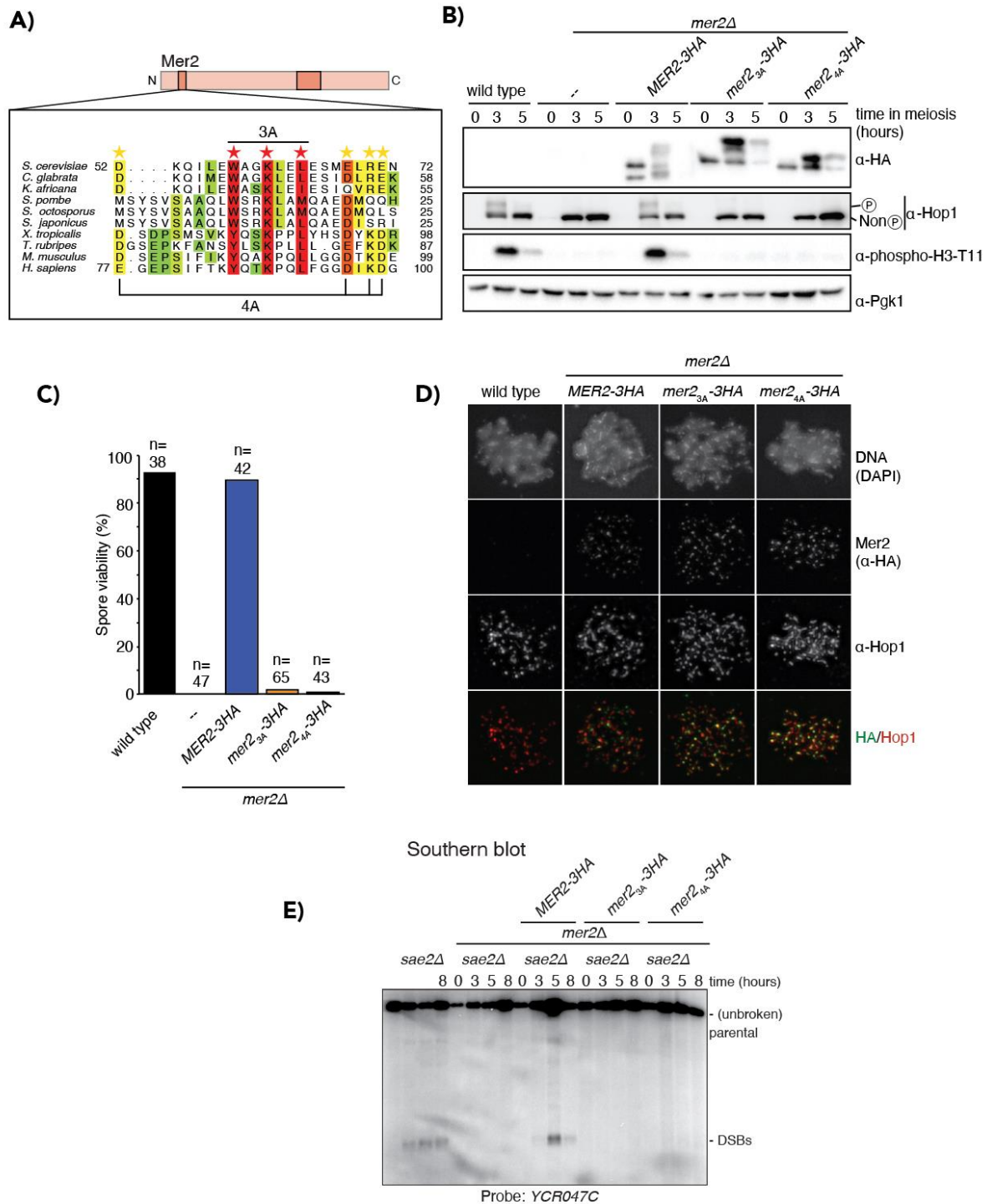
by mutating the conserved residues in Mer2. Consequently, there could be other pathways/ protein-protein interactions that are disrupted in the Mer2$^{3A/4A}$ that are essential for its function.

4.10.2 Mer2 mutants fail to interact with Mre11 and are defective in DSB formation

To investigate the possibility that mutations in the *MER2* conserved region affects Mer2 localisation to chromosomes, we performed confocal microscopy on chromosome spreads (Experiments done by Vivek Raina (Vader Lab, MPI Dortmund, Germany)). Results from the chromosome spread experiments indicated recruitment of Mer2-3HA to chromosomes during meiotic prophase (Figure 4-12 D). Furthermore, the recruitment of Mer2^{3A}-3HA and Mer2^{4A}-3HA to chromosomal foci was not disrupted (Figure 4-12 D). Thus Mer2^{3A} and Mer2^{4A} are proficient in associating to chromosomes and are likely not the reason for spore viability defects.

We next investigated the consequences of *mer2* point mutants on the induction of DSBs. For this purpose, we employed Southern blotting analysis. We constructed strains that expressed Mer2-3HA, Mer2^{3A}-3HA and Mer2^{4A}-3HA in a *mer2Δ, sae2Δ* background. *sae2Δ* cells are defective in DSB resection, making it easier to monitor and quantify the accumulated DSB levels. DSBs were observed upon expression of Mer2 in meiotic prophase while no DSB induction was seen in Mer2^{3A} and Mer2^{4A} expressing strains (Figure 4-12 E) This clearly indicated the role of conserved residues of Mer2 in its DSB forming function.

To identify potential interaction partners of Mer2 whose binding to Mer2 is affected in the Mer2$^{3A/4A}$, we carried out a yeast-two-hybrid Y2H assay with the known Mer2 binding partners of the Spo11 complex (*i.e* Rec102, Rec104, Ski8, Rec114, Spo11, Spp1 and control; data not included here; (Rousova *et al.*, 2021) (Y2H assays were performed by V. Altmannova and Weir lab colleagues). Interaction of Mer2 and Mer2 mutants with Spp1 was unaffected. While Mer2 binds Mre11 (an MRX complex protein), a marked decrease in the association of Mre11 with Mer2 was observed in instances when Mer2^{3A} and Mer2^{4A} were expressed (Figure 4-13 A). Not only does MRX complex aid in DSB repair but it is also thought to be involved in meiotic DSB formation (Borde *et al.*, 2000). Thus disruption of the Mer2-Mre11 interaction in Mer2$^{3A/4A}$ interestingly could suggest a further impaired DSB induction.

Figure 4-12: Phenotypes for point mutations in Mer2

A) Sequence alignment of Mer2 orthologs depicting the conserved coiled coil region and the NH₂-terminal *Sc*Mer2$^{52-71}$ conserved region (conserved regions in dark orange). Residues mutated to Alanine in '3A' mutants are marked by Red stars (W58A, K61A, L64A). Residues mutated to Alanine in '4A' mutants are shown in yellow stars. (D52A,

E68A, R70A, E71A). Note that the mutated residues in Mer2^{4A} are not as conserved as those in Mer2^{3A}.

B) Western blot depicting the expression of Mer2 in wild type, *mer2Δ*, *MER2-3HA mer2Δ*, *mer2-3A-3HA mer2Δ*, and *mer2-4A-3HA mer2Δ* strains. α-HA antibody was used to detect Mer2 protein, α-Hop1 was used for Hop1, α-H3 T11 phosphorylation was used to monitor Mek1 activity. α-Pgk1 was probed as a loading control. Strains used for these experiments are – yGV8, yGV4874, yGV4879, yGV4889, yGV4933

C) Quantification of spore viability for wild type, *mer2Δ*, *MER2-3HA mer2Δ*, *mer2-3A-3HA mer2Δ*, and *mer2-4A-3HA mer2Δ* strains. The number of dissected tetrads is indicated.

D) Immunofluorescence images for chromosome spreads stained for Mer2 (α-HA; is in Green), Hop1 (α-Hop1; is in Red), DAPI stained DNA is in Blue. Strains used are wild type, *mer2Δ*, *MER2-3HA mer2Δ*, *mer2-3A-3HA mer2Δ*, and *mer2-4A-3HA mer2Δ*. Southern blot depicting parental DNA and DSB fragments for strain conditions - *sae2Δ*, *mer2Δ sae2Δ*, *MER2-3HA mer2Δ sae2Δ*, *mer2-3A-3HA mer2Δ sae2Δ*, and *mer2-4A-3HA mer2Δ sae2Δ*. Samples were collected at indicated timepoints post meiotic induction. DSBs were monitored at *YCR047C* locus, a known DSB hotspot. Strains used for these experiments are – yGV4474, yGV4913, yGV4931, yGV4934, yGV4957. Sequence alignment is performed by Weir lab colleagues (A); Spore viability assay is done by Gerben Vader (C); Chromosome spreads were performed by Vivek Raina (D).

To further validate our results, recombinant Mre11 was purified and used as a bait to pulldown Mer2, Mer2^{3A} and Mer2^{4A} (Experiments performed by D. Rousova, Weir lab and colleagues). We detected a robust Mer2-Mre11 interaction in wild type Mer2 expressing strains and the binding was reduced in *MER2* mutants (Figure 4-13 B). We aimed to confirm this interaction *in vivo* and initially used Co-immunoprecipitation assay to test Mer2 interaction with Mre11 in cells undergoing meiosis (Figure 4-13 D). Under our Co-IP conditions, we did not detect Mre11 interaction with either wild type or with Mer2 mutants, although a strong interaction was detected for Hop1 (a control condition) with Mer2 in wild type Mer2 and Mer2$^{3A/4A}$ expressing strains (Figure 4-13 D). The discrepancy in the *in vitro* and the *in vivo* results might reflect an apparently transient or infrequently occurring Mer2-Mre11 interaction *in vivo*. Similar results were obtained after *in vivo* biochemical purification of Mer2 followed by IP-MS (Experiments performed by D. Rousova, Weir lab and colleagues). No Spo11 associated machinery was detected in the Mass Spec of Mer2 IP (Figure 4-13 C; and thus no

Mre11 was detected). We speculate that Mer2-Mre11 interaction *in vivo*, could be affected possibly due to post-translational modifications of Mer2 (figure 4-13 A-D) that render the interaction more transient or there could be other accessory factors of the MRX complex or the Spo11 machinery that hinder the interaction. Nonetheless, we conclude that Mer2 interacts with Mre11. The interaction is disrupted in the Mer2$^{3A/4A}$ mutants suggesting the possible involvement of the N-terminally located conserved region of Mer2 in this interaction. Further, we speculate that disruption of this interaction downregulates the introduction of DSBs in the Mer2$^{3A/4A}$ expressing strains. As MRX complex is thought to be involved in DSB induction, disruption of Mer2-Mre11 interaction could possibly be affecting the MRX mediated DSB formation.
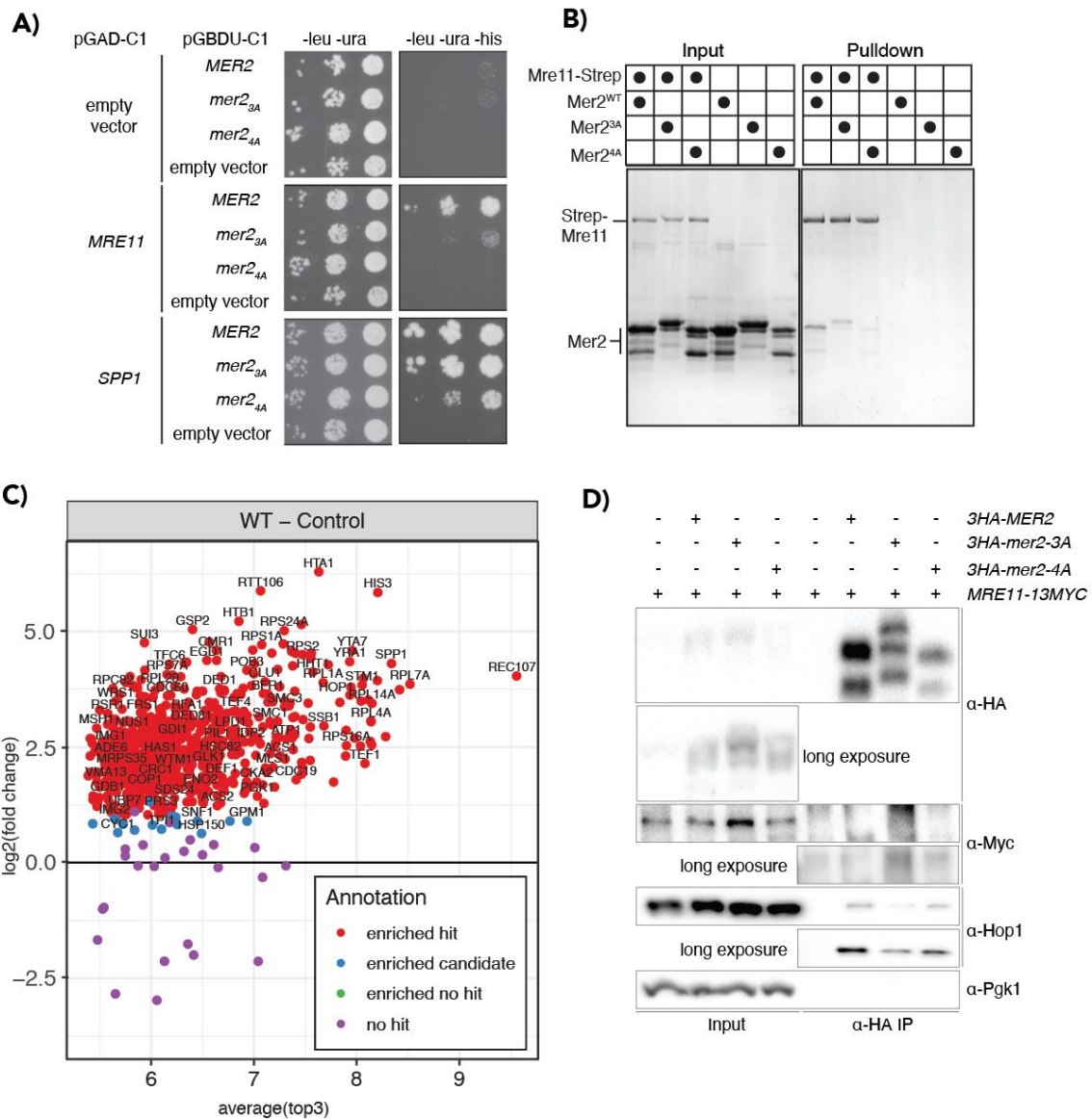
Figure 4-13: Mer2³ᴬ and Mer2⁴ᴬ disrupts interaction with Mre11 resulting in defects of DNA break formation

A) Y2H assay for Mer2-Mre11 interaction. Strains were transformed with plasmids pGAD-C1 (activation domain) and pGBDU-C1 (DNA binding domain) fused to Mre11/ Spp1 and Mer2 alleles respectively. Serial dilutions were spotted on -leu-ura (Control) plates and -leu-ura-his (selective) plates.

B) *In vitro* pulldowns of 2xStrepII-tagged Mre11 and Mer2. Mre11 was used as a bait to capture Mer2ʷᵗ, Mer2³ᴬ and Mer2⁴ᴬ. Control conditions contained Mer2ʷᵗ, Mer2³ᴬ and Mer2⁴ᴬ with beads but without Mre11. Strains used for this experiment are – yGV5052, yGV5053, yGV5057, yGV1375.

C) Protein enrichment in the Mer2ʷᵗ IP-MS.

D) Co-IPs of Mer2ʷᵗ -3HA, Mer2³ᴬ-3HA and Mer2⁴ᴬ-3HA against Mre11. Cultures were harvested at 4 hours post meiotic induction. Western blots were run and probed for α-HA antibody was used to detect Mer2 protein, α-Hop1 was used for Hop, α-Myc for Mre11 and α-Pgk1 was used as a loading control.

Y2H assay in (A), in vitro purification and pulldown in (B) and IP-MS in (C) were done by V. Altmannova, D. Rousova, John Weir (Weir lab colleagues).

Overall, in this project, we highlighted the role of Mer2 in the formation of DSBs in meiosis. We also identify and analyse the function of a conserved region in Mer2 (Mer2⁵²⁻⁷¹) that is involved in its DSB forming function. We suggest that this region is responsible for Mer2 interaction with another accessory protein of DSB machinery, Mre11. Together, our experiments indicate Mer2 as a key bridging element in the Spo11 DSB machinery that dictates its function.

Chapter 5

Discussion

A defining feature of meiosis is the biased use of the homologous chromosome as a repair template for DSB repair. Here we describe a synthetic system defined by the controlled expression of meiosis-specific factors in mitotically dividing cells that enabled us to study the inter-homolog (IH) bias. Our study focuses on Mek1, a meiosis-specific kinase that plays a central role in generating the IH mediated DSB repair (Kim *et al.*, 2010; Lao & Hunter, 2010; Niu *et al.*, 2007; Niu *et al.*, 2005; Wan *et al.*, 2004; Xu *et al*, 1997). Inactivation of Mek1 has been shown to cause sister chromatid mediated repair during meiosis (Humphryes & Hochwagen, 2014; Kim *et al.*, 2010; Niu *et al.*, 2007)). Thus, understanding how Mek1 creates homolog directed repair is a primary question that still needs to be addressed in detail. Several hypothetical models described in the literature attempt to understand the meiotic interhomolog bias. To understand this, here we attempt a novel synthetic approach whereby we ectopically express Mek1 in vegetatively dividing cells, along with accessory meiosis-specific proteins - Red1, Hop1 and demonstrate that they interact together to form a trimeric complex *i.e* the RHM complex. We use this complex to define conditions that aid in the activation of Mek1 in the ectopic so-called 'synthetic system'. Our study finds out that Red1 and Hop1 are the only two other meiosis-specific factors needed to activate Mek1. Finally, we hint towards the ectopic establishment of the inter-homolog bias upon expression of Mek1 in mitotically dividing cells. Our work lays the groundwork to explore the function of the RHM complex in DSB repair dynamics particularly aimed at studying the current models of interhomolog bias.

As a separate part of my PhD thesis research, I have been involved in a collaborative project together with the group of John Weir, at the Friedrich Miescher Laboratory in Tübingen, Germany. This project was centered around the biochemical regulation of meiotic DSB formation, with a specific focus on the Mer2 component of the DSB machinery. Before this study, it was known that Mer2 interacted with several factors involved in DSB formation, such as Spp1 and Hop1 (Acquaviva *et al.*, 2013; Karanyi *et al.*, 2018; Sommermeyer *et al.*, 2013). I analysed specific point mutants of Mer2 that emerged from extensive biochemical work done by our collaborators. These analyses suggested that a conserved amino acid stretch in Mer2's NH_2 terminal, non-structured region was crucially required to enable Spo11-dependent DSB formation. Interestingly, biochemical analysis revealed that, *in vivo*, Mer2 versions harbouring these mutations did not disrupt mapped interactions with Spp1 and Hop1. This suggested that

an additional protein-protein interaction involving these regions on Mer2 might be crucial for DSB formation. Indeed, based on a set of *in vitro* and *in vivo* experiments, Mer2 was shown to interact with Mre11, a component of the MRX complex. The MRX complex is known to be required for Spo11-dependent DSB formation, and our analysis points to a connection between Mer2 and MRX, that aids in Spo11 induced DSB formation in meiosis.

5.1 Designing a meiotic-like synthetic system

Here we design a synthetic system that expresses the RHM complex. We describe the controlled expression of meiosis-specific proteins, Red1, Hop1 and Mek1 in mitotically dividing cells. A similar approach of studying meiosis-specific proteins in ectopic environments has been made earlier in several studies to understand the role of these proteins in meiotic chromosome segregation (Monje-Casas *et al*, 2007; Mozlin *et al*, 2008; Tsubouchi & Roeder, 2006; Varela *et al*, 2010). In this study, we used an inducible galactose promoter to express Red1, Hop1 and Mek1 ectopically. We show that Red1, Hop1 and Mek1 interact to form a complex outside of its native environment (*i.e.,* the meiotic prophase). This suggests that, at least under the conditions of the synthetic system, no other meiosis-specific factors are necessary to mediate this interaction. Furthermore, the RHM complex association was seen even without the introduction of DNA damage. This is somewhat surprising as studies have indicated the role of upstream Mec1/ Tel1 signal in the recruitment of Mek1 to the Red1-Hop1 chromosomal axis (Carballo *et al.*, 2008; Subramanian *et al.*, 2016). We speculate that the possible differences in RHM complex assembly in mitotically and meiotically dividing cells could be on account of -

i) Differential protein levels in mitosis and meiosis. We observed that the expression levels of Hop1 in the synthetic system were similar to the wild type meiotic levels after 2 hours of galactose induction, while a slightly increased expression was seen at 4 hours (Figure 4-2 B). As all the Co-IP experiments were done by collecting samples at 4 hours, assembly of the RHM complex in mitosis could be possible at these higher protein concentrations without the need for DSB induced Mec1/Tel1 signalling.

ii) Cell cycle-related effects - As the cells are asynchronously dividing, effects of constitutively active Mec1 during the S-phase cannot be ruled out (Forey *et al.*, 2020). We speculate that the constitutive activity of Mec1 during the S-phase might be sufficient to a induce signal that triggers complex assembly.

In yet another approach, we designed a synthetic system whereby we expressed Red1 using an estradiol inducible system and kept Hop1 and Mek1 expression under the control of a constitutively expressing promoter (Supplementary figure 1 A, B). The constitutive expression system did not provide us with complete flexibility over monitoring and assessing the roles of individual Hop1 and Mek1 proteins in the RHM-complex. Even though we tried performing several functional experiments with the estradiol-inducible system, we concluded that the galactose induction-based synthetic system was easier to handle and continued further with it.

5.2 Conditions for activation of Mek1 in an ectopic environment

The key function of the RHM complex lies in the Mek1-triggered barrier to sister chromatid repair (BSCR). In order to lay the groundwork for the proof-of-concept functional experiments with Mek1, we initially tested the activity of the Mek1 kinase. We could effectively integrate the RHM complex in the mitotic DSB signalling pathway, leading to activation of Mek1. We show that the activation could be possible in non-physiological ectopic conditions of the synthetic system, that too, only with the help of two other meiosis-specific proteins, Red1 and Hop1. Along with the meiotic proteins, Red1 and Hop1, we also found the activation to be DNA damage dependent. Our experiments with MMS-induced DNA damage for Mek1 activation suggest that the activation is not just mediated by DSBs but also by DNA methylation-induced damage, as in the case of MMS. As Spo11 introduces DNA double-stranded breaks in the genome, we mimicked the situation by treating the synthetic system with DSB inducing drugs (phleomycin and zeocin) to obtain similar Mek1 kinase activity as observed with MMS induced DNA damage.

The necessity for the accessory proteins Red1 and Hop1 in activation of Mek1 was circumvented by artificially inducing Mek1 dimerisation by tagging with GST (Figure 4-1 C). Previous studies have reported GST mediated dimerization and activation of Mek1 in meiotic cells as well as in purified protein fractions (Niu *et al.*, 2007; Wu *et al.*, 2010). Our experiments further indicate that induction of DSBs are dispensable for GST-Mek1 activation (Figure 4-1C). It would be interesting to see if the 'active GST-Mek1' is recruited to chromosomes. Chromosomal recruitment of Mek1 is mediated via its interaction with Hop1 and Red1 (Bailis & Roeder, 1998; Carballo *et al.*, 2008; Niu *et al.*, 2007; Penedos *et al.*, 2015). GST-Mek1 expressing strains lack the meiotic axial proteins. Whether GST-Mek1 is recruited to chromosomes is unknown. Nevertheless, phosphorylation of chromosomally located histones by Mek1, possibly implies that at least some fraction of Mek1 is present on the chromosomes.

In order to elucidate the chromosomal recruitment status of our RHM complex, we performed immunofluorescence microscopy on mitotic chromosome spreads (Supplementary figure 1 C). Preliminary data from our chromosome spread experiments suggest that in Red1-Hop1-Mek1 expressing strains, Mek1 is localized to chromosomes (Supplementary figure 1 C). It would be interesting to look at the genomic Mek1 recruitment landscape in the presence and absence of DSBs. Testing this would validate the hypothesis that Mek1 recruits to chromosomes only in the presence of DSBs.

5.3 Cell cycle effect on activation of Mek1

We investigated the role of upstream DNA damage signalling kinases (Mec1/ Tel1) in the activation of Mek1. In line with previous studies where Mec1 was shown to play a role in RHM complex regulation (via Hop1 phosphorylation), we decided to analyse the effect of *mec1Δ* on the RHM complex in the synthetic system (Carballo *et al.*, 2008; Penedos *et al.*, 2015). Our experiments confirmed the role of Mec1 in the activation of Mek1. Deletion of *MEC1* led to drastic Mek1 inactivation. On the other hand, deletion of *TEL1* had no significant effect.

Next, we queried the effect of the cell cycle on Mek1 activity. Our synthetic system allowed us to understand Mek1 activation mechanisms that are difficult to investigate outside the meiotic G2/ prophase. Based on our findings, Mek1 is activated in G2/M phase of the cell cycle while it remains impaired in G1 arrested cells (Figure 4-6 A, C). To rule out the possibility that the lack of activation is due to a lack of RHM complex assembly in G1, we performed Co-immunoprecipitation assays in G1 and G2/M arrested cells. No change in interaction was observed for Red1-Hop1-Mek1 in the G1 phase (Figure 4-6 D). We speculate that the lack of Mek1 activation in G1 phase could be due to reduced Mec1 activity. Mec1 is activated in response to resected DNA (ssDNA) (Finn *et al.*, 2012; Grenon *et al.*, 2006; Hustedt *et al.*, 2013). Low DSB end resection is seen during G1 phase, which is essential for NHEJ mediated DSB repair (Daley *et al*, 2005). Alternatively, Mec1 is activated via differential mechanisms in G2/M and G1 phase (Bandhu *et al.*, 2014; Cheng *et al.*, 2013; Puddu *et al.*, 2011). Depending on the pathway of activation, Mec1 phosphorylates different downstream target proteins (Puddu *et al.*, 2011). Thus reduced Mec1 signalling in G1 phase could diminish Mek1 activity. Mec1 activity (particularly vital for RHM complex function) can be analysed by monitoring Hop1 phosphorylation mediated by Mec1 (at residue T318) in the G1 arrested cells (Carballo *et al.*, 2008). Moreover, as homologous recombination is presumably active in G1 phase diploid cells

(Smith *et al.*, 2019), this condition could be used to check if hyper resected DSB ends, lead to activation of Mek1.

## 5.4 Red1 truncations and the minimal RHM complex

To gain insight into the dependency of Red1 in RHM complex formation and activation, we performed a structure-function analysis on the domains of Red1 to understand how each of the known Red1 domains, aids in this process. In particular, we designed a series of Red1 domain truncation alleles and expressed them in the synthetic system using galactose-based induction approach. We observed a complete Red1-Hop1-Mek1 complex assembly in all of the Red1 domain deletion variants except those with closure motif deletions that are known to disrupt the Red1-Hop1 interaction (West *et al.*, 2018). Our Co-immunoprecipitation results for the Red1 closure motif deletion constructs indicated that despite the lack of Red1-Hop1 interaction, Red1 could interact with Mek1 in all of the *RED1* domain deletion variants. This result, along with our previous observation of Red1 binding to Mek1 in a Red1, Mek1 co-expressing strain, confirmed that this interaction occurs without the necessity for other meiosis-specific factors (for example, Hop1 was not needed for Red1-Mek1 interaction). Here we report the Red1-Mek1 interaction for the first time. Our data indicates the presence of two Mek1 interaction sites in Red1 as Mek1 interacts with complementary Red1 truncation constructs (for example, Red1$^{1-366}$ and Red1$^{367-827}$). Structurally, this would resemble two possible ways of interaction- i) A single Red1 molecule could wrap around a Mek1 dimer, made possible by the Red1 unstructured part. ii) A Mek1 dimer interacts with a NH2-terminal of one Red1 molecule and the C-terminal of another. More *In vitro* studies need to be done to confirm this hypothesis. Although our *in vivo* experiments point towards a clear interaction of Mek1 and Red1, no interaction was detected between the two proteins in *in vitro* biochemical studies. Using AF2 modelling and structural interpretations, we speculate that the lack of interaction seen for Red1-Mek1 *in vitro* could be due to some structural changes that occur in the *in vivo* settings that aid in the interaction only in the cells (Figure 4-4 A,B, Figure 4-7 B,C). For example, the binding of Red1 to cohesin (Sun *et al.*, 2015) might open up the Mek1 binding region of Red1 (Figure 4-10 A-F). Due to the lack of cohesin in the *in vitro* experiments, the Mek1 binding region of Red1 is no longer available for interaction.

Despite the assembly of the RHM complex in many of the Red1 domain deletion variants, activation of Mek1 was not observed unless a full-length Red1 was expressed (Figure 4-8 A). This indicates that a highly controlled assembly of full-length Red1 in the RHM

complex is required for the activation of Mek1. Possibly, a full-length Red1 protein is responsive in providing the necessary cues in the RHM complex that generates active Mek1, Ex. Red1 phosphorylation events, chromosomal recruitment or Red1 filament formation that dictates meiotic axis assembly. Interference with the above-mentioned features could result in the observed Mek1 inactivation. For example, our data indicates the involvement of Red1 NH2-terminal ARM/PH domain in Mek1 activation (Figure 4-8 A). From our *in vitro* studies, done in collaboration with Weir Lab (FMI, Tuebingen, Germany), we found that the ARML region of Red1 is necessary for Red1-Hop1 interaction (Figure 4-9 C). Using Co-immunoprecipitation experiments, we also confirm that deletion of Red1 ARM/PH domain decreases the Red1-Hop1 interaction (Figure 4-7 C). Thus, impaired Red1-Hop1 interaction could be leading to a lack of Mek1 activation in the NH_2-terminal domain deletion construct of *RED1*. Alternatively, we speculate that the ARM/PH domain of Red1 could be mediating the association between Red1 and meiotic cohesin via Red1-Rec8 interaction as mentioned in the earlier literature (Sun *et al.*, 2015; West *et al.*, 2018). The Red1-cohesin interaction presumably aids in recruiting the RHM complex to the chromosomes, which might be essential for Mek1 activation. Preliminary data from our chromosome spread experiments suggest that Red1 forms meiotic-like chromosomal structures in our synthetic system (Supplementary figure 1-C). Additionally, mitotic chromosome spread experiments with the Red1 NH_2-terminal truncation would further validate the involvement of the ARM/PH domain in RHM complex recruitment to chromosomes.

Our experiments further reveal that disruption of the Red1 filament formation leads to a lack of activate of Mek1 (Figure 4-8 A). The filament-forming region of Red1 is represented by the last residues of Red1 (Red1[1-818]) (West *et al.*, 2019). A similar region was also shown to generate higher-order assemblies in *Zygosaccharomyces rouxii* Red1 (West *et al.*, 2019). Similar oligomeric structures were also observed in SYCP2/SYCP3 and ASY3/AYS4, mammalian and Arabidopsis homologs of Red1 and the structures are essential for meiotic chromosome assembles in these organisms (West *et al.*, 2019). Earlier work has shown that Red1 filament formation is necessary for the proper meiotic chromosome axis assembly and successful completion of meiosis (Eichinger & Jentsch, 2010; Lin *et al.*, 2010; West *et al.*, 2019). In support of these studies, results from our experiments speculate that the filament formation of Red1 might be contributing to efficient Mek1 activity.
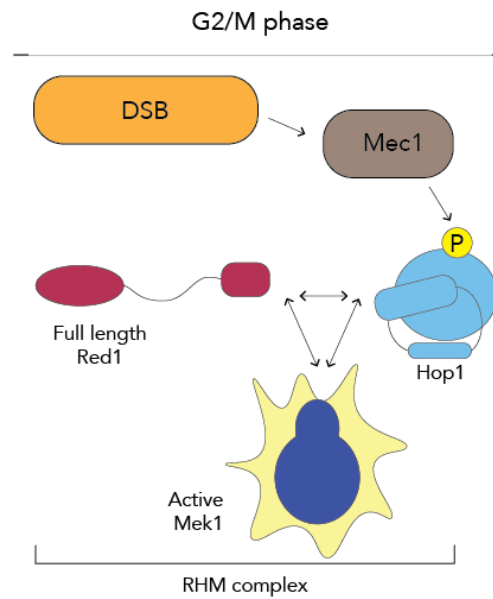
Figure 5-1: Summary of Mek1 activation conditions

Schematic representative of the summary of conditions found to be necessary for Mek1 kinase activity during this Ph.D. work. Our results indicate that in an ectopic environment, Mek1 is active only in the presence of the RHM complex and upon DSB induction. It further requires a full length Red1 and deletion of any of the domains of Red1 render it inactive. A cell cycle dependent effect was confirmed for Mek1 activity. Mek1 activity was restricted to the G2/M phase of the mitotic cell cycle. Further, we confirm that the upstream signaling of Mec1 that is activated in response to DSBs, is essential for this process. Based on earlier studies from meiosis, we speculate about possible pathways that lead to activation of Mek1 in an ectopic environment. DSBs introduced during G2/M phase due to the activity of DSB inducing drugs, are sensed by Mec1. An active Mec1 leads to phosphorylation of Hop1. The presence of phosphorylated Hop1 and a full length Red1 in the RHM complex, aids in activation of Mek1.

5.5 *In vitro* and *in vivo* studies of Mer2 protein reveal an important Mer2-Mre11 interaction that is essential for Mer2 function

A critical event that is responsible for meiotic recombination is the introduction of DNA double-stranded breaks at the onset of meiosis. To better understand the recombination process, I decided to focus on meiotic DSB formation as a part of my second project in collaboration with John Weir and colleagues (Friedrich Miescher Laboratory, Tübingen, Germany). We primarily focused on the formation of DSBs in the context of Mer2, an accessory factor of the

Spo11 DSB machinery. The role of cell cycle-dependent signals in triggering Spo11-DSBs, occur via CDK/DDK dependent phosphorylation of Mer2 (Murakami & Keeney, 2008, 2014; Wan *et al.*, 2008). As mentioned earlier, these phosphorylation events assemble and recruit other Spo11 machinery proteins to Mer2 (and thus to chromosomes).

To decipher the role of Mer2 in DSB induction, we created separation of function mutants of Mer2. Two such alleles were designed by mutating conserved residues in an N-terminally located, evolutionarily conserved patch of Mer2. The mutants, namely, *mer2-3a* and *mer2-4a* exhibited reduced spore viability similar to the *mer2Δ* phenotype, implicating the functional significance of the conserved residues. Further analysis indicated a reduction in phospho-Hop1 levels along with reduced Mek1 activation in these mutants, pointing towards a possible involvement of the conserved Mer2 region in DSB induction or DSB induced signalling (*i.e.,* likely an impaired Mec1/Tel1 activation). Additionally, *in vitro* experiments confirmed that the Mer2[3A]/ Mer2[4A] did not affect Hop1, Spp1 or nucleosome binding (Rousova *et al.*, 2021) along with no effect on mer2 chromosomal localisation as monitored by chromosome spreads. Thus we speculated the presence of an additional Mer2 binding factor that aids in its interaction with the Spo11 DSB machinery and facilitates normal levels of DSBs.

We found a novel interaction of Mer2 with Mre11, an MRX complex protein. The MRX complex was previously shown to be required for meiotic DSB formation (Johzuka & Ogawa, 1995). Thus, we speculate that *mer2Δ* mutants affect the DSB formation, possibly via disruption of Mer2-Mre11 interaction. Indeed, our southern blot data provides evidence of reduced DSB activity in *mer2-3a* and *mer2-4a* compared to the wildtype. To elucidate Mer2-Mre11 interaction, we performed several *in vitro* and *in vivo* experiments together with Weir lab and colleagues. Our Y2H results indicate a marked interaction in Mer2 and Mre11 that gets disrupted in both the *mer2-3a* and *mer2-4a* mutants. Upon *in vitro* purification and pulldown, a robust Mer2-Mre11 interaction was observed and the interaction was reduced in the Mer2 mutant conditions. We performed similar experiments *in vivo* by employing co-immunoprecipitation assay. Although robust interaction was observed between Mer2 (wild type and mutants) and Hop1, no interaction was seen between Mer2 and Mre11 (or with Rec114; a known Mer2 interacting partner). We conclude that under our Co-IP conditions, the Mer2-Mre11 interaction is transient or infrequently occurring. Similar results were observed after *in vivo* biochemical purification of Mer2 followed by IP-MS analysis. No Spo11 associated machinery was detected with the Mass-Spec of Mer2.

We infer that the apparent discrepancy between the Y2H and the pulldown data with the *in vivo* Co-IP and IP-MS experiments could be due to certain *in vivo* changes in Mer2 such as post-translational modifications (CDK/DDK dependent phosphorylation events) or additional *in vivo* binding partners such as other components of the MRX complex or the Spo11 DSB machinery that render the Mer2-Mre11 interaction transient, in *in vivo* setting. We note that introducing mutations that disrupt the Mer2-Mre11 interaction did not lead to a loss of Mre11 recruitment to DSB foci (Rousova *et al.*, 2021). This suggests that the interaction between Mer2 and Mre11 likely reflects a more 'subtle', possible allosteric regulation of meiotic DSB activity. In the future, it will be interesting to reveal how the Mer2-Mre11 controls the formation of Spo11 activity-proficient biochemical assemblies.

5.6 Modulating the inter-homolog bias in a synthetic system by ectopic expression of RHM complex

A preference for the homologous chromosome over the sister chromatid during homologous recombination marks a fundamental phenomenon that differentiates the meiotic division program from mitosis. The meiosis-specific kinase - Mek1, is a key element involved in dictating the recombination partner choice, by phosphorylating downstream target proteins. Although the underlying signalling network that occurs during the inter-homolog repair process is well studied, the exact mechanism behind the change in preference of the repair template (*i.e* from sister chromatid to homologous chromosome) still remains as a hypothetical models (Goldfarb & Lichten, 2010; Hollingsworth, 2010; Hong *et al.*, 2013; Subramanian *et al.*, 2016). Here we provide a novel synthetic system with which we study the role of Mek1 function in recombination partner choice, outside of its meiotic environment. We attempt to understand the mechanism behind changing the bias of the repair template, more specifically as proposed in the 'physical proximity model' (Subramanian *et al.*, 2016). Inter-homolog (IH) recombination is not the preferred choice of DSB repair during mitosis as it leads to loss of heterozygosity. Even so, IH recombination is not completely inhibited in mitotically dividing cells. An inter-homolog to intersister ratio (IH:IS) of 1:4 during mitosis suggests a possibility and availability of necessary conditions for the cells to undergo homolog mediated repair (Bzymek *et al.*, 2010; Humphryes & Hochwagen, 2014). We take advantage of this existing mitotic repair machinery to elucidate the function of Mek1 and understand if the expression of active Mek1 could change the IH:IS ratio in favour of homolog directed repair.

Hyperactivation of Mek1 in meiosis was previously shown to generate more inter-homolog recombination events during meiosis (Wu *et al.*, 2010). The IH preference is proposed to be due to Mek1 mediated delayed DSB repair (Goldfarb & Lichten, 2010; Wu *et al.*, 2010). The 'delayed repair' mechanism goes along with the proposed 'inhibitory' function of Mek1, where Mek1 is thought to suppress sister mediated repair by forming a localised zone of repair suppression in its vicinity (Callender & Hollingsworth, 2010; Subramanian *et al.*, 2016). As Mek1 activity is thought to be localised near sites of DSBs (Kniewel *et al.*, 2017; Subramanian *et al.*, 2016), the physically proximal sister chromatid lies in the zone of repair suppression and is inhibited from being used as a repair template (The physical proximity model). Our observations from the functional spot assay are in line with the physical proximity model. In the functional assay, to avoid the influence of Red1 expression that was shown to cause growth defect due to cell cycle arrest (Figure 4-3 A (Sopko *et al.*, 2006), I employed an active form of Mek1, *i.e.,* GST-Mek1 alone (Figure 4-11 A-C) for the purpose of the assay. Expression of GST-Mek1 in haploid asynchronous cells, led to a growth defect under DNA damaging conditions. The phenotype was specific to the expression of active form of Mek1, as no changes in growth were observed for GFP-Mek1 expressing condition (GFP-Mek1 alone is inactive in the mitotically dividing strains; Figure 4-1 C and Figure 4-5 A). Due to the lack of homologous chromosome in these cells, the only choice of repair template for homologous recombination is the sister chromatid. I speculate that the growth defect is caused by Mek1 mediated inhibition of sister chromatid mediated repair and as no other repair template is available, DSBs remain in an unrepaired state.

Next, I expressed GST-Mek1 in diploids that are homozygous or heterozygous for *GST-MEK1*. Expression of GST-Mek1 from a single *GST-MEK1* allele in diploid cells (heterozygous condition) led to the rescue of the growth phenotype on DNA damage-inducing plates. I speculate that the presence of additional homology sequences on the spatially more distal (from sites of DSBs) homologous chromosomes allows DSB repair and rescues the growth defect. However, upon increased expression of GST-Mek1 in homozygous *GST-MEK1* diploid cells, a return to decrease in growth was observed. This could be inferred as increased expression of active Mek1 leads to 'global' inhibition of DNA repair *i.e* suppression of use of homologs as well as sister chromatids for repair. Thus, the growth assay, to some extent, provides insights into the function of Mek1 that goes along with the spatial proximity model.

Based on our observations of the Mek1 functional assay, experiments could be done additionally to - i) Better understand the 'DSB repair inhibitory' function of Mek1 ii) employ

the synthetic system (specifically the expression of active GST-Mek1) to explain the biased use of homolog during meiosis iii) Artificially change the bias from the default intersister recombination repair in mitosis to inter-homolog repair similar to that occurring in meiosis. Further, the accessory roles of Red1 and Hop1 in promoting Mek1 activity could be studied by employing other functional assays such as southern blots. These assays are described in the later section.

Mek1 protein consists of three domains – an N-terminally located FHA domain, a central catalytic domain and a C-terminal domain involved in Mek1 dimerization (Niu *et al.*, 2007). Our system, along with the functional assay, can be used to study domain-wise function of Mek1. The FHA domain of Mek1 interacts with Hop1, that is phosphorylated at T318 residue. This interaction is crucial for Mek1 activation. It is similar to Rad53-Rad9 interaction, where Rad53 binds to phosphorylated Rad9 via its FHA domain (Sun *et al.*, 1998). The Mek1-Hop1 interaction further acts as a positive feedback loop that further stabilises the Hop1-T318 phosphorylation (Chuang *et al.*, 2012). The FHA domain mediated interaction of Mek1-Hop1 cannot be bypassed by ectopic dimerization of Mek1 (Niu *et al.*, 2005; Wu *et al.*, 2010). Therefore, not only the catalytic domain but also the FHA domain plays a significant role in the Mek1 function. Since there is no Hop1 expressed in the functional spot assay (done with the expression of only GST-Mek1 or GFP-Mek1), it would be interesting to know the contribution of FHA domain and the catalytic domain of Mek1 in the functional phenotype that we observed. Our preliminary experiments suggest that, indeed the FHA domain of Mek1 is involved in its function (Supplementary figure 1 D). More experiments are needed in this direction to support our initial results.

Mek1 promotes inter-homolog bias by phosphorylating several target effector proteins. Amongst its known targets is a strand exchange protein Rad54. Interaction of Rad54 and Rad51 is necessary for inter-sister homologous recombination in vegetatively dividing cells (Niu *et al.*, 2009; Raschle *et al*, 2004). Phosphorylation of Rad54 at T132 by Mek1 inhibits Rad51-Rad54 complex formation (Figure 5-2). Suppression of this interaction is a necessary factor for driving the inter-homolog recombination (Niu *et al.*, 2009). I speculate that a similar effect occurs upon the expression of active Mek1 in vegetatively dividing cells. The kinase activity of Mek1 leads to phosphorylation of Rad54 on T132, disrupting the Rad54-Rad51 complex and biasing the repair towards homolog (Figure 5-2). Thus, in haploid cells, due to the lack of homologous chromosomes available for repair, we could be observing an accumulation of DSBs leading to growth defects. To investigate whether the functional effect is due to Mek1

mediated phosphorylation of Rad54, a similar functional spot assay can be carried out in strains expressing GST-Mek1 and carrying a Rad54-T132A mutation (Niu *et al.*, 2009). The phospho-null Rad54 mutant will not show growth defect even after the expression of GST-Mek1. Additionally, a phospho-mimetic Rad54 T132D mutant could also be used to validate the speculation.
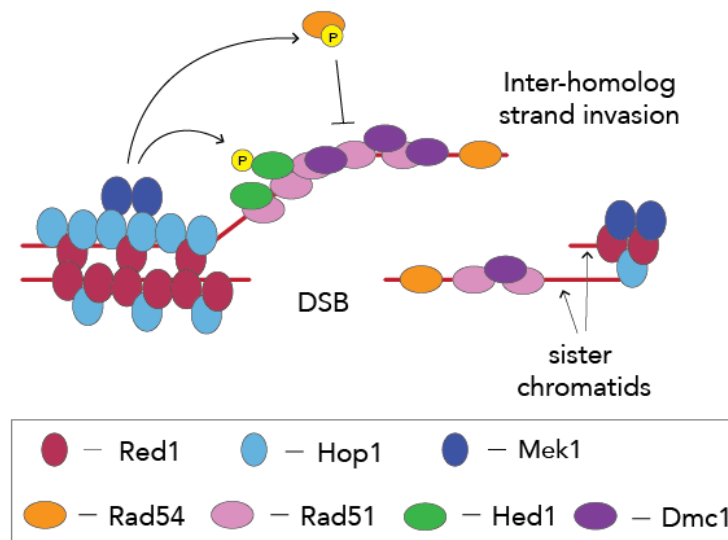
Figure 5-2: A representative schematic of the single end invasion step in the repair of DSBs during meiosis.

Chromosomal axis (sister chromatids in Red) is formed by loading of the axial proteins Red1 (maroon) and Hop1 (light blue). Mek1 (Dark blue) is recruited to the axis in a Red1 and Hop1 dependent manner. Strand invasion proteins, Rad51 (pink) and Rad54 (orange) bind to the resected strands and form nucleoprotein filaments. Mek1 phosphorylates Rad54 and Hed1 (green) in its vicinity. Phosphorylation of Rad54 at T132 by Mek1 leads to disruption of the Rad54-Rad51 interaction. Phosphorylation of Hed1 by Mek1 stabilises the Hed1-Rad51 interaction. The Rad51-Dmc1 filament invades the homologous chromosome and leads to inter-homolog recombination during meiosis.

5.7 Prospects and scope of the study

The functional assay described in the previous section provides an insight into the role of Mek1 in recombination repair. Although the experimental implications point towards a possible change in bias of the DNA repair template in the ectopic presence of Mek1, further experiments need to be done to monitor recombination frequencies, recombination

intermediates and the final byproducts. To analyse these concepts, I would employ the following assays, pre-described in the literature.

By monitoring the recombination rates in mitosis, one could determine the change in inter-sister to inter-homolog recombination frequencies. For this purpose, in future, we would employ the heteroallelic recombination assay described in (Mozlin *et al*., 2008). The assay consists of diploid cells, modified with two distinct *ade2* heteroalleles, each integrated on a different homolog at the endogenous ADE2 chromosomal locus. One allele contains *Nde*I fill in mutation resulting in a frameshift, while the other contains a I-*Sce*I cut site insertion. Both the alleles give rise to an Ade⁻ phenotype. Upon inter-homolog recombination, the mutant alleles generate an Ade⁺ recombinant phenotype, as shown in the figure 5-3. Conversely, an inter-sister recombination event still remains Ade⁻. By plating the *ade2* heteroallelic cultures on Adenine selection plates, one could determine the inter-homolog recombination events corresponding to the number of growing colonies (as Ade⁺ phenotype is observed after undergoing inter-homolog recombination). Changes in recombination by-product frequencies due to the expression of GST-Mek1/ GFP-Mek1 will be determined by employing this assay.
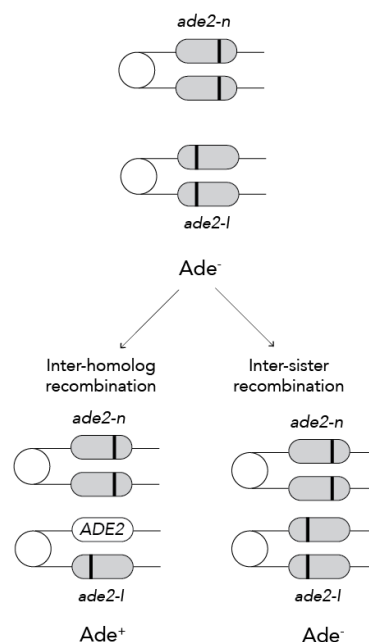
Figure 5-3: Schematic representation of the *ADE2* heteroallelic assay.
The parental homologs contain *ade2-n* and *ade2-I* heteroalleles integrated at the native ADE2 locus on the chromosome XV. The parental condition is ade⁻. Upon inter-homolog recombination, an *ADE2* allele is obtained that is Ade⁺. The intersister recombination events are also Ade⁻ in this assay.

The role of Red1 and Hop1 in the activation of Mek1 is well studied in the literature (Niu *et al.*, 2007; Niu *et al.*, 2005; Wan *et al.*, 2004). *red1Δ* or *hop1Δ* cause an increase in inter-sister recombination events (Hong *et al.*, 2013; Lao & Hunter, 2010). Moreover, phospho-Hop1 mediates the recruitment of Mek1 to chromosomes and aids in its dimerisation and activation. We have shown that Mek1 interacts with Red1 and Hop1 in the synthetic system and both the proteins are necessary for the activation of Mek1. Further investigation is needed to understand the contribution of these accessory proteins in the function of Mek1. Addressing this will help us understand if the RHM complex is autonomous in its function. While doing a spot assay with Red1, we observed a growth defect specific to its filament-forming region (Red1$^{818-827}$). Thus, neither the functional spot assay nor the heteroallelic assay could be employed for assessing the role of Red1 in the RHM complex function. We will employ an inducible site-specific DSB assay described in (Bzymek *et al.*, 2010) for this purpose. The assay was earlier used to measure mitotic recombination frequencies. It can be employed to analyse the inter-homolog and inter-sister crossovers using Southern blotting technique. We speculate that upon expression of the active RHM complex, we would observe an increase in interhomolog recombination events that will change the default IH:IS ratio - 1:4 in mitosis.
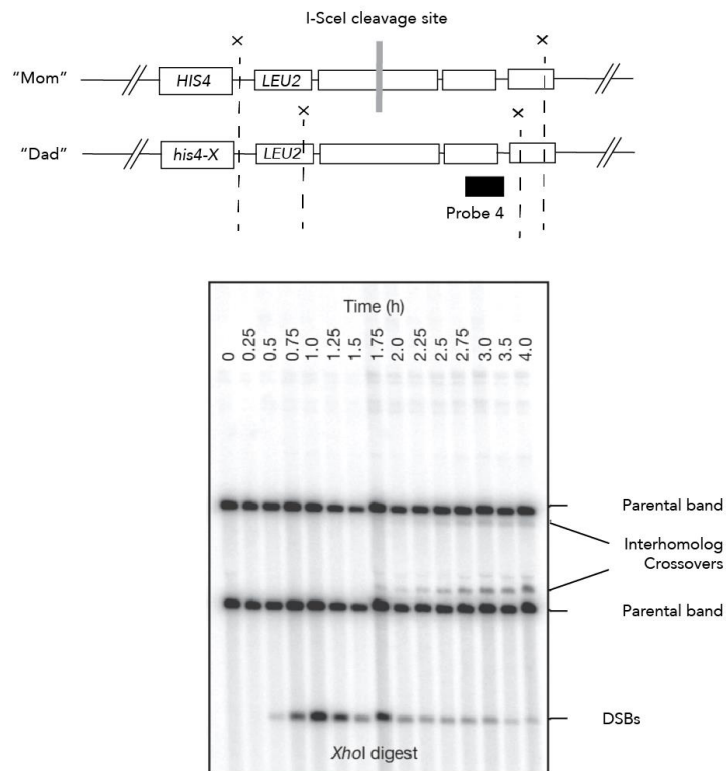
Figure 5-4: Schematic representation of the inducible site specific DSB assay

As described in *Bzymek et al. 2010*. Above is the diagram for modified *HIS4-LEU2* locus.'Mom' and 'Dad' represent the two homologous chromosomes. The Mom homolog carries an I-*Sce*I cleavage site. Upon induction of *Sce*I endonuclease, a DSB is generated at the cleave site in the Mom homolog. This DSB could be repaired by sister chromatid mediated repair or by homologous chromosomes using the 'dad' homolog. Both the homologs contain *Xho*I endonuclease cleavage sites at different locations, represented by 'X'. Treatment with *Xho*I leads to fragments of differential lengths for crossover products than the parental strands. Separation using Southern blot, allows us to assess the percent of inter-homolog recombination events occurring. We speculate that upon expression of active Mek1 (with GST-Mek1 or in the RHM complex), the inter-homolog frequency will increase in mitotically dividing cells. Figure adopted from (Bzymek *et al.*, 2010).

Our synthetic system, along with the functional assays described above, provides an excellent tool to understand the function of individual meiosis-specific proteins in modulating the interhomolog bias. It becomes difficult to analyse the individual contribution of the members in IH bias as the proteins involved being part of an intricate meiotic prophase network. Two such meiosis-specific proteins, Hed1 and Dmc1, are known to significantly contribute to meiotic interhomolog DSB repair. Mek1 promotes IH recombination by inhibition of strand exchange protein Rad51. This is achieved in two different ways – i) Phosphorylation of Rad54 on T132 that leads to disruption of Rad54-Rad51 interaction (Niu *et al.*, 2009). ii) Phosphorylation and stabilisation of a meiosis-specific Hed1 protein that binds to Rad51, inhibits its activity and disrupts the Rad54-Rad51 interaction (Busygina *et al.*, 2008; Callender *et al.*, 2016; Hollingsworth & Gaglione, 2019; Tsubouchi & Roeder, 2006). In most eukaryotic organisms, Rad51 is constitutively expressed and is necessary for inter-sister recombination. In meiosis, the strand exchange activity of Dmc1 (meiosis-specific protein), is necessary in addition to the presence of Rad51 (and not the activity), for inter-homolog repair (Bishop *et al.*, 1992; Cloud *et al.*, 2012; Woo *et al.*, 2020). It should be noted that strand exchange activity of Dmc1 is necessary but not sufficient for inter-homolog bias, as Mek1 inactivation results in inter-sister recombination even in the presence of *DMC1* (Goldfarb & Lichten, 2010; Hong *et al.*, 2013; Kim *et al.*, 2010). Thus, Hed1 and Dmc1 have emerged to be important meiosis-specific players in transducing the Mek1 kinase signal. Our functional assay in the synthetic system is a robust tool to understand the individual and targeted roles of these (and several such) meiosis-specific factors in forming the inter-homolog bias.

6.0 Summary

The meiotic cell division program culminates in the formation of four haploid gametes. Proper chromosome segregation during meiosis I is facilitated by the establishment of physical linkages between the homologous chromosome pairs. Without the homolog linkage, chromosomal missegregation events and thus the associated aneuploidy, strikingly increases. To ensure homolog pairing, introduction of programmed DNA double-stranded breaks (DSBs) occur at the onset of meiotic division. The DSBs are repaired by homologous recombination by preferential usage of DNA sequences from the homologous chromosome as a repair template. This so-called interhomolog bias is in contrast to the default sister chromatid mediated DSB repair that occurs in mitosis. An important player in achieving the interhomolog bias is a meiosis-specific kinase 'Mek1' that functions with two other accessory meiotic chromosomal axial elements - Red1 and Hop1. Here we studied the role of Mek1 in establishing the interhomolog bias by using an approach of ectopic induction. We designed a synthetic system that conditionally expresses Red1, Hop1 and Mek1 in mitotically dividing cells. We show that the Red1-Hop1-Mek1 interact to form a complex (RHM complex) in the ectopic conditions. In the process we provide evidence for a novel Red1-Mek1 independent interaction that we report for the first time. Our *in vitro* studies, performed in an attempt to reconstitute the RHM complex, provide evidence of a robust Red1-Hop1 interaction. We observe a stoichiometry of 1:1 Red1:Hop1 complex *in vitro* by employing mass photometry. We report for the first time the importance of the Red1 NH_2-terminal conserved region in interaction with Hop1. Finally, we provide a model describing the RHM complex association using Alpha Fold 2 modelling.

To understand the function of Mek1, we study the conditions necessary for Mek1 activation in the synthetic system. Mek1 activation not only requires Red1-Hop1-Mek1 complex formation but is also dependent on the presence of DSBs in the cells. However, the requirement of Red1, Hop1 and DSBs is dispensable for Mek1 activation if we perform artificial dimerisation of Mek1 by GST tagging. Furthermore, our experiments suggest that Mek1 activation requires the activity of upstream DSB sensor kinase Mec1. Our synthetic system allows us to study these meiosis-specific proteins outside the meiotic conditions, allowing us to provide evidence that activation of the RHM complex cannot be achieved in G1 arrested cells. There could be G2/M specific factors, not yet known to us, that support activation of Mek1 only in G2/M phase. Using this synthetic system, we finally demonstrate that Mek1

activation in mitosis leads to DNA damage sensitivity similar to *rad51Δ* phenotype, suggesting that RHM complex activation at least in part mediates interhomolog repair.

In a second project done in collaboration with the group of John Weir (Weir Lab, FML Tübingen), we focused on studying how DSBs are introduced in early meiotic prophase I, specifically in the context of Mer2, a Spo11 DSB machinery protein. We describe conserved residues in Mer2 that dictate its DSB forming function. Mutating these Mer2 residues to alanine, disrupts DSB forming activity in cells. Furthermore, we provide evidence that mutating the conserved residues lead to disruption of Mer2-Mre11 interaction (Mre11 is another Spo11 DSB machinery protein), suggesting a possible reason why DSB formation is affected in this condition.

6.0 Zusammenfassung

Das meiotische Zellteilungsprogramm endet mit der Bildung von vier haploiden Keimzellen. Die ordnungsgemäße Trennung der Chromosomen während der Meiose I wird durch die Erstellung physischer Bindungen zwischen den homologen Chromosomenpaaren ermöglicht. Fehlen die homologen Verknüpfungen kommt es vermehrt zu chromosomalen Fehlsegregationen und damit zu Aneuploidie. Um die homologe Paarung zu gewährleisten, werden zu Beginn der meiotischen Teilung programmierte DNA-Doppelstrangbrüche (DSBs) eingeführt. Die DSBs werden durch homologe Rekombination repariert, indem bevorzugt DNA-Sequenzen des homologen Chromosoms als Reparaturvorlage verwendet werden. Dieser so genannte interhomologe Bias steht im Gegensatz zu der DSB-Reparatur, die in der Mitose stattfindet, wobei die Sequenz der Schwesterchromatiden als Vorlage verwendet wird. Ein wichtiger Faktor bei der Erzielung des interhomologen Bias ist die Meiose-spezifische Kinase Mek1, die mit zwei anderen meiotischen chromosomalen axialen Elementen - Red1 und Hop1 - zusammenarbeitet. Hier haben wir die Rolle von Mek1 bei der Etablierung des interhomologen Bias mit Hilfe der ektopischen Induktion untersucht. Wir haben ein synthetisches System entwickelt, welches Red1, Hop1 und Mek1 in sich mitotisch teilenden Zellen konditional exprimiert. Wir zeigen, dass Red1-Hop1-Mek1 unter den ektopischen Bedingungen miteinander interagieren und einen Komplex (RHM-Komplex) bilden. Dabei liefern wir Hinweise auf eine neuartige, von Red1-Mek1 unabhängige Interaktion, über die wir zum ersten Mal berichten. Unsere in vitro-Studien liefern Beweise für eine robuste Red1-Hop1-Interaktion bei der Rekonstitution des RHM-Komplexes. Wir beobachten eine Stöchiometrie von 1:1 des Red1:Hop1-Komplexes *in vitro* mit Hilfe der Massenphotometrie. Wir berichten zum ersten Mal über die Bedeutung der konservierten NH_2-terminalen Region von Red1 für die Interaktion mit Hop1. Schließlich stellen wir ein Modell vor, das die Assoziation des RHM-Komplexes mit Hilfe von Alpha Fold 2 beschreibt.

Um die Funktion von Mek1 zu verstehen, untersuchen wir die Bedingungen, welche für die Mek1-Aktivierung in unserem synthetischen System erforderlich sind. Die Mek1-Aktivierung erfordert nicht nur die Bildung des RHM-Komplexes, sondern ist auch von der Anwesenheit von DSBs in den Zellen abhängig. Die Notwendigkeit von Red1, Hop1 und DSBs ist jedoch für die Mek1-Aktivierung entbehrlich, wenn Mek1 künstlich durch GST dimerisiert wird. Außerdem deuten unsere Experimente darauf hin, dass die Mek1-Aktivierung die Aktivität der vorgeschalteten DSB-Sensorkinase Mec1 erfordert. Mit unserem synthetischen

System können wir diese Meiose-spezifischen Proteine außerhalb der meiotischen Bedingungen untersuchen und so nachweisen, dass die Aktivierung des RHM-Komplexes nicht in G1-arretierten Zellen erfolgen kann. Es könnte G2/M-spezifische Faktoren geben, die uns noch nicht bekannt sind, und die die Aktivierung von Mek1 nur in der G2/M-Phase unterstützen. Mit diesem synthetischen System zeigen wir schlussendlich, dass die Mek1-Aktivierung in der Mitose zu einer Empfindlichkeit gegenüber DNA-Schädigung führt, die dem *rad51Δ*-Phänotyp ähnelt, was darauf schließen lässt, dass die Aktivierung des RHM-Komplexes zumindest teilweise die interhomologe Reparatur vermittelt.

In einem zweiten Projekt, das in Kollaboration mit der Gruppe von John Weir (Weir Labor, FML Tübingen) durchgeführt wurde, untersuchten wir, wie DSBs in der frühen meiotischen Prophase I eingeführt werden, insbesondere im Zusammenhang mit Mer2, einem Spo11 DSB-Maschinenprotein. Wir beschreiben konservierte Aminosäuren in Mer2, die seine DSB-bildende Funktion bestimmen. Die Mutation dieser Mer2-Aminosäuren zu Alanin verhindert die DSB-bildende Aktivität in Zellen. Darüber hinaus konnten wir nachweisen, dass die Mutation der konservierten Aminosäuren zu einer Hemmung der Interaktion zwischen Mer2 und Mre11 führt (Mre11 ist ein weiteres Spo11-DSB-Maschinenprotein), was auf einen möglichen Grund für die Beeinträchtigung der DSB-Bildung hindeutet.

7.0 Supplementary figures:
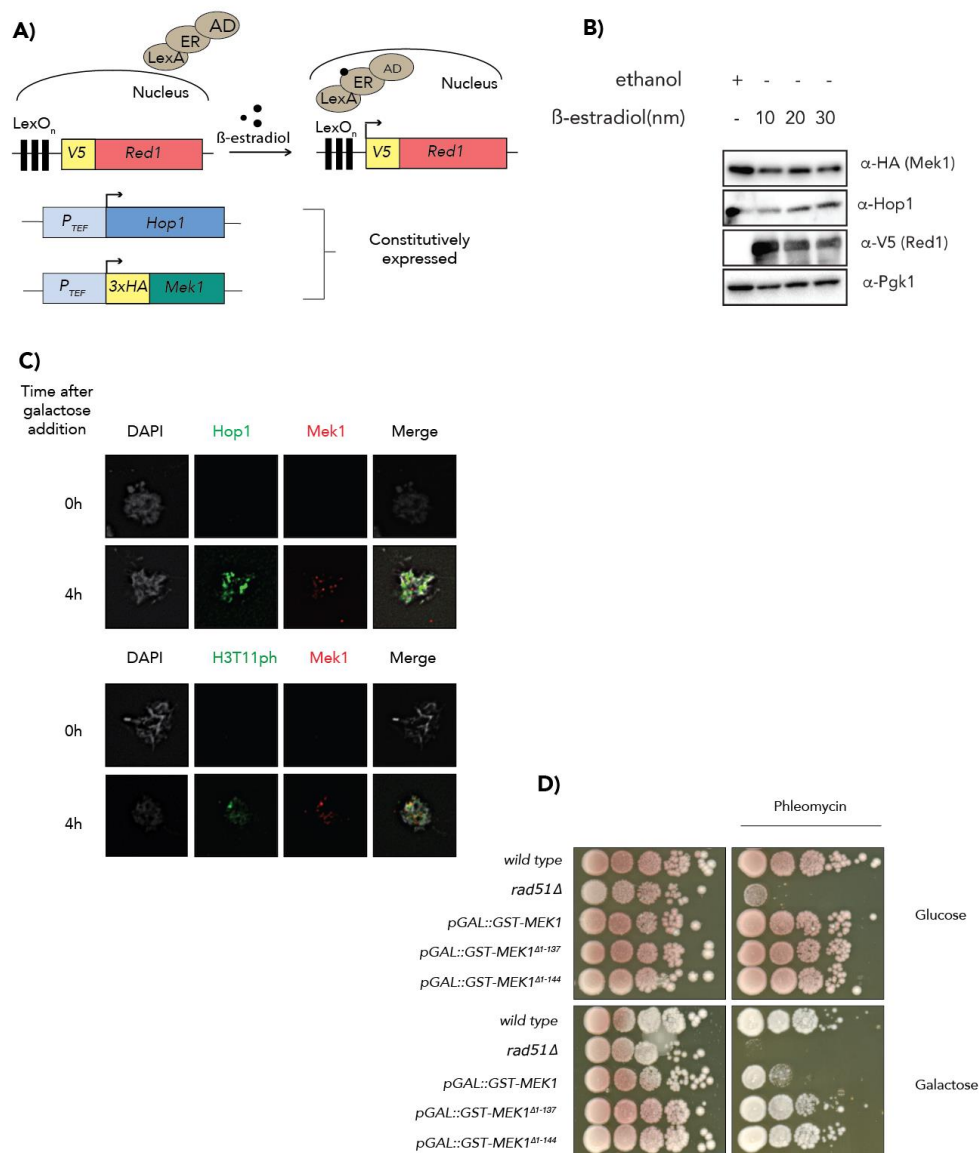
Supplementary figure 1:

A) Synthetic system with expression of Hop1 and Mek1 driven by a constitutive pTEF promoter and the expression of Red1 is carried out by LexA-LexO based induction system. LexO repeats are integrated upstream of Red1 coding region. Upon treatment with estradiol, the LexA-ER-AD binds to the LexO repeats and drives the expression of Red1.

B) Western blot depicting the constitutively expressing Hop1 (detected by α-Hop1) and Mek1 (detected by α-HA). Expression of Red1 (detected by α-V5) was dependent on estradiol treatment.

C) Representative immunofluorescence images of mitotic chromosome spreads performed at indicated time points after addition of galactose. Cultures were treated with MMS, 0.5 hours prior to galactose induction. DAPI depicts the DNA (in grey). Hop1 (in green) and Mek1 (in Red) are recruited to the chromosomes. As predicted, Hop1 binds the entire chromosome thus showing linear structures whereas Mek1 is localized to sites of DSBs hence foci like structures are visible for Mek1. Localized Mek1 is supposedly active due to presence of H3 T11 phosphorylation signal (in green).

D) 10 fold serial dilutions of strains were spotted on glucose and galactose plates supplemented with DNA damaging drug - phleomycin. Plates were incubated for 2-4 days at 30°C before imaging. A growth defect was observed for GST-Mek1 expressing strain on the DNA damaging plates. The growth defect seemed to be rescued upon deletion of the FHA domain (GST-Mek1$^{\Delta 1-137}$) and the catalytic domain of Mek1 (GST-Mek1$^{\Delta 1-144}$).
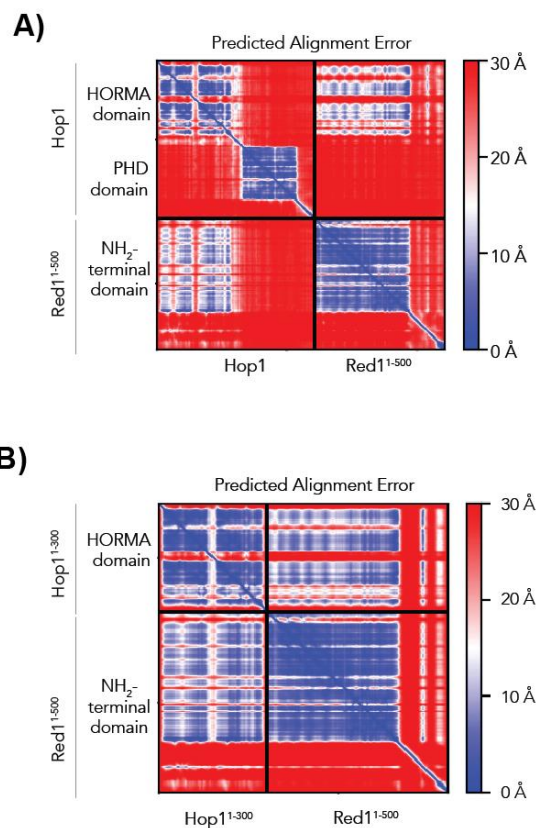
Supplementary figure 2

Predicted alignment error of Hop1-Red1 AF2 models.

A) PAE plot of the Hop1-Red1$^{1-500}$ AF2 model. The relative position of the Hop1 HORAM domain and the NH$_2$-terminal domain of Red1 was predicted to be low.

B) PAE plot of the Hop1$^{1-300}$-Red1$^{1-500}$ AF2 model.

8.0 Yeast strains

All strains are of W303 origin except the following strains that are of SK1 origin - yGV8, yGV1375, yGV4744, yGV4874, yGV4879, yGV4889, yGV4913, yGV4931, yGV4933, yGV4934, yGV4957, yGV5052, yGV5053, yGV5057, yGV49, yGV4442

Table 8-1: yeast strains

Strain number	Genotype
yGV49	*MATa/MATalpha, ho::LYS2, lys2, ura3, leu2::hisG, his4B::LEU2, ARG4/ arg4-Bgl II*
yGV104	*MATa, ade2-1, leu2-3, ura3, trp1-1, his3-11,15, can1-100, GAL, psi+,*
yGV2774	*MATa, ade2-1, leu2-3, ura3, trp1-1, his3-11,15, can1-100, GAL, psi+, mek1:TRP1-PGAL1-GST-MEK1*
yGV2812	*MATa, ade2-1, leu2-3, ura3, trp1-1, his3-11,15, can1-100, GAL, psi+, mek1:TRP1-PGAL1-GFP-MEK1*
yGV3219	*MATa, ade2-1, leu2-3, ura3, trp1-1, his3-11,15, can1-100, GAL, psi+, Hop1::His3MX6-PGAL-HOP1, mek1:TRP1-PGAL1-GFP-MEK1*
yGV3235	*MATa, ade2-1, leu2-3, ura3, trp1-1, his3-11,15, can1-100, GAL, psi+, red1::KANMX6::pGAL-3HA::RED1, hop1::His3MX6-PGAL-HOP1*
yGV3243	*MATa, ade2-1, leu2-3, ura3, trp1-1, his3-11,15, can1-100, GAL, psi+, hop1::His3MX6-PGAL-HOP1*
yGV3255	*MATa, ADE2, leu2-3, ura3, trp1-1, his3-11,15, can1-100, GAL, psi+, red1::KANMX6::pGAL-3HA::RED1, mek1:TRP1-PGAL1-GFP-MEK1*
yGV3605	*MATa, ade2-1, leu2-3, ura3, trp1-1, his3-11,15, can1-100, GAL, psi+, sml1Δ::HphMX6*

yGV3693	*MATa, ade2-1, leu2-3,112, ura3-1, trp1-1, his3-11,15, can1-100,RAD5, mec1Δ::TRP1, sml1Δ::HIS3*
yGV3719	*MATa, ade2-1, leu2-3,112, ura3-1, trp1-1, his3-11,15, can1-100, tel1Δ::URA3*
yGV3726	*MATa, ade2-1, leu2-3,112, ura3-1, trp1-1, his3-11,15, can1-100, red1::KANMX6::pGAL-3HA::RED1*
yGV3798	*MATa, ade2-1, leu2-3, ura3, trp1-1, his3-11,15, can1-100, GAL, psi+, red1::KANMX6::pGAL-3HA-345-827-red1*
yGV3799	*MATa, ade2-1, leu2-3, ura3, trp1-1, his3-11,15, can1-100, GAL, psi+, red1::KANMX6::pGAL-3HA-367-827-red1*
yGV4190	*MATa, ade2-1, leu2-3, ura3, trp1-1, his3-11,15, can1-100, GAL, psi+, red1::KANMX6::pGAL-3HA-1-730-red1::TRP1*
yGV4191	*MATa, ade2-1, leu2-3, ura3, trp1-1, his3-11,15, can1-100, GAL, psi+, red1::KANMX6::pGAL-3HA-1-818-red1::TRP1*
yGV4193	*MATa, ade2-1, leu2-3, ura3, trp1-1, his3-11,15, can1-100, GAL, psi+, red1::KANMX6::pGAL-3HA-1-346-red1::TRP1*
yGV4194	*MATa, ade2-1, leu2-3, ura3, trp1-1, his3-11,15, can1-100, GAL, psi+, red1::KANMX6::pGAL-3HA-1-367-red1::TRP1*
yGV4207	*MATalpha, ade2-1, leu2-3, ura3, trp1-1, his3-11,15, can1-100, GAL, psi+, red1::KANMX6::pGAL-3HA-345-827-red1, hop1::His3MX6-PGAL-Hop1, mek1:TRP1-PGAL1-GFP-MEK1*
yGV4393	*MATalpha, ade2-1, leu2-3, ura3, trp1-1, his3-11,15, can1-100, GAL, psi+, hop1::His3MX6-PGAL-Hop1, mek1:TRP1-PGAL1-GFP-MEK1, red1::KANMX6::pGAL-3HA-1-818-red1::TRP1*

yGV4395	*MATalpha, ade2-1, leu2-3, ura3, trp1-1, his3-11,15, can1-100, GAL, psi+, Hop1::His3MX6-PGAL-Hop1, mek1:TRP1-PGAL1-GFP-MEK1, red1::KANMX6::pGAL-3HA-1-367-red1::TRP1*
yGV4397	*MATa, ade2-1, leu2-3, ura3, trp1-1, his3-11,15, can1-100, GAL, psi+, Hop1::His3MX6-PGAL-Hop1, mek1:TRP1-PGAL1-GFP-MEK1, red1::KANMX6::pGAL-3HA-1-346-red1::TRP1*
yGV4400	*MATalpha, ade2-1, leu2-3, ura3, trp1-1, his3-11,15, can1-100, GAL, psi+, Hop1::His3MX6-PGAL-Hop1, mek1:TRP1-PGAL1-GFP-MEK1, red1::KANMX6::pGAL-3HA-1-730-red1::TRP1*
yGV4402	*MATa, ade2-1, leu2-3, ura3, trp1-1, his3-11,15, can1-100, GAL, psi+, hop1::His3MX6-PGAL-Hop1, mek1:TRP1-PGAL1-GFP-MEK1, red1::KANMX6::pGAL-3HA-367-827-red1*
yGV4442	*MATa/ MATalpha, ho::LYS2, lys2, ura3, leu2::hisG, TRP1, his4B::LEU2, MEK1-6HA::KanMX6, hop1::LEU2*
yGV4806	*MATa, ade2-1, leu2-3, ura3, trp1-1, his3-11,15, can1-100, GAL, psi+, red1::KANMX6::pGAL-3HA::RED1, Hop1::His3MX6-PGAL-Hop1, mek1:TRP1-PGAL1-GFP-MEK1*
yGV4975	*MATa, ade2-1, leu2-3, ura3, trp1-1, his3-11,15, can1-100, GAL, hpsi+, red1::KANMX6::pGAL-3HA::RED1, Hop1::His3MX6-PGAL-HOP1, mek1:TRP1-PGAL1-GFP-MEK1, mad2Δ::KanMX4*
yGV5011	*MATa, ade2-1, leu2-3,112, ura3-1, trp1-1, his3-11,15, can1-100, GAL, psi+, red1::KANMX6::pGAL-3HA::RED1, Hop1::His3MX6-PGAL-HOP1, mek1:TRP1-PGAL1-GFP-MEK1, tel1Δ ::URA3*
yGV5033	*MATa, ade2-1, leu2-3,112, ura3-1, trp1-1, his3-11,15, can1-100,RAD5, mek1:TRP1-PGAL1-GFP-MEK1, red1::KANMX6::pGAL-3HA::RED1, Hop1::His3MX6-PGAL-HOP1, mec1Δ ::TRP1, sml1Δ ::HIS3*

yGV5044	*MATa, ade2-1, leu2-3, ura3, trp1-1, his3-11,15, can1-100, GAL, psi+, sml1Δ ::HphMX6, red1::KANMX6::pGAL-3HA::RED1, Hop1::His3MX6-PGAL-HOP1, mek1:TRP1-PGAL1-GFP-MEK1*
yGV8	*MATa,ho::LYS2, lys2, ura3, leu2::hisG, his3::hisG, trp1::hisG* *MATalpha, ho::LYS2, lys2, ura3, leu2::hisG, his3::hisG, trp1::hisG*
yGV1375	*MATa, ho::LYS2, TRP, his3::hisG, ura3, LEU2, MRE11-13MYC::HIS3* *MATalpha, ho::LYS2, trp1::hisG, his3::hisG, URA3, leu2::hisG,MRE11-13MYC::HIS3*
yGV4744	*MATa, ho::LYS2, lys2, ura3, leu2::hisG, his3::hisG, trp1::hisG, sae2Δ::LEU2* *MATalpha, ho::LYS2, lys2, ura3, leu2::hisG, his3::hisG, trp1::hisG, sae2Δ::LEU2*
yGV4874	*MATa, ho::LYS2, lys2, ura3, leu2::hisG, his3::hisG, trp1::hisG, mer2Δ::HISMX6::pMER2-MER2-3HA::LEU2* *MATalpha, ho::LYS2, lys2, ura3, leu2::hisG, his3::hisG, trp1::hisG, mer2Δ::HISMX6::pMER2-MER2-3HA::LEU2*
yGV4879	*MATa, ho::LYS2, lys2, ura3, leu2::hisG, his3::hisG, trp1::hisG, mer2Δ::HISMX6::pMER2-Mer2-4A3HA::LEU2* *MATalpha, ho::LYS2, lys2, ura3, leu2::hisG, his3::hisG, trp1::hisG, mer2Δ::HISMX6::pMER2-Mer2-4A-3HA::LEU2*
yGV4889	*MATa, ho::LYS2, lys2, ura3, leu2::hisG, his3::hisG, trp1::hisG, mer2Δ::HISMX6* *MATalpha, ho::LYS2, lys2, ura3, leu2::hisG, his3::hisG, trp1::hisG, mer2Δ::HISMX*
yGV4913	*MATa, ho::LYS2, lys2, ura3, leu2::hisG, his3::hisG, trp1::hisG, mer2Δ::HISMX6, sae2Δ::LEU2* *MATalpha, ho::LYS2, lys2, ura3, leu2::hisG, his3::hisG, trp1::hisG, mer2Δ::HISMX6, sae2Δ::LEU2*
yGV4931	*MATa, ho::LYS2, lys2, ura3, leu2::hisG, his3::hisG, trp1::hisG, mer2Δ::HISMX6::pMER2-mer2-4A-3HA::LEU2, sae2Δ::LEU2* *MATalpha, ho::LYS2, lys2, ura3, leu2::hisG, his3::hisG, trp1::hisG,mer2Δ::HISMX6::pMER2-mer2-4A-3HA::LEU2,sae2Δ::LEU2*

yGV4933	*MATa, ho::LYS2, lys2, ura3, leu2::hisG, his3::hisG, trp1::hisG,* *mer2Δ::HISMX6::pMER2-mer2-3A-3HA::LEU2* *MATalpha, ho::LYS2, lys2, ura3, leu2::hisG, his3::hisG, trp1::hisG,* *mer2Δ::HISMX6::pMER2-mer2-3A-3HA::LEU2*
yGV4934	*MATalpha, ho::LYS2, lys2, ura3, leu2::hisG, his3::hisG, trp1::hisG,* *mer2Δ::HISMX6::pMER2-mer2-3A-3HA::LEU2, sae2Δ::LEU2* *MATa, ho::LYS2, lys2, ura3, leu2::hisG, his3::hisG, trp1::hisG,* *mer2Δ::HISMX6::pMER2-mer2-3A-3HA::LEU2, sae2Δ::LEU2*
yGV4957	*MATa, ho::LYS2, lys2, ura3, leu2::hisG, his3::hisG, trp1::hisG,* *mer2Δ::HISMX6::pMER2-mer2-3HA::LEU2, sae2Δ::LEU2* *MATalpha, ho::LYS2, lys2, ura3, leu2::hisG, his3::hisG,* *trp1::hisG,mer2Δ::HISMX6::pMER2-mer2-3HA::LEU2, sae2Δ::LEU2*
yGV5052	*MATa, ho::LYS2, lys2, URA3, leu2::hisG, his3::hisG, trp1::hisG,* *mer2Δ::HISMX6::pMER2-Mer2-3HA::LEU2, MRE11-13MYC::HIS3* *MATalpha, ho::LYS2, lys2, ura3, leu2::hisG, his3::hisG, trp1::hisG,* *mer2Δ::HISMX6::pMER2-Mer2-3HA::LEU2, MRE11-13MYC::HIS3*
yGV5053	*MATa, ho::LYS2, trp1::hisG, his3::hisG, URA3, leu2::hisG* *MRE11-13MYC::HIS3, rmer2Δ::HISMX6::pMER2-Mer2-3A-3HA::LEU2* *MATalpha, ho::LYS2, trp1::hisG, his3::hisG, URA3, leu2::hisG* *MRE11-13MYC::HIS3, mer2Δ::HISMX6::pMER2-Mer23A-3HA::LEU2*
yGV5057	*MATa, ho::LYS2, lys2, ura3, leu2::hisG, his3::hisG, trp1::hisG,* *mer2Δ::HISMX6::pMER2-Mer2-4A3HA::LEU2, MRE11-13MYC::HIS3* *MATalpha, ho::LYS2, trp1::hisG, his3::hisG, URA3, leu2::hisG* *MRE11-13MYC::HIS3, mer2Δ::HISMX6::pMER2-Mer2-4A-3HA::LEU2*

9.0 Bibliography

6. Acquaviva L, Székvölgyi L, Dichtl B, Dichtl BS, de La Roche Saint André C, Nicolas A, Géli V (2013) The COMPASS subunit Spp1 links histone methylation to initiation of meiotic recombination. *Science* 339: 215-218

7. Adam C, Guérois R, Citarella A, Verardi L, Adolphe F, Béneut C, Sommermeyer V, Ramus C, Govin J, Couté Y *et al* (2018) The PHD finger protein Spp1 has distinct functions in the Set1 and the meiotic DSB formation complexes. *PLoS Genet* 14: e1007223

8. Adzuma K (1992) Stable synapsis of homologous DNA molecules mediated by the Escherichia coli RecA protein involves local exchange of DNA strands. *Genes Dev* 6: 1679-1694

9. Agarwal R, Tang Z, Yu H, Cohen-Fix O (2003) Two distinct pathways for inhibiting pds1 ubiquitination in response to DNA damage. *J Biol Chem* 278: 45027-45033

10. Alberts BWJHT (2008) *Molecular biology of the cell*. Garland Science, New York

11. Allers T, Lichten M (2001) Differential timing and control of noncrossover and crossover recombination during meiosis. *Cell* 106: 47-57

12. Aouida M, Eshrif A, Ramotar D (2019) Yeast Lacking the PP2A Phosphatase Regulatory Subunit Rts1 Sensitizes rad51 Mutants to Specific DNA Damaging Agents. *Front Genet* 10: 1117

13. Aravind L, Koonin EV (1998) The HORMA domain: a common structural denominator in mitotic checkpoints, chromosome synapsis and DNA repair. *Trends Biochem Sci* 23: 284-286

14. Argunhan B, Leung WK, Afshar N, Terentyev Y, Subramanian VV, Murayama Y, Hochwagen A, Iwasaki H, Tsubouchi T, Tsubouchi H (2017) Fundamental cell cycle kinases collaborate to ensure timely destruction of the synaptonemal complex during meiosis. *Embo j* 36: 2488-2509

15. Aylon Y, Kupiec M (2005) Cell cycle-dependent regulation of double-strand break repair: a role for the CDK. *Cell Cycle* 4: 259-261

16. Bailis JM, Roeder GS (1998) Synaptonemal complex morphogenesis and sister-chromatid cohesion require Mek1-dependent phosphorylation of a meiotic chromosomal protein. *Genes Dev* 12: 3551-3563

17. Baldo V, Testoni V, Lucchini G, Longhese MP (2008) Dominant TEL1-hy mutations compensate for Mec1 lack of functions in the DNA damage response. *Mol Cell Biol* 28: 358-375

18. Bandhu A, Kang J, Fukunaga K, Goto G, Sugimoto K (2014) Ddc2 mediates Mec1 activation through a Ddc1- or Dpb11-independent mechanism. *PLoS Genet* 10: e1004136-e1004136

19. Bani Ismail M, Shinohara M, Shinohara A (2014) Dot1-dependent histone H3K79 methylation promotes the formation of meiotic double-strand breaks in the absence of histone H3K4 methylation in budding yeast. *PLoS One* 9: e96648

20. Baudat F, Buard J, Grey C, Fledel-Alon A, Ober C, Przeworski M, Coop G, de Massy B (2010) PRDM9 is a major determinant of meiotic recombination hotspots in humans and mice. *Science* 327: 836-840

21. Benjamin KR, Zhang C, Shokat KM, Herskowitz I (2003) Control of landmark events in meiosis by the CDK Cdc28 and the meiosis-specific kinase Ime2. *Genes Dev* 17: 1524-1539

22. Bergerat A, de Massy B, Gadelle D, Varoutas PC, Nicolas A, Forterre P (1997) An atypical topoisomerase II from Archaea with implications for meiotic recombination. *Nature* 386: 414-417

23. Bhargava R, Onyango DO, Stark JM (2016) Regulation of Single-Strand Annealing and its Role in Genome Maintenance. *Trends Genet* 32: 566-575

24. Bishop DK, Park D, Xu L, Kleckner N (1992) DMC1: a meiosis-specific yeast homolog of E. coli recA required for recombination, synaptonemal complex formation, and cell cycle progression. *Cell* 69: 439-456

25. Blat Y, Kleckner N (1999) Cohesins bind to preferential sites along yeast chromosome III, with differential regulation along arms versus the centric region. *Cell* 98: 249-259

26. Blat Y, Protacio RU, Hunter N, Kleckner N (2002) Physical and functional interactions among basic chromosome organizational features govern early steps of meiotic chiasma formation. *Cell* 111: 791-802

27. Blitzblau HG, Bell GW, Rodriguez J, Bell SP, Hochwagen A (2007) Mapping of meiotic single-stranded DNA reveals double-stranded-break hotspots near centromeres and telomeres. *Curr Biol* 17: 2003-2012

28. Blitzblau HG, Chan CS, Hochwagen A, Bell SP (2012) Separation of DNA replication from the assembly of break-competent meiotic chromosomes. *PLoS Genet* 8: e1002643

29. Blitzblau HG, Hochwagen A (2013) ATR/Mec1 prevents lethal meiotic recombination initiation on partially replicated chromosomes in budding yeast. *Elife* 2: e00844

30. Bolte M, Steigemann P, Braus GH, Irniger S (2002) Inhibition of APC-mediated proteolysis by the meiosis-specific protein kinase Ime2. *Proc Natl Acad Sci U S A* 99: 4385-4390

31. Borde V, Goldman AS, Lichten M (2000) Direct coupling between meiotic DNA replication and recombination initiation. *Science* 290: 806-809

32. Börner GV, Barot A, Kleckner N (2008) Yeast Pch2 promotes domainal axis organization, timely recombination progression, and arrest of defective recombinosomes during meiosis. *Proc Natl Acad Sci U S A* 105: 3327-3332

33. Börner GV, Kleckner N, Hunter N (2004) Crossover/noncrossover differentiation, synaptonemal complex formation, and regulatory surveillance at the leptotene/zygotene transition of meiosis. *Cell* 117: 29-45

34. Bowring FJ, Yeadon PJ, Stainer RG, Catcheside DE (2006) Chromosome pairing and meiotic recombination in Neurospora crassa spo11 mutants. *Curr Genet* 50: 115-123

35. Brar GA, Kiburz BM, Zhang Y, Kim JE, White F, Amon A (2006) Rec8 phosphorylation and recombination promote the step-wise loss of cohesins in meiosis. *Nature* 441: 532-536

36. Brown MS, Bishop DK (2014) DNA strand exchange and RecA homologs in meiosis. *Cold Spring Harb Perspect Biol* 7: a016659

37. Buhler C, Borde V, Lichten M (2007) Mapping meiotic single-strand DNA reveals a new landscape of DNA double-strand breaks in Saccharomyces cerevisiae. *PLoS Biol* 5: e324

38. Busygina V, Sehorn MG, Shi IY, Tsubouchi H, Roeder GS, Sung P (2008) Hed1 regulates Rad51-mediated recombination via a novel mechanism. *Genes Dev* 22: 786-795

39. Bzymek M, Thayer NH, Oh SD, Kleckner N, Hunter N (2010) Double Holliday junctions are intermediates of DNA break repair. *Nature* 464: 937-941

40. Callender TL, Hollingsworth NM (2010) Mek1 suppression of meiotic double-strand break repair is specific to sister chromatids, chromosome autonomous and independent of Rec8 cohesin complexes. *Genetics* 185: 771-782

41. Callender TL, Laureau R, Wan L, Chen X, Sandhu R, Laljee S, Zhou S, Suhandynata RT, Prugar E, Gaines WA *et al* (2016) Mek1 Down Regulates Rad51 Activity during Yeast Meiosis by Phosphorylation of Hed1. *PLoS Genet* 12: e1006226

42. Cao L, Alani E, Kleckner N (1990) A pathway for generation and processing of double-strand breaks during meiotic recombination in S. cerevisiae. *Cell* 61: 1089-1101

43. Carballo JA, Johnson AL, Sedgwick SG, Cha RS (2008) Phosphorylation of the axial element protein Hop1 by Mec1/Tel1 ensures meiotic interhomolog recombination. *Cell* 132: 758-770

44. Carpenter AT (1994) Chiasma function. *Cell* 77: 957-962

45. Cartagena-Lirola H, Guerini I, Viscardi V, Lucchini G, Longhese MP (2006) Budding Yeast Sae2 is an In Vivo Target of the Mec1 and Tel1 Checkpoint Kinases During Meiosis. *Cell Cycle* 5: 1549-1559

46. Caryl AP, Armstrong SJ, Jones GH, Franklin FC (2000) A homologue of the yeast HOP1 gene is inactivated in the Arabidopsis meiotic mutant asy1. *Chromosoma* 109: 62-71

47. Cha RS, Weiner BM, Keeney S, Dekker J, Kleckner N (2000) Progression of meiotic DNA replication is modulated by interchromosomal interaction proteins, negatively by Spo11p and positively by Rec8p. *Genes Dev* 14: 493-503

48. Chabes A, Domkin V, Thelander L (1999) Yeast Sml1, a protein inhibitor of ribonucleotide reductase. *J Biol Chem* 274: 36679-36683

49. Chambon A, West A, Vezon D, Horlow C, De Muyt A, Chelysheva L, Ronceret A, Darbyshire A, Osman K, Heckmann S *et al* (2018) Identification of ASYNAPTIC4, a Component of the Meiotic Chromosome Axis. *Plant Physiol* 178: 233-246

50. Chen SY, Tsubouchi T, Rockmill B, Sandler JS, Richards DR, Vader G, Hochwagen A, Roeder GS, Fung JC (2008) Global analysis of the meiotic crossover landscape. *Dev Cell* 15: 401-415

51. Chen X, Gaglione R, Leong T, Bednor L, de Los Santos T, Luk E, Airola M, Hollingsworth NM (2018) Mek1 coordinates meiotic progression with DNA break repair by directly phosphorylating and inhibiting the yeast pachytene exit regulator Ndt80. *PLoS Genet* 14: e1007832

52. Cheng YH, Chuang CN, Shen HJ, Lin FM, Wang TF (2013) Three distinct modes of Mec1/ATR and Tel1/ATM activation illustrate differential checkpoint targeting during budding yeast early meiosis. *Mol Cell Biol* 33: 3365-3376

53. Cherry JM, Hong EL, Amundsen C, Balakrishnan R, Binkley G, Chan ET, Christie KR, Costanzo MC, Dwight SS, Engel SR *et al* (2012) Saccharomyces Genome Database: the genomics resource of budding yeast. *Nucleic Acids Res* 40: D700-705

54. Chuang CN, Cheng YH, Wang TF (2012) Mek1 stabilizes Hop1-Thr318 phosphorylation to promote interhomolog recombination and checkpoint responses during yeast meiosis. *Nucleic Acids Res* 40: 11416-11427

55. Cimprich KA, Cortez D (2008) ATR: an essential regulator of genome integrity. *Nat Rev Mol Cell Biol* 9: 616-627

56. Ciosk R, Zachariae W, Michaelis C, Shevchenko A, Mann M, Nasmyth K (1998) An ESP1/PDS1 complex regulates loss of sister chromatid cohesion at the metaphase to anaphase transition in yeast. *Cell* 93: 1067-1076

57. Claeys Bouuaert C, Pu S, Wang J, Oger C, Daccache D, Xie W, Patel DJ, Keeney S (2021) DNA-driven condensation assembles the meiotic DNA break machinery. *Nature* 592: 144-149

58. Clerici M, Mantiero D, Guerini I, Lucchini G, Longhese MP (2008) The Yku70-Yku80 complex contributes to regulate double-strand break processing and checkpoint activation during the cell cycle. *EMBO Rep* 9: 810-818

59. Clift D, Schuh M (2013) Restarting life: fertilization and the transition from meiosis to mitosis. *Nat Rev Mol Cell Biol* 14: 549-562

60. Cloud V, Chan YL, Grubb J, Budke B, Bishop DK (2012) Rad51 is an accessory factor for Dmc1-mediated joint molecule formation during meiosis. *Science* 337: 1222-1225

61. Collins I, Newlon CS (1994) Chromosomal DNA replication initiates at the same origins in meiosis and mitosis. *Mol Cell Biol* 14: 3524-3534

62. Colomina N, Garí E, Gallego C, Herrero E, Aldea M (1999) G1 cyclins block the Ime1 pathway to make mitosis and meiosis incompatible in budding yeast. *Embo j* 18: 320-329

63. Cooper TJ, Garcia V, Neale MJ (2016) Meiotic DSB patterning: A multifaceted process. *Cell Cycle* 15: 13-21

64. Couteau F, Zetka M (2005) HTP-1 coordinates synaptonemal complex assembly with homolog alignment during meiosis in C. elegans. *Genes Dev* 19: 2744-2756

65. Crickard JB, Kaniecki K, Kwon Y, Sung P, Lisby M, Greene EC (2018) Regulation of Hed1 and Rad54 binding during maturation of the meiosis-specific presynaptic complex. *Embo j* 37

66. Cromie GA, Hyppa RW, Cam HP, Farah JA, Grewal SI, Smith GR (2007) A discrete class of intergenic DNA dictates meiotic DNA break hotspots in fission yeast. *PLoS Genet* 3: e141

67. Daley JM, Palmbos PL, Wu D, Wilson TE (2005) Nonhomologous end joining in yeast. *Annu Rev Genet* 39: 431-451

68. De Antoni A, Pearson CG, Cimini D, Canman JC, Sala V, Nezi L, Mapelli M, Sironi L, Faretta M, Salmon ED *et al* (2005) The Mad1/Mad2 complex as a template for Mad2 activation in the spindle assembly checkpoint. *Curr Biol* 15: 214-225

69. de los Santos T, Hollingsworth NM (1999) Red1p, a MEK1-dependent phosphoprotein that physically interacts with Hop1p during meiosis in yeast. *J Biol Chem* 274: 1783-1790

70. de los Santos T, Hunter N, Lee C, Larkin B, Loidl J, Hollingsworth NM (2003) The Mus81/Mms4 endonuclease acts independently of double-Holliday junction resolution to promote a distinct subset of crossovers during meiosis in budding yeast. *Genetics* 164: 81-94

71. de Massy B, Rocco V, Nicolas A (1995) The nucleotide mapping of DNA double-strand breaks at the CYS3 initiation site of meiotic recombination in Saccharomyces cerevisiae. *Embo j* 14: 4589-4598

72. De Wulf P, McAinsh AD, Sorger PK (2003) Hierarchical assembly of the budding yeast kinetochore from multiple subcomplexes. *Genes Dev* 17: 2902-2921

73. Dehé PM, Dichtl B, Schaft D, Roguev A, Pamblanco M, Lebrun R, Rodríguez-Gil A, Mkandawire M, Landsberg K, Shevchenko A *et al* (2006) Protein interactions within the Set1 complex and their roles in the regulation of histone 3 lysine 4 methylation. *J Biol Chem* 281: 35404-35412

74. Dirick L, Goetsch L, Ammerer G, Byers B (1998) Regulation of meiotic S phase by Ime2 and a Clb5,6-associated kinase in Saccharomyces cerevisiae. *Science* 281: 1854-1857

75. Doksani Y, Bermejo R, Fiorani S, Haber JE, Foiani M (2009) Replicon dynamics, dormant origin firing, and terminal fork integrity after double-strand break formation. *Cell* 137: 247-258

76. Downs JA, Lowndes NF, Jackson SP (2000) A role for Saccharomyces cerevisiae histone H2A in DNA repair. *Nature* 408: 1001-1004

77. Dudásová Z, Dudás A, Chovanec M (2004) Non-homologous end-joining factors of Saccharomyces cerevisiae. *FEMS Microbiol Rev* 28: 581-601

78. Earnshaw WC, Tomkiel JE (1992) Centromere and kinetochore structure. *Curr Opin Cell Biol* 4: 86-93

79. Eichinger CS, Jentsch S (2010) Synaptonemal complex formation and meiotic checkpoint signaling are linked to the lateral element protein Red1. *Proc Natl Acad Sci U S A* 107: 11370-11375

80. Engebrecht J, Hirsch J, Roeder GS (1990) Meiotic gene conversion and crossing over: their relationship to each other and to chromosome synapsis and segregation. *Cell* 62: 927-937

81. Engebrecht JA, Voelkel-Meiman K, Roeder GS (1991) Meiosis-specific RNA splicing in yeast. *Cell* 66: 1257-1268

82. Enserink JM, Smolka MB, Zhou H, Kolodner RD (2006) Checkpoint proteins control morphogenetic events during DNA replication stress in Saccharomyces cerevisiae. *J Cell Biol* 175: 729-741

83. Feng J, Fu S, Cao X, Wu H, Lu J, Zeng M, Liu L, Yang X, Shen Y (2017) Synaptonemal complex protein 2 (SYCP2) mediates the association of the centromere with the synaptonemal complex. *Protein Cell* 8: 538-543

84. Ferdous M, Higgins JD, Osman K, Lambing C, Roitinger E, Mechtler K, Armstrong SJ, Perry R, Pradillo M, Cuñado N *et al* (2012) Inter-homolog crossing-over and synapsis in Arabidopsis meiosis are dependent on the chromosome axis protein AtASY3. *PLoS Genet* 8: e1002507

85. Finn K, Lowndes NF, Grenon M (2012) Eukaryotic DNA damage checkpoint activation in response to double-strand breaks. *Cell Mol Life Sci* 69: 1447-1473

86. Forey R, Poveda A, Sharma S, Barthe A, Padioleau I, Renard C, Lambert R, Skrzypczak M, Ginalski K, Lengronne A *et al* (2020) Mec1 Is Activated at the Onset of Normal S Phase by Low-dNTP Pools Impeding DNA Replication. *Mol Cell* 78: 396-410.e394

87. Fowler KR, Sasaki M, Milman N, Keeney S, Smith GR (2014) Evolutionarily diverse determinants of meiotic DNA break and recombination landscapes across the genome. *Genome Res* 24: 1650-1664

88. Freese EB, Chu MI, Freese E (1982) Initiation of yeast sporulation of partial carbon, nitrogen, or phosphate deprivation. *J Bacteriol* 149: 840-851

89. Friedberg EC, Aguilera A, Gellert M, Hanawalt PC, Hays JB, Lehmann AR, Lindahl T, Lowndes N, Sarasin A, Wood RD (2006) DNA repair: from molecular mechanism to human disease. *DNA Repair (Amst)* 5: 986-996

90. Fukunaga K, Kwon Y, Sung P, Sugimoto K (2011) Activation of protein kinase Tel1 through recognition of protein-bound DNA ends. *Mol Cell Biol* 31: 1959-1971

91. Garcia V, Gray S, Allison RM, Cooper TJ, Neale MJ (2015) Tel1(ATM)-mediated interference suppresses clustered meiotic double-strand-break formation. *Nature* 520: 114-118

92. Garcia V, Phelps SE, Gray S, Neale MJ (2011) Bidirectional resection of DNA double-strand breaks by Mre11 and Exo1. *Nature* 479: 241-244

93. Gardner RD, Burke DJ (2000) The spindle checkpoint: two transitions, two pathways. *Trends Cell Biol* 10: 154-158

94. Gerton JL, DeRisi J, Shroff R, Lichten M, Brown PO, Petes TD (2000) Global mapping of meiotic recombination hotspots and coldspots in the yeast Saccharomyces cerevisiae. *Proc Natl Acad Sci U S A* 97: 11383-11390

95. Gerton JL, Hawley RS (2005) Homologous chromosome interactions in meiosis: diversity amidst conservation. *Nat Rev Genet* 6: 477-487

96. Glynn EF, Megee PC, Yu HG, Mistrot C, Unal E, Koshland DE, DeRisi JL, Gerton JL (2004) Genome-wide mapping of the cohesin complex in the yeast Saccharomyces cerevisiae. *PLoS Biol* 2: E259

97. Goldfarb T, Lichten M (2010) Frequent and efficient use of the sister chromatid for DNA double-strand break repair during budding yeast meiosis. *PLoS Biol* 8: e1000520

98. Goldmark JP, Fazzio TG, Estep PW, Church GM, Tsukiyama T (2000) The Isw2 chromatin remodeling complex represses early meiotic genes upon recruitment by Ume6p. *Cell* 103: 423-433

99. Gray S, Cohen PE (2016) Control of Meiotic Crossovers: From Double-Strand Break Formation to Designation. *Annu Rev Genet* 50: 175-210

100. Greenwell PW, Kronmal SL, Porter SE, Gassenhuber J, Obermaier B, Petes TD (1995) TEL1, a gene involved in controlling telomere length in S. cerevisiae, is homologous to the human ataxia telangiectasia gene. *Cell* 82: 823-829

101. Grenon M, Magill CP, Lowndes NF, Jackson SP (2006) Double-strand breaks trigger MRX- and Mec1-dependent, but Tel1-independent, checkpoint activation. *FEMS Yeast Res* 6: 836-847

102. Handel MA, Schimenti JC (2010) Genetics of mammalian meiosis: regulation, dynamics and impact on fertility. *Nat Rev Genet* 11: 124-136

103. Hartwell LH (1974) Saccharomyces cerevisiae cell cycle. *Bacteriol Rev* 38: 164-198

104. Hassold T, Hunt P (2001) To err (meiotically) is human: the genesis of human aneuploidy. *Nat Rev Genet* 2: 280-291

105. Henderson KA, Kee K, Maleki S, Santini PA, Keeney S (2006) Cyclin-dependent kinase directly regulates initiation of meiotic recombination. *Cell* 125: 1321-1332

106. Henderson KA, Keeney S (2004) Tying synaptonemal complex initiation to the formation and programmed repair of DNA double-strand breaks. *Proceedings of the National Academy of Sciences of the United States of America* 101: 4519

107. Heyer WD, Li X, Rolfsmeier M, Zhang XP (2006) Rad54: the Swiss Army knife of homologous recombination? *Nucleic Acids Res* 34: 4115-4125

108. Hochwagen A (2008) Meiosis. *Curr Biol* 18: R641-r645

109. Hochwagen A, Amon A (2006) Checking your breaks: surveillance mechanisms of meiotic recombination. *Curr Biol* 16: R217-228

110. Hochwagen A, Tham WH, Brar GA, Amon A (2005) The FK506 binding protein Fpr3 counteracts protein phosphatase 1 to maintain meiotic recombination checkpoint activity. *Cell* 122: 861-873

111. Holliday R (2007) A mechanism for gene conversion in fungi. *Genet Res* 89: 285-307

112. Hollingsworth NM (2010) Phosphorylation and the creation of interhomolog bias during meiosis in yeast. *Cell Cycle* 9: 436-437

113. Hollingsworth NM, Gaglione R (2019) The meiotic-specific Mek1 kinase in budding yeast regulates interhomolog recombination and coordinates meiotic progression with double-strand break repair. *Curr Genet* 65: 631-641

114. Hollingsworth NM, Goetsch L, Byers B (1990) The HOP1 gene encodes a meiosis-specific component of yeast chromosomes. *Cell* 61: 73-84

115. Hollingsworth NM, Ponte L (1997) Genetic interactions between HOP1, RED1 and MEK1 suggest that MEK1 regulates assembly of axial element components during meiosis in the yeast Saccharomyces cerevisiae. *Genetics* 147: 33-42

116. Hollingsworth NM, Ponte L, Halsey C (1995) MSH5, a novel MutS homolog, facilitates meiotic reciprocal recombination between homologs in Saccharomyces cerevisiae but not mismatch repair. *Genes Dev* 9: 1728-1739

117. Holm L (2020) Using Dali for Protein Structure Comparison. *Methods Mol Biol* 2112: 29-42

118. Hong EL, Shinohara A, Bishop DK (2001) Saccharomyces cerevisiae Dmc1 protein promotes renaturation of single-strand DNA (ssDNA) and assimilation of ssDNA into homologous super-coiled duplex DNA. *J Biol Chem* 276: 41906-41912

119. Hong S, Sung Y, Yu M, Lee M, Kleckner N, Kim KP (2013) The logic and mechanism of homologous recombination partner choice. *Mol Cell* 51: 440-453

120. Hornig NC, Knowles PP, McDonald NQ, Uhlmann F (2002) The dual mechanism of separase regulation by securin. *Curr Biol* 12: 973-982

121. Huertas P, Cortés-Ledesma F, Sartori AA, Aguilera A, Jackson SP (2008) CDK targets Sae2 to control DNA-end resection and homologous recombination. *Nature* 455: 689-692

122. Humphryes N, Hochwagen A (2014) A non-sister act: recombination template choice during meiosis. *Exp Cell Res* 329: 53-60

123.   Hunter N, Borts RH (1997) Mlh1 is unique among mismatch repair proteins in its ability to promote crossing-over during meiosis. *Genes Dev* 11: 1573-1582

124.   Hunter N, Kleckner N (2001) The single-end invasion: an asymmetric intermediate at the double-strand break to double-holliday junction transition of meiotic recombination. *Cell* 106: 59-70

125.   Hustedt N, Gasser SM, Shimada K (2013) Replication checkpoint: tuning and coordination of replication forks in s phase. *Genes (Basel)* 4: 388-434

126.   Ira G, Pellicioli A, Balijja A, Wang X, Fiorani S, Carotenuto W, Liberi G, Bressan D, Wan L, Hollingsworth NM *et al* (2004) DNA end resection, homologous recombination and DNA damage checkpoint activation require CDK1. *Nature* 431: 1011-1017

127.   Jessop L, Lichten M (2008) Mus81/Mms4 endonuclease and Sgs1 helicase collaborate to ensure proper recombination intermediate metabolism during meiosis. *Mol Cell* 31: 313-323

128.   Johnston M (1987) A model fungal gene regulatory mechanism: the GAL genes of Saccharomyces cerevisiae. *Microbiol Rev* 51: 458-476

129.   Johzuka K, Ogawa H (1995) Interaction of Mre11 and Rad50: two proteins required for DNA repair and meiosis-specific double-strand break formation in Saccharomyces cerevisiae. *Genetics* 139: 1521-1532

130.   Jumper J, Evans R, Pritzel A, Green T, Figurnov M, Ronneberger O, Tunyasuvunakool K, Bates R, Žídek A, Potapenko A *et al* (2021) Applying and improving AlphaFold at CASP14. *Proteins* 89: 1711-1721

131.   Kaplan N, Moore IK, Fondufe-Mittendorf Y, Gossett AJ, Tillo D, Field Y, LeProust EM, Hughes TR, Lieb JD, Widom J *et al* (2009) The DNA-encoded nucleosome organization of a eukaryotic genome. *Nature* 458: 362-366

132.   Kar FM, Hochwagen A (2021) Phospho-Regulation of Meiotic Prophase. *Front Cell Dev Biol* 9: 667073

133.   Karanyi Z, Halasz L, Acquaviva L, Jonas D, Hetey S, Boros-Olah B, Peng F, Chen D, Klein F, Geli V *et al* (2018) Nuclear dynamics of the Set1C subunit Spp1 prepares meiotic recombination sites for break formation. *J Cell Biol* 217: 3398-3415

134.   Kariyazono R, Oda A, Yamada T, Ohta K (2019) Conserved HORMA domain-containing protein Hop1 stabilizes interaction between proteins of meiotic DNA break hotspots and chromosome axis. *Nucleic Acids Res* 47: 10166-10180

135.   Kassir Y, Granot D, Simchen G (1988) IME1, a positive regulator gene of meiosis in S. cerevisiae. *Cell* 52: 853-862

136.   Keeney S (2001) Mechanism and control of meiotic recombination initiation. *Curr Top Dev Biol* 52: 1-53

137.   Keeney S (2008) Spo11 and the Formation of DNA Double-Strand Breaks in Meiosis. *Genome Dyn Stab* 2: 81-123

138.   Keeney S, Giroux CN, Kleckner N (1997) Meiosis-specific DNA double-strand breaks are catalyzed by Spo11, a member of a widely conserved protein family. *Cell* 88: 375-384

139.   Keeney S, Kleckner N (1995) Covalent protein-DNA complexes at the 5' strand termini of meiosis-specific double-strand breaks in yeast. *Proc Natl Acad Sci U S A* 92: 11274-11278

140.   Keeney S, Lange J, Mohibullah N (2014) Self-organization of meiotic recombination initiation: general principles and molecular pathways. *Annu Rev Genet* 48: 187-214

141.   Kerr GW, Sarkar S, Arumugam P (2012) How to halve ploidy: lessons from budding yeast meiosis. *Cell Mol Life Sci* 69: 3037-3051

142.   Khil PP, Smagulova F, Brick KM, Camerini-Otero RD, Petukhova GV (2012) Sensitive mapping of recombination hotspots using sequencing-based detection of ssDNA. *Genome Res* 22: 957-965

143.   Kim KP, Weiner BM, Zhang L, Jordan A, Dekker J, Kleckner N (2010) Sister cohesion and structural axis components mediate homolog bias of meiotic recombination. *Cell* 143: 924-937

144.   Kleckner N (1996) Meiosis: how could it work? *Proc Natl Acad Sci U S A* 93: 8167-8174

145.   Kleckner N (2006) Chiasma formation: chromatin/axis interplay and the role(s) of the synaptonemal complex. *Chromosoma* 115: 175-194

146.   Klein F, Mahr P, Galova M, Buonomo SB, Michaelis C, Nairz K, Nasmyth K (1999) A central role for cohesins in sister chromatid cohesion, formation of axial elements, and recombination during yeast meiosis. *Cell* 98: 91-103

147.   Kniewel R, Murakami H, Liu Y, Ito M, Ohta K, Hollingsworth NM, Keeney S (2017) Histone H3 Threonine 11 Phosphorylation Is Catalyzed Directly by the Meiosis-Specific Kinase Mek1 and Provides a Molecular Readout of Mek1 Activity in Vivo. *Genetics* 207: 1313-1333

148.   Kugou K, Fukuda T, Yamada S, Ito M, Sasanuma H, Mori S, Katou Y, Itoh T, Matsumoto K, Shibata T *et al* (2009) Rec8 guides canonical Spo11 distribution along yeast meiotic chromosomes. *Mol Biol Cell* 20: 3064-3076

149.   Lai YJ, Lin FM, Chuang MJ, Shen HJ, Wang TF (2011) Genetic requirements and meiotic function of phosphorylation of the yeast axial element protein Red1. *Mol Cell Biol* 31: 912-923

150.   Lam I, Keeney S (2014) Mechanism and regulation of meiotic recombination initiation. *Cold Spring Harb Perspect Biol* 7: a016634

151.   Lao JP, Cloud V, Huang CC, Grubb J, Thacker D, Lee CY, Dresser ME, Hunter N, Bishop DK (2013) Meiotic crossover control by concerted action of Rad51-Dmc1 in homolog template bias and robust homeostatic regulation. *PLoS Genet* 9: e1003978

152.   Lao JP, Hunter N (2010) Trying to avoid your sister. *PLoS Biol* 8: e1000519

153.   Lee B, Amon A (2001) Meiosis: how to create a specialized cell cycle. *Curr Opin Cell Biol* 13: 770-777

154.   Lee PS, Petes TD (2010) From the Cover: mitotic gene conversion events induced in G1-synchronized yeast cells by gamma rays are similar to spontaneous conversion events. *Proc Natl Acad Sci U S A* 107: 7383-7388

155.   Lempiäinen H, Halazonetis TD (2009) Emerging common themes in regulation of PIKKs and PI3Ks. *Embo j* 28: 3067-3073

156.   Li J, Hooker GW, Roeder GS (2006) Saccharomyces cerevisiae Mer2, Mei4 and Rec114 form a complex required for meiotic double-strand break formation. *Genetics* 173: 1969-1981

157.   Li X, Heyer WD (2008) Homologous recombination in DNA repair and DNA damage tolerance. *Cell Res* 18: 99-113

158.   Lin FM, Lai YJ, Shen HJ, Cheng YH, Wang TF (2010) Yeast axial-element protein, Red1, binds SUMO chains to promote meiotic interhomologue recombination and chromosome synapsis. *Embo j* 29: 586-596

159.   Liu J, Wu TC, Lichten M (1995) The location and structure of double-strand DNA breaks induced during yeast meiosis: evidence for a covalently linked DNA-protein intermediate. *Embo j* 14: 4599-4608

160.   Liu Y, Gaines WA, Callender T, Busygina V, Oke A, Sung P, Fung JC, Hollingsworth NM (2014) Down-regulation of Rad51 activity during meiosis in yeast prevents competition with Dmc1 for repair of double-strand breaks. *PLoS Genet* 10: e1004005

161.   Longtine MS, McKenzie A, 3rd, Demarini DJ, Shah NG, Wach A, Brachat A, Philippsen P, Pringle JR (1998) Additional modules for versatile and economical PCR-based gene deletion and modification in Saccharomyces cerevisiae. *Yeast* 14: 953-961

162.   Lorenz A, Wells JL, Pryce DW, Novatchkova M, Eisenhaber F, McFarlane RJ, Loidl J (2004) S. pombe meiotic linear elements contain proteins related to synaptonemal complex components. *J Cell Sci* 117: 3343-3351

163.   Lundin C, North M, Erixon K, Walters K, Jenssen D, Goldman AS, Helleday T (2005) Methyl methanesulfonate (MMS) produces heat-labile DNA damage but no detectable in vivo DNA double-strand breaks. *Nucleic Acids Res* 33: 3799-3811

164.   Luo S, Tong L (2017) Molecular mechanism for the regulation of yeast separase by securin. *Nature* 542: 255-259

165.   Luo X, Fang G, Coldiron M, Lin Y, Yu H, Kirschner MW, Wagner G (2000) Structure of the Mad2 spindle assembly checkpoint protein and its interaction with Cdc20. *Nat Struct Biol* 7: 224-229

166.   MacKenzie AM, Lacefield S (2020) CDK Regulation of Meiosis: Lessons from S. cerevisiae and S. pombe. *Genes (Basel)* 11

167.   Maleki S, Neale MJ, Arora C, Henderson KA, Keeney S (2007) Interactions between Mei4, Rec114, and other proteins required for meiotic DNA double-strand break formation in Saccharomyces cerevisiae. *Chromosoma* 116: 471-486

168.   Malumbres M, Barbacid M (2005) Mammalian cyclin-dependent kinases. *Trends Biochem Sci* 30: 630-641

169.   Mankouri HW, Hickson ID (2006) Top3 processes recombination intermediates and modulates checkpoint activity after DNA damage. *Mol Biol Cell* 17: 4473-4483

170.   Mantiero D, Clerici M, Lucchini G, Longhese MP (2007) Dual role for Saccharomyces cerevisiae Tel1 in the checkpoint response to double-strand breaks. *EMBO Rep* 8: 380-387

171.   Mapelli M, Massimiliano L, Santaguida S, Musacchio A (2007) The Mad2 conformational dimer: structure and implications for the spindle assembly checkpoint. *Cell* 131: 730-743

172.   Markowitz TE, Suarez D, Blitzblau HG, Patel NJ, Markhard AL, MacQueen AJ, Hochwagen A (2017) Reduced dosage of the chromosome axis factor Red1 selectively disrupts the meiotic recombination checkpoint in Saccharomyces cerevisiae. *PLoS Genet* 13: e1006928

173.   Marston AL (2014) Chromosome segregation in budding yeast: sister chromatid cohesion and related mechanisms. *Genetics* 196: 31-63

174.   Marston AL, Amon A (2004) Meiosis: cell-cycle controls shuffle and deal. *Nat Rev Mol Cell Biol* 5: 983-997

175.   Martini E, Diaz RL, Hunter N, Keeney S (2006) Crossover homeostasis in yeast meiosis. *Cell* 126: 285-295

176.   McAinsh AD, Tytell JD, Sorger PK (2003) Structure, function, and regulation of budding yeast kinetochores. *Annu Rev Cell Dev Biol* 19: 519-539

177.   McMahill MS, Sham CW, Bishop DK (2007) Synthesis-dependent strand annealing in meiosis. *PLoS Biol* 5: e299

178.   Melo J, Toczyski D (2002) A unified view of the DNA-damage checkpoint. *Curr Opin Cell Biol* 14: 237-245

179.   Mendenhall MD, Hodge AE (1998) Regulation of Cdc28 cyclin-dependent protein kinase activity during the cell cycle of the yeast Saccharomyces cerevisiae. *Microbiol Mol Biol Rev* 62: 1191-1243

180.   Mercier R, Mézard C, Jenczewski E, Macaisne N, Grelon M (2015) The molecular biology of meiosis in plants. *Annu Rev Plant Biol* 66: 297-327

181.   Michaelis C, Ciosk R, Nasmyth K (1997) Cohesins: chromosomal proteins that prevent premature separation of sister chromatids. *Cell* 91: 35-45

182.   Mieczkowski PA, Dominska M, Buck MJ, Lieb JD, Petes TD (2007) Loss of a histone deacetylase dramatically alters the genomic distribution of Spo11p-catalyzed DNA breaks in Saccharomyces cerevisiae. *Proc Natl Acad Sci U S A* 104: 3955-3960

183.   Monje-Casas F, Prabhu VR, Lee BH, Boselli M, Amon A (2007) Kinetochore orientation during meiosis is controlled by Aurora B and the monopolin complex. *Cell* 128: 477-490

184.   Moore CW (1988) Internucleosomal Cleavage and Chromosomal Degradation by Bleomycin and Phleomycin in Yeast. *Cancer Research* 48: 6837-6843

185.   Morrow DM, Tagle DA, Shiloh Y, Collins FS, Hieter P (1995) TEL1, an S. cerevisiae homolog of the human gene mutated in ataxia telangiectasia, is functionally related to the yeast checkpoint gene MEC1. *Cell* 82: 831-840

186.   Mozlin AM, Fung CW, Symington LS (2008) Role of the Saccharomyces cerevisiae Rad51 paralogs in sister chromatid recombination. *Genetics* 178: 113-126

187.   Muller HJ (1916) The mechanism of crossing-over.

188.   Murakami H, Keeney S (2008) Regulating the formation of DNA double-strand breaks in meiosis. *Genes Dev* 22: 286-292

189.   Murakami H, Keeney S (2014) Temporospatial coordination of meiotic DNA replication and recombination via DDK recruitment to replisomes. *Cell* 158: 861-873

190. Murakami H, Nurse P (2001) Regulation of premeiotic S phase and recombination-related double-strand DNA breaks during meiosis in fission yeast. *Nat Genet* 28: 290-293

191. Murton BL, Chin WL, Ponting CP, Itzhaki LS (2010) Characterising the binding specificities of the subunits associated with the KMT2/Set1 histone lysine methyltransferase. *J Mol Biol* 398: 481-488

192. Musacchio A, Desai A (2017) A Molecular View of Kinetochore Assembly and Function. *Biology (Basel)* 6

193. Myers S, Bottolo L, Freeman C, McVean G, Donnelly P (2005) A fine-scale map of recombination rates and hotspots across the human genome. *Science* 310: 321-324

194. Myung K, Kolodner RD (2003) Induction of genome instability by DNA damage in Saccharomyces cerevisiae. *DNA Repair (Amst)* 2: 243-258

195. Nakada D, Matsumoto K, Sugimoto K (2003) ATM-related Tel1 associates with double-strand breaks through an Xrs2-dependent mechanism. *Genes Dev* 17: 1957-1962

196. Nandabalan K, Roeder GS (1995) Binding of a cell-type-specific RNA splicing factor to its target regulatory sequence. *Mol Cell Biol* 15: 1953-1960

197. Nassif N, Penney J, Pal S, Engels WR, Gloor GB (1994) Efficient copying of nonhomologous sequences from ectopic sites via P-element-induced gap repair. *Mol Cell Biol* 14: 1613-1625

198. Neale MJ, Pan J, Keeney S (2005) Endonucleolytic processing of covalent protein-linked DNA double-strand breaks. *Nature* 436: 1053-1057

199. Neiman AM (2011) Sporulation in the budding yeast Saccharomyces cerevisiae. *Genetics* 189: 737-765

200. Newlon CS (1988) Yeast chromosome replication and segregation. *Microbiol Rev* 52: 568-601

201. Niu H, Li X, Job E, Park C, Moazed D, Gygi SP, Hollingsworth NM (2007) Mek1 kinase is regulated to suppress double-strand break repair between sister chromatids during budding yeast meiosis. *Mol Cell Biol* 27: 5456-5467

202. Niu H, Wan L, Baumgartner B, Schaefer D, Loidl J, Hollingsworth NM (2005) Partner choice during meiosis is regulated by Hop1-promoted dimerization of Mek1. *Mol Biol Cell* 16: 5804-5818

203. Niu H, Wan L, Busygina V, Kwon Y, Allen JA, Li X, Kunz RC, Kubota K, Wang B, Sung P *et al* (2009) Regulation of meiotic recombination via Mek1-mediated Rad54 phosphorylation. *Mol Cell* 36: 393-404

204.   Novak JE, Ross-Macdonald PB, Roeder GS (2001) The budding yeast Msh4 protein functions in chromosome synapsis and the regulation of crossover distribution. *Genetics* 158: 1013-1025

205.   Ogino K, Masai H (2006) Rad3-Cds1 mediates coupling of initiation of meiotic recombination with DNA replication. Mei4-dependent transcription as a potential target of meiotic checkpoint. *J Biol Chem* 281: 1338-1344

206.   Oh S, Lee J, Swanson SK, Florens L, Washburn MP, Workman JL (2020) Yeast Nuak1 phosphorylates histone H3 threonine 11 in low glucose stress by the cooperation of AMPK and CK2 signaling. *Elife* 9

207.   Oh S, Suganuma T, Gogol MM, Workman JL (2018) Histone H3 threonine 11 phosphorylation by Sch9 and CK2 regulates chronological lifespan by controlling the nutritional stress response. *Elife* 7

208.   Oh SD, Lao JP, Hwang PY, Taylor AF, Smith GR, Hunter N (2007) BLM ortholog, Sgs1, prevents aberrant crossing-over by suppressing formation of multichromatid joint molecules. *Cell* 130: 259-272

209.   Ohkura H (2015) Meiosis: an overview of key differences from mitosis. *Cold Spring Harb Perspect Biol* 7

210.   Okaz E, Argüello-Miranda O, Bogdanova A, Vinod PK, Lipp JJ, Markova Z, Zagoriy I, Novak B, Zachariae W (2012) Meiotic prophase requires proteolysis of M phase regulators mediated by the meiosis-specific APC/CAma1. *Cell* 151: 603-618

211.   Osman K, Yang J, Roitinger E, Lambing C, Heckmann S, Howell E, Cuacos M, Imre R, Dürnberger G, Mechtler K *et al* (2018) Affinity proteomics reveals extensive phosphorylation of the Brassica chromosome axis protein ASY1 and a network of associated proteins at prophase I of meiosis. *Plant J* 93: 17-33

212.   Padmore R, Cao L, Kleckner N (1991) Temporal comparison of recombination and synaptonemal complex formation during meiosis in S. cerevisiae. *Cell* 66: 1239-1256

213.   Page SL, Hawley RS (2004) The genetics and molecular biology of the synaptonemal complex. *Annu Rev Cell Dev Biol* 20: 525-558

214.   Pan D, Brockmeyer A, Mueller F, Musacchio A, Bange T (2018) Simplified Protocol for Cross-linking Mass Spectrometry Using the MS-Cleavable Cross-linker DSBU with Efficient Cross-link Identification. *Anal Chem* 90: 10990-10999

215.   Pan J, Sasaki M, Kniewel R, Murakami H, Blitzblau HG, Tischfield SE, Zhu X, Neale MJ, Jasin M, Socci ND *et al* (2011) A hierarchical combination of factors shapes

the genome-wide topography of yeast meiotic recombination initiation. *Cell* 144: 719-731

216. Panizza S, Mendoza MA, Berlinger M, Huang L, Nicolas A, Shirahige K, Klein F (2011) Spo11-accessory proteins link double-strand break sites to the chromosome axis in early meiotic recombination. *Cell* 146: 372-383

217. Pâques F, Haber JE (1999) Multiple pathways of recombination induced by double-strand breaks in Saccharomyces cerevisiae. *Microbiol Mol Biol Rev* 63: 349-404

218. Paulovich AG, Hartwell LH (1995) A checkpoint regulates the rate of progression through S phase in S. cerevisiae in response to DNA damage. *Cell* 82: 841-847

219. Pelttari J, Hoja MR, Yuan L, Liu JG, Brundell E, Moens P, Santucci-Darmanin S, Jessberger R, Barbero JL, Heyting C *et al* (2001) A meiotic chromosomal core consisting of cohesin complex proteins recruits DNA recombination proteins and promotes synapsis in the absence of an axial element in mammalian meiotic cells. *Mol Cell Biol* 21: 5667-5677

220. Penedos A, Johnson AL, Strong E, Goldman AS, Carballo JA, Cha RS (2015) Essential and Checkpoint Functions of Budding Yeast ATM and ATR during Meiotic Prophase Are Facilitated by Differential Phosphorylation of a Meiotic Adaptor Protein, Hop1. *PLoS One* 10: e0134297

221. Peters JM, Nishiyama T (2012) Sister chromatid cohesion. *Cold Spring Harb Perspect Biol* 4

222. Petes TD (2001) Meiotic recombination hot spots and cold spots. *Nat Rev Genet* 2: 360-369

223. Petronczki M, Siomos MF, Nasmyth K (2003) Un ménage à quatre: the molecular biology of chromosome segregation in meiosis. *Cell* 112: 423-440

224. Petukhova G, Stratton S, Sung P (1998) Catalysis of homologous DNA pairing by yeast Rad51 and Rad54 proteins. *Nature* 393: 91-94

225. Petukhova G, Sung P, Klein H (2000) Promotion of Rad51-dependent D-loop formation by yeast recombination factor Rdh54/Tid1. *Genes Dev* 14: 2206-2215

226. Pratto F, Brick K, Khil P, Smagulova F, Petukhova GV, Camerini-Otero RD (2014) DNA recombination. Recombination initiation maps of individual human genomes. *Science* 346: 1256442

227. Prieler S, Penkner A, Borde V, Klein F (2005) The control of Spo11's interaction with meiotic recombination hotspots. *Genes Dev* 19: 255-269

228. Prugar E, Burnett C, Chen X, Hollingsworth NM (2017) Coordination of Double Strand Break Repair and Meiotic Progression in Yeast by a Mek1-Ndt80 Negative Feedback Loop. *Genetics* 206: 497-512

229. Puddu F, Piergiovanni G, Plevani P, Muzi-Falconi M (2011) Sensing of replication stress and Mec1 activation act through two independent pathways involving the 9-1-1 complex and DNA polymerase ε. *PLoS Genet* 7: e1002022

230. Putnam CD, Jaehnig EJ, Kolodner RD (2009) Perspectives on the DNA damage and replication checkpoint responses in Saccharomyces cerevisiae. *DNA Repair (Amst)* 8: 974-982

231. Rabitsch W, Schellongowski P, Staudinger T, Hofbauer R, Dufek V, Eder B, Raab H, Thell R, Schuster E, Frass M (2003) Comparison of a conventional tracheal airway with the Combitube in an urban emergency medical services system run by physicians. *Resuscitation* 57: 27-32

232. Raschle M, Van Komen S, Chi P, Ellenberger T, Sung P (2004) Multiple interactions with the Rad51 recombinase govern the homologous recombination function of Rad54. *J Biol Chem* 279: 51973-51980

233. Reitz D, Grubb J, Bishop DK (2019) A mutant form of Dmc1 that bypasses the requirement for accessory protein Mei5-Sae3 reveals independent activities of Mei5-Sae3 and Rad51 in Dmc1 filament stability. *PLoS Genet* 15: e1008217

234. Rockmill B, Engebrecht JA, Scherthan H, Loidl J, Roeder GS (1995) The yeast MER2 gene is required for chromosome synapsis and the initiation of meiotic recombination. *Genetics* 141: 49-59

235. Rockmill B, Voelkel-Meiman K, Roeder GS (2006) Centromere-proximal crossovers are associated with precocious separation of sister chromatids during meiosis in Saccharomyces cerevisiae. *Genetics* 174: 1745-1754

236. Rosenberg SC, Corbett KD (2015) The multifaceted roles of the HORMA domain in cellular signaling. *J Cell Biol* 211: 745-755

237. Rousova D, Nivsarkar V, Altmannova V, Raina VB, Funk SK, Liedtke D, Janning P, Muller F, Reichle H, Vader G *et al* (2021) Novel mechanistic insights into the role of Mer2 as the keystone of meiotic DNA break formation. *Elife* 10

238. Sakuno T, Watanabe Y (2015) Phosphorylation of cohesin Rec11/SA3 by casein kinase 1 promotes homologous recombination by assembling the meiotic chromosome axis. *Dev Cell* 32: 220-230

239. San Filippo J, Sung P, Klein H (2008) Mechanism of eukaryotic homologous recombination. *Annu Rev Biochem* 77: 229-257

240.   San-Segundo PA, Roeder GS (1999) Pch2 links chromatin silencing to meiotic checkpoint control. *Cell* 97: 313-324

241.   Sanchez Y, Desany BA, Jones WJ, Liu Q, Wang B, Elledge SJ (1996) Regulation of RAD53 by the ATM-like kinases MEC1 and TEL1 in yeast cell cycle checkpoint pathways. *Science* 271: 357-360

242.   Sando N, Miyake S (1971) Biochemical changes in yeast during sporulation. I. Fate of nucleic acids and related compounds. *Dev Growth Differ* 12: 273-283

243.   Sasaki M, Lange J, Keeney S (2010) Genome destabilization by homologous recombination in the germ line. *Nat Rev Mol Cell Biol* 11: 182-195

244.   Sasanuma H, Hirota K, Fukuda T, Kakusho N, Kugou K, Kawasaki Y, Shibata T, Masai H, Ohta K (2008) Cdc7-dependent phosphorylation of Mer2 facilitates initiation of yeast meiotic recombination. *Genes Dev* 22: 398-410

245.   Schalbetter SA, Fudenberg G, Baxter J, Pollard KS, Neale MJ (2019) Principles of meiotic chromosome assembly revealed in S. cerevisiae. *Nat Commun* 10: 4795

246.   Schiffrin B, Radford SE, Brockwell DJ, Calabrese AN (2020) PyXlinkViewer: A flexible tool for visualization of protein chemical crosslinking data within the PyMOL molecular graphics system. *Protein Sci* 29: 1851-1857

247.   Schwacha A, Kleckner N (1995) Identification of double Holliday junctions as intermediates in meiotic recombination. *Cell* 83: 783-791

248.   Schwacha A, Kleckner N (1997) Interhomolog bias during meiotic recombination: meiotic functions promote a highly differentiated interhomolog-only pathway. *Cell* 90: 1123-1135

249.   Schwartz EK, Heyer WD (2011) Processing of joint molecule intermediates by structure-selective endonucleases during homologous recombination in eukaryotes. *Chromosoma* 120: 109-127

250.   Schwartz MF, Duong JK, Sun Z, Morrow JS, Pradhan D, Stern DF (2002) Rad9 phosphorylation sites couple Rad53 to the Saccharomyces cerevisiae DNA damage checkpoint. *Mol Cell* 9: 1055-1065

251.   Shi X, Kachirskaia I, Walter KL, Kuo JH, Lake A, Davrazou F, Chan SM, Martin DG, Fingerman IM, Briggs SD *et al* (2007) Proteome-wide analysis in Saccharomyces cerevisiae identifies several PHD fingers as novel direct and selective binding modules of histone H3 methylated at either lysine 4 or lysine 36. *J Biol Chem* 282: 2450-2455

252.   Shinohara A, Shinohara M (2004) Roles of RecA homologues Rad51 and Dmc1 during meiotic recombination. *Cytogenet Genome Res* 107: 201-207

253.   Shonn MA, McCarroll R, Murray AW (2000) Requirement of the spindle checkpoint for proper chromosome segregation in budding yeast meiosis. *Science* 289: 300-303

254.   Shuster EO, Byers B (1989) Pachytene arrest and other meiotic effects of the start mutations in Saccharomyces cerevisiae. *Genetics* 123: 29-43

255.   Smagulova F, Gregoretti IV, Brick K, Khil P, Camerini-Otero RD, Petukhova GV (2011) Genome-wide analysis reveals novel molecular features of mouse recombination hotspots. *Nature* 472: 375-378

256.   Smith AV, Roeder GS (1997) The yeast Red1 protein localizes to the cores of meiotic chromosomes. *J Cell Biol* 136: 957-967

257.   Smith HE, Mitchell AP (1989) A transcriptional cascade governs entry into meiosis in Saccharomyces cerevisiae. *Mol Cell Biol* 9: 2142-2152

258.   Smith HE, Su SS, Neigeborn L, Driscoll SE, Mitchell AP (1990) Role of IME1 expression in regulation of meiosis in Saccharomyces cerevisiae. *Mol Cell Biol* 10: 6103-6113

259.   Smith KN, Penkner A, Ohta K, Klein F, Nicolas A (2001) B-type cyclins CLB5 and CLB6 control the initiation of recombination and synaptonemal complex formation in yeast meiosis. *Curr Biol* 11: 88-97

260.   Smith MJ, Bryant EE, Joseph FJ, Rothstein R (2019) DNA damage triggers increased mobility of chromosomes in G1-phase cells. *Mol Biol Cell* 30: 2620-2625

261.   Sommermeyer V, Béneut C, Chaplais E, Serrentino ME, Borde V (2013) Spp1, a member of the Set1 Complex, promotes meiotic DSB formation in promoters by tethering histone H3K4 methylation sites to chromosome axes. *Mol Cell* 49: 43-54

262.   Sopko R, Huang D, Preston N, Chua G, Papp B, Kafadar K, Snyder M, Oliver SG, Cyert M, Hughes TR *et al* (2006) Mapping pathways and phenotypes by systematic gene overexpression. *Mol Cell* 21: 319-330

263.   Sourirajan A, Lichten M (2008) Polo-like kinase Cdc5 drives exit from pachytene during budding yeast meiosis. *Genes Dev* 22: 2627-2632

264.   Spingola M, Ares M, Jr. (2000) A yeast intronic splicing enhancer and Nam8p are required for Mer1p-activated splicing. *Mol Cell* 6: 329-338

265.   Stanzione M, Baumann M, Papanikos F, Dereli I, Lange J, Ramlal A, Tränkner D, Shibuya H, de Massy B, Watanabe Y *et al* (2016) Meiotic DNA break formation requires the unsynapsed chromosome axis-binding protein IHO1 (CCDC36) in mice. *Nat Cell Biol* 18: 1208-1220

266. Steiner WW, Schreckhise RW, Smith GR (2002) Meiotic DNA breaks at the S. pombe recombination hot spot M26. *Mol Cell* 9: 847-855

267. Storlazzi A, Tessé S, Gargano S, James F, Kleckner N, Zickler D (2003) Meiotic double-strand breaks at the interface of chromosome movement, chromosome remodeling, and reductional division. *Genes Dev* 17: 2675-2687

268. Strich R, Surosky RT, Steber C, Dubois E, Messenguy F, Esposito RE (1994) UME6 is a key regulator of nitrogen repression and meiotic development. *Genes Dev* 8: 796-810

269. Stuart D, Wittenberg C (1998) CLB5 and CLB6 are required for premeiotic DNA replication and activation of the meiotic S/M checkpoint. *Genes Dev* 12: 2698-2710

270. Sturtevant AH (1915) The behavior of the chromosomes as studied through linkage. *Zeitschrift für induktive Abstammungs- und Vererbungslehre* 13: 234-287

271. Subramanian VV, Hochwagen A (2014) The meiotic checkpoint network: step-by-step through meiotic prophase. *Cold Spring Harb Perspect Biol* 6: a016675

272. Subramanian VV, MacQueen AJ, Vader G, Shinohara M, Sanchez A, Borde V, Shinohara A, Hochwagen A (2016) Chromosome Synapsis Alleviates Mek1-Dependent Suppression of Meiotic DNA Repair. *PLoS Biol* 14: e1002369

273. Subramanian VV, Zhu X, Markowitz TE, Vale-Silva LA, San-Segundo PA, Hollingsworth NM, Keeney S, Hochwagen A (2019) Persistent DNA-break potential near telomeres increases initiation of meiotic recombination on short chromosomes. *Nat Commun* 10: 970

274. Sun H, Treco D, Szostak JW (1991) Extensive 3'-overhanging, single-stranded DNA associated with the meiosis-specific double-strand breaks at the ARG4 recombination initiation site. *Cell* 64: 1155-1161

275. Sun X, Huang L, Markowitz TE, Blitzblau HG, Chen D, Klein F, Hochwagen A (2015) Transcription dynamically patterns the meiotic chromosome-axis interface. *Elife* 4

276. Sun Z, Fay DS, Marini F, Foiani M, Stern DF (1996) Spk1/Rad53 is regulated by Mec1-dependent protein phosphorylation in DNA replication and damage checkpoint pathways. *Genes Dev* 10: 395-406

277. Sun Z, Hsiao J, Fay DS, Stern DF (1998) Rad53 FHA domain associated with phosphorylated Rad9 in the DNA damage checkpoint. *Science* 281: 272-274

278. Sym M, Engebrecht JA, Roeder GS (1993) ZIP1 is a synaptonemal complex protein required for meiotic chromosome synapsis. *Cell* 72: 365-378

279. Symington LS (2016) Mechanism and regulation of DNA end resection in eukaryotes. *Crit Rev Biochem Mol Biol* 51: 195-212

280. Szostak JW, Orr-Weaver TL, Rothstein RJ, Stahl FW (1983) The double-strand-break repair model for recombination. *Cell* 33: 25-35

281. Tan TL, Kanaar R, Wyman C (2003) Rad54, a Jack of all trades in homologous recombination. *DNA Repair (Amst)* 2: 787-794

282. Tang S, Wu MKY, Zhang R, Hunter N (2015) Pervasive and essential roles of the Top3-Rmi1 decatenase orchestrate recombination and facilitate chromosome segregation in meiosis. *Mol Cell* 57: 607-621

283. Tannous EA, Burgers PM (2021) Novel insights into the mechanism of cell cycle kinases Mec1(ATR) and Tel1(ATM). *Crit Rev Biochem Mol Biol* 56: 441-454

284. Terentyev Y, Johnson R, Neale MJ, Khisroon M, Bishop-Bailey A, Goldman AS (2010) Evidence that MEK1 positively promotes interhomologue double-strand break repair. *Nucleic Acids Res* 38: 4349-4360

285. Tonami Y, Murakami H, Shirahige K, Nakanishi M (2005) A checkpoint control linking meiotic S phase and recombination initiation in fission yeast. *Proc Natl Acad Sci U S A* 102: 5797-5801

286. Torres-Ramos CA, Prakash S, Prakash L (2002) Requirement of RAD5 and MMS2 for postreplication repair of UV-damaged DNA in Saccharomyces cerevisiae. *Mol Cell Biol* 22: 2419-2426

287. Tóth A, Rabitsch KP, Gálová M, Schleiffer A, Buonomo SB, Nasmyth K (2000) Functional genomics identifies monopolin: a kinetochore protein required for segregation of homologs during meiosis i. *Cell* 103: 1155-1168

288. Traven A, Heierhorst J (2005) SQ/TQ cluster domains: concentrated ATM/ATR kinase phosphorylation site regions in DNA-damage-response proteins. *Bioessays* 27: 397-407

289. Tromer EC, Wemyss TA, Ludzia P, Waller RF, Akiyoshi B (2021) Repurposing of synaptonemal complex proteins for kinetochores in Kinetoplastida. *Open Biol* 11: 210049

290. Tsubouchi H, Roeder GS (2006) Budding yeast Hed1 down-regulates the mitotic recombination machinery when meiotic recombination is impaired. *Genes Dev* 20: 1766-1775

291. Tsubouchi T, Roeder GS (2005) A synaptonemal complex protein promotes homology-independent centromere coupling. *Science* 308: 870-873

292. Tudyka T, Skerra A (1997) Glutathione S-transferase can be used as a C-terminal, enzymatically active dimerization module for a recombinant protease inhibitor, and functionally secreted into the periplasm of Escherichia coli. *Protein Sci* 6: 2180-2187

293. Uhlmann F, Lottspeich F, Nasmyth K (1999) Sister-chromatid separation at anaphase onset is promoted by cleavage of the cohesin subunit Scc1. *Nature* 400: 37-42

294. Ui A, Seki M, Ogiwara H, Onodera R, Fukushige S, Onoda F, Enomoto T (2005) The ability of Sgs1 to interact with DNA topoisomerase III is essential for damage-induced recombination. *DNA Repair (Amst)* 4: 191-201

295. Ur SN, Corbett KD (2021) Architecture and Dynamics of Meiotic Chromosomes. *Annu Rev Genet* 55: 497-526

296. Usui T, Ogawa H, Petrini JH (2001) A DNA damage response pathway controlled by Tel1 and the Mre11 complex. *Mol Cell* 7: 1255-1266

297. Vader G (2015) Pch2(TRIP13): controlling cell division through regulation of HORMA domains. *Chromosoma* 124: 333-339

298. Vader G, Blitzblau HG, Tame MA, Falk JE, Curtin L, Hochwagen A (2011) Protection of repetitive DNA borders from self-induced meiotic instability. *Nature* 477: 115-119

299. Vader G, Musacchio A (2014) HORMA domains at the heart of meiotic chromosome dynamics. *Dev Cell* 31: 389-391

300. van Heemst D, Heyting C (2000) Sister chromatid cohesion and recombination in meiosis. *Chromosoma* 109: 10-26

301. van Werven FJ, Amon A (2011) Regulation of entry into gametogenesis. *Philos Trans R Soc Lond B Biol Sci* 366: 3521-3531

302. Varela E, Schlecht U, Moina A, Fackenthal JD, Washburn BK, Niederhauser-Wiederkehr C, Tsai-Pflugfelder M, Primig M, Gasser SM, Esposito RE (2010) Mitotic expression of Spo13 alters M-phase progression and nucleolar localization of Cdc14 in budding yeast. *Genetics* 185: 841-854

303. Vialard JE, Gilbert CS, Green CM, Lowndes NF (1998) The budding yeast Rad9 checkpoint protein is subjected to Mec1/Tel1-dependent hyperphosphorylation and interacts with Rad53 after DNA damage. *Embo j* 17: 5679-5688

304. Vincenten N, Kuhl LM, Lam I, Oke A, Kerr AR, Hochwagen A, Fung J, Keeney S, Vader G, Marston AL (2015) The kinetochore prevents centromere-proximal crossover recombination during meiosis. *Elife* 4

305.   Wan L, de los Santos T, Zhang C, Shokat K, Hollingsworth NM (2004) Mek1 kinase activity functions downstream of RED1 in the regulation of meiotic double strand break repair in budding yeast. *Mol Biol Cell* 15: 11-23

306.   Wan L, Niu H, Futcher B, Zhang C, Shokat KM, Boulton SJ, Hollingsworth NM (2008) Cdc28-Clb5 (CDK-S) and Cdc7-Dbf4 (DDK) collaborate to initiate meiotic recombination in yeast. *Genes Dev* 22: 386-397

307.   Wang TF, Kleckner N, Hunter N (1999) Functional specificity of MutL homologs in yeast: evidence for three Mlh1-based heterocomplexes with distinct roles during meiosis in recombination and mismatch correction. *Proc Natl Acad Sci U S A* 96: 13914-13919

308.   Wang Y, Chang CY, Wu JF, Tung KS (2011) Nuclear localization of the meiosis-specific transcription factor Ndt80 is regulated by the pachytene checkpoint. *Mol Biol Cell* 22: 1878-1886

309.   Watanabe Y (2004) Modifying sister chromatid cohesion for meiosis. *J Cell Sci* 117: 4017-4023

310.   Watanabe Y (2012) Geometry and force behind kinetochore orientation: lessons from meiosis. *Nat Rev Mol Cell Biol* 13: 370-382

311.   West AM, Rosenberg SC, Ur SN, Lehmer MK, Ye Q, Hagemann G, Caballero I, Usón I, MacQueen AJ, Herzog F *et al* (2019) A conserved filamentous assembly underlies the structure of the meiotic chromosome axis. *Elife* 8

312.   West AMV, Komives EA, Corbett KD (2018) Conformational dynamics of the Hop1 HORMA domain reveal a common mechanism with the spindle checkpoint protein Mad2. *Nucleic Acids Res* 46: 279-292

313.   Westermann S, Cheeseman IM, Anderson S, Yates JR, 3rd, Drubin DG, Barnes G (2003) Architecture of the budding yeast kinetochore reveals a conserved molecular core. *J Cell Biol* 163: 215-222

314.   Williamson DH, Johnston LH, Fennell DJ, Simchen G (1983) The timing of the S phase and other nuclear events in yeast meiosis. *Exp Cell Res* 145: 209-217

315.   Wojtasz L, Daniel K, Roig I, Bolcun-Filas E, Xu H, Boonsanay V, Eckmann CR, Cooke HJ, Jasin M, Keeney S *et al* (2009) Mouse HORMAD1 and HORMAD2, two conserved meiotic chromosomal proteins, are depleted from synapsed chromosome axes with the help of TRIP13 AAA-ATPase. *PLoS Genet* 5: e1000702

316.   Woltering D, Baumgartner B, Bagchi S, Larkin B, Loidl J, de los Santos T, Hollingsworth NM (2000) Meiotic segregation, synapsis, and recombination

checkpoint functions require physical interaction between the chromosomal proteins Red1p and Hop1p. *Mol Cell Biol* 20: 6646-6658

317.   Woo TT, Chuang CN, Higashide M, Shinohara A, Wang TF (2020) Dual roles of yeast Rad51 N-terminal domain in repairing DNA double-strand breaks. *Nucleic Acids Res* 48: 8474-8489

318.   Woo TT, Chuang CN, Wang TF (2021) Budding yeast Rad51: a paradigm for how phosphorylation and intrinsic structural disorder regulate homologous recombination and protein homeostasis. *Curr Genet* 67: 389-396

319.   Wu HY, Ho HC, Burgess SM (2010) Mek1 kinase governs outcomes of meiotic recombination and the checkpoint response. *Curr Biol* 20: 1707-1716

320.   Xu L, Kleckner N (1995) Sequence non-specific double-strand breaks and interhomolog interactions prior to double-strand break formation at a meiotic recombination hot spot in yeast. *Embo j* 14: 5115-5128

321.   Xu L, Weiner BM, Kleckner N (1997) Meiotic cells monitor the status of the interhomolog recombination complex. *Genes Dev* 11: 106-118

322.   Yadav VK, Claeys Bouuaert C (2021) Mechanism and Control of Meiotic DNA Double-Strand Break Formation in S. cerevisiae. *Front Cell Dev Biol* 9: 642737

323.   Yilmaz D, Furst A, Meaburn K, Lezaja A, Wen Y, Altmeyer M, Reina-San-Martin B, Soutoglou E (2021) Activation of homologous recombination in G1 preserves centromeric integrity. *Nature* 600: 748-753

324.   Yuan L, Liu JG, Hoja MR, Wilbertz J, Nordqvist K, Höög C (2002) Female germ cell aneuploidy and embryo death in mice lacking the meiosis-specific protein SCP3. *Science* 296: 1115-1118

325.   Yuan L, Liu JG, Zhao J, Brundell E, Daneholt B, Höög C (2000) The murine SCP3 gene is required for synaptonemal complex assembly, chromosome synapsis, and male fertility. *Mol Cell* 5: 73-83

326.   Zakharyevich K, Ma Y, Tang S, Hwang PY, Boiteux S, Hunter N (2010) Temporally and biochemically distinct activities of Exo1 during meiosis: double-strand break resection and resolution of double Holliday junctions. *Mol Cell* 40: 1001-1015

327.   Zeman MK, Cimprich KA (2014) Causes and consequences of replication stress. *Nat Cell Biol* 16: 2-9

328.   Zetka MC, Kawasaki I, Strome S, Müller F (1999) Synapsis and chiasma formation in Caenorhabditis elegans require HIM-3, a meiotic chromosome core component that functions in chromosome segregation. *Genes Dev* 13: 2258-2270

329.   Zhang L, Kim KP, Kleckner NE, Storlazzi A (2011) Meiotic double-strand breaks occur once per pair of (sister) chromatids and, via Mec1/ATR and Tel1/ATM, once per quartet of chromatids. *Proc Natl Acad Sci U S A* 108: 20036-20041

330.   Zhao X, Muller EG, Rothstein R (1998) A suppressor of two essential checkpoint genes identifies a novel protein that negatively affects dNTP pools. *Mol Cell* 2: 329-340

331.   Zhuk AS, Stepchenkova EI, Pavlov YI, Inge-Vechtomov SG (2016) EVALUATION OF EFFECTIVENESS OF SYNCHRONIZATION METHODS OF CELL DIVISION IN YEAST SACCHAROMYCES CEREVISIAE. *Tsitologiia* 58: 936-946

332.   Zickler D, Kleckner N (1999) Meiotic chromosomes: integrating structure and function. *Annu Rev Genet* 33: 603-754

333.   Zou L, Elledge SJ (2003) Sensing DNA damage through ATRIP recognition of RPA-ssDNA complexes. *Science* 300: 1542-1548

Acknowledgements

As the course of this doctoral work comes to an end, I would like to express my gratitude to all those who stood by my side throughout this journey. During these years, I have become a better thinker which has resulted in scientific, professional and personal development. Thus, first and foremost, I would like to thank Dr. Gerben Vader for giving me the opportunity to pursue doctoral research in his lab. I really appreciate his continuous support and guidance throughout the process. He introduced me to yeast genetics, taught me concepts with enthusiasm and encouraged me to try new experiments and learn. He taught me how to design experiments, troubleshoot problems and extract information from the data. Our scientific discussions have provoked me to become a better researcher as I am on this day. After the lab shifted to a new location, he kept on guiding me remotely and supported me in every possible way. I am forever indebted to him especially for his support during the last years.

I would like to thank Dr. Andrea Musacchio for mentoring me and making me feel welcome in his lab. His suggestions and continuous feedback have helped me a lot to make progress in my projects. He has supported me in understanding my scientific interests. I would like to express my deepest gratitude to him for agreeing to be my supervisor, my thesis committee member and examiner for my Ph.D. defence.

I am grateful to Dr. John Weir for collaborating with us. I am thankful to him for giving me the opportunity to work on a project designed by him. His scientific inputs and ideas have helped develop my project tremendously. I am thankful to all the Weir lab members for their scientific and experimental contributions to this work. I would like to acknowledge my thesis committee members, Dr. Matias Hernandez and Dr. Heinz Neumann, for their ideas and inputs during the TAC meetings. They have always been available for discussions and encouraged me to keep up the work. My thanks go to all the Vader and Musacchio lab members for their advice and help. I am particularly thankful to Dr. Richard Cardoso da Silva for helping me with designing the experiments, introducing me to new scientific methods and for scientific discussions. I would also like to thank Dr. Duccio Conti, Julia Schweighofer and Dr. Valentina Piano for checking this thesis.

Finally, I would like to extend my gratitude to my family for trusting and believing in me. They have been supportive throughout my life. I am forever grateful to my mother and

The curriculum vitae is not included in the online version for data protection reasons

Andrea Musacchio
Abteilung für mechanistische Zellbiologie

MAX-PLANCK-INSTITUT
FÜR MOLEKULARE PHYSIOLOGIE

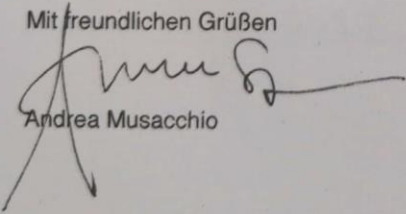MPI für molekulare Physiologie, Otto-Hahn-Str. 11, 44227 Dortmund

Universität Duisburg-Essen
Fakultät für Biologie
Prof. Dr. Stefan Westermann
Promotionsausschuss
Schützenbahn 70
45127 Essen

5. April 2022

Erklärung:

Hiermit erkläre ich, gem. § 6 Abs. (2) g) der Promotionsordnung der Fakultät für Biologie zur Erlangung der Dr. rer. nat., dass ich das Arbeitsgebiet, dem das Thema „A synthetic system to study the establishment of meiotic interhomolog-specific DNA repair by the Red1-Hop1-Mek1 complex" zuzuordnen ist, in Forschung und Lehre vertrete und den Antrag von Frau Vaishnavi Nivsarkar befürworte und die Betreuung auch im Falle eines Weggangs, wenn nicht wichtige Gründe dem entgegenstehen, weiterführen werde.
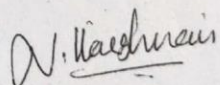
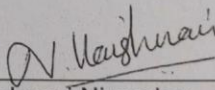Mit freundlichen Grüßen

Andrea Musacchio

Universität Duisburg-Essen
Fakultät für Biologie
Prof. Dr. Stefan Westermann
Promotionsausschuss
Schützenbahn 70

45127 Essen

Erklärung:

Hiermit erkläre ich, gem. § 7 Abs. (2) d) + f) der Promotionsordnung der Fakultät für Biologie zur Erlangung des Dr. rer. nat., dass ich die vorliegende Dissertation selbständig verfasst und mich keiner anderen als der angegebenen Hilfsmittel bedient, bei der Abfassung der Dissertation nur die angegeben Hilfsmittel benutzt und alle wörtlich oder inhaltlich übernommenen Stellen als solche gekennzeichnet habe.

Dortmund, 05.04.2022

_____
Vaishnavi Nivsarkar

Universität Duisburg-Essen
Fakultät für Biologie
Prof. Dr. Stefan Westermann
Promotionsausschuss
Schützenbahn 70

45127 Essen

Erklärung:

Hiermit erkläre ich, gem. § 7 Abs. (2) e) + g) der Promotionsordnung der Fakultät für Biologie zur Erlangung des Dr. rer. nat., dass ich keine anderen Promotionen bzw. Promotionsversuche in der Vergangenheit durchgeführt habe und dass diese Arbeit von keiner anderen Fakultät/Fachbereich abgelehnt worden ist.

Dortmund, 05. 04. 2022

Vaishnavi Nivsarkar

DuEPublico

Duisburg-Essen Publications online